Technical Report Documentation Page

1. Report No.	2. Government Accession No.	3. Recipient's Catalog No.
FHWA/TX-94+1306-1F		

4. Title and Subtitle	5. Report Date
LONG-TERM PERFORMANCE EVALUATION OF POLYMER-MODIFIED ASPHALT CONCRETE PAVEMENTS	*November 1993*
	6. Performing Organization Code
7. Author(s)	8. Performing Organization Report No.
William E. Elmore, Thomas W. Kennedy, Mansour Solaimanian, and Pablo Bolzan	*Research Report 1306-1F*
9. Performing Organization Name and Address	10. Work Unit No. (TRAIS)
Center for Transportation Research *The University of Texas at Austin* *3208 Red River, Suite 200* *Austin, Texas 78705-2650*	11. Contract or Grant No. *Research Study 0-1306*
	13. Type of Report and Period Covered
12. Sponsoring Agency Name and Address	*Final*
Texas Department of Transportation *Research and Technology Transfer Office* *P. O. Box 5051* *Austin, Texas 78763-5051*	14. Sponsoring Agency Code

15. Supplementary Notes

Study conducted in cooperation with the U. S. Department of Transportation, Federal Highway Administration
Research Study Title: "Long-Term Performance Evaluation of Polymer-Modified Asphalt Concrete Pavements"

16. Abstract

Following the five-year study performed to investigate the behavior of binders and asphalt mixtures containing polymer modifiers, it was determined that an insufficient amount of time had elapsed to allow any determinations to be made based upon the special field test sections. The study reported herein was to extend that initial time and to study in depth those special test sections, using visual observations coupled with resulting tests performed on samples extracted from the sections and comparisons with the original data developed in the original research. The research includes laboratory testing of field samples, determining the aging effect on the control and modified binders and corresponding effect on the mixtures, and visual evaluations. Retained samples of the original asphalts were also evaluated for potential performance as determined by the performance-based asphalt binder specification developed by the Strategic Highway Research Program.

Four hot mix pavement field projects were constructed in the Tyler, Lufkin, San Antonio, and Childress Districts (10, 11, 15, and 25, respectively), and two seal coat projects were placed in the Odessa and Bryan Districts (6 and 17).

17. Key Words	18. Distribution Statement
binders, asphalt mixtures, polymer modifiers, field test sections, visual observations, samples, laboratory testing, aging effect, performance, specification, hot mix pavement, seal coat, surface treatments, thermal cracking, fatigue cracking, distress	*No restrictions. This document is available to the public through the National Technical Information Service, Springfield, Virginia 22161.*

19. Security Classif. (of this report)	20. Security Classif. (of this page)	21. No. of Pages	22. Price
Unclassified	*Unclassified*	*218*	

Form DOT F 1700.7 (8-72) Reproduction of completed page authorized

LONG-TERM PERFORMANCE EVALUATION OF POLYMER-MODIFIED ASPHALT CONCRETE PAVEMENTS

by

William E. Elmore
Thomas W. Kennedy
Mansour Solaimanian
Pablo Bolzan

Research Report Number 1306-1F

Research Project 0-1306 (3-9-92/3-1306)

Long-Term Performance Evaluation of Polymer-Modified Asphalt Concrete Pavements

conducted for the

TEXAS DEPARTMENT OF TRANSPORTATION

in cooperation with the

U.S. Department of Transportation
Federal Highway Administration

by the

CENTER FOR TRANSPORTATION RESEARCH

Bureau of Engineering Research
THE UNIVERSITY OF TEXAS AT AUSTIN

November 1993

IMPLEMENTATION STATEMENT

The benefits obtained when polymers are blended with asphalt cements are apparent from the data developed in this and the previous research study (Research Study 492). The need to carefully evaluate the properties developed between individual asphalts and a polymer should be incorporated into the Texas Department of Transportation (TxDOT) procedures, along with the proper test methods capable of measuring those properties. The findings of this report support changes in test and design procedures. In addition, the data from the field test sections provide a base for the continuing monitoring of the effect of polymer modification of asphalts under a wide variety of environmental conditions.

Prepared in cooperation with the Texas Department of Transportation and the U.S. Department of Transportation, Federal Highway Administration

DISCLAIMERS

Thomas W. Kennedy (Texas No. 29596)
Research Supervisor

PREFACE

This is the final report for Research Project 3-9-92/3-1306, "Long-Term Performance Evaluation of Polymer-Modified Asphalt Concrete Pavements." This study was established to provide for the continuation of the field evaluation of special test sections constructed under the original research project, 3-9-87/1-492, "Mix Design Procedures and Considerations for Polymer-Modified Asphalt Compatibility and Stability." The previous study was also conducted by the Center for Transportation Research, The University of Texas at Austin, for and in cooperation with the Texas Department of Transportation (TxDOT). This report presents the findings, conclusions, and recommendations based upon the laboratory and final field sampling of HMAC mixtures and seal coats placed in six of the TxDOT districts.

The success of this project was possible only through the close cooperation and assistance of the individual district personnel involved and the guidance of Darren Hazlett of the Materials and Tests Division, who represented the Texas Department of Transportation as Technical Coordinator (Technical Panel Chairman, now referred to as Project Director).

The authors also gratefully acknowledge the input and effort of Eugene Betts and Chayatan Phromsorn and the close support of the Center for Transportation Research staff.

ABSTRACT

Following the five-year study performed to investigate the behavior of binders and asphalt mixtures containing polymer modifiers, it was determined that an insufficient amount of time had elapsed to allow any determinations to be made based upon the special field test sections. The study reported herein was to extend that initial time and to study in depth those special test sections, using visual observations coupled with resulting tests performed on samples extracted from the sections and comparisons with the original data developed in the original research. The research includes laboratory testing of field samples, determining the aging effects on the control and modified binders and the corresponding effects on the mixtures, and visual evaluations. Retained samples of the original asphalts were also evaluated for potential performance as determined by the performance-based asphalt binder specification developed by the Strategic Highway Research Program.

Four hot mix pavement field projects were constructed in the Tyler, Lufkin, San Antonio, and Childress Districts (10, 11, 15, and 25, respectively), and two seal coat projects were placed in the Odessa and Bryan Districts (6 and 17).

TABLE OF CONTENTS

LIST OF FIGURES

LIST OF TABLES

SUMMARY

The use of polymers to modify asphalt binders for asphalt concrete mixtures and seal coats and surface treatments resulted in a five-year study into the use of polymer addition to improve the properties of asphalt binders. This research (Research Project 3-9-87/1-492, "Mix Design Procedures and Considerations for Polymer-Modified Asphalt Compatibility and Stability") was conducted by the Center for Transportation Research at The University of Texas at Austin for the Texas Department of Transportation. The primary objectives were to determine any benefits of polymer modification resulting in reducing (1) thermal and fatigue cracking, (2) moisture damage, and (3) permanent deformation. A major part of this research was the construction of 28 test sections in six districts (Odessa, Tyler, Lufkin, San Antonio, Bryan, and Childress) utilizing seven different polymers including SBS, SBR, EVA, and SBR/Polyolefin.

A determination was made at the conclusion of the original research that an insufficient amount of time had elapsed for the test sections to begin to show recognizable signs of distress. This two-year project was initiated to address this deficiency and to provide an evaluation of the performance of the asphalt binders under varying environmental and traffic conditions and in comparison with one another, utilizing the available parent asphalt.

Final cores were obtained and the various tests performed for comparison with the original values in the initial study. In addition, available retained samples of the original asphalts were tested for classification by the Strategic Highway Research Project's Performance-Based Binder Specification. These results were compared to the existing conditions of the individual test sections to determine whether the asphalt used met the project site and condition requirements as measured by that specification.

This report provides the information required to aid in the selection of the desired combination of asphalt and polymer modifiers to meet individual project requirements.

CHAPTER 1

INTRODUCTION

The continuing distress caused by the increasing traffic loads, traffic volumes, and higher tire pressures led the Texas Department of Transportation (TxDOT) to sponsor a major research study, beginning in the spring of 1987, to study the potential benefits of polymer modification of asphalts. The study involved both laboratory testing and field implementation. Primarily, the research was directed to reducing the basic types of distress, which included:

(1) **Thermal Cracking,**
(2) **Fatigue Cracking**, and
(3) **Permanent Deformation.**

In addition, it was realized that environmental factors such as temperature and moisture increased the severity of any such distress, and, therefore, the following were included for consideration:

(4) **Moisture Damage** and
(5) **Aging.**

The resulting three-year project, Research Study 492, "Mix Design Procedures and Considerations for Polymer-Modified Compatibility and Stability" (Ref 34), was completed in 1991.

DEFINITIONS

For the purposes of definition, the following descriptions of distress are quoted here from the final report on that study.

Thermal Cracking occurs in two forms, low-temperature cracking and thermal fatigue. Thermal cracks are transverse cracks which run perpendicular to the direction of traffic and are often spaced equidistant from one another. As the temperature is reduced, the pavement structure tends to shrink. This shrinkage is resisted by the internal strength of the pavement structure and by the friction which is developed between the pavement undersurface and the underlying layer. Development of frictional forces causes tensile stresses to develop in the pavement. The magnitude of these stresses is dependent on the stiffness, the coefficient of expansion of the material, the rate of temperature change, and the magnitude of the temperature change. Low-temperature cracking takes place when the tensile stress induced by a single drop in temperature exceeds the tensile strength of the asphalt mixture. Similarly, repeated thermal cycles may cause the pavement to crack as the result of thermal fatigue.

Fatigue Cracking, also called alligator cracking, is caused by the action of repeated loads induced by moving traffic. Fatigue cracking susceptibility increases with higher loads, with increasing repetitions of loads, and/or with inadequate support in one or more of the pavement or underlying layers, which causes the HMAC to experience higher strains. The problem of preventing fatigue cracking is further compounded because the desirable mixture properties for increased fatigue life are different for thick and for thin pavements. Thick sections require stiffer materials for minimal fatigue, and thin sections require less stiff or more flexible materials.

Permanent Deformation on rural highways is manifested by wheel path rutting. However, in urban areas and at the intersections, where heavy vehicles move slowly or stop frequently, both rutting and shoving can occur. Rutting in HMAC can be caused by either overdensification from traffic or shear flow of the mixture. Shoving is caused only by shear flow of the mixture. In general, the more severe premature rutting failures and distortion problems of HMAC are related to lateral flow of the asphalt or shear distortion rather than to one-dimensional densification. These types of distress (rutting and shoving) are a function of the shearing resistance of the materials. The shearing resistance of HMAC is a function of the interparticle cohesion and friction as well as the amount of stress applied to the material. The cohesion of the mixture depends on the amount and properties of the asphalt binder in the mix.

Moisture Damage occurs in two forms, loss of cohesion and loss of adhesion. Loss of adhesion or stripping involves the physical separation of the asphalt binder and the aggregate, primarily due to the action of moisture and traffic. Loss of cohesion involves failure of the asphalt film itself. Both forms of damage are characterized by a reduction in strength and stiffness of the asphalt mixture.

Aging occurs primarily as the result of oxidation, which causes hardening of the asphalt. This increased stiffness (due to the hardening) can cause increased cracking as a result of temperature changes or repeated loads.

OBJECTIVES OF RESEARCH STUDY 492

The specific objectives of Research Study 492 were:

(1) To define the properties desired in a polymer-modified binder.
(2) To select tests which best measure or quantify these properties for hot mixed asphalt concrete.
(3) To evaluate proper design procedures for hot mixed asphalt concrete.
(4) To establish specifications for modified binders for each application.

To accomplish these objectives, the following work plan was adopted:

(1) To select materials.
(2) To determine properties of polymer-modified binders in the laboratory.
(3) To determine engineering properties of polymer-modified mixtures in the laboratory.
(4) To construct field test sections for the polymer-modified mixtures and control mixtures.
(5) To monitor field performance for long-term evaluation.

Since polymer additives are asphalt-dependent for their engineering properties, it is important to provide a means of determining the long-term performance characteristics of polymer-modified asphalt concrete pavements. The purpose of this research project, Research Study 1306, "Long-Term Performance Evaluation of Polymer-Modified Asphalt Concrete Pavements," is to develop this information based upon the service history generated by the test pavements constructed in the 492 study.

OBJECTIVES OF RESEARCH STUDY 1306

The objectives of this study were:

(1) To establish a long-term monitoring program to follow the performance of the test pavement sections.

(2) To determine the critical engineering properties which will predict long-term performance.

(3) To evaluate and document this performance in a variety of load and climatic environments.

This report summarizes the results of the evaluations conducted on the experimental field sections placed as a major part of the initial study and reported in Research Study 492-1F, "Mix Design Procedures and Considerations for Polymer-Modified Asphalt Compatibility and Stability" (Ref 34). The theoretical background is provided in Chapter 2, much of which is a repeat from the earlier study and is made a part of this report in the interest of clarity. Chapter 3 explains the experimental program developed in this study, and the resulting data and discussion are presented in Chapter 4. A part of Chapter 4 contains the results of performing the recommended Strategic Asphalt Research Program performance-related asphalt binder tests on the retained asphalt binders remaining from the original construction of the field sections.

CHAPTER 2

BACKGROUND

The viscoelastic behavior of an asphalt mixture is given by the viscoelastic properties of the asphalt binder used in the mixture. The asphalt binder as a part of the asphalt mixture is subjected to traffic-related stresses and thermal-induced stresses within a large combination range of loading times and temperatures throughout its service life. The ideal binder should be capable of reducing to a minimum permanent residual strains at high service temperatures under repeated loading, and should also be able to relieve the thermal stresses induced by the temperature changes. At the intermediate service temperature range, the binder should maintain its flexibility to avoid load-related fatigue cracking. In addition, the viscosity of the ideal asphalt at normal mixing temperatures in a mix should be sufficiently low as to ensure that the mixture can be processed and applied under typical conditions with conventional equipment. A few asphalts exist that approach this description, but most vary significantly. Even the so-called "good" asphalts generally need some degree of improvement with the ever-increasing performance requirements being imposed on asphalt pavements.

It has long been recognized that both the crude source and the subsequent refining methods determine the physical and chemical properties of the resultant asphalt cement. Due to the unstable nature of the petroleum supply source to the industry, more and more crude sources are being supplied to every refinery, and almost all asphalt refineries are blending two or more crude sources in their production. This blending occurs even within a given oil field or given strata with the mixing of crudes from different wells.

Conventional asphalt cements often do not have the properties to simultaneously satisfy the requirements represented by the different forms of distress that are being encountered. It was readily determined that it would be necessary to utilize the asphalt modifiers that are available on the market to produce an asphalt binder that would provide the engineering properties required. Modification of asphalt cement binders to improve properties has received much attention in the highway paving industry over the past few years. To accomplish the objectives of the original study, Research Study 492, it was necessary to select potential modifiers and to develop a means of determining asphalt-additive compatibility, binder characteristics, and mixture design procedures sensitive to these modified asphaltic binders. Polymer additives are currently dominating this emerging industry and producers of polymer additives are increasing at a rapid rate. This then became the focus of the parent study, Research Study 492 (Ref 34).

An extensive literature search was conducted to determine the known characteristics of various polymers and the effects of using these polymers to modify asphalt cements. In addition, included in the search were studies on the applications of both adopted testing standards and innovative modifications to them that referred to the use of these modified binders. A listing of some of the more pertinent sources is given as References 1-21.

In the laboratory portion of the 492 study, AC-10 and AC-20 grades of asphalt from Texas Fuel and Asphalt, Texaco, Shamrock, and Fina were used to evaluate the various test methods and procedures. The same asphalt sources, plus Total, Gulf, and Exxon, were used in the field test portion, with the location of each depending upon individual economic feasibility.

In Research Study 492, the following materials properties were determined for each binder:

- Temperature Susceptibility:
  - Penetration Index, PI
  - Penetration-Viscosity Number, PVN
- Durability Indicators:
  - Penetration Ratio (77°F) (25°C)
  - Kinematic Viscosity Ratio (275°F) (135°C)
  - Absolute Viscosity Ratio (140°F) (60°C)
- Stiffness Modulus:
  - Stiffness-Temperature Susceptibility
- Cracking Temperature:
  - Limiting Stiffness Method
  - Critical Stress Method
- Force Ductility:
  - Asphalt Modulus
  - Asphalt-Polymer Modulus
  - Maximum True Stress
  - Maximum True Strain
  - Area Under Stress-Strain Curve
- Schweyer Constant Stress Rheometer:
  - Shear Susceptibility
  - Apparent Viscosity
  - Constant Power Viscosity
  - Constant Power Viscosity-Temperature Susceptibility
- Compatibility:
  - Hot Storage Stability Test

A brief discussion and the formulae used to determine these values have been summarized from Research Study 492 and are made a part of this report as Appendix A.

LABORATORY TESTING OF CORE SAMPLES

Several tests were performed in the laboratory on the core samples taken periodically from the field road test sections prior to the extraction of the binder for the previously listed tests. The testing protocol in the 492 study measured the following engineering properties:

- Marshall Stability Test (ASTM D1559):
  - Marshall Stability
  - Marshall Flow or Flow Index
- Hveem Stability Test (Tex-208-F):
  - Hveem Stability

Indirect Tensile Strength Test (Tex-226-F):
- Indirect Tensile Strength
- Tensile Strain at Failure
- Secant Modulus

Indirect Tension Test for Resilient Modulus (ASTM D4123):
- Resilient Modulus
- Poisson's Ratio

Indirect Tensile Fatigue Test:
- Fatigue Constants, K_1 and K_2
- Permanent Deformation Characteristic Parameters (Alpha and Gnu)
- Indirect Tensile Creep Test
- Tensile Creep Compliance

Moisture Sensitivity Test (Tex-531-C):
- Tensile Strength Ratio (TSR)

Again, a brief summary identifying these tests and corresponding formulae are included as part of this report in Appendix A.

FIELD TEST SITES

Field test sites in six Texas DOT districts (Figure 2.1) were chosen and constructed with the close cooperation of District, Contractor, Asphalt, and Modifier representatives. Two of the districts, Bryan and Odessa, had test sites consisting of seal coat construction, and the remaining four, San Antonio, Tyler, Lufkin, and Childress, consisted of new hot mix asphalt concrete pavement. The number of polymers being evaluated in each district varied, depending upon the size of the project and the ability to transport to the construction site a properly blended modified asphalt binder.

The polymers that were included in the field test program in at least one location were:

(1) Goodyear UP 70 (SBR);
(2) Polysar NS 175 (SBR);
(3) Elf Styrelf (SBS);
(4) Exxon Polybilt 103 (EVA);
(5) Dow (SBR/Polyolefin);
(6) Shell Kraton D1101 (SBS); and
(7) Crafco Rubber C107.

In this research study polymers were grouped into two basic categories. An "elastomer" is a polymer which exhibits elastic or rubber-like characteristics. When distorted and released it will tend to recover its original shape and size. A "plastomer" is a polymer which demonstrates plastic-like properties. When distorted and released it will tend to remain deformed and not recover its original size and shape. Some of the available polymers were combinations of the two and, as such, exhibited properties to some extent of both.

Styrene Butadiene Rubber (SBR) is an elastomer and was added to the asphalt in this study as a latex emulsion.

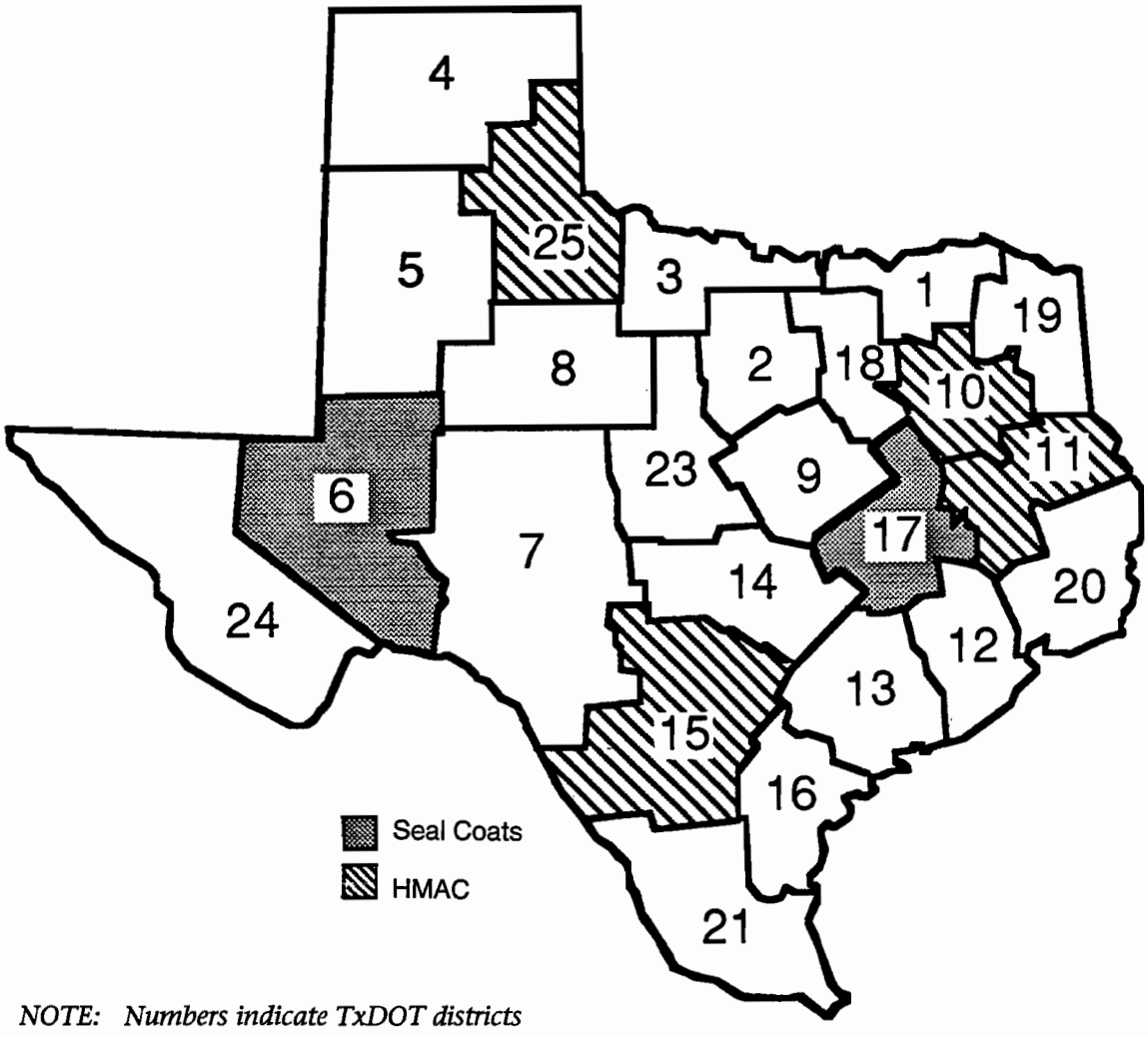

NOTE: Numbers indicate TxDOT districts

Figure 2.1 Location of field test sections

Styrene Butadiene Block Copolymer (SBS) is an elastomeric polymer and is a solid, rubbery material. Two different polymers of this type were used in this study: one was blended with the asphalt by using a high-shear mixing process; the other was the result of the polymer reacting with the asphalt and sulfur.

Ethylene Vinyl Acetate Copolymer (EVA) is a solid, plastomeric material and was blended with the binder prior to adding to the mixture.

SBR/Polyolefin is a combination of a SBR latex and a functionalized polyolefin. In this case it is a blend of an elastomeric polymer and a plastomeric polymer (polyolefin). It is not a copolymer of these two types but, instead, a physical blend of two distinct polymers.

Recycled Tires consisted of tread buffings, primarily those from passenger car tires.

Fibers for this study consisted of a mixture of polyethylene and kevlar fibers. This mixture was added during the mixing cycle.

Each district test pavement consisted of a well-identified section for each of the polymers being tested in that pavement and, with two exceptions, a control section using the same asphalt *un*modified. The exceptions were the Tyler District and the Childress District, which used a completely different asphalt. Another exception was the addition of 1 percent by weight of lime to every mixture in the Childress District test sections.

Identical aggregates were used for all test sections within each district. Table 2.1, Summary of Materials for Field Test Projects, is from the initial research, described in Research Report 492-1F, which indicates the materials used in each of the test sections in each of the participating districts.

Both batch and drum mix plants were used in the research and are represented here. Districts 11, 25, and 10 (Lufkin, Childress, and Tyler, respectively) utilized the drum mix plant, and District 15 (San Antonio) used a batch plant for the production of the project hot mix. All of the polymer-modified binders were pre-blended, and the mixing temperatures were between 310° and 350°F (154° and 177°C). The initial breakdown compaction occurred at temperatures between 250° and 280°F (121° and 138°C), and compaction was then completed on each test section using a vibratory roller, a pneumatic roller, and a static wheel roller.

TABLE 2.1 SUMMARY OF MATERIALS FOR FIELD TEST PROJECTS

Location of Field Project	Test Section Number	Aggregates	Asphalt Source & Grade	Binder Content, % Field +	Binder Content, % Design ++	Polymer Source	Polymer Type	Polymer Designation	Polymer Content %	Appendix*
	1		TFA AC-10	4.6	-	Goodyear	SBR	UP 70	3%	A
	2	Sandstone 31%	TFA AC-10	4.6	-	Elf	SBS	Styrelf-13	3%	A
District 15	3	Limestone 27%	TFA AC-20	4.6	4.8	-	-	-	-	A
	4	Limestone	TFA AC-20	4.6	-	Exxon	EVA	Polybilt 103	3%	A
San Antonio	5	Screenings 19%	TFA AC-10	6.3	6.3	Crafco	Recy. tires	Genstar C107	18%	A
	6	Field Sand 23%	TFA AC-10	4.6	-	Polysar	SBR	NS 175	3%	A
	7		TFA AC-20	4.6	-	Dow	SBR/Polyolefin		5%	A
		LtWt. Type D 56%								
District 11	1	Coarse Sandstone	Texaco AC-20	6.8	6.8	-	-	-	-	B
Lufkin	2	Screenings 10%	Texaco AC-10	6.8	-	Elf	SBS	Styrelf-13	3%	B
	3	Fine Sndstone Screenings 15% Field Sand 19%	Texaco AC-10	6.8	-	Goodyear	SBR	UP 70	3%	B
	1		Shamrock AC-20	5.0	5.4	-	-	-	-	C
District 25	2	Crushed Gravel 51%	Fina AC-10	5.0	5.8	Goodyear	SBR	UP 70	3%	C
Childress	3	Screenings 49%	Fina AC-10	5.0	5.4	Elf	SBS	Styrelf-13	3%	C
	4	Lime 1% by weight	Fina AC-10	5.0	5.0	Shell	SBS	Kraton D1101	3%	C
	5	of aggregates	Fina AC-10	5.0	5.4	Shell	SBS	Kraton D1101	6%	C
	1		Total AC-20	4.6	4.9	-	-	-	-	D
District 10	2	Crushed Stone 65%	Fina AC-10	4.6	-	Goodyear	SBR	UP 70	3%	D
Tyler	3	Screenings 15%	Fina AC-10	4.6	-	Elf	SBS	Styrelf-13	3%	D
	4	Field Sand 20%	Exxon AC-10	4.6	-	Exxon	EVA	Polybilt 103	3%	D
	5		Gulf AC-10	4.6	-	Shell	SBS	Kraton D1101	3%	D
	1		Fina AC-5	0.35 Gal/SqYd		Goodyear	SBR	UP 70	2%	E
District 17	2	Pre- Coated	Fina AC-10	0.35 Gal/SqYd		-	-	-	-	E
Bryan	3	Aggregates	Exxon AC-10	0.35 Gal/SqYd		Shell	SBS	Kraton D1101	3%	E
	4		Exxon AC-10	0.35 Gal/SqYd		Elf	SBS	Styrelf-13	3%	E
	1		Fina AC-5	0.35 Gal/SqYd		Exxon	EVA	Polybilt 103	3.2%	E
District 6	2	Pre- Coated	Fina AC-5	0.35 Gal/SqYd		Shell	SBS	Kraton D1101	4.5%	E
Odessa	3	Aggregates	Fina AC-5	0.35 Gal/SqYd		Goodyear	SBR	UP 70	2%	E
	4		Fina AC-5	0.35 Gal/SqYd		-	-	-	-	E

* Details are contained in the indicated Appendices
\+ Binder content used for the field test project mixtures
++ Laboratory design optimum binder content

CHAPTER 3

EXPERIMENTAL PROGRAM

FIELD TEST PROGRAM

In the field sampling program, samples of plant-mixed mixtures of both the control and polymer-modified test sections, together with samples of asphalt cements, polymer-modified binders, and aggregates, were initially obtained in the original study and shipped to the asphalt research laboratory at The University of Texas at Austin. Cores were then scheduled to be taken from each of the test sections on a yearly basis. At the time core samples were obtained, a visual inspection and evaluation was made.

In the two districts where seal coat test sections were placed, monitoring was conducted primarily by visual inspection. If performance difference was noted, such as by significant aggregate loss, samples of the binder were to be obtained from the surface of the roadway for comparison to the original binder properties.

Test Program

The laboratory tests to be conducted on the core samples taken from the test sections were selected from a modification of the testing protocol established in the previous project, Research Study 492. These were:

(1) Indirect Tensile Strength at 39°, 77°, and 104°F (4°, 25°, and 40°C)
(2) Resilient Modulus at 39°, 77°, and 104°F (4°, 25°, and 40°C)
(3) Stability (Marshall and Hveem)
(4) Air Voids/Density Determination

The asphalt binder was then scheduled to be extracted from the tested cores and the following additional tests then performed on the recovered binder for evaluation and comparison to the test values on the original binders:

(a) Penetration at 77°F (25°C)
(b) Viscosity at 140° and 275°F (60° and 135°C)
(c) Force Ductility at 39°F (4°C)
(d) Constant Stress Scheweyer Rheometer at 39°, 60°, 77°, 90°, and 140°F (4°, 16°, 25°, 32°, and 40°C)
(e) Creep Testing
(f) Fatigue Testing

The availability of the recommended performance-based asphalt binder specification developed by the Asphalt Research Group of the Strategic Highway Research Program provided the ability to enhance the testing and evaluation of this research. With the approval of the TxDOT Technical Coordinator (Project Director), the remaining retained samples of the original asphalt binders were tested in accordance with that specification with the Dynamic Shear Rheometer and the Bending Beam Rheometer.

Modification to the Experimental Program

In this research study, the basic plan developed in Research Study 492 (and recommended to be continued) was followed. Core samples were collected and visual evaluations made on each of the test sections once a year.

After review of the test data developed over the testing period to date, it was decided in a meeting with the TxDOT Technical Advisor to modify the experimental program by deleting the Scheweyer Rheometer as being of no value at this point in the evaluation of the field test sections. In addition, the Marshall and Hveem stability tests were dropped from the list of tests to be performed on the recovered cores. Both the researchers and the Technical Advisor were of the opinion that little benefit could be obtained from the tests.

In addition, a preliminary review of the data also led the researchers and the TxDOT advisors to decide not to perform both the creep and fatigue tests at this time. These tests were considered to be predictive of the future condition of the test pavements rather than able to give further insight into the existing condition of the section at the time of sampling. Sufficient samples were obtained at the coring of the pavements to provide for these tests to be performed if time permitted; the samples also would provide a limited backup in the event any of the scheduled tests had to be repeated.

A total of 15 cores were randomly selected in each test section from locations in the wheel paths. During the final on-site evaluations, photographs were taken of the surface condition of each test section to provide a reference for future use if necessary.

Individual district personnel continued to provide critical services of traffic control, performing the actual coring and preparing the cores for shipment to The University of Texas asphalt research laboratory.

As previously stated, the recent completion of the SHRP Asphalt Research Program has yielded the recommended performance-based asphalt binder specifications. Test procedures requiring two additional pieces of equipment, the Dynamic Shear Rheometer (DSR) and the Bending Beam Rheometer (BBR), are a part of that specification. In order to see if those tests could forecast what has occurred to the test pavements, the tests have been run on all of the retained asphalt binder samples. A description of tests, procedures, and resulting data is furnished later in the report.

Site plans of the test sections, together with the physical location of the test pavements as previously shown in Research Study 492, are included herein as Figures 3.1 through 3.4.

Modified Test Plan

Based upon the modifications to the experimental program, the test plan for the cores obtained from the field sections was modified as follows:

Three cores — Indirect Tensile Test at 77°F (25°C)
Three cores — Indirect Tensile Test at 104°F (40°C)
Three cores — (1) Resilient Modulus at 77°F (25°C)
(2) Resilient Modulus at 39°F (4°C)
(3) Indirect Tensile Test at 39°F (4°C)

The remaining cores were held as a backup in the event of a need to retest, or for performing the creep test if time allowed and it was considered necessary.

Seal coat sections were to be visually evaluated and sampling of the binder to be attempted only if conditions appeared to require it.

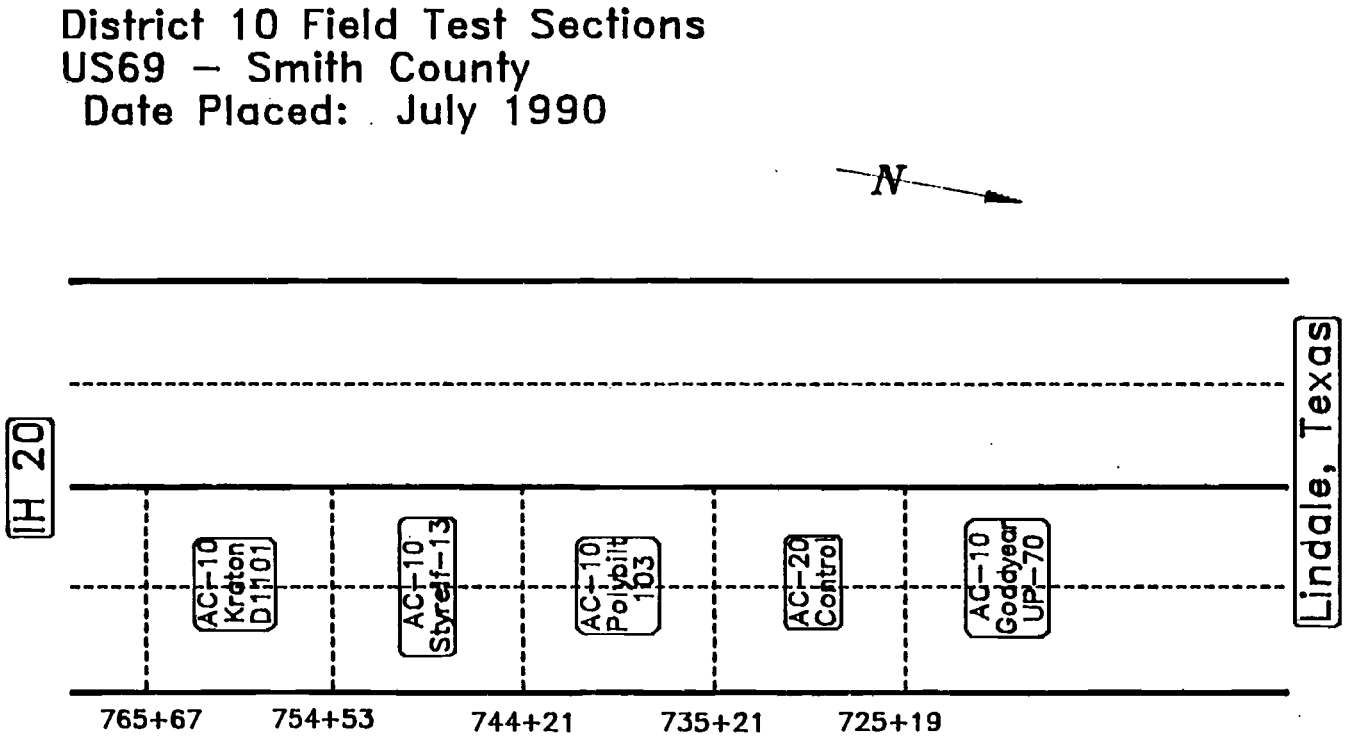

Figure 3.1 Schematic illustration of field test section

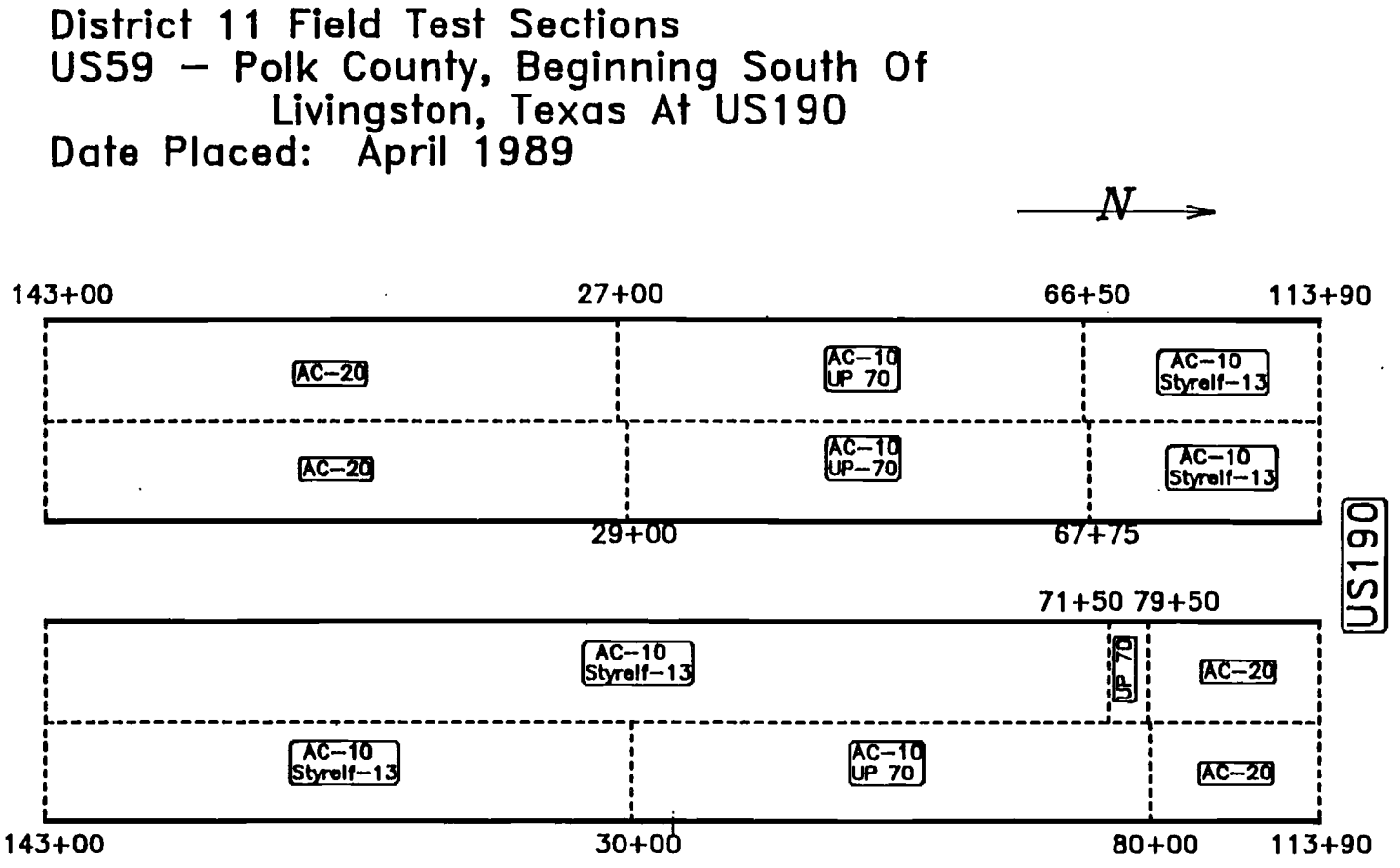

Figure 3.2 Schematic illustration of field test section

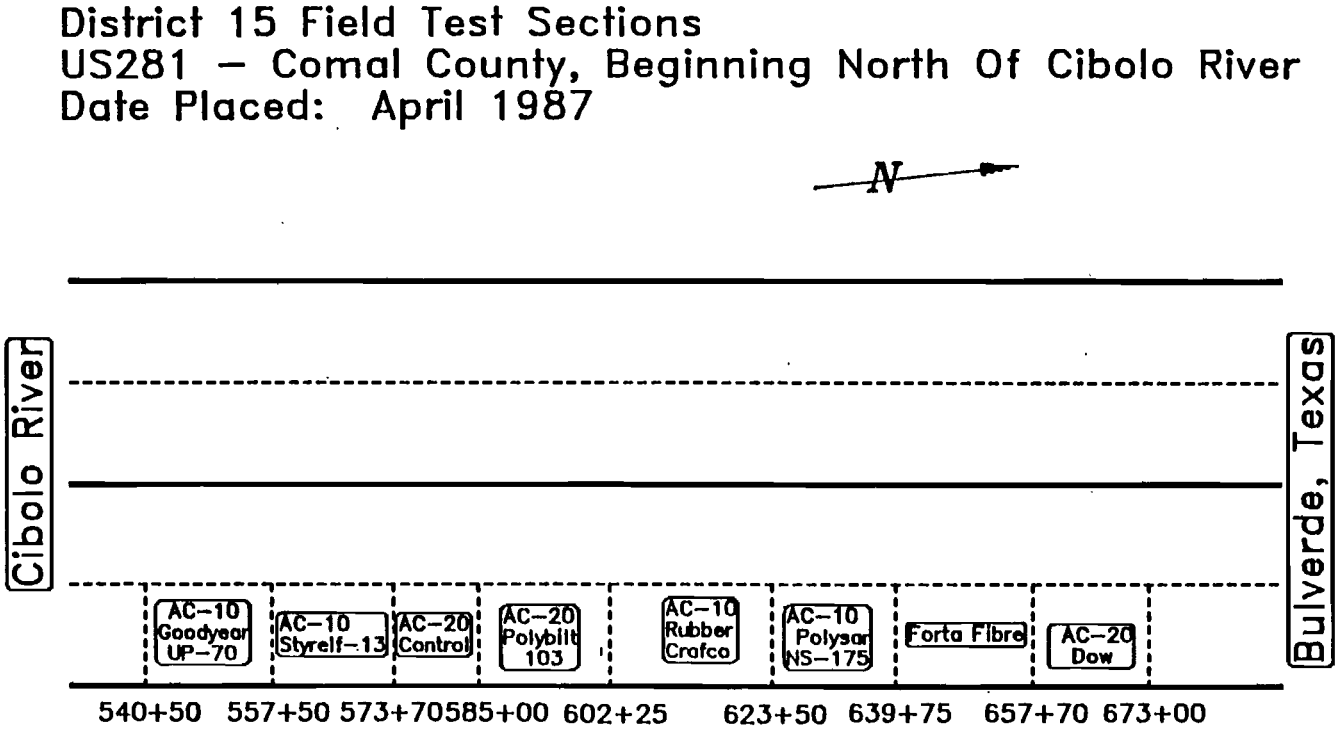

Figure 3.3 Schematic illustration of field test section

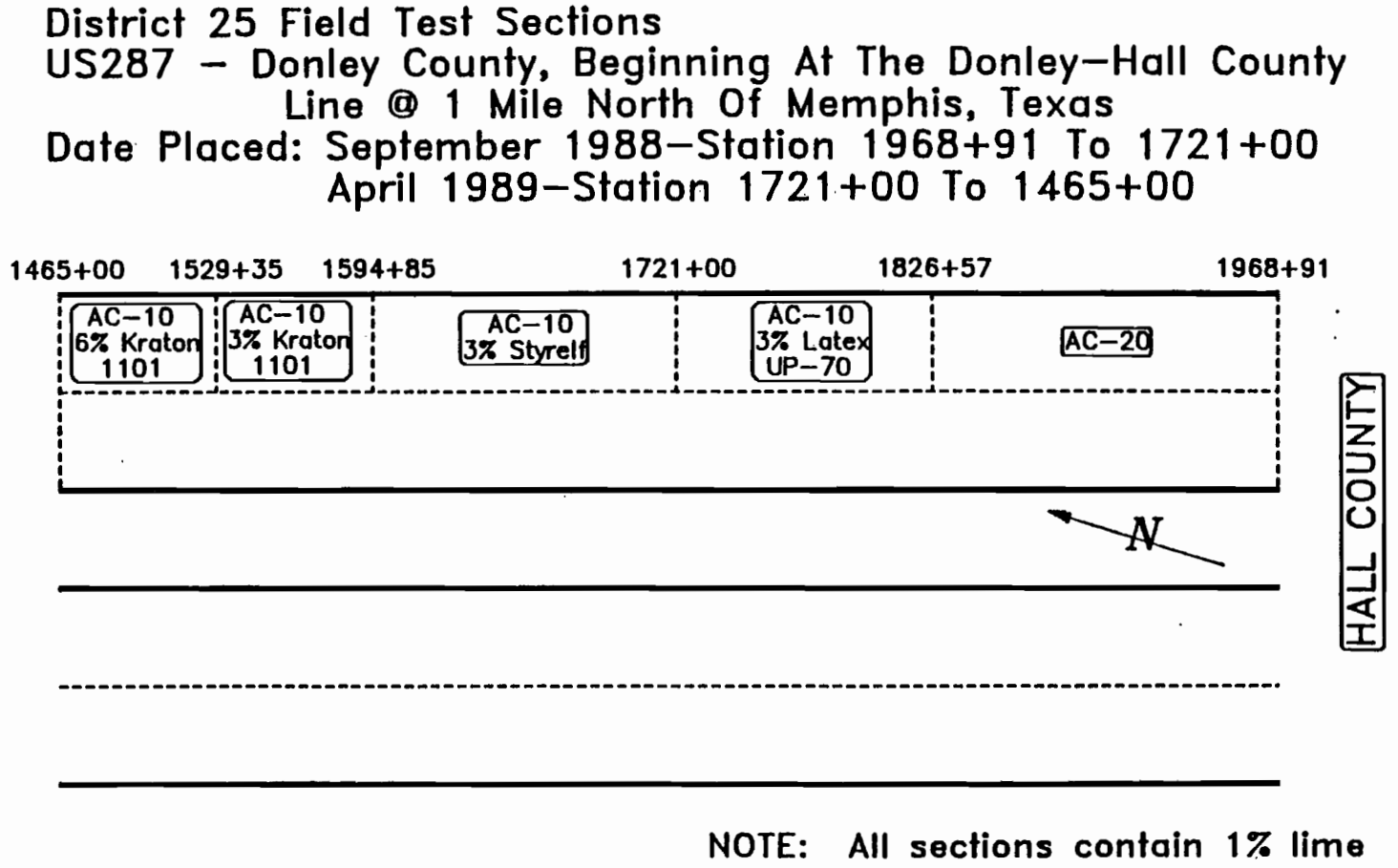

Figure 3.4 Schematic illustration of field test section

CHAPTER 4

TEST RESULTS AND DISCUSSION

VISUAL EVALUATION

Visual evaluations were made of the condition of the test pavements each time core samples were obtained. In addition, during the final sampling scheduled under this study, photographs were taken in the event they were needed to provide a record for later use. For the purpose of brevity, only the final evaluations are described in this report since these were the most pertinent.

The seal coat test pavements are included in the visual evaluations, but there has been no evidence at the end of this phase of the study to justify attempting to sample the asphalt in these sections.

SEAL COAT SECTIONS

Odessa District (6), Winkler County, SH 18

These sections were placed on September 7, 1990. Three polymer-modified sections were included in this test site for comparison to the control asphalt, Fina AC-5. The last visual inspection and evaluation revealed no excessive amounts of bleeding or aggregate loss. The modified sections were all modifications of the Fina AC-5: 3.2% Exxon Polybilt 103, 4.6% Kraton D1101, and 2% Goodyear UP70. Based upon the existing apparent lack of distress, no further evaluations were planned or conducted.

Bryan District (17), Robertson County, US 79

These sections were placed August 10, 1990. Again, there were three modified sections for comparison with the control. In this case, however, the control section was constructed with a Fina AC-10 and the asphalts to be modified were from two different refineries: Fina AC-5 modified with 2% Goodyear UP-70 and Exxon AC-10 modified with 3% Kraton D1101 and 3% Styrelf. Here again there were no visual signs of appreciable bleeding or aggregate loss, and no further evaluations were made.

HOT MIX ASPHALT SECTIONS

Tyler District (10), Smith County, US 69

These test sections were constructed in July 1990. Four different asphalts were used to provide four modified asphalts and one control: Total AC-20 was the control section asphalt; Fina AC-10 with Goodyear UP70 (SPR_g) and Styrelf-13 (SBS_e), Exxon AC-10 with Polybilt 103 (EVA_e), and Gulf AC-10 with Kraton D1101 (SBS_s) were the modified asphalts.

The final visual inspection was made at the time the pavements were three years old. All sections were in good shape with no visible cracking and with negligible to no damage of any type visually notable.

Lufkin District (11), Polk County, US 59

These test sections were constructed in April 1989. The control section asphalt was a Texaco AC-20, and two modifiers were used to modify a Texaco AC-10: Goodyear UP70 (SBR_g) and Styrelf-13 (SBS_e).

There was no significant rutting in any of the sections at this time. Test sections of the modified asphalts were placed in both the northbound and the southbound lanes.

Styrelf-13 (SBS_e) Sections

There are four test sections with this modifier, one for each southbound lane and one for each northbound lane. The samples were obtained from the southbound outside lane. Visual inspection of all the sections indicated approximately the same type and level of distress. There were both longitudinal and transverse cracks which in some locations were beginning to intersect and form widely spaced pattern or map cracking. The cracks were not wide, and there was no apparent movement at this point. Some slight degree of surface spalling was also noted.

Goodyear UP70 (SBR_g) Sections

There were again four test sections, placed similarly to the Styrelf-13 sections. The core samples were also taken from the southbound outside lane. There were both longitudinal and transverse cracking but lesser amounts of the horizontal type. There was some evidence of breaking of the mixture along the edge of the crack. Even though the cracks were reasonably tight, the edges indicated that there was the possibility of some movement.

AC-20 Control

The AC-20 unmodified sections were also configured in a similar pattern, with the samples obtained from the northbound lane. Here there were still both transverse and longitudinal cracking but predominantly more longitudinal cracking. The transverse cracks appeared to be tighter than those in the other sections, but the longitudinal cracks were a little more open.

San Antonio District (15), Comal County, US 281

Six of the seven polymer asphalt modifiers were used in constructing these test sections in April 1987. Not only were more sections placed for evaluation, but these are the oldest of all those placed in this study. The only modifier not available was the Kraton D1101 (SBS_s). All used asphalt from the same source, but two grades, AC-10 and AC-20, were required in order to meet the manufacturer's recommended mixing procedures for the modified sections and the unmodified control section.

The control section and the Dow (SBR/Pd) section used the TFA AC-20, and TFA AC-10 was the asphalt modified by Goodyear UP70 (SBR_g), Styrelf-13 (SBS_e), Polybilt 103 (EVA_e), Crafco's Genstar C107, and Polysar NS-175 (SBR_p).

Several of the sections exhibited severe distress, and it is expected that corrective maintenance will need to be performed.

Goodyear UP70 (SBR_g) Section

This section had considerable longitudinal and transverse cracking that is proceeding into map or pattern cracking. There is minor rutting in the wheel path and the cracks show evidence of some pumping.

Styrelf-13 (SBS_e) Section

This section was in good condition, with no cracks apparent upon visual inspection. There did appear to be minor rutting in the wheel path in some places.

Polybilt 103 (EVA_e) Section

This section is suffering severe distress, with heavy alligator cracking in addition to both longitudinal and transverse open cracks.

Genstar C107 Section

This section is suffering moderate distress with significant longitudinal and transverse cracking. At this time, the cracks are not wide, nor is there any indication of spalling on the edges of the cracks that would indicate pumping. The longitudinal cracks are more predominant than the transverse.

Polysar NS-175 (SBR_p) Section

This section is in basically good condition. Some transverse cracks are visible but many of these appear actually to have partially healed themselves.

Dow (SBR/Pd) Section

This section is another of those suffering severe distress. The section is badly cracked, in both the longitudinal and transverse directions, developing pattern cracking which is already approaching alligator cracking in many locations. The edges of the cracks are raveling and indicating movement.

Control

The control section is suffering moderate distress, with a significant number of longitudinal and transverse cracks that so far have not developed into pattern or map cracking. The cracks do have signs of raveling at their edges.

Childress District (25), Donley County, US 287

These sections were constructed in April 1989. Three of the modifiers were used at this location to modify an AC-10 asphalt furnished by Fina. One difference was that two sections were placed with the same modifier but different percentages. Shamrock AC-20 was the asphalt used for the control section. In addition, all sections contained mixtures that were produced with aggregates that were prior treated with 1% lime. The modifiers used with the Fina AC-10 were Goodyear UP70 (SBR_g), Styrelf-13 (SBS_e), and Kraton D1101 (SBS_s) at 3% and 6%.

Kraton D1101 (SBS_s) (6%) Section

Visual inspection of this section indicated that the general condition was satisfactory, although some areas of alligator cracking were noted. There did not appear to be any additional longitudinal or transverse cracking.

Kraton D1101 (SBS_s) (3%) Section

This section was found visually to be in as good a condition as the 6% section, with the exception that no places with alligator cracking were observed.

Styrelf-13 (SBS_e) Section

This section was in good condition with no noticeable cracks or rutting. There was one 50-foot-long (80.5-meter-long) longitudinal crack between the wheel paths at

one location. The single occurrence would indicate that this crack is unrelated to the present study of the modifiers.

Goodyear UP70 (SBR_g) Section

This section was found to be in a moderately distressed condition, with longitudinal cracking and slight rutting in the outside wheel path.

Control

This section visually appeared to be in a light to moderate state of distress. Small longitudinal cracks were noted in the outside wheel path.

ASPHALT BINDER CLASSIFICATION BY SHRP PERFORMANCE GRADE AND LINEAR VISCOELASTIC CHARACTERIZATION

Samples of the original binders used in the initial research project, Research Study 492, were retained for potential further testing. This section of the report summarizes the testing carried out to determine the linear viscoelastic (LVE) properties of the unmodified asphalts and polymer-modified asphalts used in that project and further studied here. Measurement of the LVE properties was not an original part of the work plan for Research Study 1306. However, the recent successful completion of the Strategic Highway Research Program (SHRP) provided a performance-based specification (AASHTO MP1) for asphalt binders. This specification provides a potential means for the selection of asphalt binders that will perform properly under the field conditions to be encountered.

The LVE properties are calculated in order to both rheologically characterize and classify the binders according to the current SHRP Asphalt Binder Specification (AASHTO MP1) (Figures B-1 and B-2 of Appendix B). To this end, a comprehensive evaluation of the physical properties of the asphalt binders was performed using the SHRP test equipment and protocols. The data obtained from the testing, along with environmental and traffic considerations, enabled a comparison between the performance predicted by SHRP specifications and the actual behavior of materials placed.

The SHRP Asphalt Binder Specification is oriented to fundamental rheology based on the measurement of the linear thermo-viscoelastic properties of the binders, in both simple shear and simple flexion, and their failure properties (direct tension mode). Thus, the specification is designed to provide performance-related properties that can be related in a rational manner to pavement performance under the actual traffic and environmental loadings.

Some of the main features of the new asphalt binder specifications are as follows. The coefficient of viscosity is measured at high temperatures (pumping, mixing, and compaction temperature ranges) and, for safety reasons, the Cleveland open cup flash point temperature is retained in use. The loss on heating after the Rolling Thin-Film Oven Test (RTFOT) is calculated as a quality control for the asphalt binders. The complex modulus and stiffness are measured for both the anticipated traffic-related loading and representative regional climatic temperatures. Temperature susceptibility, aging index, and empirical testing were not considered by SHRP in the new

specifications, since these characteristics could not be properly related to pavement performance.

The unique feature of the SHRP specification, as mentioned before, is the measurement of fundamental asphalt properties at high, medium, and low temperatures representative of the anticipated pavement service temperature range. This feature addresses the main distress mechanisms in the pavement: plastic deformation, load-associated fatigue cracking, and low-temperature thermal shrinkage cracking.

The rheological characterization of the binders is carried out utilizing a series of tests capable of measuring the fundamental engineering material properties. Dynamic Shear Modulus, Flexural Creep Stiffness and slope of the log stiffness versus log time relationship, and Failure Strain in Direct Tension are the main binder physical properties measured in both unmodified and modified asphalts.

A list of the specification tests and standards pertaining to the SHRP Asphalt Binder Specification (AASHTO MP1) and application follows.

SHRP ASPHALT BINDER SPECIFICATION: SUMMARY OF THE PRACTICE

Tank asphalt binder conditioning:

- Flash point in °F (°C) (AASHTO T 48)
- Viscosity at 275°F (135°C) (ASTM D 4402)
- Shear modulus (G*) and phase angle (delta) at 10 rad/sec. and at specification test temperature (Ref SHRP B-003, AASHTO TP5)

RTFOT asphalt binder (ASTM D 2872) conditioning:

- Mass loss (ASTM D 2872)
- Shear modulus (G*) and phase angle (delta) at 10 rad/sec. and at specification test temperature (Ref SHRP B-003, AASHTO TP5)

PAV asphalt binder (Ref SHRP B-005, AASHTO PP1) conditioning:

- Shear modulus (G*) and phase angle (delta) at 10 rad/sec. and at specification test temperature (Ref SHRP B-003, AASHTO TP5)
- Creep stiffness (S) and slope (m) of the log S vs. log time at 60 seconds and at specification test temperature (Ref SHRP B-002, AASHTO TP1)
- Failure strain in direct tension at 1mm/min. (Ref SHRP B-004, AASHTO TP3) and at specification test temperature *as necessary*

The complex modulus and phase angle (G*, δ), and stiffness (S(t,T)) are measured at various temperatures related to the environment most commonly found at the field construction site. Maximum and minimum asphalt pavement temperatures are indicated in the upper part of the binder specification (Figure B-1). The asphalt binder specification uses the designation PG x y , where PG stands for Performance Graded, x designates the high pavement design temperature, and y designates the low pavement design temperature.

Hence, an asphalt PG 64-28 would meet the specification for an average high 7-day pavement temperature of less than 148°F (64°C), and a one-time low pavement temperature greater than -21°F (-28°C). While it is obvious that the PG 64-28 is going to

meet all the requirements for all high temperatures less than 148°F (64°C), that is not the case for the low temperatures, since the requirements for fatigue resistance at intermediate temperatures are stricter in the next lower high temperature grade. Thus, the binder that meets PG 64-28 grade will not meet PG 58-28.

The maximum pavement temperature is obtained from maximum air temperature and some other factors (Ref 32). The maximum air temperature for each year is selected as the highest average value of maximum temperatures for 7 consecutive days. The average of all the values obtained this way for a minimum of twenty years is used to determine the maximum pavement temperature. The design maximum temperature is selected at 0.8 inches (22 mm) depth of pavement.

The minimum surface pavement design temperature is defined as the minimum surface pavement temperature expected over the design life of the pavement and can be estimated from the SUPERPAVE program (Ref 23). There are also temperature contour maps of the United States and Canada that contain the average 7-day maximum pavement temperature and the minimum surface pavement design temperature values. For fatigue criteria, an intermediate pavement design temperature is used. It is selected as the approximate average of the maximum and minimum pavement design temperatures.

High-temperature viscosity measurements are conducted using the Brookfield Thermosel Apparatus described in ASTM D 4402 instead of the capillary tube viscometers used in current asphalt cement specifications. The purpose is two-fold: to ensure adequate viscosity at 275°F (135°C) for pumpability, and to provide viscosity measurements at high temperatures in order to depict the mixing and compaction viscosity-temperature profile for mixture design. Several reasons prompted the replacement of the capillary viscosity because of its inappropriate low shear rates, unknown shear rates, less accurate temperature control, more difficult cleaning, inability to test non-Newtonian binders, and lesser repeatability and reproducibility.

Tenderness during mixing and laydown because of the asphalt binder is taken into consideration in the SHRP specification by setting a minimum value of the parameter represented by the complex modulus (G^*) divided by the phase angle (δ), $G^*/\sin\delta$. In rheology this is termed the inverse of the loss compliance (1/J"). This parameter is also used as the specification criterion for rutting because of the good correlation found between the $G^*/\sin\delta$ values and asphalt mixture permanent deformations (Ref 24). The measurement of G^* and delta for the rutting resistance specification is performed on the asphalt binder after it has been conditioned with the RTFOT. This represents the potential for rutting that can occur early in the service life of the pavement. This parameter is measured at the high temperatures representative of high in-service temperatures, and at 10 rad/sec., which is representative of the loading time of a passing truck traveling at 50 mph (80 km/h).

Load-associated fatigue cracking is considered in the specification by limiting the value of the loss modulus ($G^*.\sin\delta$) measured at intermediate temperatures and at 10 rad/sec. (1.59 Hz) on the asphalt residue after the long-term aging test (PAV). The value of the loss modulus was found to be directly related to the continuous dissipation of energy that takes place in the asphalt binder under repeated cyclic loading (Ref 25). The energy dissipation is the result of viscoelastic and plastic flow mechanisms. In the energy dissipation criterion for fatigue developed by SHRP, it was hypothesized that

failure under cyclic loading occurs when the energy absorbed in each cycle in excess of a certain non-damaging amount accumulates to a critical value. For specification purposes, the value of $G^*.\sin\delta$ is limited to a maximum value of 720 psi (5 MPa) measured at 10 rad/sec. and at the anticipated pavement design temperatures.

Thermal shrinkage cracking occurs when rapid temperature drops cause the development of thermal stresses which exceed the tensile strength of the pavement. The concept of limiting stiffness, and of limiting stiffness temperature, was developed in Canada (Ref 26). According to this concept, thermal cracking will develop when the binder reaches a critical stiffness value at a certain loading time and a critical temperature. At temperatures below the critical one, the pavement will experience thermal cracking. This criterion assumes that cracking can be developed after a single temperature drop below the limiting stiffness temperature. In the SHRP binder specification, the limiting stiffness value was chosen as 43,000 psi (300 MPa) measured at 60 seconds at a temperature 50°F (10°C) higher than the anticipated minimum pavement temperature. The limiting stiffness concept as developed by Readshaw (Ref 26) states that the binder will develop cracking when the stiffness overcomes the limit of 29,000 psi (200 MPa) measured at the minimum pavement temperature and at 2 hours loading time. Because of the common temperature dependency of the binders at very low temperatures, the stiffness at T min. after 2 hours loading time is practically equal to the stiffness at T min. + 50°F (10°C) at 60 seconds, which obviously saves a great deal of time in the testing phase. The importance of time dependency in studying the development of thermal cracking is also addressed in the SHRP binder specification by setting a minimum value of the slope of the creep curve.

The aging or hardening of asphalt binders occurs during the mixing and laydown process and during service. The laboratory tests that determine quantitatively the resistance of binders to hardening during the production process are the rolling thin-film oven test (RTFOT, ASTM D 2872) and the thin-film oven test (TFOT, ASTM D 1754). The RTFOT is a part of the SHRP Asphalt Binder Specification. The loss on heating test is suitable for ranking asphalt binders according to their tendency to harden and indicates whether a material has been contaminated with light oils.

To simulate long-term aging in the field, the pressure aging test was adopted by SHRP. Standard thin-film oven test pans containing the residue from the RTFOT are placed in a pressure vessel at an air pressure of 300 psi (2.1 MPa) and age for 20 hours at temperatures for that asphalt grade. This test simulates field aging during the first five to ten years.

In summary, the new SHRP asphalt binder specification is performance-related. Fundamental binder rheological properties are included that can be related to fundamental mixture properties and, therefore, to pavement performance. The specification also provides adequate high- and low-temperature measurements that take into account the non-Newtonian behavior of modified asphalts and some unmodified asphalts. In addition, short-term aging is considered with the RTFOT, and long-term in-service aging is given by the PAV.

Testing Procedures

The rheological characterization of the retained samples of the original modified and unmodified binders tested was accomplished by conducting the following tests in

accordance with the SHRP Asphalt Binder Specification, SHRP test protocols, and ASTM and AASHTO standards:

SHRP B-007	
ASTM D 4402	Viscosity Determinations of Unfilled Asphalts Using the Brookfield Thermosel Apparatus
SHRP B-003	
AASHTO TP5	Determining Rheological Properties of Asphalt Binder Using a Dynamic Shear Rheometer (DSR)
ASTM D 2872	Test Method for Effect of Heat and Air on Rolling Film of Asphalt (Rolling Thin Film Oven Test)
SHRP B-005	
AASHTO PP1	Accelerated Aging of Asphalt Binder Using a Pressurized Aging Vessel (PAV)
SHRP B-002	
AASHTO TP1	Determining the Flexural Creep Stiffness of Asphalt Binder Using the Bending Beam Rheometer (BBR)
SHRP P-1001	
AASHTO MP1	Standard Specification for Performance Graded Asphalt Binder
SHRP P-1002	
AASHTO PP6	Standard Practice for Grading or Verifying the Performance Grade of an Asphalt Binder

The consistency of the unaged binders was measured at 275°F (135°C), which is the test temperature at which all the binders must have a viscosity that ensures pumpability during storage. The parameters relating the fundamental asphalt binder properties to field performance were analyzed. The tests were performed on the available retained asphalts in accordance with the SHRP protocol and the results are given in Appendix B. These procedures, as they relate to this study, are discussed in Appendix B.

Discussion of Test Results

An analysis of the results of testing the original samples is discussed by District.

The results of two replicate viscosity measurements for asphalts are shown in Tables B-1, B-6, B-11, B-16, and B-21 (Appendix B). As can be seen, all of the asphalts are far below the maximum viscosity limit of 30 Poise (3 Pa.s) stipulated by SHRP.

District 10

Tables B-2 through B-4 provide the average of three-replicate linear-viscoelastic parameter measurements of the control and modified binders for District 10 at the temperatures at which each binder meets the specification limits. To better illustrate the differences among the binders properties, a bar-plot of the loss modulus, storage modulus, and tan delta for tank and aged conditions is presented in Figures B-3, B-4, and B-5. Furthermore, a 2D bar-plot of the rutting resistance factor ($G^*/\sin\delta$) and the fatigue resistance factor ($G^* \sin\delta$) is shown in Figures B-6, B-7, and B-8.

The bar-plots reveal several characteristic features. When the control binder is compared with the modified ones in District 10, the first distinctive point that emerges is that two of the modified binders pass the specification limits for high temperature at 136°F (58°C), while the rest do this at 148°F (64°C). One can assume that the binders Control (Total), SBR_g (Goodyear), and SBS_e (Elf) will have better high-temperature properties (rutting resistance) than binders EVA_e (Exxon) and SBS_s (Shell).

An interesting feature common to all the binders is that tan delta (tanδ), the ratio of the loss modulus G" to the storage modulus G', is much lower in the modified binders than in the control binder for both tank and RTFOT conditions in the high-temperature region. At intermediate temperatures and after the long-term aging process (PAV), tan∂ for the modified binders is larger than for the control ones. It can be noticed that the ratio between tanδ of the modified asphalt and tanδ of the control asphalt, at intermediate temperatures and after the PAV, is much lower than for tank and RTFOT conditions at higher temperatures.

Another general trend is observed in that the storage modulus ($G' = G^* \cos\delta$), which grows with aging, does so in a lesser amount after the RTFOT (high temperatures) than after the PAV (intermediate temperatures). The loss modulus also experiences an increase after the aging tests. At intermediate temperatures and after the PAV, the difference between G' and G" is smaller than at high temperatures. In only one case (control asphalt), G' exceeds G" after the PAV test. This binder has the lowest tanδ. Tanδ conveys no physical magnitude, but is a measure of the ratio of energy lost to energy stored in a cyclic deformation. High tanδ values mean high heat dissipation and low elastic component; conversely, low tanδ values occur with increasing storage modulus values. It is of interest that tanδ passes through a minimum at high temperatures and/or low frequencies where a strong elastic network in the binder would be highly desirable for rutting resistance purposes. By the same token, at intermediate temperatures, to avoid fatigue cracking, lower tanδ value means lower energy dissipation, which is the parameter linked to fatigue resistance. It is important to note that the value of tanδ by itself is not sufficient to evaluate the performance of a binder with respect to rutting or fatigue resistance. Thus, two different binders can have the same tanδ value, but one of them may have a higher value of G', which implies comparatively more storage energy, and, therefore, more capacity of recoverable deformation. An adequate balance between the loss modulus and the storage modulus is very important in order to obtain good fatigue resistance properties in the binder.

The SHRP Asphalt Research Program chose $G^*/\sin\delta$ and $G^*\sin\delta$ as parameters to evaluate asphalt binder rutting resistance and fatigue resistance, respectively. These parameters take into consideration at the same time both the complex shear modulus and the phase angle.

Rutting Resistance

Complex shear modulus and phase angle were measured at 136°F (58°C) and 10 rad/sec. for binders EVA_e (Exxon) and SBS_s (Shell), and at 148°F (64°C) and 10 rad/sec. for binders Control (Total), SBR_g (Goodyear) and SBS_e (Elf). As stated earlier, these are the temperatures at which the binders comply with the limits established in the SHRP binder specification. The results of the tests are shown in Tables B-2 and B-3. Figures B-3

through B-5 illustrate the LVE parameters in 2D bar-plots, while Figures B-6 and B-7 illustrate the rutting factor G*/sinδ in 2D bar-plots.

All the asphalt binders must have a minimum value of G*/sinδ before and after the RTFOT. However, binders within the same grade can have different G*/sinδ values above the minimum value. For instance, binder SBS_e (Elf) could be ranked as the best performance grade for rutting resistance among the District 10 binders, since it has the highest G*/sinδ at 148°F (64°C) after the RTFOT. It also has the highest storage modulus and the lowest phase angle.

Between the two binders tested at 136°F (58°C), asphalt SBS_s (Shell) should perform better than asphalt EVA_e (Exxon) for rutting resistance, given its higher G*/sinδ value after the RTFOT. It can be noticed that storage modulus for asphalt SBS_s is almost double than for asphalt EVA_e. The following is the ranking of District 10 binders for resistance to permanent deformation based on the value of G*/sinδ and the test temperature:

(1) SBS_e (Elf)
(2) Control (Total)
(3) SBR_g (Goodyear)
(4) SBS_s (Shell)
(5) EVA_e (Exxon)

The higher the temperature at which the binder attains the limit value of G*/sinδ, the better the resistance to permanent deformation. The higher the value of G*/sinδ measure at a given temperature, the higher the rutting resistance.

Fatigue Resistance

The energy dissipated or lost as heat per cycle of sinusoidal deformation is directly related to the out-of-phase component of the shear complex modulus or loss modulus G*sinδ, which constitutes an indirect measurement of fatigue resistance of the binder. Figure B-8 compares the values of this parameter for the binders tested. Observation of these 2D bar-charts reveals a reduction in the energy loss of the modified asphalts compared to the base asphalt after the PAV, with the exception of asphalt SBR_g (Goodyear).

G*sinδ was measured at 72°F (22°C) for asphalts Control (Total), SBR_g (Goodyear), and SBS_e (Elf); at 66°F (19°C) for asphalt SBS_s (Shell); and at 61°F (16°C) for asphalt EVA_e (Exxon). These are the limiting temperatures for these binders for the fatigue criteria in the SHRP specification. The EVA binder showed the lowest value of G*sinδ and at the lowest temperature, which makes it the best-ranked asphalt insofar as fatigue resistance is concerned. As previously stated, this asphalt EVA_e has the lowest G" among all of the binders, and the lowest tan delta (tanδ) among the modified binders. The ranking of the asphalt binders for District 10 for fatigue resistance based on the value of G*sinδ and the test temperature is as follows:

(1) EVA_e (Exxon)
(2) SBS_s (Shell)
(3) SBS_e (Elf)
(4) SBR_g (Goodyear) and Control (Total)

The lower the temperature at which the asphalt meets the limiting G*sinδ, the better the load-related fatigue cracking resistance. The lower the value of G*sinδ at a

given temperature, the lower the possibilities that the binder undergoes fatigue cracking.

Low-Temperature Cracking Resistance

Table B-5 provides the test results from the Bending Beam Rheometer for District 10 asphalt binders. Asphalts Control, SBR_g, and SBS_e (Elf) met the specification at 10°F (-12°C), while asphalts EVA_e and SBS_s (Shell) met the limiting values at 0° to -1°F (-18°C). However, and despite the former three asphalts meeting the specification limit values at the same temperature, their stiffness and m-values are slightly different. The same thing happens with asphalts EVA_e and SBS_s (Shell). The following is a ranking of these binders according to the lowest temperature at which they reach the limiting stiffness value, and according to the lowest stiffness within the same temperature:

(1) EVA_e (Exxon)
(2) SBS_s (Shell)
(3) Control (Total)
(4) SBR_g (Goodyear)
(5) SBS_e (Elf)

Asphalt EVA_e (Exxon) has a lower stiffness value at 0° to -1°F (-18°C) than asphalt SBS_s (Shell), although they are close. Control asphalt has the lowest stiffness value among the binders tested at 10°F (-12°C). It is interesting to note that asphalt SBS_e (Elf) has the highest stiffness among the binders tested at -10°F (-12°C), but also has the highest m-value. If the ranking were done based on the m-value, asphalt SBS_e (Elf) should be placed in the third position.

District 11

Three binders, Control (Texaco), SBR_g (Goodyear) and SBS_e (Elf) were evaluated with the SHRP asphalt binder tests for District 11 (Table B-6). Tables B-7, B-8, and B-9 present the linear-viscoelastic properties of the binders measured at 148°F (64°C) and 158°F (70°C) by means of the DSR under different sample conditionings (tank, RTFOT, and PAV). In this case it can be seen from the table that both asphalts Control (Texaco) and SBR_g (Goodyear) satisfy the minimum required criteria for $G^*/\sin\delta$ at 148°F (64°C), while asphalt SBS_e (Elf) meets the minimum criteria at 158°F (70°C), one grade higher than the other two.

Figures B-8, B-9, and B-10 illustrate the differences in the values of G", G', and tan delta for the binders studied. At 148°F (64°C) the binder modified with SBR_g (latex) shows lower shear complex modulus than the Control (Texaco) binder. It has a higher tan delta and a lower storage modulus than the neat asphalt at high temperatures. Asphalt SBS_e (Elf) met the minimum value for $G^*/\sin\delta$ at a higher temperature than Control (Texaco) and SBR_g (Goodyear) asphalts; therefore it should have higher rutting resistance than the latter binders.

Rutting Resistance

According to the results observed in Tables B-7 and B-8 and in Figures B-10 and B-11, and based on both the test temperatures and values of G*/sinδ, the asphalts for District 11 can be ranked for rutting resistance as follows:

(1) SBS_e (Elf)
(2) Control (Texaco)
(3) SBR_g (Goodyear)

Asphalt SBS_e (Elf) attained the limiting value of G*/sinδ at the highest temperature. Asphalts Control (Texaco) and SBR_g (Goodyear) met the specification limit value at lower test temperature than asphalt SBS_e (Elf). Asphalt Control (Texaco) had a higher value of G*/sinδ than asphalt SBR_g (Goodyear) (Figure B-13).

Fatigue Resistance

From examination of the 3D bar-plots in Figure B-14, it is evident that asphalts Control (Texaco) and SBR_g (Goodyear) have better intermediate-temperature properties than asphalt SBS_e (Elf) for District 11. Asphalt SBR_g has lower G*sinδ than asphalt Control. It also has lower G" and tan delta, and its storage modulus is higher than that of asphalt Control. These asphalts can be ranked for fatigue resistance, based on both the test temperature and the G*sinδ value, as follows:

(1) SBR_g (Goodyear)
(2) Control (Texaco)
(3) SBS_e (Elf)

As can be noticed, asphalt SBR_g has the highest ranking for fatigue resistance but the lowest for rutting resistance. The reverse is true of asphalt SBS_e, which has the best permanent deformation resistance but the lowest fatigue cracking resistance. Nonetheless, while both asphalts can be classified for the same low-temperature grade (-8°F [-22°C]), asphalt SBS_e meets the high-temperature requirements at one grade higher (158°F [70°C]) than asphalt SBR_g (148°F [64°C]).

Low-Temperature Cracking Resistance

Table B-10 shows the flexural creep stiffness and m-values at 60 seconds as measured by the Bending Beam Rheometer at the test temperatures indicated. According to the results obtained the District 11, binders can be ranked as follows:

(1) Control (Texaco)
(2) SBS_e (Elf)
(3) SBR_g (Goodyear)

Asphalt Control (Texaco) attained the limiting stiffness value at the lowest temperature (0° to -1°F [-18°C]) at 60 seconds. Asphalt SBS_e (Elf) reached the lowest stiffness between the binders tested at 10°F (-12°C) and 60 seconds.

District 15

Asphalts modified with two different latexes—(1) ethylene-vinyl-acetate and (2) a blend of latex with polyolefin—were tested, along with a control asphalt, in District 15. A summary of the testing of asphalt binders is given in Table B-11. Table B-12 provides the linear-viscoelastic function values of the binders in their tank condition (unaged) obtained from DSR at three temperatures: 136°F (58°C) for asphalt SBR_g (Goodyear),

148°F (64°C) for asphalts Control (TFA) and SBR_p (Polysar), and 158°F (70°C) for asphalts EVA_e (Exxon) and SBR/Pd (Dow). Figures B-15 through B-27 show the bar-plots in the tank, RTFOT, and PAV conditions of the viscoelastic functions for the binders tested. Asphalts EVA_e (Exxon) and SBR/Pd (Dow) showed the highest performance grade at high temperatures. Asphalt SBR/Pd (Dow) has the highest storage modulus, while asphalt EVA_e (Exxon) has the lowest tan delta. All the modified binders, except binder SBR_g (Goodyear), have higher G' and lower tan delta values than the control binder, both before and after the RTFOT. After the RTFOT, all the binders, modified and unmodified, have experienced an increase in G' and a decrease in tan delta values.

Rutting Resistance

From the 2D bar-charts, based on the results obtained from the DSR in terms of $G^*/\sin\delta$, the binders for District 15 can be ranked for rutting resistance as follows:

(1) SBR/Pd (Dow)
(2) EVA_e (Exxon)
(3) Control (TFA)
(4) SBR_p (Polysar)
(5) SBR_g (Goodyear)

Asphalt SBR/Pd (Dow) has the highest $G^*/\sin\delta$ value at 158°F (70°C) and 10 rad/sec., whereas asphalt SBR_g (Goodyear) possesses the lowest value of this parameter, measured at 136°F (58°C) and 10 rad/sec. (Figures B-18 and B-19).

Fatigue Resistance

The fatigue performance of binders pertaining to District 15, based on the values of $G^*\sin\delta$ and the temperatures at which the binders attain the maximum value permitted for this parameter in the SHRP binder specification, is as follows:

(1) SBR_g (Goodyear)
(2) SBR_p (Polysar)
(3) EVA_e (Exxon)
(4.) SBR/Pd (Dow)
(5) Control (TFA)

The lowest value of $G^*\sin\delta$ was attained at 66°F (19°C) and 10 rad/sec. for asphalt SBR_g (Goodyear), while asphalt Control (TFA) reached the limiting $G^*\sin\delta$ value at 77°F (25°C) and 10 rad/sec. (Figure B-20).

Low-Temperature Cracking Resistance

In this district the limiting temperatures are 21°F and 10°F (-6°C and -12°C), as can be seen in Table B-15. The stiffnesses of asphalts Control (TFA), EVA_e (Exxon), and SBR/Pd (Dow) are far below than the limiting value of 43,000 psi (300 MPa). This is due to the fact that the m-values of these binders were lower than 0.30 at temperatures lower than 21°F (-6°C). Therefore, because of the minimum m-value, and not for the

maximum stiffness, these binders had to be tested at 21°F (-6°C). The ranking of binders in District 15 is as follows:

(1) SBR_p (Polysar)
(2) SBR_g (Goodyear)
(3) EVA_e (Exxon)
(4) SBR/Pd (Dow)
(5) Control (TFA)

If the m-value is to be a first consideration in the ranking, then Control (TFA) asphalt should occupy the third position, followed by asphalts EVA_e and SBR/Pd.

District 25

In this District the following asphalt binders were tested: Control (Shamrock), SBS_e (Elf), and two asphalts containing SBS_s (Shell) polymer at two levels—3% and 6% (Table B-16). Tables B-17 through B-20 and Figures B-21 through B-23 show the test data and graphs, respectively, for the above binders. In the tank condition, asphalt SBS_s 6% (Shell) attained the minimum value of $G^*/\sin\delta$ at one grade higher (158°F [70°C]) than the other three binders (148°F [64°C]). After the RTFOT, all the binders meet the specification limit at the same temperature, 148°F (64°°C). Asphalt SBS_s 6% (Shell) displays the highest $G^*/\sin\delta$, followed by SBS_e (Elf), SBS_s 3% (Shell), and Control (Shamrock). The control asphalt has the highest tan delta value and the lowest storage modulus at 148°F (64°C) and 10 rad/sec. in both conditions, before and after the RTFOT. Under these conditions it is reasonable to expect lower rutting resistance in this binder when it is compared to the modified binders. The lowest tan delta and the highest G' were exhibited by binder SBS_s 6% (Shell), as expected.

At intermediate temperatures and 10 rad/sec., asphalt SBS_s 6% (Shell) attained the limit value for $G^*\sin\delta$ at 61°F (16°C), which is the lowest test temperature among the binders tested. This is very important, since this parameter controls the low starting point temperature for creep stiffness, and generally means better low-temperature properties for the binder.

Rutting Resistance

Based on the dynamic shear results at high temperature obtained for asphalts from District 25, asphalt SBS_s 6% (Shell) should perform better than the rest of the binders from a rutting resistance standpoint. The following is the ranking of the binders for rutting resistance (Figure B-25):

(1) SBS_s 6% (Shell)
(2) SBS_e (Elf)
(3) SBS_s 3% (Shell)
(4) Control (Shamrock)

All the binders meet the SHRP asphalt binder specification at the same temperature (148°F [64°C]) in the high temperature region. Asphalt SBS_s 6% (Shell) has the highest $G^*/\sin\delta$ value at 148°F (64°C) and 10 rad/sec.

Fatigue Resistance

In the control of load-related fatigue cracking, the recommended specification criterion is based on the dissipated energy, which is related to $G^*.\sin\delta$ (loss modulus) in a dynamic shear test. Since fatigue occurs at low to intermediate temperatures and after

the pavement has been in service for a certain period of time, the fatigue resistance factor is calculated based on the results from a dynamic shear test after the binder has been subjected to the RTFOT and PAV aging tests. According to the data collected from the pertinent tests, the binders can be ranked as follows (Figure B-26):

(1) SBS_s 6% (Shell)
(2) Control (Shamrock)
(3) SBS_s 3% (Shell)
(4) SBS_e (Elf)

The lowest temperature at which the binders reached a G*sinδ of less than 720 psi (5 MPa) was 61°F (16°C), and corresponded to asphalt SBS_s 6% (Shell). The lowest value of G*sinδ measured was 467 psi (3.23 MPa) for asphalt SBS_s 3% (Shell) at 72°F (22°C) and 10 rad/sec.

Low-Temperature Cracking Resistance

Asphalts Control (Shamrock), SBS_e (Elf), and SBS_s 3% (Shell) were tested at 10°F (-12°C), while asphalt SBS_s 6% (Shell) was tested at 0° to -1°F (-18°C) (Table B-20). The ranking based on temperature and stiffness is as follows:

(1) SBS_s 6% (Shell)
(2) Control (Shamrock)
(3) SBS_e (Elf)
(4) SBS_s 3% (Shell)

The lowest test temperature corresponded to asphalt SBS_s 6% (Shell); the other three binders were tested at 10°F (-12°C), and at 60 seconds their stiffness value was reported.

District 17

The binders tested in this district were used in seal coats designed to evaluate the effectiveness of polymers for high traffic volume, aggregate retention, bleeding resistance, etc., in seal coats. Of particular interest are the high- and low-temperature properties of these binders; therefore the SHRP test was also performed. The asphalts used in this district were identified as follows: Control (Fina), SBR_g (Goodyear), SBS_s (Shell), and SBS_e (Elf). The polymer content was 3% for the SBS asphalts and 2% for the SBR asphalt binder.

Tables B-21 through B-24 provide information on the test data collected from the dynamic shear test carried out at the temperature (136°F [58°C]) at which all the binders show a G*/sinδ value higher than 0.15 psi (1 kPa) (tank condition) and higher than 0.32 psi (2.2 kPa) (RTFOT condition), and at 10 rad/sec. Figures B-27 through B-29 illustrate the viscoelastic functions of the binders tested. It can be noticed that there is a huge difference in the tan delta values between the modified binders and the control binder. This stems from the very low value of G' for asphalt Control (Fina) when compared to the other three binders. Asphalt SBS_e (Elf) presents the highest storage and loss modulus and the lowest tan delta after the RTFOT. The binder modified with 2% latex shows about one-half the value of tan delta when compared to the control asphalt, while the binders modified with either SBS display a tan delta value around seven times lower than that of the control asphalt.

According to the SHRP specification, the maximum allowable value of G*.sinδ is 720 psi (5 MPa) in order to satisfy fatigue criteria at the test temperature. At intermediate temperatures, the lowest temperature at which the binders attain a value of G*sinδ lower than 720 psi (5 MPa) was 61°F (16°C); this corresponded to asphalt SBS_s (Shell), as can be seen in Figure B-31. Asphalts SBR_p (Polysar) and SBS_e (Elf) have a G*sinδ limiting value at 66°F (19°C), whereas asphalt Control (Fina) attains this value at 72°F (22°C).

Rutting Resistance

The ranking of the District 17 asphalts, according to their rutting resistance (Figures B-30 and B-31) based on the SHRP binder specification, is as follows:

(1) SBS_e (Elf)
(2) SBS_s (Shell)
(3) Control (Fina)
(4) SBR_g (Goodyear)

All the binders attained the limiting G*/sinδ value at 136°F (58°C) and 10 rad/sec. Asphalt SBS_e (Elf) has the highest G*/sinδ at that temperature and those loading conditions.

Fatigue Resistance

The load-associated fatigue cracking resistance as measured by the fatigue factor G*sinδ (Figure B-32) of the District 17 binders is as follows:

(1) SBS_s (Shell)
(2) SBS_e (Elf)
(3) SBR_g (Goodyear)
(4) Control (Fina)

Asphalt SBS_s (Shell) met the SHRP Asphalt Binder Specification at 61°F (16°C) and 10 rad/sec., the lowest temperature for the binders tested. The Control asphalt reached the limiting G*sinδ at 72°F (22°C) and 10 rad/sec., while asphalts SBS_e (Elf) and SBR_g (Goodyear) did not surpass G*sinδ = xx psi (G*sinδ = 5 MPa) at 66°F (19°C) and 10 rad/sec.

Low-Temperature Cracking Resistance

Table B-25 shows the values of the creep stiffness and the slope of the logarithm of the stiffness versus the logarithm of the time curve as measured by BBR. These binders show the highest m-values of all the binders tested in this study. Based on test temperature and stiffness values, the binders can be ranked as follows:

(1) SBS_s (Shell)
(2) SBS_e (Elf)
(3) SBR_g (Goodyear)
(4) Control (Fina)

SHRP ASPHALT BINDER SPECIFICATION: BINDERS CLASSIFICATION

The testing carried out according to the SHRP Asphalt Binder Test Protocols permits the classification of the control and modified binders of each district as follows:

District 10		
	Control (Total)	PG 64-22
	SBR_g (Goodyear)	PG 64-22
	SBS_e (Elf)	PG 64-22
	EVA_e (Exxon)	PG 58-28
	SBS_s (Shell)	PG 58-28
District 11		
	Control (Texaco)	PG 64-28
	SBR_g (Goodyear)	PG 64-22
	SBS_e (Elf)	PG 70-22
District 15		
	Control (TFA)	PG 64-16
	SBR_g (Goodyear)	PG 58-22
	SBR_p (Polysar)	PG 64-22
	EVA_e (Exxon)	PG 70-16
	SBR/Pd (Dow)	PG 70-16
District 25		
	Control (Shamrock)	PG 64-22
	SBS_e (Elf)	PG 64-22
	SBS_s (Shell) 3%	PG 64-22
	SBS_s (Shell) 6%	PG 64-28
District 17		
	Control (Fina)	PG 58-22
	SBR_g (Goodyear)	PG 58-22
	SBS_s (Shell)	PG 58-28
	SBS_e (Elf)	PG 58-28

The asphalts EVA_e (Exxon) and SBS_s (Shell) in District 10 have better low-temperature properties than asphalts Control (Total), SBR_g (Goodyear), and SBS_e (Elf). However, the latter asphalt binders are one grade higher in the high temperature range than the former.

Summary of Findings

Performance Grade Asphalts and Actual Pavement Performance

The performance of the different test sections placed in four of the TxDOT districts has been monitored periodically in order to evaluate and compare the control sections with the sections containing modified asphalts. A surface condition survey by field inspection of the test sections was carried out in July 1993 in order to determine whether any deterioration has occurred, and what level of severity is present. On the other hand, the classification testing of the asphalt binders done in accordance with SHRP Asphalt Binder Specification (AASHTO MP1), along with the traffic and environmental conditions of each site, allowed the comparison between the structural

conditions shown by the test sections with what is predicted by the SHRP tests in terms of rutting, load-associated fatigue cracking, and low-temperature cracking resistance.

Table B-26 shows the average 7-day maximum pavement design temperature, and the minimum pavement design temperature, for the five districts studied. These values were calculated from the climatic database from the weather stations closest to each site considered. The maximum design pavement temperature is estimated based on the maximum air temperature and the latitude of the site, while the minimum design pavement temperature is assumed to be equal to the minimum air temperature (Ref 32). The maximum pavement temperature has been calculated for the 0.8-inch (20-mm) depth. In calculating both minimum and maximum pavement temperatures, twice the standard deviation has been added to the average value. This way a 98 percent reliability is obtained.

According to the maximum and minimum pavement design temperatures, the binders to be selected for the different districts fall in the performance grades PG 64-16, PG 64-22, and PG 64-28.

Next is an analysis of the performance of each binder in each district as surveyed in July 1993. The performance grade of the binders used in the construction of each test section was determined following the SHRP binder test protocols and the Standard Specification for Performance-Graded Asphalt Binder (AASHTO PP6). Table B-27 shows a summary of the asphalt binder grading by the SHRP guidelines and the field observations for each district.

Tyler District 10, Smith County, US 69

The test pavement sections were constructed in July 1990. Construction involved pavement overlay of two lanes of the original highway. The approximate test section dimensions were: 2 inches thick, 24 feet wide, and 1,000 feet long (5.1 cm thick, 7.4 m wide, and 304.8 m long). A total of five test sections were constructed by District 10 of TxDOT, assisted by the Center for Transportation Research, The University of Texas at Austin. The average daily traffic (ADT) was estimated at 15,500 vehicles for the test section.

The final visual inspection was made at the time the pavements were three years old. Each section present condition is discussed as follows:

SBS_s (Shell) Test Section: Generally in good condition, no visible cracks, slight rutting in wheel path. The original asphalt has been classified as a PG 58-28. According to climatic data the binder should meet PG 64-22 if maximum pavement design temperature is taken at a depth of 0.8 inches (20 mm), with 98 percent reliability. This means that this asphalt does not meet the high temperature range if the 0.8-inch (20-mm) maximum pavement design temperature is adopted. This binder should not undergo either load-related fatigue cracking or low-temperature cracking, but may rut if the maximum pavement temperature at the 0.8-inch (20-mm) depth is considered critical. This might explain the slight rutting observed in the wheel path.

SBS_e (Elf) Test Section: No cracking or rutting was visible at the time of inspection, only polishing of surface aggregate. This asphalt should meet PG 64-22 according to the maximum and minimum pavement temperatures estimated from the weather data. Data from the SHRP asphalt binder tests

permitted the classification of this binder as PG 64-22. This literally means that no major distresses are expected in the pavement as a consequence of the asphalt used under the climatic conditions considered. The pavement performance of this test section confirms the performance expected so far, and from the binder standpoint.

EVA_e (Exxon) Test Section: No cracking was visible; a very slight rutting in the outside wheel path is shown. The original asphalt classifies as PG 58-28, which is in agreement with the symptoms observed: no cracking, slight rutting.

Control (Total) Test Section: The same conditions were found as for EVA_e. However, this binder classifies as PG 64-22, and, therefore, no rutting should be experienced in the asphalt mixture as a contribution from the binder.

SBR_g (Goodyear) Test Section: There is no cracking reported in this section. Unlike the cases of the last two sections described, there is no rutting observed in this test section. The asphalt was classified as PG 64-22, and this agrees with the performance grade expected.

Lufkin District 11, Polk County, US 59

Three test pavements were constructed on US 190 in April 1989. A pavement overlay was placed in four lanes of the highway. The thickness varied from approximately 1 to 1-1/2 inches (2.54 to 3.81 cm). Two polymer-modified binders and one unmodified binder were used in the asphalt mixtures placed in the test sections.

SBS_e (Elf) Test Section: There are four test sections with this modifier, one for each southbound lane and one for each northbound lane. The samples were obtained from the southbound outside lane. Visual inspection of all the sections indicated approximately the same type and level of distress. Medium-severity-level longitudinal and horizontal fatigue cracking has been reported. The cracks were not wide, and there was no apparent movement at this point. Some slight degree of surface spalling was also noted. The performance grade according to the weather data should be PG 64-16 if the maximum pavement design temperature is taken at a 0.8-inch (20-mm) depth, with 98 percent reliability. This asphalt meets PG 70-22; therefore, no permanent deformation nor fatigue, nor low-temperature cracking are expected as a consequence of the binder selected.

SBR_g (Goodyear) Test Section: There were again four test sections placed similarly to the SBS_e (Elf) sections. The core samples were also taken from the southbound outside lane. The existing distress included horizontal cracking, breaking up of edges, and some longitudinal cracking. Even though the cracks were reasonably tight, the edges indicated that there was the possibility of some movement. The asphalt classifies as PG 64-22, which satisfies the criteria required by PG 64-16.

Control (Texaco) Test Section: The distress patterns existing in this section are medium-severity-level longitudinal and horizontal cracking, tighter than others on horizontal but predominantly more longitudinal cracking. The transverse cracks appeared to be tighter than those of the other sections, but the longitudinal cracks were a little more open. This binder meets PG 64-28; thus, no permanent deformation nor thermal or load-related cracking should be expected.

San Antonio District 15, Comal County, US 281

A total of seven test sections were constructed on US 281 in Comal County, Texas, in April 1987, and involved the pavement overlay of one lane of the highway. Each test section was approximately 1 to 1-1/2 inches thick, 12 feet wide, and 1,500 feet long (2.5 to 3.8 cm thick, 3.7 m wide, and 457 m long). The average daily traffic was estimated at 2,650 vehicles for the test pavement.

Six of the seven polymer asphalt modifiers were used in constructing these test sections. Not only were more sections placed for evaluation, but these are the oldest of all those placed in this study. The only modifier not available was the SBS_s (Shell) or Kraton D1101. All used asphalt from the same source, but two viscosity grades, AC-10 and AC-20, were required in order to meet the manufacturer's recommended mixing procedures for the modified sections and the unmodified control section.

The control section and the SBR/Pd (Dow) section used the TFA AC-20, and TFA AC-10 was the asphalt modified by SBR_g (Goodyear UP-70), SBS_e (Elf Styrelf-13), EVA_e (Exxon Polybilt 103), Crafco's Genstar C107, and SBR_p (Polysar NS-175).

Several of the sections exhibited severe distress and it is expected that corrective maintenance will need to be performed in the near future.

SBR_g (Goodyear) Test Section: This section had considerable longitudinal and transverse cracking that is proceeding into map or pattern cracking. There is minor rutting in the wheel path and some of the cracks show evidence of some pumping. The binder meets PG 58-22, and according to the weather data it should meet PG 64-16 if the maximum pavement design temperature is taken at a depth of 0.8 inches (20 mm).

Control (TFA) Test Section: High-severity-level longitudinal and horizontal cracking (block cracking or alligator cracking) and raveling at edges are the main distresses present at this time. The asphalt meets PG 64-16 according to the SHRP asphalt binder test data obtained.

EVA_e (Exxon) Test Section: This is another section displaying high-severity-level fatigue cracking plus both longitudinal and transverse open cracks. This asphalt meets PG 70-16, one grade higher in the high temperature region, but one grade lower in the low temperature region, which may explain the interconnecting cracks caused by fatigue failure of the asphalt concrete surface.

SBR_p (Polysar) Test Section: This section presents good surface condition. Some transverse cracks are visible, but many of these appear actually to have partially healed themselves. The binder meets SHRP PG 64-22 requirements.

SBR/Pd (Dow) Test Section: This section is another of those suffering severe distress. The section is badly cracked in both the longitudinal and transverse directions, developing pattern cracking which is already proceeding into alligator cracking in many locations. The edges of the cracks are raveling and indicating movement. The binder, like asphalt EVA_e, responds to a PG 70-16 in the SHRP Asphalt Binder Specification. This asphalt is one grade higher than the PG 64-16 performance grade based on the climatic data.

Childress District 25, Donley County, US 287

Two test sections, Control and SBR_g (Goodyear) binders, were placed on US 287 in Donley County, Texas, in September 1988. Three test sections, SBS_e (Elf) and SBS_s (Shell), the latter with both 3% and 6% polymer content, were placed in April 1989. Asphalt AC-10 furnished by Fina was used with the modifiers, while Shamrock AC-20 was the asphalt used for the control section. Each test section was approximately 1 to 1-1/2 inches thick (2.54 to 3.81 cm thick).

Control (Shamrock) Test Section: The only distress reported so far is the presence of small longitudinal cracks in outside wheel path. The binder classifies as PG 64-22; it should meet PG 64-28 in accordance with the design pavement temperatures estimated from the climatic data. Some low-temperature pavement failures may be expected if the temperature falls below -8°F (-22°C) during the pavement service life.

SBS_e (Elf) Test Section: The pavement surface appears to be in good condition, remaining rut- and crack-free as of July 1993. Only one 50-foot-long (15-meter-long) longitudinal crack between the wheel paths is reported. The single occurrence would indicate that this crack is unrelated to this study of the modifiers. This asphalt meets PG 64-22, which is one grade below the low temperature range estimated in accordance with the climatic data recorded in the last twenty years. This does not indicate that during the remaining service life of this section a sudden drop in the temperature below -8°F (-22°C) will not produce thermal cracking.

SBS_s 3% (Shell) Test Section: In general, this section is in good condition. This binder meets PG 64-22, and the same concepts concerning low-temperature behavior of the above-described binder apply.

SBS_s 6% (Shell) Test Section: This section is still in fairly good shape, although some alligator cracking is apparently beginning to form; nevertheless, there does not appear to be any additional longitudinal or transverse cracking noted throughout most of the section. The binder meets PG 64-28, which constitutes the only asphalt binder that agrees with the performance grade estimated from the climatic data in this area.

Asphalt Binder Durability Properties as Measured by Conventional Tests on Original, Laboratory-Aged, and Field-Aged Binders

The measurement of the changes in asphalt binders consistency with aging in terms of penetrations and capillary viscosities was carried out on unaged and aged samples. Penetration at 77°F (25°C), absolute viscosity at 140°F (60°C), and kinematic viscosity at 275°F (135°C) were performed on original samples of the asphalt binders, on samples aged in laboratory using the Rolling Thin-Film Oven Test (RTFOT, ASTM D 2872), and on recovered binders from samples cored from each test section after an in-service time that spans between 34 and 73 months depending upon the test section.

Penetration and viscosity tests present several shortcomings in estimating the change in the rheological properties that an asphalt undergoes during manufacture and in service (Ref 27). These tests were performed on the asphalt binders recovered from the field for comparison with the tests originally conducted in the initial project. When

Research Study 492 was conducted, there were no other tests available to measure the linear viscoelastic properties of the binders, such as the SHRP Asphalt Binder Tests (Dynamic Shear Rheometer, Bending Beam Rheometer, etc.), which were developed recently.

Asphalt binder properties are affected by the presence of oxygen, by ultra-violet radiation, and by changes in temperature. These external influences cause a hardening in the binder, which is manifested by a decrease in penetration and by increases in softening point, viscosity, stiffness, and shear complex modulus. The binder becomes stiffer under the influence of the environment through oxidation and loss of volatiles, i.e., oxidative and exudative hardening, and evaporative hardening. While it is valid to quantify the age hardening of the binders through a penetration test or a capillary viscosity test, it is not valid to compare the results between two different asphalts if one or both of them are shear-dependent under the test conditions. The shear rate is asphalt-specific and varies within the sample during the test period. By measuring penetrations and viscosities at different temperatures on original and aged binders, several consistency parameters have been used to evaluate asphalt hardening. Penetration Index (PI), Penetration-Viscosity-Number (PVN) and Viscosity-Temperature-Susceptibility (VTS) are among the most commonly used (Ref 28). Penetration tests are empirical in nature; their main shortcoming is that the stress fields within the test specimen cannot be defined. The strains developed during the test are very large (non-linear behavior), vary within the sample, and cannot be easily calculated. The Penetration Index is based on the measurement of penetrations at two temperatures, or by measuring penetration at one temperature along with the softening point. Time and temperature effects are confounded in this parameter since they cannot be separated. It was considered that this index was not appropriate to define the durability properties of the recovered binders, since no good correlation exists between this parameter and field performance (Ref 29).

The Coefficient of Viscosity constitutes a fundamental property when calculated through the use of capillary viscometer so long as Newtonian fluids are tested. Absolute and kinematic viscosities are conducted using capillary tubes at 140°F (60°C) and 275°F (135°C), respectively. Most unaged asphalt cements are Newtonian at 140°F (60°C), but are not Newtonian when they have been subjected to an aging process, when modified with polymers, or when exhibiting complex flow properties. Since this method is not appropriate for aged binders or for modified binders and because shear rates cannot be measured in the capillary viscometers, the use of this method is of no benefit. Susceptibility parameters that include this property are not reliable either to characterize asphalt properties or to measure the effect of oxidative hardening.

At high mixing temperatures, most asphalt cements exhibit a linear viscoelastic behavior permitting the measurement of the kinematic viscosity at 275°F (135°C) neglecting the shear rate, although some polymer-modified binders exhibit significant shear rate dependency when tested in capillary viscometers. The Penetration-Viscosity Number (PVN) is obtained through penetration and capillary viscosity measurements, and, therefore, does not adequately describe the effect of aging on the temperature dependency of the binder. The other temperature susceptibility parameter mentioned earlier was the VTS, based on viscosities at 140°F (60°C) and 275°F (135°C), and it could be a good indicator of this property if the binder behaves in a Newtonian manner within that temperature range. However, there were many controversial results encountered

using these parameters, and it was determined that it would not be possible to rely on them.

Temperature susceptibility parameters can be misleading when used to forecast the effect of aging. Asphalts are viscoelastic materials whose properties depend both on time of loading and on temperature. Without separating these two properties, the temperature-dependency parameter will vary at different loading times. Since the temperature susceptibility is, therefore, not constant, and aging is not necessarily the same at all temperature ranges, it was decided not to calculate PI, PVN, or VTS parameters from the penetration and viscosity values obtained on the final set of field samples.

Despite the errors induced in using the capillary measured viscosities when testing fluids that behave in a non-Newtonian manner, historically the test has been used in an attempt to measure the age hardening, either in the laboratory by the RTFOT or in service in the field. Therefore, the capillary viscosities were measured at two temperatures in order to compare the values obtained with those reported in the initial study, Research Project 492, and with the previous fundamental understanding of the values resulting from this test. Two viscosity ratios were calculated: Absolute Aging Index and Kinematic Aging Index. The first ratio is based upon the viscosity before and after aging measured at 140°F (60°C), and the second is similarly measured before and after aging at 275°F (135°C). Each of these ratios was calculated for the asphalt binders aged in the laboratory and in the field test pavements.

The results obtained at 140°F (60°C) in many cases are not comparable with others at that temperature or with the values at higher temperatures, since the binder does not behave as a pure viscous fluid but as a viscoelastic liquid. Consequently, not only viscosity is being measured but also delayed elasticity. As stated earlier, the viscosities so obtained are not able to separate temperature and time of loading effects.

The aging index based on capillary viscosity at 140°F (60°C) is higher than the corresponding ones based on kinematic viscosity at 275°F (135°C). It would appear that since the oxidation process is more pronounced at higher temperatures, the ratio between viscosities before and after aging in the binder measured at 140°F (60°C) should be lower than the ratio at 275°F (135°C). In reality this is not the case, because in vacuum capillary viscometry we are measuring viscosity plus delayed elastic effects at a much longer loading time (smaller shear rates) than at higher temperatures. In asphalt rheology it is known that the oxidative hardening produces an increase in the stiffness (or the shear complex modulus) of that asphalt (Ref 30). This, in turn, increases with temperature, with increasing loading time, and with decreasing frequency, or with a combination of these factors. Thus, the higher the temperature and/or the lower the frequency or the longer the loading time, the larger the gap between the modulus measured before and after the aging process.

Since it is not possible to measure the shear rate of the material flowing through the viscometer and since this flow rate is asphalt-specific at a given temperature, it is not correct to compare viscosities among asphalts that display different shear rates during the test at a given temperature.

Asphalt binder properties in terms of penetration and viscosity before and after laboratory and field aging are given in Appendix C. A discussion by field test pavement site of the test results follows.

District 10

The **penetration test** results on the binders for the District 10 (Tyler) test site are shown in Table C-1 (Appendix C). The penetration tests were conducted in accordance with the procedures set forth in ASTM D 5 at 77°F (25°C), 100 grams, and 5 seconds. The Laboratory Retained Penetration in percent was obtained by dividing the penetration obtained after the Rolling Thin-Film Oven Test (RTFOT, ASTM D 2872) by the penetration performed on the original binder. The Field Retained Penetration is a similar ratio between the penetration on the recovered binder after 34 months in-service time and the penetration on the original binder. The penetration value after the RTFOT simulates the drop in penetration due to hardening by both oxidation and evaporation observed during the manufacture of an asphalt concrete in an asphalt mixing plant.

The penetration values of the original binders fall within the range 74-112. Asphalt Control (Total) has the lowest penetration (74), while asphalt EVA_e (Exxon) has the highest one (112). After the RTFOT, the penetration values are about 40 percent lower. After 34 months in service, the lowest penetration measured was the asphalt modified with the polymer SBS_e (Elf) at 44, while the highest was the asphalt modified with EVA_e (Exxon) at 90.

The control asphalt was classified as an AC-20. The modified binders were the product of the blending of an AC-10 asphalt with a 3% polymer content. As a result of blending the AC-10 with the different polymers, the resultant product became an asphalt with an approximate grade of AC-20, with one exception: asphalt EVA_e (Exxon). This modified binder appears to remain an AC-10 after modification when measured by penetration and absolute viscosity values (Tables C-1 and C-2).

Comparing the field-retained penetration and the laboratory retained penetration values (Figure C-1), the recovered binders indicate the possible effect of the polymer additive used. The control asphalt (Total) retained 60 percent of its original penetration after laboratory RTFOT aging. After 34 months of field aging, this asphalt binder has retained the same percentage of penetration when compared to the value of the original material prior to aging. Asphalts SBR_g (Goodyear), SBS_e (Elf), and SBS_s (Shell) have shown a lower percentage of retained penetration value after 34 months in the road than after the RTFOT. Asphalt SBS_e (Elf) displayed the largest difference in retained penetration after field aging and after the RTFOT, while asphalt SBS_s (Shell) showed the smallest difference. Asphalt EVA_e (Exxon) aged considerably more after the RTFOT than after being in the road for 34 months, with a field retained penetration of 80 percent.

In comparing the laboratory rolling thin-film oven test (RTFOT) aging and field aging for 34 months, the control and modified binders do not show the same hardening pattern. Although all of the laboratory-aged asphalts varied by less than 10 percent, asphalts SBS_e (Elf) and EVA_e (Exxon) have the highest retained penetration value after the RTFOT, and asphalt EVA_e (Exxon) has a significantly higher retained penetration value after 34 months in the field.

In summary, penetration results show different behavioral patterns among the different asphalt systems tested. Laboratory aging indicated that asphalts SBS_e (Elf) and EVA_e (Exxon) were the least aging-susceptible, while asphalts Control and SBR_g (Goodyear) were the most prone to aging. Field performance indicates somewhat different results, since, after 34 months in service, although asphalt EVA_e (Exxon) has retained more penetration than in the laboratory and is the binder that seems the least

aged of all, asphalt SBS_e (Elf) appears to be the binder that has aged the most. These binders have exhibited no cracking and only a slight rutting in sections built with SBS_s (Shell) and EVA_e (Exxon), and are in generally good condition after a performance life of slightly less than three years.

Table C-2 shows test data on absolute viscosities measured by vacuum capillary viscometry (ASTM D 2171) on original, laboratory-aged, and field-aged binders from District 10. Figure C-2 depicts the differences between the laboratory absolute aging index and the field absolute aging index after 34 months in service. Asphalts Control, SBR_g (Goodyear), SBS_e (Elf), and EVA_e (Exxon) showed higher field absolute aging indexes than the laboratory absolute aging index, while asphalt SBS_s (Shell) showed higher laboratory absolute aging index than the field absolute aging index. Under normal circumstances, the aging index of a recovered binder is higher than that of the original binder aged with either the TFOT or the RTFOT. A possible explanation for the behavioral pattern encountered in asphalt SBS_s (Shell) could be polymer degradation or binder contamination during the manufacturing of the asphalt mixture.

Asphalt SBS_e (Elf) has the largest gap between both indexes, which is consistent with the results found in penetration tests. At the other extreme, asphalt SBS_s (Shell) has the narrowest gap between aging indexes.

In Figure C-3 the field retained penetration is plotted versus the absolute aging index. There is a weak trend, suggesting that the higher the retained penetration, the lower the aging index.

In Figure C-4 some incongruencies can be seen among the aging index values. Asphalts Control, EVA_e (Exxon), and SBS_s (Shell) indicate a lower aging index after 34 months in the field than after the RTFOT in the laboratory. Only two asphalts, SBR_g (Goodyear) and SBS_e (Elf), have a higher field kinematic aging index than their laboratory kinematic aging index. In this case, asphalt SBR_g (Goodyear) displays the largest aging index on the recovered binders, while asphalt SBS_s (Shell) exhibits the lowest. According to this index, asphalt EVA_e (Exxon) is the one that has aged the most in the laboratory, while asphalt SBR_g (Goodyear) has aged the most in the field.

These incongruencies among the different tests and binders may be the result of at least three main factors: the use of empirical tests (penetration); the use of fundamental tests (capillary viscosities), which are incapable of separating temperature and loading time effects; and the use of a single-point aging index which does not adequately characterize the changes in the rheological properties of the binders. In addition, there is the problem of whether the asphalt in the laboratory and the asphalt in the mixing plant are identical, and, if so, was the actual aging process adequately similar for both.

Figure C-5 compares the three indexes, field retained penetration, field absolute aging index, and field kinematic aging index. As can be gathered, there is no correlation; lack of agreement among them is due to the already-explained diverse factors such as single-point measurements, different loading times, non-Newtonian behavior, etc.

Figure C-6 shows the relationship between retained penetration of the recovered binders and their kinematic aging index. The trend is stronger than that shown in Figure C-5 for retained penetration versus absolute aging index, with the higher retained penetrations clearly indicating lower aging indexes.

The only sign of distress encountered in District 10, as of May 1993, was a slight rutting in the EVA_e (Exxon) and SBS_s (Shell) sections. These two binders have shown higher values of penetration and lower viscosities on the recovered samples than the rest of the binders. This may be the only linkage between pen and viscosity tests and field performance.

District 11

In this district, only three test sections were placed: Asphalt Control (Texaco AC-20), SBS_e (Elf), and SBR_g (Goodyear). These three asphalt binders were tested for penetration at 77°F (25°C). Test data are indicated in Table C-4. Figure C-7 shows the laboratory retained penetration versus field retained penetration. In this figure, as expected, the three recovered binders' retained penetration values are lower than the retained penetration values of the binders aged and measured in the laboratory. In addition, asphalt SBS_e (Elf) had the largest difference between both retained penetration values.

No significant differences were found between the test sites after 49 months in the field. Asphalt SBS_e (Elf) has apparently aged a little more than the other two binders in terms of retained penetration.

Table C-5 shows the viscosities measured at 140°F (60°C) on original, laboratory-aged and field-aged binders. Figure C-8 compares the laboratory absolute aging index with the field absolute aging index. There is a significantly higher aging in the binders recovered from the field than in the binders aged in the laboratory. Asphalt SBR_g (Goodyear) showed the highest field aging index, and asphalt Control the lowest. Asphalt SBR_g (Goodyear) also showed the largest gap between both indexes.

There is no apparent correlation between the field retained penetration and the absolute aging index for the three asphalt binders tested, as shown in Figure C-9.

At higher temperatures (275°F [135°C]), the kinematic viscosities were measured and are shown in Table C-6. Figure C-10 compares the kinematic aging indexes of the three binders tested. It can be seen that the aging index in the field is larger than the aging index in the laboratory. However, the differences between field and laboratory kinematic aging indexes are narrower than they are at 140°F (60°C), as shown in Figure C-11. Also, it can be seen that the highest retained penetration does not correlate with the aging indexes. Recovered asphalt SBR_g (Goodyear) has the highest aging index and recovered asphalt Control the lowest at both temperatures, 140°F (60°C) and 275°F (135°C).

Again, there is no apparent correlation between the retained penetration and the kinematic aging index, as can be seen in Figure C-12.

According to the distresses reported in this district, a medium severity level of longitudinal and horizontal cracking was observed in all three sections after 49 months. There has been no rutting reported. It is important to bear in mind that the penetration values of the all recovered binders were very low (21 to 27), that the absolute viscosities have increased between eight and twelve times, and the kinematic viscosities have increased from two to more than three times the original viscosities after 49 months in service. In summary, very low penetrations and high aging indexes correlate with the medium-severity-level fatigue cracking found in the field. However, while the pavement distresses observed are fairly similar in the three sections, the relative values of

penetrations and viscosities of the binders tested suggest quite different behavior among them.

According to the aging indexes, the modified binders have undergone more aging than the control.

District 15

At the time of initial placement there was indication that some of the asphalts may have exceeded maximum temperature limits prior to mixing. This did not completely explain the different distress levels found to exist between the sections.

Six asphalt binders were recovered from cores from the field after 73 months and tested for penetration and capillary viscosity. Table C-7 shows the test values for the penetration on the original, laboratory-aged, and field-aged binders. Figure C-13 illustrates the retained penetration values for the laboratory samples and recovered field samples. Field retained penetration is much smaller (about 60 percent less) than the laboratory retained penetration in all but the SBR/Pd (Dow) binder. This binder showed a 65 percent retained penetration on its recovered residue after 73 months in the field. As shown in Table C-7, except for SPR/Pd (Dow), all of the recovered binders had extremely low penetration values. A report from Sisko and Brunstrum (Ref 31) relates the authors' observations in the study of cracks in asphalt concrete in the field and outlines what they found to be acceptable and unacceptable values of penetration at 77°F (25°C), viscosity at 140°F (60°C), and viscosity at 275°F (135°C). Based upon their findings, a penetration of 24, a viscosity at 140°F of 47, 818 Poises, and a viscosity at 275°F of 1,216 cSt were found to be unacceptable values.

Viscosities at 140°F (60°C) could not be performed on the recovered field samples because of the very high stiffness values, and at this test temperature the binders would not flow under the 12-inch (30-cm) Hg vacuum. Consequently, there are no aging index values available at this temperature. Table C-8 does show the results of absolute viscosity measurements performed on the original and laboratory-aged samples. All of the viscosity values were high after the RTFOT, but those of asphalts EVA_e (Exxon) and SBR/Pd (Dow) were exceptionally high. This is another indication of the inadequacy of the vacuum capillary viscosity method when dealing with modified asphalts and aged asphalt binders.

The kinematic viscosities for the asphalt binders are shown in Table C-9. Figure C-14 compares laboratory kinematic aging index and field kinematic aging index. Only one binder showed a field kinematic aging index lower than its laboratory kinematic aging index, asphalt SBR/Pd (Dow). Asphalt EVA_e (Exxon) had the highest field kinematic aging index, followed closely by asphalt Control.

Poor correlation was found between field retained penetration and field kinematic aging index, as seen in Figure C-16.

Figure C-15 compares retained penetration and aging index of the recovered binders after 73 months. Some of the binder test data appear to correlate well, while others are contradictory.

Several of the sections in this test pavement exhibited severe types of distress. Sections constructed with asphalt binders SBR_g (Goodyear), Control (TFA), EVA_e (Exxon), and SBR/Pd (Dow) exhibited a high severity level of cracking (longitudinal and transverse). Accordingly, the penetration values on the recovered samples were very

low (23), and their kinematic aging indexes very high (over 10 times higher in asphalts Control and EVA_e (Exxon)). However, asphalt SBR/Pd (Dow) does not show the same trend in penetration and viscosity values. Its retained penetration is the highest, and its field kinematic aging index the lowest. There does not appear to be a correlation between these values and the performance of asphalt SBR/Pd (Dow). Asphalts SBR_p (Polysar) and SBS_e (Elf) exhibited a reasonably good surface condition. There is good correlation between their existing distress conditions and their field kinematic aging indexes (2.71 and 1.89, respectively), and no correlation with their recovered penetration values (27 and 18, respectively).

District 25

Age hardening in both the field and the laboratory as measured by penetration is indicated in Table C-10. Figure C-17 depicts the laboratory retained penetration and field retained penetration for each binder tested. The retained penetration from the recovered field samples is lower than the retained penetration from the laboratory-aged samples. The largest gap between these two parameters is found in asphalt Control and the smallest in modified asphalt SBS_s (Shell) with 6% polymer content. Asphalts SBS_e (Elf) and SBS_s 3% (Shell) have a 3% polymer content. After 56 months of service exposure, asphalt SBS_s 6% (Shell) showed the largest retained penetration. In general, with the exception of asphalt SBS_e (Elf), the modified binders have retained more of their original penetration than the control asphalt.

Changes in the vacuum capillary viscosities with aging are indicated in Table C-11. The comparison between the laboratory absolute aging index and the field absolute aging index is shown in Figure C-18. Absolute viscosity at 140°F (60°C) could not be performed on modified asphalt SBS_s 6% (Shell) because of its high stiffness value. Asphalt Control had the highest field aging index, while asphalt SBS_s 3% (Shell) had the lowest among the three binders tested. Figure C-19 shows the correlation found (poor to none) between retained penetration and absolute aging index of the recovered binders. The Control binder has apparently aged more than the modified binders.

Table C-12 shows the kinematic viscosity values of the four binders field tested. Asphalt Control had the highest value field kinematic aging index, as seen in Figure C-20. The widest gap between these two parameters was found in asphalt SBS_e (Elf), while the narrowest was found in asphalt SBS_e 6% (Shell). A fairly good correlation between field retained penetration and field kinematic aging index is indicated in Figure C-21.

In Figure C-22, the field retained penetration, field absolute aging index and field kinematic aging index are shown. Some correlation was found between field retained penetration and field kinematic aging index. There is no correlation between field retained penetration and the absolute field aging index, nor between field absolute aging index and field kinematic aging index.

Accordingly, it could be expected that asphalt SBS_s 6% (Shell) will perform the best, given its highest value of retained penetration and lowest kinematic aging index. The field survey condition report indicated that the section built with this binder is still in fairly good condition, although some low level of severity of alligator cracking was noted. The other three sections were reported in good condition, remaining rut- and crack-free as of May 1993 despite their low penetration values and high viscosity values

after 48 months in service. Therefore, no correlation between binder performance, retained penetration and aging index values, and observed field conditions was found for this test site at this length of service.

Summary of Findings

1. While some degree of correlation was found between penetrations (77°F [25°C], 100 grams, 5 seconds) and field performance (for instance, in District 25, penetrations were all below 27 after 73 months and the majority of the test sections were cracked), it is difficult to establish any sound relationship given the empirical nature of the penetration test.

2. The most critical index used in this report has been the aging index based on the absolute viscosity measured at 140°F (60°C) with capillary tubes. Not only was there no correlation between this parameter and retained penetration or with the aging index from the kinematic viscosity, but also in some cases the test could not be run owing to the stiff nature of the recovered asphalts. When the asphalt binder is not Newtonian-like, it is totally incorrect to utilize the vacuum absolute viscosity method. Also, it is not correct to compare viscosities of different asphalt systems if they are shear-dependent, since there is no chance to measure or control the shear rate developed in the binder during the test.

3. The field kinematic aging index, defined as the ratio between the kinematic viscosity of the recovered asphalt binder over the kinematic viscosity of the original asphalt binder, has shown some correlation with retained penetration and—most importantly—with field performance. However, this did not hold true for field-aged asphalt binders that exhibited non-linear behavior at the test temperature (275°F [135°C]).

4. There was no correlation among the different indexes—retained penetration, absolute aging index, and kinematic aging index—measured in the recovered asphalt binders. It was explained in the report that penetration tests are not suitable for measuring asphalt rheological properties due to unknown field strains, shear stress variability within the sample, and inability of to differentiate between temperature and loading time effects. With regard to the capillary viscosities, it was said that despite the fact that these tests are more fundamental in nature, they have the shortcoming both of (a) not being able to measure shear rate in the sample during the test and (b) not being able to keep it constant. When the material is shear-dependent, particularly aged asphalts and polymer-modified asphalts, the results are not comparable and are totally misleading.

5. Asphalt consistency increases with aging, and, while it is possible to detect it through a penetration test or a capillary viscosity test, neither method can produce comparable results when the binder is shear-dependent.

6. The relationship between pavement performance and the durability of asphalt binders—the latter being defined as the ability to retain original rheological properties during the service life of the pavement—should be evaluated through tests capable of measuring fundamental, rather than empirical, properties of the binders. The linear viscoelastic properties, such as stiffness or shear complex modulus, etc., are the fundamental properties of the binders that contribute to pavement durability, and they should be measured under the load and temperature conditions found in the field.

Asphalt Concrete Mixtures from Field Test Sites

Air Voids

Table D-1 (Appendix D) presents the data for the air voids of the cores obtained from the field. There is a large variation in the air void levels. The lowest air voids were found in the Lufkin District (11), with an average of 2 percent, and the highest voids were obtained in the Childress District (25), with an average of 8 percent. Within each individual field project, there was found to be a maximum of 2 percent variation between the test sections. The standard deviation for air voids is approximately 1 to 1.5 percent, which is a typical value found in most pavements.

It has been established that changes in air voids significantly influence the engineering characteristics of asphalt pavements. Plots of the various engineering properties measured in the laboratory are provided as a function of air voids, and the results are discussed in the pertinent sections.

Tensile Strain at Failure

The numerical values of maximum tensile strain at failure, for different districts and different temperatures, are presented in Tables D-2 through D-13. A summary of the results is presented in Table 4.1. These results were compared with the tensile strain values obtained in Research Study 492 on laboratory-compacted mixtures (Ref 34), as shown in Table D-14 and in Figure D-1. In general, it is obvious that field cores exhibited a more brittle behavior compared to laboratory compacted mixtures which were made using unaged binder. The tensile strains of field cores are two to four times lower than those of the laboratory-compacted specimens. Scatter plots in Figures D-2 through D-4 indicate the relationship between tensile strain at failure and air voids. While no clear pattern is noticed for most cases, some indicate lower tensile strain for higher air voids. This could be justified, probably, because higher void content increases the potential for aging, which makes the material more brittle. The values for Poisson's ratio had to be assumed in order to calculate the tensile strain. The values of 0.2, 0.3, and 0.4 were used for this parameter, respectively, for 39°F (4°C), 77°F (25°C), and 104°F (40°C).

The maximum tensile strain at failure for the different asphalt binders is presented in the bar charts of Figures D-5 through D-7 (Appendix D). A summary of results is presented in Figure 4.1. Each value for each binder was obtained as the average of maximum tensile strength for three cores. As expected, as the temperature increases, the material exhibits a more ductile behavior (tensile strain at failure increases). In general, it can be observed that mixtures with AC-10 polymer-modified binders exhibited equal or higher tensile strengths at failure than the mixtures with unmodified AC-20 asphalt binders. This is a positive contribution at cold temperatures, since it provides the more ductile behavior of the mixture, which is desirable at cold temperatures. In the Lufkin and Childress Districts (11 and 25), mixtures with SBS polymers (SBS_e and SBS_s) indicate a less brittle behavior at 39°F (4°C) than the mixtures with the SBR polymers (SBR_g and SBR_p), as shown in Figure 4.1. These results are in agreement with the findings in the laboratory study carried out during Research Study 492. In the case of the Tyler and San Antonio Districts (10 and 15), there was not a firm indication regarding less brittle behavior of SBS mixtures in contrast to SBR mixtures at cold temperatures.

Indirect Tensile Strength

The numerical values of indirect tensile strength, for different districts and different temperatures, are presented in Tables D-2 through D-13. A summary of the results is presented in Table 4.1. These results were compared with the indirect tensile strain values obtained in the 492 study on laboratory-compacted mixtures (Ref 34), as shown in Table D-15 and in Figure D-8. In general, the aged cores exhibit about 10 to 60 percent higher tensile strength than do the laboratory mixtures at 104°F (40°C). However, at 77°F (25°C) and 39°F (4°C), the cores yield approximately two to four times higher strength than do the laboratory mixes.

Figures D-9 through D-11 show the variation of the tensile strength values as a function of air voids for different field projects. In ten of the cases (out of twelve), there is a very clear trend of higher tensile strength values for lower air voids. The plots of tensile strength at 77°F (25°C) for the Lufkin District (11), however, do not exhibit such a clear trend, probably because the air voids of the different cores for this test site are so close that the effect of variables not being considered becomes important.

Bar-charts of Figures D-12 through D-14 (Appendix D) display tensile strength values obtained for different mixtures. A summary of results is shown in Figure 4.2. In general, it appears that the effect of polymers on tensile strength depends on the type and the amount of the polymer as well as on the type of the asphalt binder. Based on these figures, it seems fair to conclude that at 39°F (4°C), mixtures with SBR-modified AC-10 have higher tensile strength than mixtures with unmodified AC-20 (except in the Childress District). At 77°F (25°C), SBR mixtures have tensile strength equal to or higher than that of the unmodified AC-20 mixtures. The SBR (Polysar) section in the San Antonio District (15) exhibits consistently higher tensile strength than the AC-20 section for all test temperatures. Except for the case of tensile strength at 104°F (40°C) and at 39°F (4°C) for the Tyler District (10), the SBS_e (Styrelf) mixture exhibits a higher tensile strength than the AC-20 sections at all temperatures. Also in the Childress District (25) at all temperatures, the SBS_s 3% polymer (3% Kraton) yields higher tensile strength and SBS_s 6% (6% Kraton) yields lower tensile strength than the control section. Obviously, the amount of polymer can significantly influence the mixture strength. The section with tire rubber in the San Antonio District (15) exhibited significantly lower strength than did all the other sections at all temperatures.

Figures D-15 through D.-7 show the relationship between the indirect tensile strength and the tensile strain at failure for different mixtures and different temperatures. In some cases, a pattern of lower strain for the mixtures with higher strength is observed. However, in some other cases, no clear pattern is found.

Secant Modulus

The numerical values of secant modulus, for different districts and different temperatures, are presented in Tables D-2 through D-13. A summary of the results is presented in Table 4.2. These results were compared with the secant moduli obtained in the 492 study on laboratory-compacted mixtures (Ref 34), as shown in Table D-16 and in Figure D.18. This figure indicates that the secant moduli of field cores are two to four times higher than those of laboratory mixtures. The secant moduli are presented as a function of air voids in scatter plots, Figures D-19 through D-21. In some cases, a trend of lower moduli for higher air voids is observed. The values for Poisson's ratio had to be

assumed in order to calculate the secant modulus. The values of 0.2, 0.3, and 0.4 were used for this parameter, respectively, for 39°F (4°C), 77°F (25°C), and 104°F (40°C).

Bar-charts of secant modulus for different districts and different test sections are presented in Figures D-22 through D-24. A summary of results is presented in Figure 4.3. In general, field cores from the test sections which had shown higher secant modulus in the 492 laboratory study (laboratory-compacted laboratory mixtures) also exhibited higher modulus during this study (Figure D-18). However, it can be seen that this conclusion does not hold true for all mixes. At 39°F (4°C), the Styrelf polymer (SBS_e [Elf]) indicated a significantly higher secant modulus than the AC-20 sections for the Tyler and San Antonio Districts (10 and 15), and a lower modulus for the Lufkin and Childress Districts (11 and 25). This is contrary to the findings of the 492 laboratory study, which indicated that this parameter was lower for Styrelf mixtures compared to unmodified AC-20 mixtures. The AC-10 Kraton (SBS_s)-modified test sections, in general, had lower secant moduli than AC-20 sections at all temperatures for the Tyler and Children Districts (10 and 25), which were the only two districts where they were used. This is consistent with the findings of the 492 laboratory study. At 77°F (25°C), test sections with Styrelf (SBS_e) yielded secant moduli comparable to the those obtained for AC-20 sections, while at 104°F (40°C), the Styrelf mixtures had consistently lower secant moduli than the AC-20 sections for all districts.

The secant moduli of test sections with UP-70 polymer (SBR_g [Goodyear]) vary without any apparent pattern. At 77°F (25°C), the AC-20 and SBR_g sections yielded moduli consistently very close for all districts and all temperatures. At 104°F (40°C), in two cases (Tyler and San Antonio Districts), the AC-20 mixtures had significantly higher moduli than the SBR_g sections, while in the other two districts the results were close.

The relationship between the secant modulus and the indirect tensile strength at different temperatures and for different districts is shown in scatter plots, Figures D-26 through D-28. In almost in all cases, a pattern of higher secant modulus for materials with higher strength is noticed.

Resilient Modulus

The numerical values of resilient modulus are presented in Tables D-17 through D-20 (Appendix D). A summary of results is presented in Table 4.2. Graphs of resilient moduli of different mixtures are provided in Figures D-28 through D-29., and a summary of results is presented in Figure 4.4. Except in the Tyler District (10), all the AC-10 polymer-modified mixtures have a lower resilient modulus at 77°F (25°C) than the control AC-20 mixtures. At 39°F (4°C) in the Tyler and Childress Districts (10 and 25), most polymers yielded a higher mixture resilient modulus than the AC-20 sections, while in the Lufkin and San Antonio Districts (11 and 15), the control sections have higher moduli than the polymer-modified sections. EVA_e and SBS_s 6% (6% Kraton) sections yielded lower moduli than the control sections at both 39°F (4°C) and 77°F (25°C) temperatures. The values for Poisson's ratio had to be assumed in order to calculate the resilient modulus. The values of 0.2, 0.3, and 0.4 were used for this parameter, respectively, for 39°F (4°C), 77°F (25°C), and 104°F (40°C).

Figures D-30 and D-31 show the relationship between the resilient modulus and the indirect tensile strength for different districts. A trend of higher modulus for mixtures with higher tensile strength is observed in most cases.

RELATIONSHIP BETWEEN LABORATORY STUDY AND FIELD PERFORMANCE

To evaluate the effectiveness of different polymers, it seems most reasonable to compare the performance of different test sections against each other within the same field project (i.e., in the same district) in order to minimize the effect of uncontrolled variables. Results are questionable when comparing a test section treated with a certain polymer in one district with a test section treated with the same polymer in a different district because of the influence of the large number of factors which could not be controlled in this research study. For example, type and amount of asphalt cement and aggregates used in different districts were dependent upon an economical selection and came from different sources. In addition, pavements have aged to different periods (three to six years) and have been exposed to different climatic conditions; moreover, construction practices vary between districts and contractors, even though they all may satisfy specification limits. However, as far as all the above factors are concerned, test sections of the same field project are not very different, and comparison of these sections with one another will be more meaningful. Even so, care should be taken in carrying out such comparisons, because in some of the projects, the control asphalt cements are from a different source than the modified sections.

Rutting did not appear to be significant in any of the projects, while longitudinal, horizontal, and alligator cracking were severe in some of the projects. The test sections in the San Antonio District (15) field project experienced more severe distress than the other projects. Six out of eight test sections in this project exhibited severe cracking. The test sections in the Tyler District (10) appeared to be the least damaged compared to other projects.

During the laboratory study carried out in Research Study 492, it was found that for the San Antonio District (15), the Styrelf (SBS_e) mixture exhibited the most ductile behavior, while the AC-20 control mixture, the SBR/Polyolefin (Dow) mixture, and the Polybilt (EVA_e) mixture exhibited the least ductile behavior. The Polysar NS-175(SBR_p) mixture also showed more ductile behavior than others during that laboratory study, even though not as high as the Styrelf mixture. The UP-70(SBR_g) mixture exhibited an intermediate behavior.

These results were obtained based on the indirect tensile strength tests at three different temperatures. The mixture with higher maximum tensile strain at failure was considered more ductile. This ductility ranking of the San Antonio District (15) mixtures was in agreement with the cracking that initiated in the test sections of this district during the very cold February of 1990, three years after construction. The most ductile mixtures experienced the least amount of cracking, and the mixtures which had shown relatively more brittle behavior during that laboratory study experienced the most severe cracking. These findings, however, cannot be generalized to other districts, since the Styrelf sections in the Lufkin District (11) indicated some longitudinal and horizontal cracking (as in the control and latex sections), even though, during the laboratory study phase, the same ductile trend as for the San Antonio District (15) was observed. It should be mentioned that testing the cores of the San Antonio District (15) project after six years of exposure to traffic and climate did not yield the same ductility ranking as the original laboratory testing did.

The recent laboratory study on field cores in this project, as well as the original laboratory study on laboratory-compacted plant mixtures (Research Project 492) indicates that, in some cases, the tensile strength and resilient modulus of cores from different test sections vary within a wide range. However, even the sections with lower tensile strength than others did not exhibit noticeable permanent deformation after several years' exposure to traffic and climate.

The values for tensile strain at failure and total instantaneous resilient modulus (Tables 4.1 and 4.2, respectively) were plotted on the fatigue criteria graph developed during the AAMAS study (Reference 33). The results are shown in Figures D-32 through D-35 of Appendix D. The mixtures plotting above the fatigue line are expected to have satisfactory resistance against fatigue distress, while those falling below the line are expected to perform poorly. For each of the figures shown, there are two populations of points. The group to the left indicates values for the 77°F (25°C) testing, while the values to the right of the figure indicate the 39°F (4°C) testing. The points for 39°F (4°C) mostly fall below the line for all districts and all mixtures, while the points for 77°F (25°C) fall above the line—except for the San Antonio District (15), where most of the test sections exhibited the most severe cracking among all the districts.

TABLE 4.1 AVERAGE VALUES OF INDIRECT TENSILE STRENGTH AND STRAIN AT FAILURE FOR CORES FROM DIFFERENT FIELD PROJECTS (1)

Section	ITS(2) psi 39 F	ITS(2) psi 77 F	ITS(2) psi 104 F	StF(3) E-03 39 F	StF(3) E-03 77 F	StF(3) E-03 104 F
District 10						
Control	358	215	67	1.3	6.8	7.8
Goodyear,SBR,Latex	492	248	51	1.3	7.9	10.7
Elf,SBS,Styrelf	423	248	49	0.8	8.1	8.4
Shell,SBS,Kraton	347	139	42	2.6	9.2	7.5
Exxon,EVA,Polybilt	392	151	34	1.9	7.1	6.7
District 11						
Control	484	215	77	2.0	9.2	9.2
Goodyear,SBR,Latex	507	250	80	1.9	9.1	10.4
Elf,SBS,Styrelf	525	220	70	2.6	10.2	10.7
District 15						
Control	372	186	77	1.1	3.6	4.4
Goodyear,SBR,Latex	419	180	72	1.1	3.6	5.7
Elf,SBS,Styrelf	479	196	83	1.1	4.4	6.1
Exxon,EVA,Polybilt	366	161	71	1.5	2.4	3.4
Crafco,Rubber,Genstar	270	120	63	1.3	3.4	6.0
Polysar,SBR,Latex	475	207	85	1.5	5.1	6.6
Fiber	336	181	73	1.7	3.6	5.6
DOW,SBR,Polyolefin	352	143	68	1.4	3.5	4.5
District 25						
Control	378	160	52	1.2	4.8	7.8
Goodyear,SBR,Latex	367	166	52	1.1	4.7	8.1
Elf,SBS,Styrelf	364	168	58	1.4	4.6	8.1
Shell,SBS,Kraton,3%	401	191	58	1.6	6.5	9.2
Shell,SBS,Kraton,6%	295	119	53	2.1	7.1	9.9

NOTES:
(1) Results are reported as the average of measurements on three specimens
(2) ITS: Indirect Tesile Strength
(3) StF: Maximum Tensile Srength at Failure from ITS

1 psi = 6895 pascal
1 Δ°F = 0.556 Δ°C

TABLE 4.2 AVERAGE VALUES OF VARIOUS MODULI FOR CORES FROM DIFFERENT FIELD PROJECTS

Section	MRi(2) E06,psi 39 F	MRi(2) E06,psi 77 F	MRt(3) E06,psi 39 F	MRt(3) E06,psi 77 F	MS(4) E03,psi 39 F	MS(4) E03,psi 77 F	MS(4) E03,psi 104 F
District 10							
Control	5.31	2.52	4.78	1.94	465	60	19
Goodyear,SBR,Latex	7.96	2.63	7.04	1.90	628	60	10
Elf,SBS,Styrelf	6.33	3.09	5.86	2.32	839	59	11
Shell,SBS,Kraton	7.87	1.48	6.30	1.09	220	32	13
Exxon,EVA,Polybilt	4.87	1.58	4.12	1.24	343	41	12
District 11							
Control	6.57	1.91	6.15	1.44	389	45	19
Goodyear,SBR,Latex	5.48	1.68	5.01	1.18	436	53	17
Elf,SBS,Styrelf	4.19	1.24	3.51	1.04	333	42	15
District 15							
Control	9.58	4.97	8.68	2.23	604	100	40
Goodyear,SBR,Latex	7.62	2.34	7.33	1.80	804	97	28
Elf,SBS,Styrelf	7.81	2.85	7.43	2.16	888	94	30
Exxon,EVA,Polybilt	6.66	2.65	5.98	2.43	423	131	47
Crafco,Rubber,Genstar	6.28	2.93	5.94	2.32	338	71	29
Polysar,SBR,Latex	9.40	2.86	8.37	2.28	525	81	30
Fiber	6.14	1.98	5.50	1.81	495	96	34
DOW,SBR,Polyolefin	5.21	1.83	4.87	1.61	415	83	36
District 25							
Control	5.40	2.22	4.50	1.94	522	68	14
Goodyear,SBR,LAtex	7.19	1.64	5.81	1.33	535	69	14
Elf,SBS,Styrelf	6.54	1.90	5.89	1.46	411	72	16
Shell,SBS,Kraton,3%	6.47	2.09	5.95	1.46	418	57	14
Shell,SBS,Kraton,6%	4.65	1.31	4.16	0.96	184	33	12

NOTES:
(1) Results are reported as the average of measurements on three specimens
(2) MRi: Instantaneous Resilient Modulus
(3) MRt: Total Resilient Modulus
(4) MS: Secant Modulus from Indirect Tensile Test at Peak Load

1 psi = 6895 pascal
1 Δ°F = 0.556 Δ°C

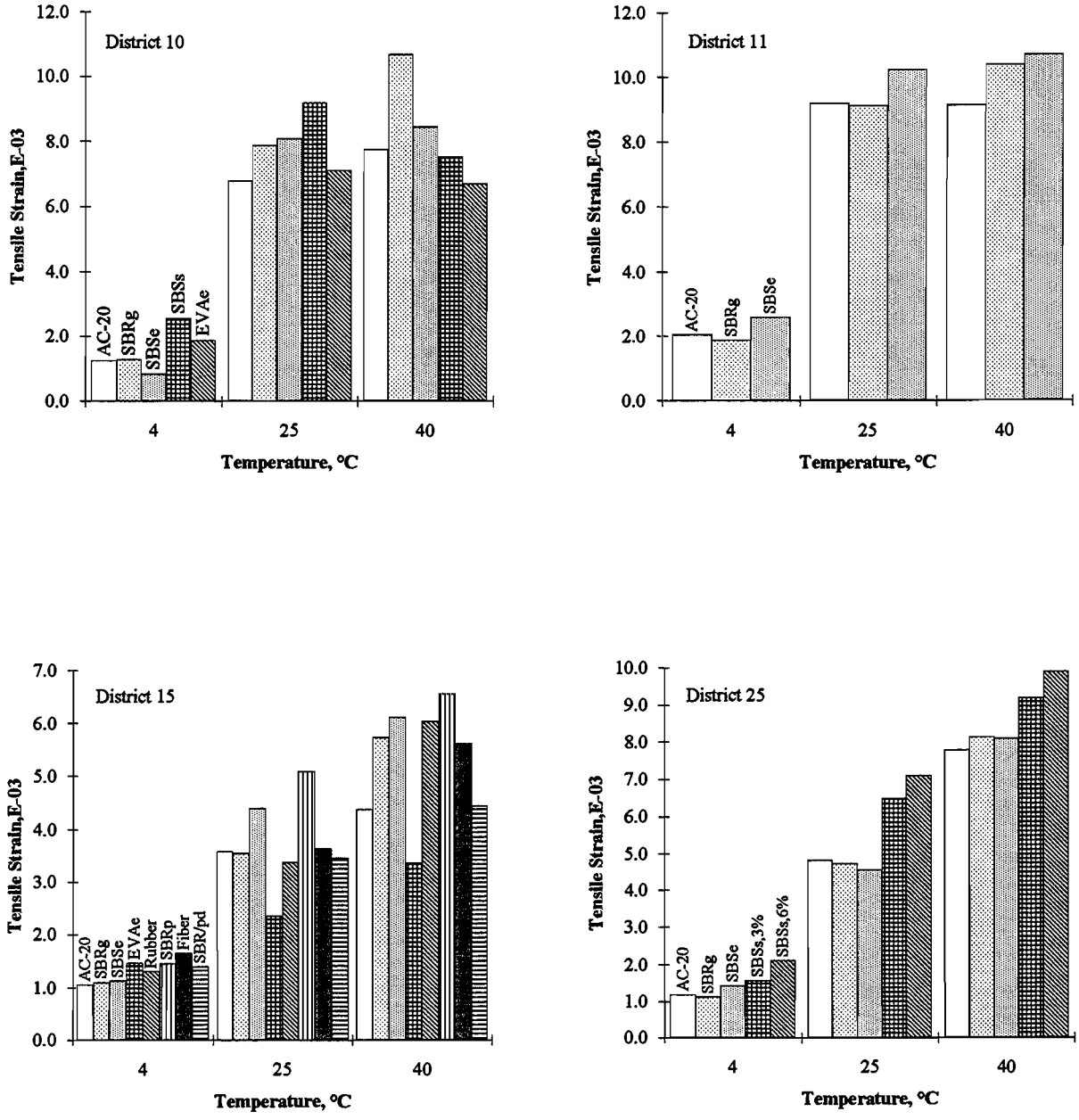

Figure 4.1 Maximum tensile strain at failure for different polymer-modified mixtures at different temperatures

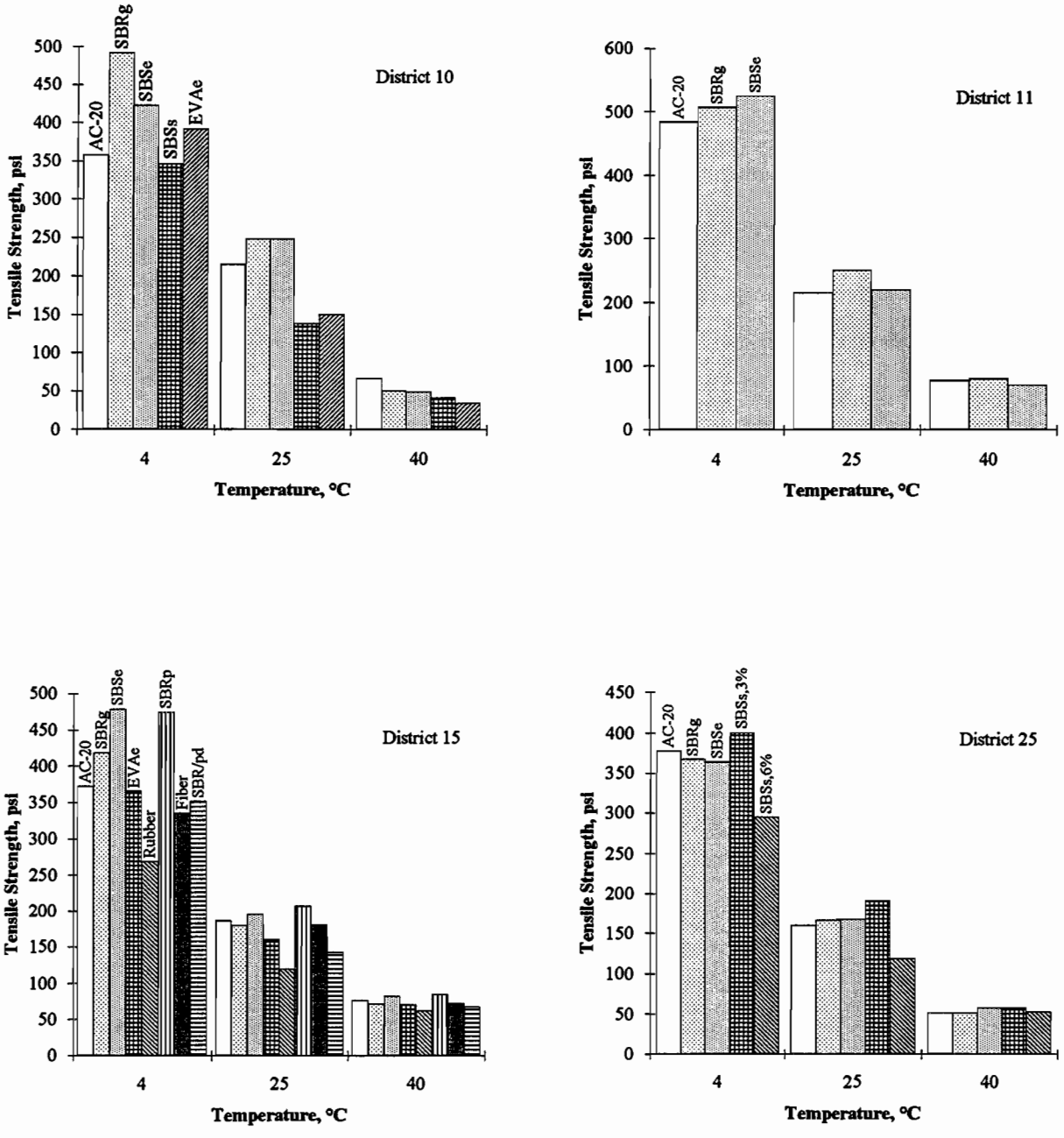

Figure 4.2 Indirect tensile strength for different polymer-modified mixtures at different temperatures

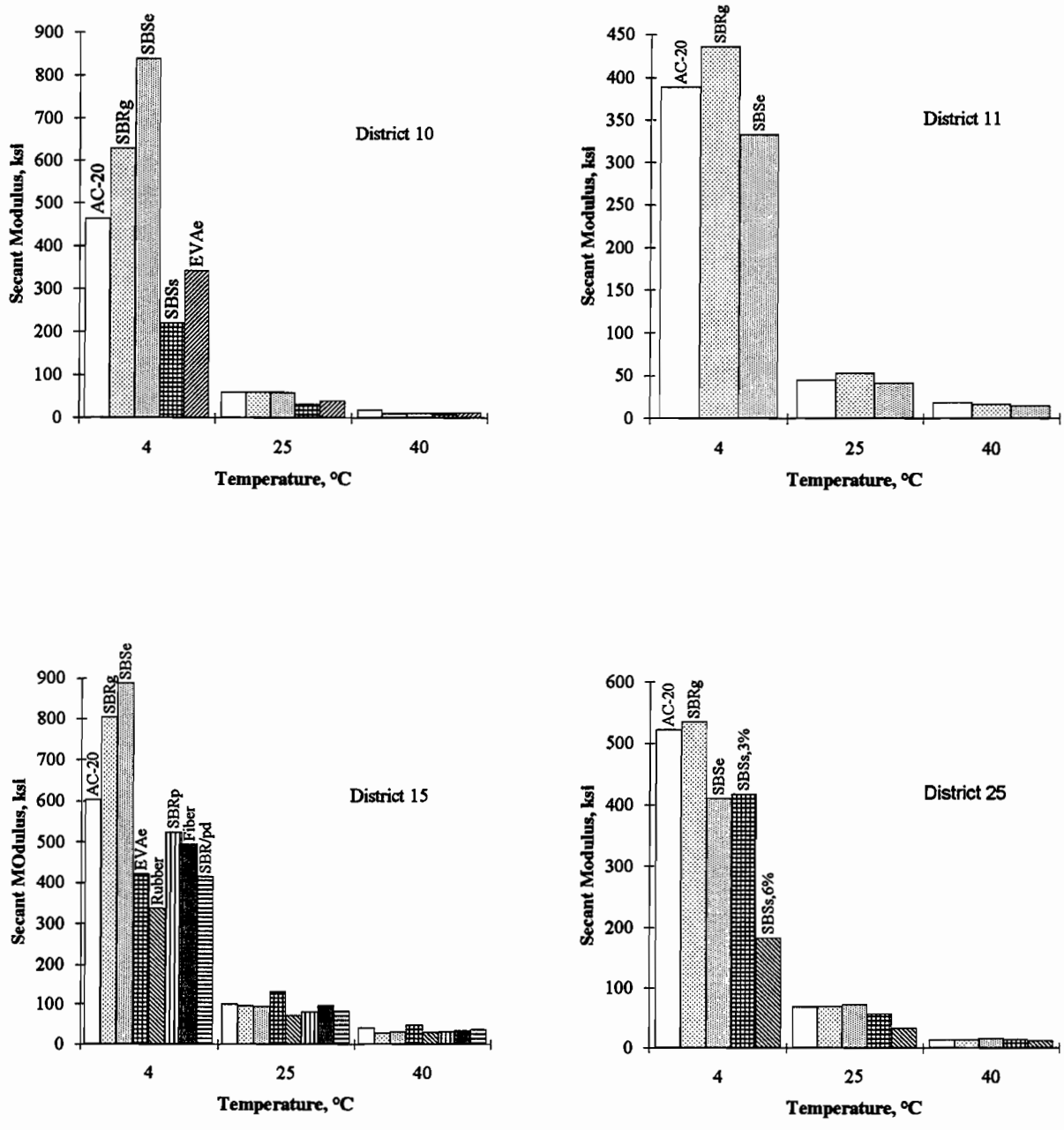

Figure 4.3 Secant modulus at peak load for different polymer-modified mixtures at different temperatures

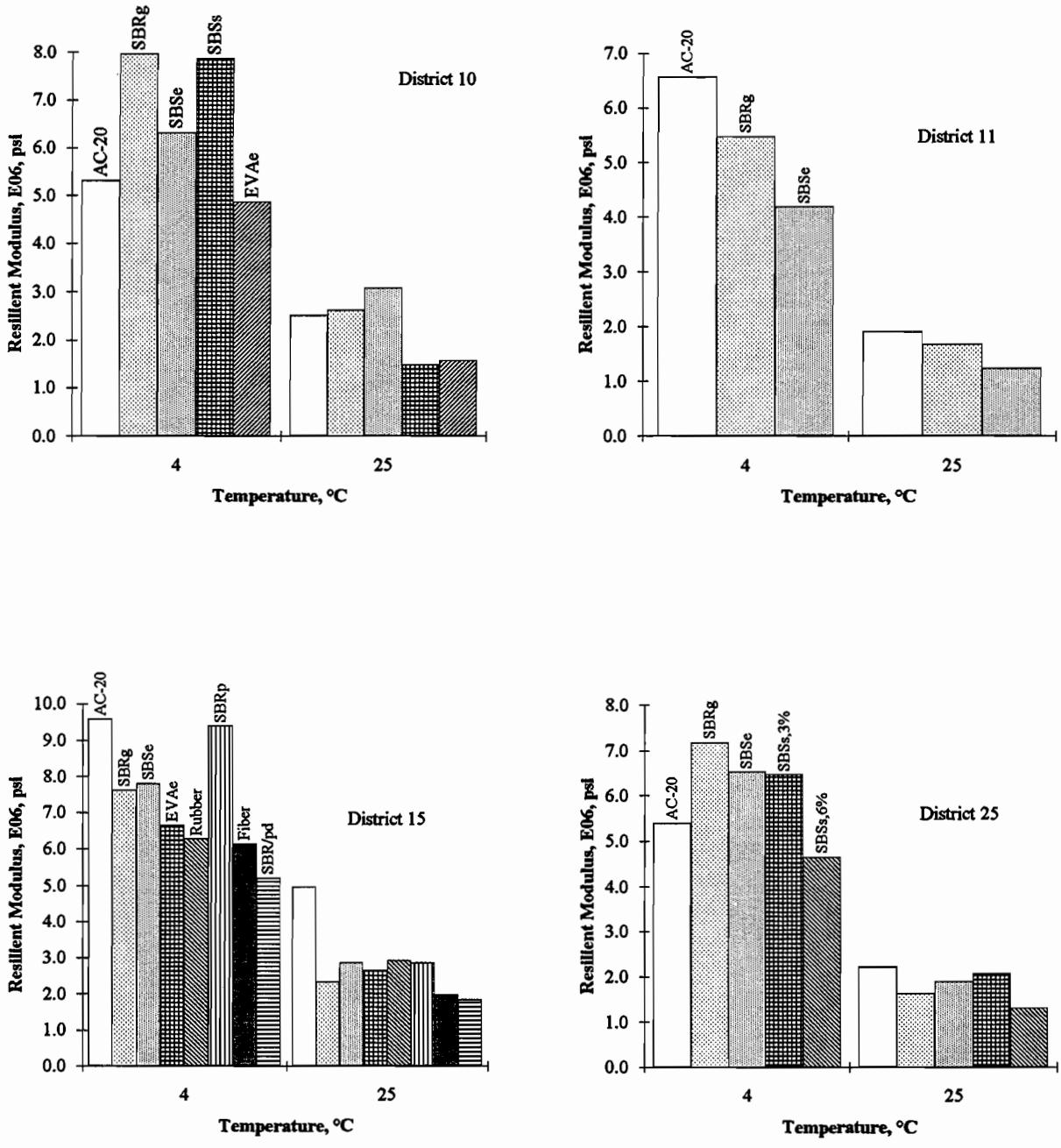

Figure 4.4 Resilient modulus for different polymer-modified mixtures at different temperatures

CHAPTER 5

CONCLUSIONS AND RECOMMENDATIONS

The long-term effect of the use of the polymer modifications was studied from three viewpoints:

(1) Effect on the Binder Properties Based upon Conventional Tests;
(2) Binder Selection Based upon SHRP Recommended Protocol; and
(3) Visual Condition and Physical Tests of the Mixture.

CONCLUSIONS

The following conclusions are drawn based on the findings of this study:

Conventional Binder Testing

1. The empirical nature of the penetration test made it difficult to establish a sound relationship between the penetrations found to exist in the asphalt binders recovered from road samples and the condition of the test section.

2. The aging index, based upon the absolute viscosity measured at 140°F (60°C) with capillary tubes, was the prime method of evaluating changes in the binders with time in service. With new technology available, it is apparent that there can be no correlation with retained penetrations and the kinematic viscosity when the asphalt binder is no longer Newtonian from either aging or polymer modification.

3. The viscosities of different asphalt systems cannot be compared when they are shear-dependent, since there is no way to measure or control the shear rate developed in the binder during the test.

4. The kinematic aging index based on the field-recovered binders, defined as the ratio of the kinematic viscosity of the recovered asphalt binder over the kinematic viscosity of the original asphalt binder, appears to show some degree of correlation with retained penetration and field performance. An exception occurs when the field-aged asphalt binder exhibits non-linear behavior at the test temperature of 275°F (135°C).

5. No correlation was found between the different indexes—retained penetration, absolute aging index, and kinematic aging index—as measured on the recovered asphalt binders. It was determined that penetration tests were not suitable for measuring asphalt rheological properties under conditions of unknown field strains, shear stress variability within the sample, and inability to differentiate between temperature and loading time effects.

SHRP Binder Testing

1. The SHRP Asphalt Binder Test Protocols were employed in order to classify the original binders used in the asphalt mixtures placed in Project 1306. As a result, the binders have been classified in seven grades: PG 58-22, PG 58-28, PG 64-16, PG 64-22, PG 64-28, PG 70-16, and PG 70-22.

2. Climatic data from each district for each project were collected and a SHRP Asphalt Binder classification was performed based on the weather data. As a result, the following grades were found: PG 64-16, PG 64-22, and PG 64-28. Differences between

the binder requirements based on the environmental data and the SHRP classification obtained based on the testing of the binders would be expected to be reflected in the performance of the binder in service. The service life of the majority of the test sections is considered too short (in time) to allow for this comparison.

3. No distinctive pattern was found between unmodified and modified binders' performance, nor among the performance of the same modified binder types, when compared between districts. This is considered to be the case owing to the many factors affecting the performance of an asphalt mixture, such as pavement structure, volumetric composition, binder type, location, traffic, etc.

4. In some cases a close agreement was found between the observed pavement performance and asphalt binders' classification based on the SHRP guidelines. In others, there was no correlation, a phenomenon which might have been influenced by factors other than the binder alone. It is important to bear in mind that selection of the asphalt binder based on SHRP criteria does not necessarily guarantee that the pavement will not rut or crack, since these types of distresses are influenced by other factors in addition to the binder alone.

Asphalt Mixtures

These conclusions are based upon the testing of samples obtained from the district field test sections:

1. None of the field test sections exhibited considerable permanent deformation.

2. The test sections in the San Antonio District (15), after six years of exposure to traffic and environment, exhibited the most severe cracking.

3. The least amount of distress was found in the Tyler District (10), which was also one of the more recently placed test sites.

4. The aged field cores showed a significantly more brittle behavior than previously indicated in the unaged laboratory-compacted mixtures.

5. The secant and resilient moduli, as well as the tensile strength of the field cores, were also significantly higher than those of the laboratory-compacted mixtures.

6. Neither the AC-10 polymer-modified nor the AC-20 unmodified control sections in the Tyler District (10) exhibited any distress at this point.

7. In the Lufkin District (11), both the AC-20 unmodified and the AC-10 polymer-modified sections exhibited longitudinal and horizontal cracking.

8. In the San Antonio District (15), only the SBR_p (Polysar) and SBS_e (Styrelf) sections were free of major distress. All of the remaining sections had severe cracking to varying degrees.

9. Also in the San Antonio District, the mixtures which had shown the most ductile behavior during the previous laboratory study (Research Study 492) also indicated the least amount of cracking under service.

10. In the San Antonio District, which had the longest period of service, the two AC-20 polymer-modified sections had a significantly higher degree of distress than the sections with polymer-modified AC-10.

11. The SBS sections in the Childress District in general exhibited a higher degree of performance than the SBR and the AC-20 control section.

General

1. The polymer-modified test sections placed as seal coats in the Odessa (6) and Bryan (17) Districts did not exhibit any distress at this time, and, for that reason, were not made a part of this report. The retained samples of the original asphalts used in the Bryan District were available and were made a part of the SHRP binder tests.

2. It is not possible to effectively compare the performance of the individual polymers between district test sites because of the widely different conditions of length of service, environment, traffic, parent asphalt, construction techniques, and pavement structure design involved. Recommendations can be made to some degree based on performance within the test sites themselves.

RECOMMENDATIONS

1. Asphalt and polymers should not be arbitrarily combined but should be the result of testing the modified asphalt for service in the anticipated environment.

2. Conventional asphalt tests have been found to be either misleading or incorrect with respect to polymer-modified and/or aged asphalt binders. The SHRP asphalt binder tests are recommended:

Dynamic Shear,
Bending Beam,
Rotational Viscosity,
PAV Aging,
RTFOT, and
Direct Tension.

3. The relationship between pavement performance and the durability of asphalt binders, the latter being defined as the ability to retain the original rheological properties during the service life of the pavement, should be evaluated by the tests capable of measuring fundamental properties of the binders instead of the empirical ones.

4. The linear viscoelastic properties, such as stiffness or shear complex modulus, etc., are the fundamental properties that contribute to pavement durability and should be measured under the load and temperature conditions anticipated in service.

5. Both pavement visual inspection and laboratory tests on core samples in the one district with the longest service life (San Antonio) indicate that AC-20 polymer-modified binders will not perform as satisfactorily as AC-10 polymer-modified binders. It is therefore recommended that caution be used before attempting to modify an asphalt AC grade above that of AC-10.

6. The relatively short service life of the majority of the test pavements, combined with the degree of distress found to have occurred on the pavement longest in service, points to the need for the Department to continue at least a low level of visual evaluation on these sites. The need for further in-depth testing at any or all of the test sites can then be evaluated.

7. It was outside the scope (both time and funding) of this project, but it has been determined that a significant amount of valuable information can be developed from additional testing on samples already obtained from the test sections. It is therefore recommended that the Department:

(a) Perform the Dynamic Shear, Rotational Viscosity and Bending Beam tests on asphalts extracted from the last core samples. Results should be compared with the data from tests on aged and unaged binders and compared to the existing visual condition of the test pavements.

(b) Perform the fatigue and creep tests on the cores remaining from the final core sampling and testing.

(c) Re-examine the fatigue and creep formulas developed in the previous 492 study to determine any additional benefit when compared to the latest field observations.

REFERENCES

1. Terrel, R. L., and J. L. Walter, "Modified Asphalt Pavement Materials—The European Experience," Association of Asphalt Paving Technologists, Vol 55, 1986.

2. Schweyer, H. E., L. L. Smith, and G. W. Fish, "A Constant Stress Rheometer for Asphalt Cements," Association of Asphalt Paving Technologists, Vol 45, 1976.

3. Shuler, T. S., C. Adams, and M. Lamborn, "Asphalt-Rubber Binder Laboratory Performance," Research Report 347-1F, Texas Transportation Institute, The Texas A&M University System, College Station, August 1985.

4. Pfeiffer, J., and P. F. VanDoomeal, "The Rheological Properties of Asphaltic Bitumen," Journal of the Institute of Petroleum Technologists, Vol 22, 1936.

5. McKeon, N. W., "Transverse Pavement Cracking Related to Hardness of Asphalt Cement," Canadian Technical Asphalt Association, Vol 13, 1968.

6. Anderson, K. O., and S. C. Leang, "Evaluation of Asphalt Cements for Low Temperature Performance," paper presented at the 66th Annual Meeting of the Transportation Research Board, Washington, D.C., 1987.

7. Bonnaure, F., G. Gest, A. Gravois, and P. Uge, "A New Method of Predicting Stiffness of Asphalt Paving Mixtures," Association of Asphalt Paving Technologists, 1977.

8. Burgess, R. A., D. Kopvillem, and F. D. Young, "St. Anne Test Road—Relationship Between Predicted Fracture Temperature and Low Temperature Field Performance," Association of Asphalt Paving Technologists, 1971.

9. Hills, J. F., "Predicting the Fracture of Asphalt Mixes by Thermal Stresses," Journal of the Petroleum Institute, 1974.

10. Anderson, D. I., and M. L. Willey, "Force Ductility—An Asphalt Performance Indicator," Association of the Asphalt Paving Technologists, Vol 45, 1976.

11. Reiner, M., and G. W. Blair, "Rheological Terminology," *Rheology: Theory and Applications*, Vol 4, Academic Press Inc., New York, 1956.

12. Tia, M., and B. E. Ruth, "Basic Rheological Concepts Established by H. F. Schweyer," ASTM STP 941, 1987.

13. Hadley, William O., W. Ronald Hudson, and Thomas W. Kennedy, "A Method of Estimating Tensile Properties of Materials Tested in Indirect Tension," Research Report 98-7, Center for Highway Research, The University of Texas at Austin, July 1970.

14. Anagnos, James N., and Thomas W. Kennedy, "Practical Method of Conducting the Indirect Tensile Test," Research Report 98-10, Center for Highway Research, The University of Texas at Austin, August 1972.

15. Kennedy, Thomas W., and James N. Anagnos, "Procedures for the Static and Repeated-Load Indirect Tensile Test," Research Report 183-14, Center for Transportation Research, The University of Texas at Austin, August 1983.

16. Kennedy, T. W., and D. Navarro, "Fatigue and Repeated-Load Elastic Characteristics of In-Service Asphalt-Treated Materials," Research Report 183-2, Center for Highway Research, The University of Texas at Austin, January 1975.

17. Adedimila, Adedare S., and Thomas W. Kennedy, "Fatigue and Resilient Characteristics of Asphalt Mixtures by Repeated-Load Indirect Tensile Test," Research Report 183-5, Center for Highway Research, The University of Texas at Austin, August 1975.

18. Kennedy, T. W., J. Vallejo, and R. Haas, "Permanent Deformation Characteristics of Asphalt Mixtures by Repeated-Load Indirect Tensile Test," Research Report 183-7, Center for Highway Research, The University of Texas at Austin, June 1976.

19. Williams, M. L., R. F. Landel, and J. D. Ferry, "Visco-Elastic Properties of Polymers," Journal of American Chemical Society, Vol 77, 1955.

20. Hondros, G., "The Evaluation of Poisson's Ratio and the Modulus of Materials of a Low Tensile Resistance by the Brazilian (Indirect Tensile) Test with Particular Reference to Concrete," Australian Journal of Applied Science, Vol 10, No. 3.

21. Texas Department of Transportation, "Manual of Testing Procedures."

22. Texas State Department of Highways and Public Transportation, "Standard Specifications for Construction of Highways, Streets and Bridges, 1982."

23. *The SUPERPAVE™ Mix Design Manual for New Construction and Overlays*, Strategic Highway Research Program (SHRP), Vols 3 and 4, National Research Council, Washington, D.C., 1993.

24. Finn, F., Monismith, C., Hicks, G., and Leahy, R., "Validation of SHRP Binder Specification Through Mix Testing," preprints of the 1993 Annual Meeting of the Association of Asphalt Paving Technologists, Vol 62, 1993.

25. *SHRP A-002A Binder Characterization and Evaluation*, Draft Final Report, Vol III, Strategic Highway Research Program, National Research Council, Washington, D.C., 1992.

26. Readshaw, E. E., "Asphalt Specifications in British Columbia for Low Temperature Performance," Proceedings of the Association of Asphalt Paving Technologists, Vol 43, 1974, p 285.

27. Anderson, D., et al, "Physical Properties of Asphalt Cement and the Development of Performance-Related Specifications," Journal of the Association of Asphalt Paving Technologists, Vol 60, 1991, p 437.

28. Puzinauskas, V. P., "Properties of Asphalt Cements," The Asphalt Institute Research Report No. 80-2 (RR-80-2), November 1980.

29. Finn, F., et al, "Summary Report on Asphalt Properties and Relationship to Pavement Performance: Literature Review," SHRP-A/IR-90-015, Strategic Highway Research Program, National Research Council, May 1990.

30. Bolzan, P. E., "Controlled Stress Dynamic Mechanical Analysis on Asphalt and Polymer-Modified Asphalts," SHRP A-001 Contract Report, Center for Transportation Research, The University of Texas at Austin, October 1991.

31. Sisko, A. W., and Brunstrum, L. C., "The Rheological Properties of Asphalts in Relation to Durability and Pavement Performance," Proceedings of the Association of Asphalt Paving Technologists, Vol 37, 1968, p 448.

32. Solaimanian, M., and T. W. Kennedy, "Predicting Maximum Pavement Temperature Using Maximum Air Temperature and Hourly Solar Radiation," Proceedings of the 72nd Annual Meeting of the Transportation Research Board, Washington, D.C., January 1993.

33. "Asphalt-Aggregate Mixture Analysis System, AAMAS," National Cooperative Highway Research Report 338, Transportation Research Board, Washington, D.C., March 1991.

34. Kennedy, Thomas W., Hassan Torshizi, and David R. Jones IV, "Mix Design Procedures and Considerations for Polymer-Modified Asphalt Compatibility and Stability," Research Report 492-1F, Center for Transportation Research, The University of Texas at Austin, June 1992.

Note: The Center for Highway Research, The University of Texas at Austin (Refs 13, 14, 16, 17, and 18) was renamed the Center for Transportation Research, The University of Texas at Austin (Refs 15, 30, and 34) in November 1979.

APPENDIX A

DEFINITIONS AND FORMULAE FROM RESEARCH STUDY 492 AS APPLICABLE TO THIS STUDY

APPENDIX A

LABORATORY BINDER TESTS, RS 492

Penetration. The penetration test is an empirical measure of consistency and was performed in accordance with ASTM Designation D5. Penetration values were used to determine the temperature susceptibility of the binders in terms of penetration index (PI) or penetration-viscosity number (PVN).

Kinematic Viscosity. The ratio between the applied shear stress and shear rate of the liquid is the viscosity and the kinematic viscosity is then the ratio of the viscosity to the density of the liquid. This value is determined by ASTM D2170, measured in centistokes at 275°F.

Absolute viscosity. Viscosity grading of the asphalt binders was determined at 140°F using the ASTM D2171 method and was measured in the standard unit of poises. The 140°F temperature is used because it approximates the temperature normally accepted as the maximum temperature for asphaltic pavements during the summer months in the United States.

Softening Point. Softening point is measured by the ring andball method in accordance with ASTM D2398 and is defined as the temperature at which an asphalt cement cannot support its own weight and starts flowing. The purpose was to determine the temperature at which a phase change occurs in the asphalt. This value was used to determine the temperature susceptibility of the binders in terms of a penetration index (PI).

Rolling Thin Film Oven Test (RTFOT). This test is performed in accordance with ASTM D2872 causes a controlled aging of the asphalt by the combined effect of heat and air applied to a moving film of asphalt cement. This test is supposed to approximate the change in the properties of the asphalt binder during conventional plant mixing.

Penetration Index (PI). The penetration index is commonly used as a means of estimating the temperature susceptibility of asphalt cement. There are several methods to determine the PI of the binders. The procedure followed in this research used the penetration and softening point. By this procedure an assumption is made that all asphalts have a common penetration of 800 at their softening point. The relationship between penetration and softening point that was used to determine the PI of the asphalt binders is:

$$PI = \frac{30}{1+90(PTS)} - 10$$

where,

PTS = Penetration Temperature Susceptibility

$$PTS = \frac{\log(800) - \log(Pen)}{T_{R\&B} - T_{Pen}}$$

$T_{R\&B}$ = Softening Point, F
Pen = Penetration at 77°F

An increase in the PI value indicates an apparent decrease in the temperature susceptibility of the material. The Penetration Index determined by this method is identified in this report as PI(Pen/SP).

Penetration Viscosity Number (PVN). The Penetration-Viscosity Number is another method of estimating the temperature susceptibility of asphalt cements that was developed when the PI failed to provide good correlation with observed pavement cracking at low temperatures in colder regions. The PVN in this research is based upon penetration at 77°F and viscosity at 140°F.

PVN can be calculated using the following relationship:

$$PVN = \frac{4{,}258 - 0.7967(\log(Pen)) - \log(Vis)}{0.7591 - 0.1858(\log(Pen))} x\ (-1.5)$$

where,

Pen = Penetration at 77°F
Vis = Kinematic Viscosity at 275°F

Both PI and PVN values were calculated because the data needed to develop them was available and the two values have been believed to correlate to low temperature performance of HMAC pavements. The correlation of PI and PVN may occasionally yield apparent contradictory data but recent research indicates that both methods of predicting temperature susceptibility may have merit.

Penetration and Viscosity Ratios. These values determined by measuring the respective property before and after aging in the Rolling Thin Film Oven. For normal or conventional asphalt binders, the ratio for viscosity should always have a value greater than one and a value of less than one for the penetration ratio because of the oxidative hardening resulting from the RTFOT. Values close to one by either method for the binders used in asphalt paving indicate a better resistance to oxidative hardening during plant mixing, laydown and subsequent service life.

Stiffness Modulus. Stiffness modulus is the ratio of stress to strain. Since this modulus is dependent on the test temperature and the duration of the applied stress, it was used to estimate the low-temperature cracking susceptibility of the HMAC. Since it is generally believed that at low temperatures the asphalt binder controls the stiffness of HMAC mixtures, controlling this stiffness will improve the low temperature properties of a HMAC pavement.

Limiting Stiffness Method. A simple method for predicting the cracking temperature of asphalt binders is to estimate the temperature at which the binder reaches a critical "limiting stiffness". Based upon research performed on a test road by Canadian researchers, the temperature at which the asphalt binder stiffness reaches 145,000 psi at a half-hour loading time was selected as the predicted cracking temperature.

Critical Stress Method. The predicted cracking temperature of the pavement was assumed, based upon research reported in Study 492, to be the thermal stress developed in the binder as it cooled and was calculated by:

$$\sigma_t = \Sigma (Si \times \alpha_A \times \Delta T)$$

where,

Si = Asphalt stiffness at a one hour loading time at a series of temperature intervals, ΔT.

α_A = Coefficient of linear thermal contraction, assumed to be 2 x 10E-4 in/in/°C

The calculated cracking temperature was taken as the temperature at which a stress of 73 psi is induced.

Force Ductility. The force ductility test is a modification of the asphalt ductility test (ASTM D113). The following properties were measured in the force ductility test:

- Asphalt Modulus
- Asphalt-Polymer Modulus
- Maximum True Stress
- Maximum True Strain
- Area under Stress/Strain Curve

Two slopes were evaluated. The initial lope of the stress-strain curve in the linear region under primary loading is referred to as the "asphalt modulus". A second slope was observed for certain blends of asphalt and polymer which is characterized by secondary loading and labeled the "asphalt-polymer modulus".

Schweyer Rheometer. The Schweyer Rheometer is a constant stress rheometer that produces a rheogram of apparent viscosity versus shear rate. Generally, the plot of the shear stress (τ) vs rate of shear (γ) on a logarithmic scale will describe a straight line which may represented by a power formula:

$$\tau = A\gamma^C$$

where

C = Slope of the straight line of the log-log plot

A = Apparent viscosity at a shear rate of 1 reciprocal second

The Schweyer "C" parameter (slope) is used as a measure of the shear susceptibility or deviation from Newtonian behavior. Binders with slopes of one are defined as Newtonian fluids and are not shear susceptible and, therefore, have a constant apparent viscosity over a range of shear rates. Where C is less than one, the binder is a shear thinning fluid and when C is greater than one the fluid is termed shear thickening. The viscosity-temperature susceptibility was measured from the log plot of the viscosity vs. the test temperature.

Compatibility Test. Recognizing that compatibility of the polymer modifiers with the asphalt has been a major concern of both construction and state personnel, a hot storage stability test was used to determine any settlement or separation and the results of these tests were reported in the report on Study 492. In those

tests, the modified binder was stored for two days at 165°F in 50 mm diameter cans. Following the cooling period, the top and bottom of the sample was separated and the penetration test was performed on each part. The modified binders were classified as follows:

- Compatible- less than 10% difference in penetration between the top and bottom
- Incompatible- more than 10% difference in penetration between the top and bottom

LABORATORY TESTING OF CORES, RS 492

Marshall Stability Test. The Marshall stability and flow values were determined in accordance with ASTM D1559 on a 4 inch specimen loaded at 140°F and a constant deformation rate of 2 inches per minute. The maximum load, expressed in pounds, is the Marshall stability value and the vertical deformation corresponding to the maximum load, expressed in inches, is the flow value.

Hveem Stability Test. The Hveem stability was determined by the Texas DOT Test Method Tex-208-F. The 4 inch cores sampled from the test road, at a temperature of 140 °F, were loaded at a rate of 0.05 inches per minute to a vertical load of 5000 pounds. The resultant horizontal at the maximum vertical loading was measured and the Hveem stability value calculated as follows:

$$S = \frac{22.2}{P_h D_2 / (P_v - P_h) + 0.222}$$

where

S = Hveem Stability, %
P_v = Applied vertical pressure (160 psi)
P_h = Transmitted horizontal pressure at P_v= 160 psi
D_2 = Displacement of the stabilometer fluid to increase the horizontal pressure from 5 to 100 psi, measured in revolutions of a calibrated pump handle.

Indirect Tensile Test. A vertical load is applied directly along the vertical diametral plan of the 4-inch core. The load is distributed over a 0.5 inch wide curved steel loading strip to produce a uniform tensile stress. The horizontal and vertical deformations and the applied load re measured during the test. The tensile strength, tensile strain at failure, the modulus of elasticity, and Poisson's ratio were then calculated.

Indirect tensile strength was measured in accordance with Texas DOT Test Method Tex-226-F with the addition of two test temperatures (39° and 104°F) to the prescribed 77°F to determine the effect of temperature on tensile strength of the cores. Tensile strength was calculated using the following equation for 4-inch diameter specimens:

where

S_t = Tensile strength,psi

$$S_t = 0.156 \frac{P_{max}}{t}$$

P_{max} = Total applied vertical load at failure, lbs
t = Thickness or height of the specimen, in.

Tensile strain at failure was calculated using the following equation for the 4-inch cores:

$$\epsilon_f = \Delta H \times \frac{0.1185\nu + 0.3896}{0.02494\nu + 0.0673}$$

where

ϵ_f = Strain at failure
ΔH = Horizontal deformation in inches at failure or deformation at maximum or peak load
υ = Poisson's ratio

Secant Modulus was calculated as the elastic modulus using the peak load and maximum tensile strain from the indirect tensile test. It should be pointed out that the secant modulus can be defined in different ways. In this study the same formula used for determining the Young's Modulus of Elasticity is used to calculate the Secant Modulus. This also agrees with the method previously used in RS 492. The equation used to calculate the secant modulus is:

$$M_s = \frac{P_{ult}}{t \cdot H_{pk}} (0.27 + \nu)$$

where

M_s = Secant Modulus
P_{ult} = Ultimate load from indirect tensile test (peak load)
H = Horizontal deformation at peak load
t = Specimen thickness
υ = Poisson's ratio

Resilient Modulus. The resilient modulus was determined using the repeat-load indirect tensile test in ASTM D4123 and was calculated using the resilient, or instantaneously recoverable, horizontal and vertical deformations after approximately 200 load cycles. The equation used to calculate the modulus is:

$$E_R = \frac{P_R}{t\, H_R} (0.27 + \nu_R)$$

where,

E_R = Resilient modulus,psi
P_R = Applied repeated load,lbs
t = Specimen thickness,inches
H_R = Horizontal resilient deformation,inches
υ_R = Resilient Poisson's ratio

Poisson's Ratio (υ) was calculated from both the horizontal and vertical displacements using the following relationship:

$$\nu = 3.59\ DR - 0.27$$

where

DR = $\Delta H/\Delta V$ = The deformation ratio measured during the indirect tensile test.
ΔH = The recoverable horizontal deformation measured during the resilient modulus test.
ΔV = The recoverable vertical deformation measured during the resilient modulus test.

Indirect Tensile Fatigue Test. The indirect tensile test configuration was used to measure the fatigue properties of the HMAC core samples based on the reasoning that the indirect tensile test simulates the state of stress in the lower portion of pavement layer.

Fatigue life relationships were expressed in terms of initial strain for the controlled-stress test as follows:

$$N_f = K_1 (1/\epsilon_{mix})^{K_2}$$

where

N_f = Number of repetitions or load applications to failure.
K_1 and K_2 = Fatigue constants (regression constants).
ϵ_{mix} = Initial strain in the core = the applied dynamic stress divided by the average static modulus of elasticity.

Alpha and Gnu. The alpha and gnu functions were measured using the indirect tensile test based on the first 1,000 load cycles and are used to describe the permanent deformation characteristics of the HMAC pavement samples. Both are mathematically defined as follows:

Alpha = 1-S
Gnu = IS/ϵ_r

where

S = Slope of the logarithm of number of load repetitions (N) versus logarithm of the accumulated permanent strain (Ep).
I = Intercept of the straight line (arithmetic strain value) with the accumulated permanent strain axis,i.e., value at which number of load repetitions scale equals 1.
ϵ_r = Resilient or recoverable strain.

Creep Test. The creep test value could not be determined in the normal manner since it is dependent on the state of the stress being uniaxial. The equation for creep compliance for the indirect tensile creep test was developed in the initial study developing the field test sites (RS 492).

The creep compliance property is an important indicator of several additional properties such as permanent deformation, temperature susceptibility and fracture properties.

Tensile Strength Ratio. The indirect tensile test was used to determine the tensile strength ratio (TSR) of wet and dry specimens to provide an estimation of the moisture susceptibility of the HMAC compacted mixtures. The procedure as defined in the Texas DOT Test Method Tex-531-C was used to determine the TSR.

$$TSR = \frac{St(conditioned)}{St(unconditioned)}$$

where

St = Indirect tensile Strength
Conditioned = vacuum saturated with water
Unconditioned = dry at room temperature

APPENDIX B

DEFINITIONS AND PROCEDURES RELATED TO SHRP ASPHALT BINDER SPECIFICATION AND TABLES AND GRAPHS

APPENDIX B

Viscosity Measurements using the Brookfield Thermosel Apparatus

The method is outlined in ASTM D 4402 and in SHRP B-007. A rotational type viscometer is used to determine the coefficient of viscosity of an asphalt binder at high temperatures (80 to 300°C). The Brookfield Thermosel Viscometer measures the relative resistance to rotation of a small sample of binder (8.0 to 13.0 ml) through a torque on a coaxial-cylinder spindle rotating in a special thermostatically controlled sample holder. The spindle is driven by a synchronous motor through a calibrated spring and its deflection is indicated by a digital display. In digital models, the relative angular position of the pivot shaft is detected by an RVDT (rotary variable displacement transducer) and is read off on a digital display. By varying the speed and the spindle dimensions, a variety of viscosity ranges can be measured. The resistance to flow is proportional to the spindle's speed of rotation and geometry. A factor is applied to the torque dial reading to yield the coefficient of viscosity in centipoises or millipascal seconds. The coaxial-cylinder spindle geometry provides defined shear rates in the range of 0.08 to 93.0 reciprocal seconds, depending on spindle dimensions and viscometer model.

In order to ensure adequate pumpability, the maximum viscosity permitted in the SHRP specifications is 3 Pa.s at 135°C. This measurement is done on the unaged binder.

Dynamic Mechanical Analysis using the Dynamic Shear Rheometer

A controlled stress dynamic shear rheometer (DSR) was used for the testing of the binders in dynamic (oscillatory) shear using parallel plate test geometry. In a controlled stress DSR test, a sinusoidal stress is applied to a specimen and the resulting strain is monitored as a function of frequency at a given temperature. The complex shear modulus,G* (maximum peak-to-peak stress divided by the maximum peak-to-peak strain) and the phase angle, δ,

between the applied stress and the resulting strain are reported. It is believed that higher complex shear moduli and lower phase angle contribute to increase resistance to permanent deformation (rutting).

Lower complex moduli and lower phase angles are believed to improve fatigue resistance properties. As one can observe, the properties of the binder that mitigate fatigue damage, in fact, decrease the resistance to rutting.

The DSR is used to determine the rheological properties of the asphalt binders at the upper and intermediate range of service temperatures where rutting and fatigue are the primary distress mechanisms.

In testing asphalt binders, the specimen is placed between parallel plates of different diameters; (25mm for high temperatures and 8mm for intermediate temperatures), and different thicknesses (1mm at high temperatures and 2mm at intermediate temperatures). During testing, one of the parallel plates is oscillated with respect to the other at pre-selected frequencies and rotational deformation amplitudes. The testing is performed keeping the strains small enough in order to conduct the measurement within the linear range of behavior of the binder. This linear viscoelastic region has to be determined for each binder, temperature, and geometry used. The test specimen is maintained at the test temperature to within +- 0.1 °C . Keeping a rigorous temperature control is of paramount importance since over most of the region of interest for specification testing, there is an approximately 20% variation in the shear complex modulus per degree C. Specification testing requires a test frequency of 10 rad/s, although frequency sweeps at different temperatures are conducted when the construction of the Mastercurve is required.

SHRP B-003 and AASHTO TP5 describe the test methodology to follow in order to obtain G* and δ at 10 rad/sec. and at different test temperatures. In the SHRP (AASHTO MP1) specifications, a minimum value of $G^*/\sin\delta$ is specified to control rutting, and a maximum value of $G^*.\sin\delta$ is specified to control fatigue. The frequency of 10 rad/sec is used to simulate moderate speed traffic.

The dynamic shear testing was conducted using a dynamic shear rheometer at high and medium temperature levels representative of service temperatures most commonly found in Texas. The following parameters considered as part of the SHRP specification, were analyzed:

- Value of G*/sin delta measured at the maximum pavement temperature on tank material (tenderness).
- Value of G*/sin delta measured at the maximum pavement temperature on RTFOT residue (rutting resistance).
- Value of G*.sin delta measured at the intermediate pavement temperature on PAV residue (fatigue resistance).

The dynamic shear testing was performed according to the SHRP protocol that calls for a frequency of 10 radians per second, and test temperatures related to the maximum and minimum pavement temperatures as indicated in the specification. The linear viscoelastic region was determined for every binder at each temperature by performing stress sweep tests. In reporting the results, other linear viscoelastic parameters such as storage and loss moduli, tan delta, delta, etc. as well as $G^*/\sin\delta$ and $G^*\sin\delta$ were also provided.

Low-temperature rheology analysis using the Bending Beam Rheometer

The low-temperature physical properties of the asphalt binders are characterized by using a prismatic specimen (dimensions: 120 x 10 x 10 mm) loaded in three-point bending with a constant load (the beam is supported at the ends and loaded in the center). The bending beam rheometer (SHRP B-002, AASHTO TP1) allows determination of the flexural creep stiffness of the binder at temperatures below 0°C and within the linear viscoelastic response range. The method is applicable to asphalt binders having flexural creep stiffness values from 30 MPa to 1 GPa.

The rheometer system consists of the rheometer unit, a temperature controlled bath, and a data acquisition system using a PC. The creep behavior of a binder at low temperatures can be monitored with the BBR, the deflection is monitored during 240

seconds while a load of 100 gms. is kept constant. This is particularly important at low temperatures where temperature dependency of the asphalts are similar, and time dependency is the main factor that makes one asphalt different from the other.

The low-temperature stiffness of the asphalt binder is related to the low-temperature thermal cracking in the pavement, and the slope of the log stiffness versus log temperature curve is related to low-temperature thermal shrinkage cracking, that can occur due to thermal cycling.

The test is conducted at the minimum pavement temperature plus 10°C by applying a constant load of 100 grams during 240 seconds. A maximum value is specified for the creep stiffness at the test temperature and at 60 seconds to control thermal cracking. A minimum value for the slope m of the log stiffness versus log time at 60 seconds is specified to control the rate at which the stiffness changes with time at low temperatures. A low creep stiffness coupled with a high m-value are desirable to avoid the accumulation of stresses to a level where low temperature cracking would occur.

A maximum value of the flexural creep stiffness along with a minimum value of the slope of the log S(t) versus log (t) curve are included in the SHRP binder specification in order to avoid thermal shrinkage cracking in the low temperature range. A maximum value of 300,000 kPa (300 MPa) is placed on creep stiffness as measured by the Bending Beam Rheometer (SHRP B-002) at 60 seconds and at a temperature 10°C higher than the minimum pavement temperature. The rate at which the asphalt binder stiffness changes at low temperatures is controlled by means of the m-value. An m-value greater than 0.30 is required in the SHRP specification.

The initial temperature for the low temperature measurements is guided by the temperature at which the loss modulus $G^*\sin\delta$ was measured. For instance, asphalt Control (Total) passed the fatigue criteria at 22°C, therefore the starting temperature for this binder for BBR is -18°C, which is the temperature below 22°C in the same column (SHRP Binder Specification) for grade PG 64-. However, the temperature at which the binder finally passed the Stiffness

requirement was -12°C.

A comparison between the measured and the calculated flexural creep stiffness was included as prescribed in the BBR protocol. The stiffness is first measured in the BBR and the results are plotted in a log-log chart. The plotted data over a limited testing time from 8 to 240 seconds can be represented by a second order polynomial. From this equation, and with the measured stiffness, the calculated stiffness can be obtained. The same applies for the m-value. Calculated and measured values should not be different in more than 1%. As seen in the tables, there is a very close agreement between measured and calculated values.
The limiting stiffness temperature concept is being used in the SHRP binder specifications as a mean of predicting low-temperature thermal shrinkage cracking in the pavement. In this case, the limiting stiffness temperature is the test temperature at which a limiting stiffness of 300 MPa is reached at 60 seconds loading time. Also, the value of the slope of the creep curve, m = dlogJ(t)/ dlog t, should be higher than 0.30 in order to avoid thermal cracking.

Short and Long-term accelerated aging of Asphalt Binders

Durability of an asphalt binder is a characteristic that describes its resistance to chemical and physical changes caused by environmental exposure. Asphalt binders harden as a result of irreversible oxidative aging and reversible stearic hardening. The first one is directly related to the chemistry of the binder and the changes produced as a consequence of the interaction of oxygen from the air with the chemical components in the binder. The second one is still not very well understood and is related to a physio-chemical process where strongly polar functional groups in the binder orient themselves into agglomerates resulting in a build up of a structure that stiffens the binder. The most important factor in the durability of an asphalt binder is its age-hardening process due to oxygen, solar radiation, temperatures and volumetric proportions in the asphalt mixture.

Two procedures were used to simulate the aging that takes

place in a binder during mixing and lay-down operations, and in-service: the Rolling Thin Film Oven Test (ASTM D 2872, AASHTO T 240) and the Pressure Aging Vessel Test (SHRP B-005, AASHTO PP1). The former reproduces the hardening (loss of volatiles) of the binder during the mixing operations while the latter simulates the oxidation of the binder on the road during the first 5 to 10 years of service life.

The Rolling Thin Film Oven Test is stipulated in the SHRP binder specification to be applied to the tank asphalt before it can be tested in the DSR for rutting resistance. The RTFOT residue is further aged by means of the PAV before it is tested in the DSR to measure fatigue cracking resistance, and in the BBR to measure low-temperature creep properties of the binder.

The pressure aging apparatus consists of an stainless steel pressure aging vessel and a temperature chamber. Air pressure is provided by a cylinder of dry, clean compressed air with a pressure regulator. The vessel accommodates 10 sample pans placed in a sample rack. A forced draft oven is used as a temperature chamber. The PAV is conducted for 20 hours in a vessel pressurized with air to 2.1 MPa and at different temperatures according to the binder grade.

TABLE B-1 SUMMARY OF SHRP SPECIFICATION TESTING FOR DISTRICT 10 ASPHALT BINDERS

Tests	Brookfield Viscosity mPa.s	DSR, °C			BBR °C	Class.
Conditioning	Tank	Tank	RTFOT	PAV	PAV	PG
Binder						
Control (TOTAL)	440	64	64	22	-12	**64-22**
SBR (Goodyear)	960	64	58	22	-12	**64-22**
SBS (Elf)	840	64	64	22	-12	**64-22**
EVA (Exxon)	380	58	58	16	-18	**58-28**
SBS (Shell)	480	58	58	19	-18	**58-28**

TABLE B-2 LINEAR-VISCOELASTIC PROPERTIES OF THE ASPHALT BINDERS AS MEASURED BY THE DSR (DISTRICT 10 — TANK)

Cond.	Tank				
Binder	Control (Total)	SBR (Goodyear)	SBS (Elf)	EVA (Exxon)	SBS (Shell)
Test Temp. deg.C	64	64	64	58	58
G*,kPa	1.04	1.12	1.57	1.85	1.71
G',kPa	0.05	0.12	0.32	0.73	0.37
G",kPa	1.04	1.11	1.54	1.70	1.55
δ,°	87	84	78	67	76
sinδ	1.00	1.00	0.98	0.92	0.97
G*/sinδ kPa	**1.04**	**1.12**	**1.60**	**2.01**	**1.76**
tanδ	20.00	9.25	4.81	2.33	4.19

TABLE B-3 LINEAR-VISCOELASTIC PROPERTIES OF THE ASPHALT BINDERS AS MEASURED BY THE DSR (DISTRICT 10 — RTFOT)

Cond.	RTFOT				
Binder	Control (Total)	SBR (Goodyear)	SBS (Elf)	EVA (Exxon)	SBS (Shell)
Test Temp. deg.C	64	58	64	58	58
G*,kPa	2.73	4.16	2.97	2.53	2.89
G',kPa	0.26	0.59	0.73	0.39	0.62
G",kPa	2.71	4.11	2.88	2.50	2.83
δ,°	85	82	76	81	77
sinδ	1.00	0.99	0.97	0.99	0.97
G*/sinδ kPa	**2.73**	**4.20**	**3.06**	**2.56**	**2.98**
tanδ	10.42	6.97	3.96	6.41	4.57

TABLE B-4 LINEAR-VISCOELASTIC PROPERTIES OF THE ASPHALT BINDERS AS MEASURED BY THE DSR (DISTRICT 10 — PAV)

Cond.	PAV				
Binder	Control (Total)	SBR (Goodyear)	SBS (Elf)	EVA (Exxon)	SBS (Shell)
Test Temp. deg.C	22	22	22	16	19
G*,MPa	6.44	5.53	5.26	4.43	5.41
G',MPa	4.61	3.28	2.85	3.05	3.15
G",MPa	4.49	4.45	4.42	3.22	4.39
δ,°	44	54	57	47	54
sinδ	0.70	0.81	0.84	0.73	0.81
G*.sinδ MPa	**4.47**	**4.47**	**4.41**	**3.24**	**4.38**
tanδ	0.97	1.36	1.55	1.06	1.39

TABLE B-5 FLEXURAL CREEP STIFFNESS AS MEASURED BY THE BENDING BEAM RHEOMETER (DISTRICT 10)

Asphalt binder	Test Temperature,° C	Stiffness, MPa,60sec.		m-value 60 sec.	
		M[1]	C[2]	M[1]	C[2]
Control (Total)	-12	171	170.5	0.31	0.305
SBR (Goodyear)	-12	212	211.2	0.33	0.332
SBS (Elf)	-12	228	227.0	0.35	0.348
EVA (Exxon)	-18	242	241.5	0.32	0.322
SBS (Shell)	-18	286	285.3	0.31	0.318

Notes:

1: Measured Stiffness and m-value by the BBR

2: Calculated Stiffness and m-value by a second degree polynomial equation according to SHRP B-002 (AASHTO TP1).

TABLE B-6 SUMMARY OF SHRP SPECIFICATION TESTING FOR DISTRICT 11 ASPHALT BINDERS

Tests	BrookfieldViscosity,mPa.s	DSR, ° C			BBR ° C	Class.
Conditioning / Binder	Tank	Tank	RTFOT	PAV	PAV	PG
Control (Texaco)	640	64	64	19	-18	**64-28**
SBR (Goodyear)	1340	64	64	19	-12	**64-22**
SBS (Elf)	760	70	70	22	-12	**70-22**

TABLE B-7 LINEAR-VISCOELASTIC PROPERTIES OF THE ASPHALT BINDERS AS MEASURED BY THE DSR (DISTRICT 11 — TANK)

Cond.	Tank		
Binder	Control (Texaco)	SBR (Goodyear)	SBS (Elf)
Test Temp. deg.C	64	64	70
G*,kPa	1.63	1.21	1.14
G',kPa	0.37	0.26	0.07
G",kPa	1.58	1.18	1.13
δ,°	77	78	86
sinδ	0.97	0.98	1.00
G*/sinδ kPa	**1.68**	**1.23**	**1.14**
tanδ	4.27	4.54	16.14

TABLE B-8 LINEAR-VISCOELASTIC PROPERTIES OF THE ASPHALT BINDERS AS MEASURED BY THE DSR (DISTRICT 11 — RTFOT)

Cond.	RTFOT		
Binder	Control (Texaco)	SBR (Goodyear)	SBS (Shell)
Test Temp. deg.C	64	64	70
G*,kPa	2.41	2.22	2.40
G',kPa	0.59	0.39	0.27
G",kPa	2.34	2.17	2.38
δ,°	76	80	84
sinδ	0.97	0.98	0.99
G*/sinδ kPa	**2.49**	**2.27**	**2.42**
tanδ	3.97	5.56	8.81

TABLE B-9 LINEAR-VISCOELASTIC PROPERTIES OF THE ASPHALT BINDERS AS MEASURED BY THE DSR (DISTRICT 11 — PAV)

Cond.	PAV		
Binder	Control (Texaco)	SBR (Goodyear)	SBS (Elf)
Test Temp. deg.C	19	19	22
G*,kPa	5.90	6.47	5.19
G',kPa	3.57	4.82	3.59
G",kPa	4.70	4.31	3.74
δ,°	53	42	46
sinδ	0.80	0.67	0.72
G*.sinδ kPa	**4.71**	**4.33**	**3.73**
tanδ	1.32	0.89	1.04

TABLE B-10 FLEXURAL CREEP STIFFNESS AS MEASURED BY THE BENDING BEAM RHEOMETER (DISTRICT 11)

Asphalt binder	Test Temperature,° C	Stiffness, MPa 60 sec.		m-value 60 sec.	
		M[1]	C[2]	M[1]	C[2]
Control (Texaco)	-18	298	295.7	0.31	0.322
SBR (Goodyear)	-12	200	198.5	0.31	0.307
SBS (Elf)	-12	165	165.2	0.33	0.327

Notes:

1. Measured Stiffness and m-value by the BBR.
2. Calculated Stiffness and m-value by a second degree polynomial equation according to SHRP B-002 (AASHTO TP1).

TABLE B-11 SUMMARY OF SHRP SPECIFICATION TESTING FOR DISTRICT 15 ASPHALT BINDERS

Tests	BrookfieldViscosity,mPa.s	DSR, °C			BBR °C	Class.
Conditioning / Binder	Tank	Tank	RTFOT	PAV	PAV	PG
Control (TFA)	480	64	64	25	-6	**64-16**
SBR (Goodyear)	500	58	58	19	-12	**58-22**
SBR (Polysar)	520	64	64	19	-12	**64-22**
EVA (Exxon)	960	70	70	19	-6	**70-16**
SBR/Polyolef (Dow)	1280	70	70	19	-6	**70-16**

TABLE B-12 LINEAR-VISCOELASTIC PROPERTIES OF THE ASPHALT BINDERS AS MEASURED BY THE DSR (DISTRICT 15 — TANK)

Cond.	Tank				
Binder	Control (TFA)	SBR (Goodyear)	SBR (Polysar)	EVA (Exxon)	SBR/P (Dow)
Test Temp. deg.C	64	58	64	70	70
G*,kPa	1.68	1.48	1.05	1.35	1.46
G',kPa	0.13	0.18	0.12	0.20	0.21
G",kPa	1.68	1.46	1.04	1.34	1.45
δ,°	86	83	83	82	82
$\sin\delta$	1.00	0.99	0.99	0.99	0.99
$G^*/\sin\delta$ kPa	**1.68**	**1.50**	**1.06**	**1.36**	**1.47**
$\tan\delta$	12.92	8.11	8.67	6.70	6.90

TABLE B-13 LINEAR-VISCOELASTIC PROPERTIES OF THE ASPHALT BINDERS AS MEASURED BY THE DSR (DISTRICT 15 — RTFOT)

Cond.	RTFOT				
Binder	Control (TFA)	SBR (Goodyear)	SBR (Polysar)	EVA (Exxon)	SBR/P (Dow)
Test Temp. deg.C	64	58	64	70	70
G*,kPa	4.54	4.50	2.29	5.19	5.62
G',kPa	0.70	0.96	0.42	1.87	1.93
G",kPa	4.48	4.39	2.25	4.85	5.27
δ,°	81	78	80	69	70
sinδ	0.99	0.98	0.99	0.93	0.94
G*/sinδ kPa	**4.48**	**4.59**	**2.26**	**5.58**	**5.99**
tanδ	6.40	4.57	5.36	2.59	2.73

TABLE B-14 LINEAR-VISCOELASTIC PROPERTIES OF THE ASPHALT BINDERS AS MEASURED BY THE DSR (DISTRICT 15 — PAV)

Cond.	PAV				
Binder	Control (TFA)	SBR (Goodyear)	SBR (Polysar)	EVA (Exxon)	SBR/P (Dow)
Test Temp. deg.C	25	19	19	19	19
G*,MPa	6.24	5.96	6.25	8.05	8.55
G',MPa	4.74	4.53	4.09	6.73	7.26
G",MPa	4.06	3.87	4.09	4.40	4.51
δ,°	41	40	41	33	32
sinδ	0.66	0.66	0.66	0.55	0.53
G*.sinδ MPa	**4.12**	**3.93**	**4.13**	**4.43**	**4.53**
tanδ	0.86	0.85	1.00	0.65	0.62

TABLE B-15 FLEXURAL CREEP STIFFNESS AS MEASURED BY THE BENDING BEAM RHEOMETER (DISTRICT 15)

Asphalt binder	Test Temperature, ° C	Stiffness, MPa 60 sec.		m-value 60 sec.	
		M[1]	C[2]	M[1]	C[2]
Control (TFA)	-6	96	95.4	0.33	0.331
SBR (Goodyear)	-12	126	125.0	0.32	0.331
SBR (Polysar)	-12	125	124.7	0.33	0.342
EVA (Exxon)	-6	70	69.5	0.32	0.341
SBR/Polyolefin(Dow)	-6	78	77.6	0.30	0.301

Notes:

1. Measured Stiffness and m-value by the BBR.
2. Calculated Stiffness and m-value by a second degree polynomial equation according to SHRP B-002 (AASHTO TP1).

TABLE B-16 SUMMARY OF SHRP SPECIFICATION TESTING FOR DISTRICT 25 ASPHALT BINDERS

Tests	BrookfieldViscosity,mPa.s	DSR, ° C			BBR ° C	Class.
Conditioning / Binder	Tank	Tank	RTFOT	PAV	PAV	PG
Control (Shamrock)	640	64	64	19	-12	**64-22**
SBS (Elf)	780	64	64	22	-12	**64-22**
SBS,3% (Shell)	580	64	64	22	-12	**64-22**
SBS,6% (Shell)	980	70	64	16	-18	**64-28**

TABLE B-17 LINEAR-VISCOELASTIC PROPERTIES OF THE ASPHALT BINDERS AS MEASURED BY THE DSR (DISTRICT 25 — TANK)

Cond.

	Tank			
Binder	Control (Shamrock)	SBS (Elf)	SBS,3% (Shell)	SBS,6% (Shell)
Test Temp. deg.C	64	64	64	70
G*,kPa	1.21	1.34	1.37	1.32
G',kPa	0.06	0.35	0.43	0.88
G",kPa	1.21	1.30	1.30	0.99
δ,°	87	75	72	48
sinδ	1.00	0.96	0.95	0.74
G*/sinδ kPa	**1.21**	**1.40**	**1.30**	**1.78**
tanδ	20.17	3.71	3.02	1.13

TABLE B-18 LINEAR-VISCOELASTIC PROPERTIES OF THE ASPHALT BINDERS AS MEASURED BY THE DSR (DISTRICT 25 — RTFOT)

Cond.

	RTFOT			
Binder	Control (Shamrock)	SBS (Elf)	SBS,3% (Shell)	SBS,6% (Shell)
Test Temp. deg.C	64	64	64	64
G*,kPa	2.57	2.53	2.51	2.66
G',kPa	0.26	0.80	0.70	1.31
G",kPa	2.55	2.40	2.41	2.32
δ,°	84	72	74	61
sinδ	1.00	0.95	0.96	0.88
G*/sinδ kPa	**2.57**	**2.67**	**2.62**	**3.02**
tanδ	9.81	3.00	3.44	1.77

TABLE B-19 LINEAR-VISCOELASTIC PROPERTIES OF THE ASPHALT BINDERS AS MEASURED BY THE DSR (DISTRICT 25 — PAV)

Cond.	PAV			
Binder	Control (Shamrock)	SBS (Elf)	SBS,3% (Shell)	SBS,6% (Shell)
Test Temp. deg.C	19	22	22	16
G*,MPa	6.99	5.30	4.41	5.81
G',MPa	5.53	3.54	2.98	4.23
G",MPa	4.28	3.94	3.25	3.99
δ,°	38	48	47	43
sinδ	0.62	0.74	0.73	0.68
G*.sinδ MPa	**4.30**	**3.94**	**3.23**	**3.96**
tanδ	0.77	1.11	1.09	0.94

TABLE B-20 FLEXURAL CREEP STIFFNESS AS MEASURED BY THE BENDING BEAM RHEOMETER (DISTRICT 25)

Asphalt binder	Test Temperature,° C	Stiffness,MPa 60 sec.		m-value 60 sec.	
		M[1]	C[2]	M[1]	C[2]
Control (Shamrock)	-12	168	167.5	0.30	0.317
SBS (Elf)	-12	173	172.5	0.33	0.352
SBS,3% (Shell)	-12	181	179.0	0.31	0.307
SBS,6% (Shell)	-18	207	207.3	0.31	0.317

Notes:

1. Measured Stiffness and m-value by the BBR
2. Calculated Stiffness and m-value in accordance with SHRP B-002 (AASHTO TP1)

TABLE B-21 SUMMARY OF SHRP SPECIFICATION TESTING FOR DISTRICT 17 ASPHALT BINDERS

Tests	BrookfieldViscosity,mPa.s	DSR, ° C			BBR ° C	Class.
Conditioning	Tank	Tank	RTFOT	PAV	PAV	PG
Binder						
Control (Fina)	320	58	58	22	-12	**58-22**
SBR (Goodyear)	620	58	58	19	-12	**58-22**
SBS (Shell)	460	58	58	16	-18	**58-28**
SBS (Elf)	560	58	58	19	-18	**58-28**

TABLE B-22 LINEAR-VISCOELASTIC PROPERTIES OF THE ASPHALT BINDERS AS MEASURED BY THE DSR (DISTRICT 17 — TANK)

Cond.

	Tank			
Binder	Control (Fina)	SBR (Goodyear)	SBS (Shell)	SBS (Elf)
Test Temp. deg.C	58	58	58	58
G*,kPa	1.30	1.26	1.47	1.63
G',kPa	0.02	0.08	0.32	0.34
G",kPa	1.30	1.26	1.44	1.59
δ,°	89	86	78	78
sinδ	1.00	1.00	0.98	0.98
G*/sinδ kPa	**1.30**	**1.26**	**1.50**	**1.66**
tanδ	65.00	15.75	4.50	4.68

TABLE B-23 LINEAR-VISCOELASTIC PROPERTIES OF THE ASPHALT BINDERS AS MEASURED BY THE DSR (DISTRICT 17 — RTFOT)

Cond.	RTFOT			
Binder	Control (Fina)	SBR (Goodyear)	SBS (Shell)	SBS (Elf)
Test Temp. deg.C	58	58	58	58
G*,kPa	2.40	2.26	2.44	2.65
G',kPa	0.08	0.16	0.53	0.64
G",kPa	2.40	2.25	2.39	2.58
δ,°	88	86	78	76
sinδ	1.00	1.00	0.98	0.97
G*/sinδ kPa	**2.40**	**2.26**	**2.49**	**2.73**
tanδ	30.00	14.06	4.51	4.03

TABLE B-24 LINEAR-VISCOELASTIC PROPERTIES OF THE ASPHALT BINDERS AS MEASURED BY THE DSR (DISTRICT 17 — PAV)

Cond.

	PAV			
Binder	Control (Fina)	SBR (Goodyear)	SBS (Shell)	SBS (Elf)
Test Temp. deg.C	22	19	16	19
G*,MPa	5.51	5.14	5.57	3.94
G',MPa	2.95	2.75	3.35	2.07
G",MPa	4.66	4.34	4.45	3.36
δ,°	58	58	53	58
sinδ	0.85	0.85	0.80	0.85
G*.sinδ MPa	**4.67**	**4.37**	**4.45**	**3.35**
tanδ	1.58	1.58	1.33	1.62

TABLE B-25 FLEXURAL CREEP STIFFNESS AS MEASURED BY THE BENDING BEAM RHEOMETER (DISTRICT 17)

Asphalt binder	Test Temperature,° C	Stiffness, MPa 60 sec.		m-value 60 sec.	
		M[1]	C[2]	M[1]	C[2]
Control (Fina)	-12	229	227.9	0.35	0.368
SBR (Goodyear)	-12	172	172.0	0.39	0.413
SBS (Shell)	-18	217	216.2	0.34	0.358
SBS (Elf)	-18	282	279.1	0.33	0.332

Notes:

1. Measured Stiffness and m-value by the BBR
2. Calculated Stiffness and m-value in accordance with SHRP B-002 (AASHTO TP1)

TABLE B-26 PAVEMENT TEMPERATURES FOR TxDOT DISTRICTS FOR PROJECT 1306

County	Station	D	Max. Temp. °C	Min. Temp. °C	PG
Bexar	San Antonio WSFO	15	61.8	-15	64-16
Angelina	Lufkin FAA AP	11	61.8	-15	64-16
Childress	Childress 3W	25	63.4	-23	64-28
Smith	Tyler	10	61.3	-17	64-22
Brazos	College Station 6W	17	62.4	-19	64-22
Brazos	College Station FAA AP	17	61.7	-17	64-22

D = District
Max.Temp. = maximum pavement temperature at the 20 mm depth
Min.Temp. = minimum pavement temperature at the surface
PG = performance grade asphalt

TABLE B-27 SHRP GRADING OF POLYMER-MODIFIED ASPHALT BINDERS AND SUMMARY OF FIELD OBSERVATIONS FOR DIFFERENT FIELD PROJECTS

District	Location	Polymer	Asphalt Grade	Source	Req'd PG (1)	Meas. PG (2)	G* sind MPa	Temp. C G*sind	Field Observation	PAV., AGE YEAR
10	Tyler	None	AC-20	TOTAL	64-22	64-22	4.38	19	Slight Rut, No Crack	3
10	Tyler	Goodyear,SBR,Latex	AC-10	FINA	64-22	64-22	4.47	22	No Rut, No Crack	3
10	Tyler	Elf,SBS,Styrelf	AC-10	FINA	64-22	64-22	4.41	22	No Rut, No Crack	3
10	Tyler	Shell,SBS,Kraton	AC-10	FINA	64-22	58-16 / 28	4.47	22	Slight Rut, No Crack	3
10	Tyler	Exxon,EVA,Polybilt	AC-10	FINA	64-22	58-28	3.24	16	Slight Rut, No Crack	3
11	Lufkin	None	AC-20	TEXACO	64-16	64-28	4.71	19	Tight Longitudinal & Horizontal Cracks	4
11	Lufkin	Goodyear,SBR,Latex	AC-10	TEXACO	64-16	64-22	4.33	19	Mostly Horizontal Cracks, Not much Logitudinal	4
11	Lufkin	Elf,SBS,Styrelf	AC-10	TEXACO	64-16	70-22	3.73	22	Longitudinal & Horizontal Cracks Going to Alligator	4
15	San Anto	None	AC-20	TFA	64-16	64-16	4.12	25	Heavy Longitudinal & Horizontal Cracks, Edge Ravel	6
15	San Anto	Goodyear,SBR,Latex	AC-10	TFA	64-16	58-22	3.93	19	Slight Rutting, Horizontal & Longitudinal Map Cracks	6
15	San Anto	Elf,SBS,Styrelf	AC-10	TFA	64-16	**** (3)	**** (3)	**** (3)	No Apparent Crack, Only Surface Polish	6
15	San Anto	Exxon,EVA,Polybilt	AC-20	TFA	64-16	70-16	4.43	19	Severe Horizontal, Logintudinal, and Aligator Cracks	6
15	San Anto	Crafco,Rubber,Genstar	AC-10	TFA	64-16	**** (3)	**** (3)	**** (3)	Slight Longitudinal and Transverse Cracks, More Longi	6
15	San Anto	Polysar,SBR,Latex	AC-10	TFA	64-16	64-22	4.13	19	Good Surface,Faint Transverse Crack	6
15	San Anto	Fiber	AC-10	TFA	64-16	**** (3)	**** (3)	**** (3)	Widespread Transverse & Longitudinal Cracks	6
15	San Anto	DOW,SBR,Polyolefin	AC-20	TFA	64-16	70-16	4.53	19	Badly Cracked, Transverse, Longitudinal to Alligator	6
25	Childress	None	AC-20	SHAMRAK	64-28	64-22	4.30	19	Small Longitudinal Cracks in Outside Wheel Path	4.5
25	Childress	Goodyear,SBR,Latex	AC-10	FINA	64-28	**** (3)	**** (3)	**** (3)	Longitudinal Cracks in Outside Wheel Patth,Minor Rut	4.5
25	Childress	Elf,SBS,Styrelf	AC-10	FINA	64-28	64-22	3.94	22	Good Shape, No Rut, No Crack	4.5
25	Childress	Shell,SBS,Kraton,3%	AC-10	FINA	64-28	64-22	3.23	22	Good Shape, No Rut, No Crack	4.5
25	Childress	Shell,SBS,Kraton,6%	AC-10	FINA	64-28	64-28	3.96	16	General Good Shape, A few Alligator Cracks	4.5

NOTES:

(1) Req'd PG: Required binder grade is based on averaged highest 7-day maximum daily temperature+2*std.dev. at 20 mm depth and average lowest temperature+2*std.dev. at the surface.

(2) Meas. PG: Measured binder grade is based on SHRP binder testing on the retained original asphalts.

(3) Cells filled with *** indicate that the original binder was not available for SHRP testing.

SHRP Binder Specification (AASHTO MP1)

Performance Grade	PG 46			PG 52							PG 58					PG 64				
	34	40	46	10	16	22	28	34	40	46	16	22	28	34	40	16	22	28	34	40
Average 7-day Maximum Pavement Design Temperature, °C[a]	<46			<52							<58					<64				
Minimum Pavement Design Temperature, °C[a]	>-34	>-40	>-46	>-10	>-16	>-22	>-28	>-34	>-40	>-46	>-16	>-22	>-28	>-34	>-40	>-16	>-22	>-28	>-34	>-40
Original Binder																				
Flash Point Temp, AASHTO T48: Min., °C	230																			
Viscosity, ASTM D 4402:[b] Max, 3 Pa-s (3000 cP) Test Temp, °C	135																			
Dynamic Shear, TP 5:[c] G*/sin δ, Min, 1.0 kPa Test Temp @ 10 rad/s, °C	46			52							58					64				
Rolling Thin Film Oven Residue (AASHTO T 240)																				
Mass Loss, Max, percent	1.00																			
Dynamic Shear, TP 5: G* /sin δ, Min, 2.2 kPa Test Temp @ 10 rad/s, °C	46			52							58					64				
Pressure Aging Vessel Residue (AASHTO PP 1)																				
PAV Aging Temperature, °C	90			90							100					100				
Dynamic Shear, AASHTO TP 5: G* sin δ, Max, 5,000 kPa Test Temp @ 10 rad/s, °C	10	7	4	25	22	19	16	13	10	7	25	22	19	16	13	28	25	22	19	16
Physical Hardening[e]	Report																			
Creep Stiffness, AASHTO TP 1:[f] S, Max, 300 MPa, m - value, Min, 0.30 Test Temp @ 60s, °C	-24	-30	-36	0	-6	-12	-18	-24	-30	-36	-6	-12	-18	-24	-30	-6	-12	-18	-24	-30
Direct Tension, AASHTO TP 3:[f] Failure Strain, Min, 1.0% Test Temp @1.0 mm/min, °C	-24	-30	-36	0	-6	-12	-18	-24	-30	-36	-6	-12	-18	-24	-30	-6	-12	-18	-24	-30

Notes:

a Pavement temperatures can be estimated from air temperatures using an algorithm contained in the SUPERPAVE software may be provided by the specifying agency, or by following the procedures as outlined in PPX.

b This requirement may be waived at the discretion of the specifying agency if the supplier warrants that the asphalt binder can be adequately pumped and mixed at temperatures that meet all applicable safety standards.

c For quality control of unmodified asphalt cement production, measurement of the viscosity of the original asphalt cement may be substituted for dynamic shear measurements of G*/sin δ at test temperatures where the asphalt is a Newtonian fluid. Any suitable standard means of viscosity measurement may be used, including capillary or rotational viscometry (AASHTO T201 or T202).

d The PAV aging temperature is based on simulated climatic conditions and is one of three temperatures 90°C, 100°C or 110°C. The PAV aging temperature is 100°C for PG 64- and above, except in desert climates, where it is 110°C.

e Physical Hardening—TP1 is performed on a set of asphalt beams according to Section 13.1, except the conditioning time is extended to 24 hrs± 10 minutes at 10°C above the minimum performance temperature. The 24-hour stiffness and m-value are reported for information puposes only.

f If the creep stiffness is below 300 MPa, the direct tension test is not required. If the creep stiffness is between 300 and 600 MPa the direct tension failure strain requirement can be used in lieu of the creep stiffness requirement. The m-value requirement must be satisfied in both cases.

Figure B-1 Performance-based asphalt binder specification

SHRP Binder Specification (AASHTO MP1)

Performance Grade	PG 70						PG 76					PG 82				
	10	16	22	28	34	40	10	16	22	28	34	10	16	22	28	34
Average 7-day Maximum Pavement Design Temperature, °C [a]	<70						<76					<82				
Minimum Pavement Design Temperature, °C [a]	>-10	>-16	>-22	>-28	>-34	>-40	>-10	>-16	>-22	>-28	>-34	>-10	>-16	>-22	>-28	>-34
Original Binder																
Flash Point Temp, AASHTO T48: Min., °C	230															
Viscosity, ASTM D 4402: [b] Max, 3 Pa-s (3000 cP) Test Temp, °C	135															
Dynamic Shear, TP 5: [c] G*/sin δ, Min, 1.0 kPa Test Temp @ 10 rad/s, °C	70						76					82				
Rolling thin film oven (T240)																
Mass Loss, Max, percent	1.00															
Dynamic Shear, TP 5: G* /sin δ, Min, 2.2 kPa Test Temp @ 10 rad/s, °C	70						76					82				
PAV Aging Temperature, °C	100(110)						100(110)					100(110)				
Dynamic Shear, AASHTO TP 5: G* sin δ, Max, 5,000 kPa Test Temp @ 10 rad/s, °C	34	31	28	25	22	19	37	34	31	28	25	40	37	34	31	28
Physical Hardening [e]	**Report**															
Creep Stiffness, AASHTO TP 1: [f] S, Max, 300 MPa, m - value, Min, 0.30 Test Temp @ 60s, °C	0	-6	-12	-18	-24	-30	0	-6	-12	-18	-24	0	-6	-12	-18	-24
Direct Tension, AASHTO TP 3: [f] Failure Strain, Min, 1.0% Test Temp @1.0 mm/min, °C	0	-6	-12	-18	-24	-30	0	-6	-12	-18	-24	0	-6	-12	-18	-24

Figure B-1 Performance-based asphalt binder specification (continued)

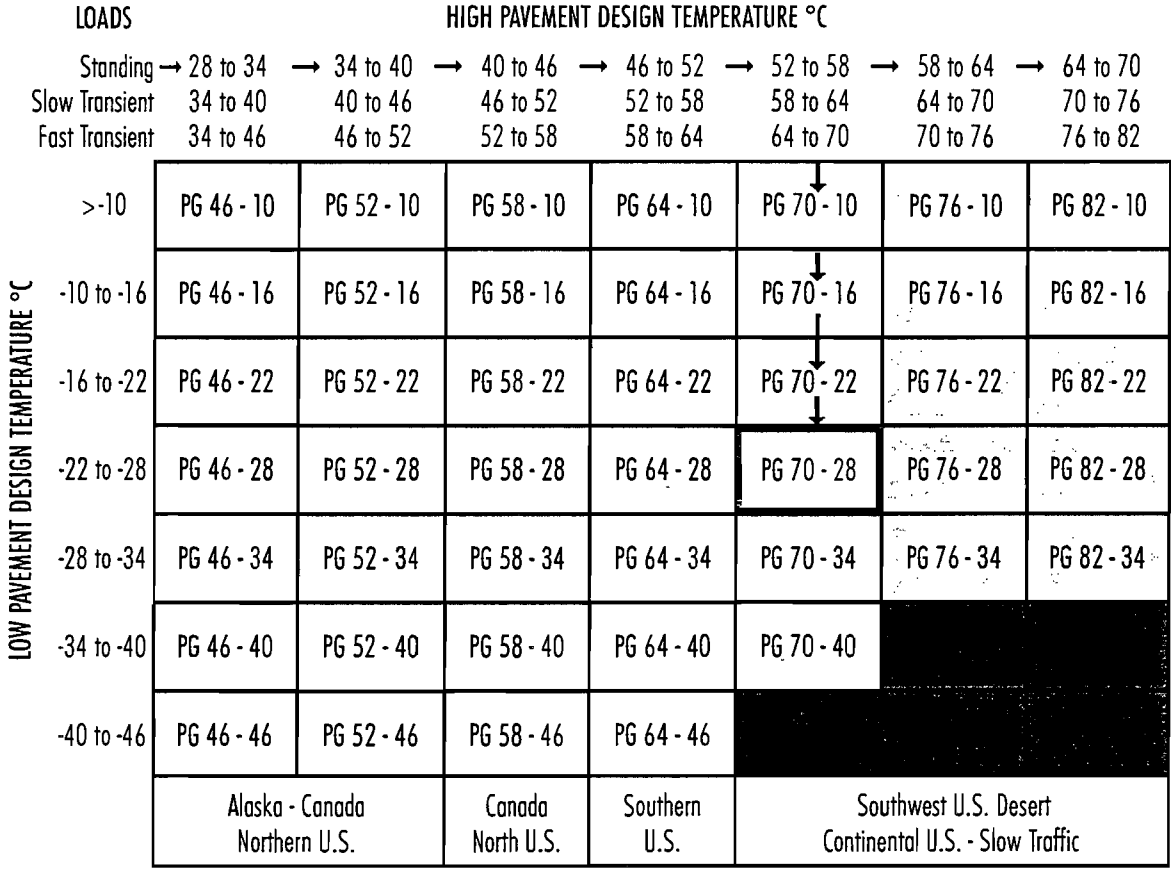

1. Select the type of loading.
2. Move horizontally to the high pavement design temperature.
3. Move down to the low pavement design temperature.
4. Identify the binder grade.

☐ Prevalent North American Grades

Example: Standing Load, High Design Temperature = 57 °C
Low Design Temperature = -25 °C
Grade = PG 70 - 28

Figure B-2 Recommendation for selecting binder performance grades

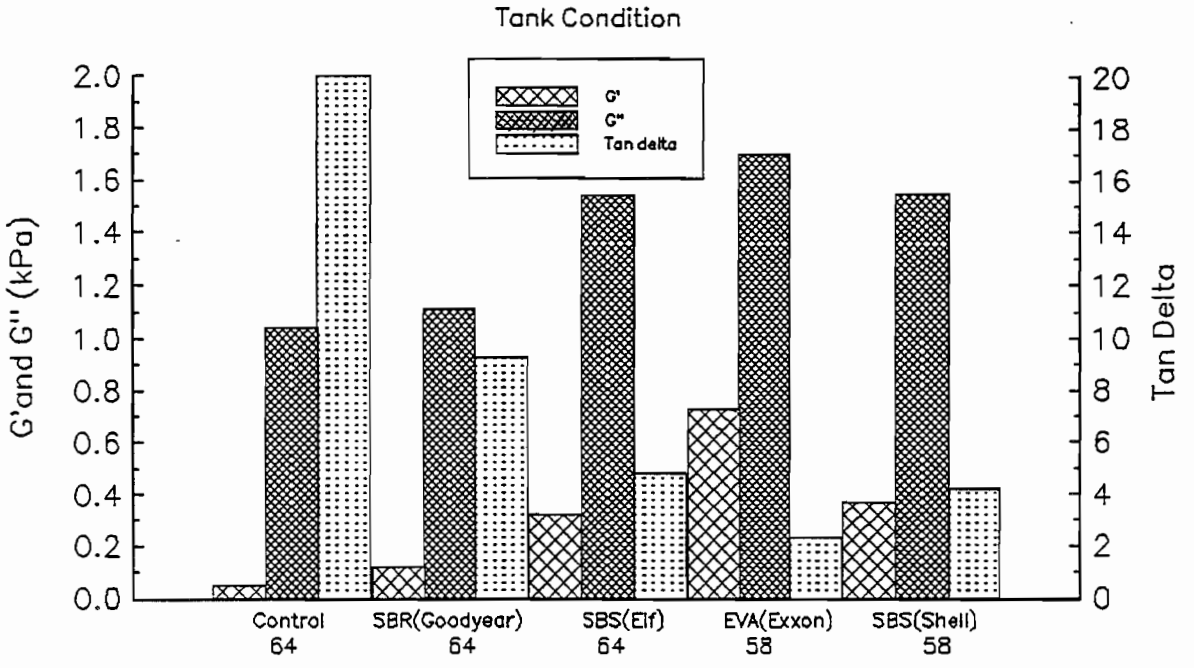

Figure B-3 Storage, loss modulus, and tan delta for District 10 binders (tank condition)

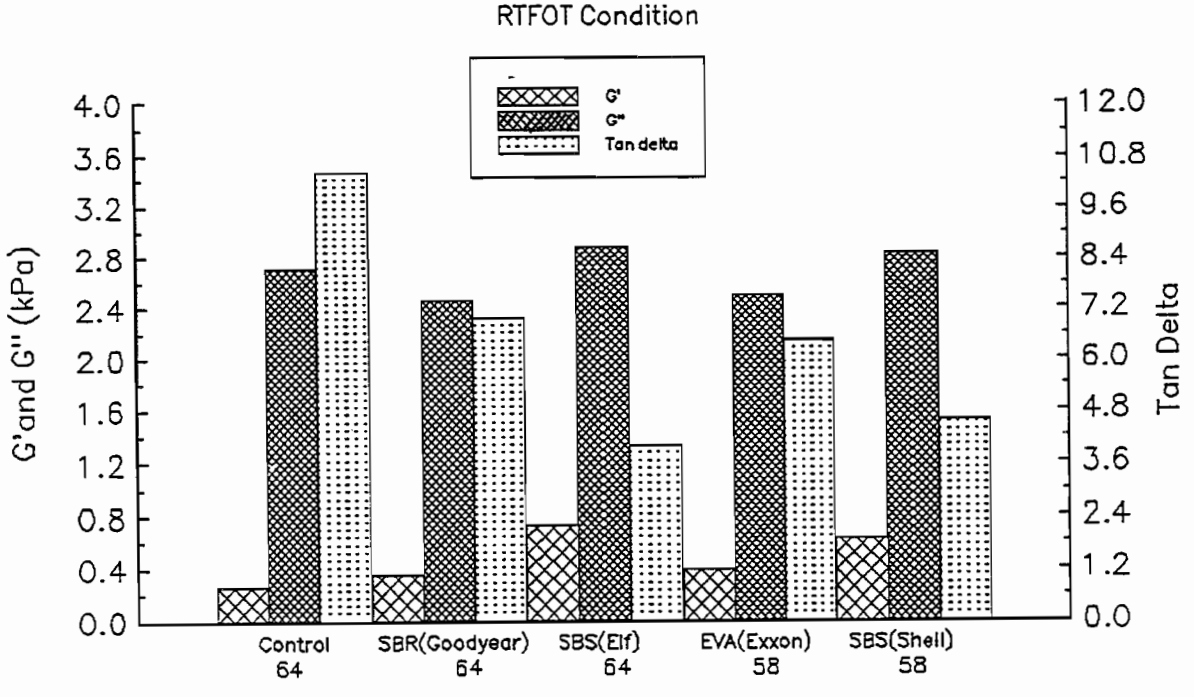

Figure B-4 Storage, loss modulus, and tan delta for District 10 binders (RTFOT condition)

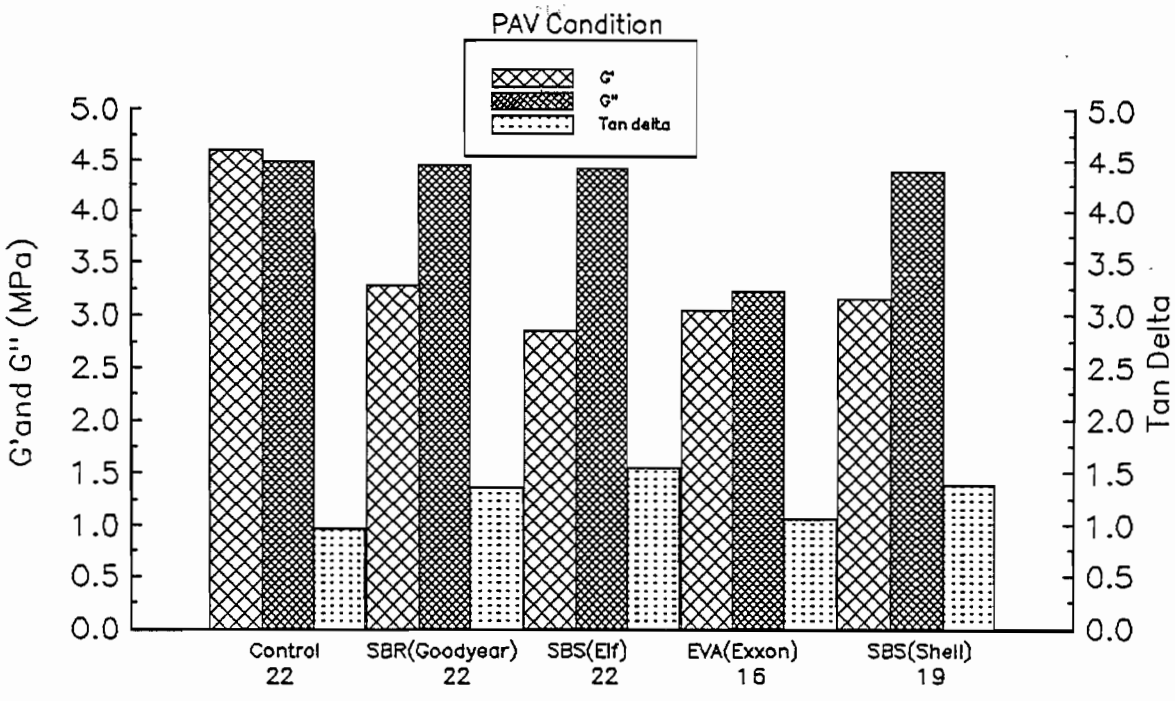

Figure B-5 Storage, loss modulus, and tan delta for District 10 binders (PAV condition)

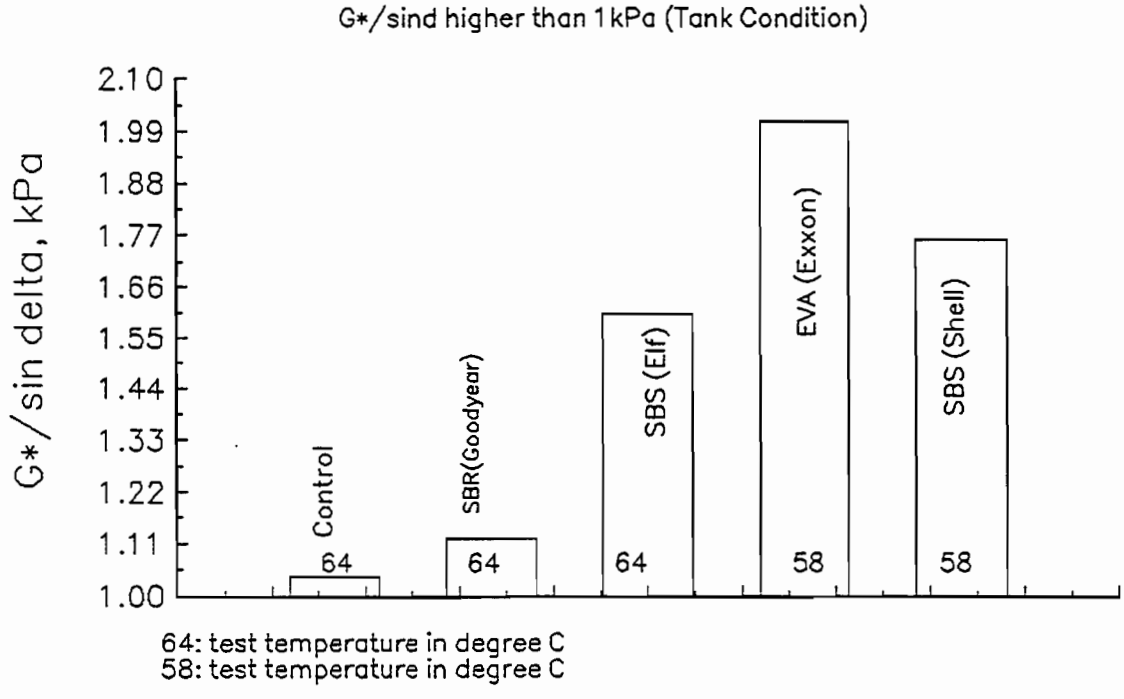

Figure B-6 Ranking of District 10 binders (tank condition)

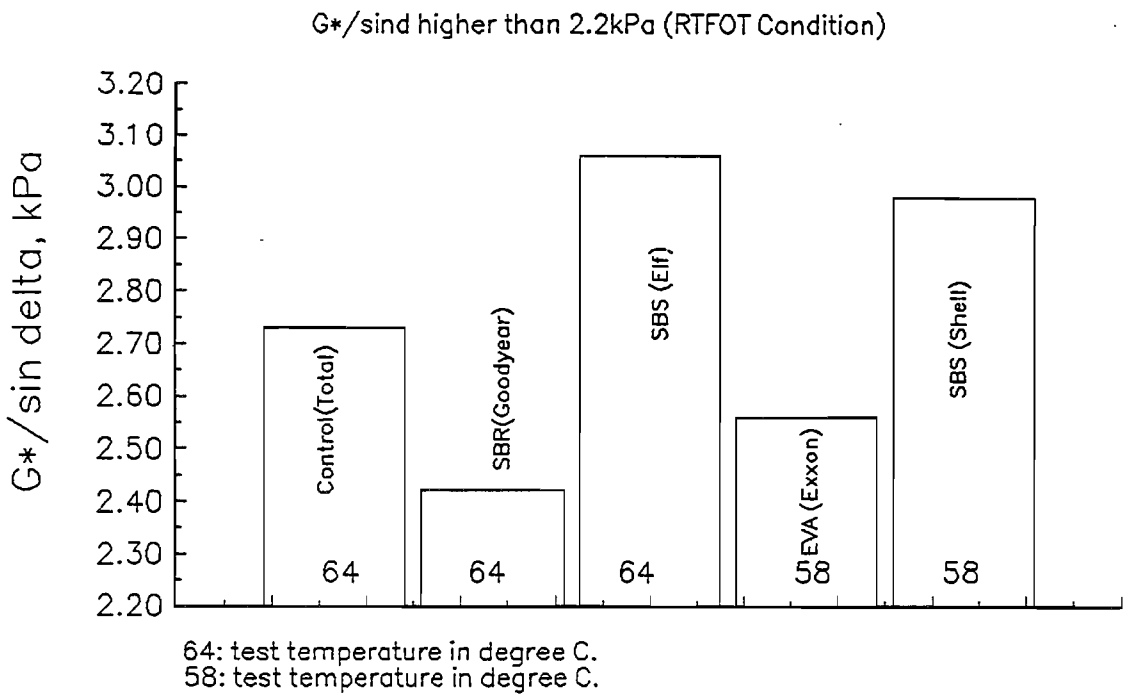

Figure B-7 Ranking of District 10 binders (RTFOT condition)

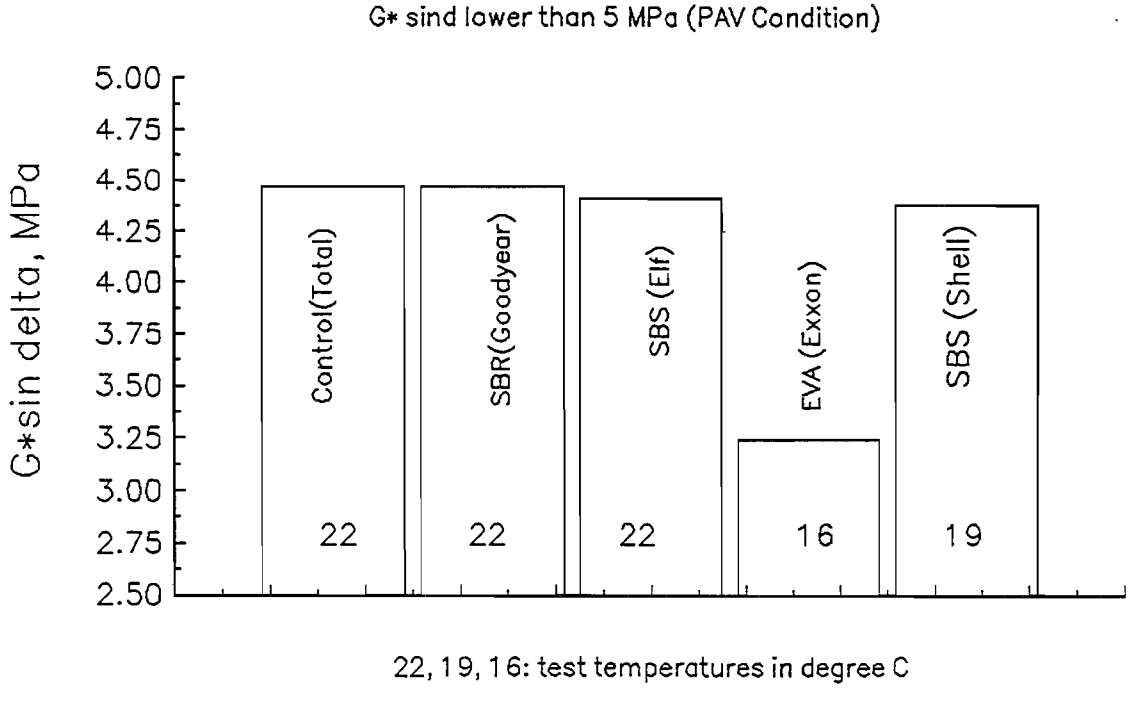

Figure B-8 Ranking of District 10 binders (PAV condition)

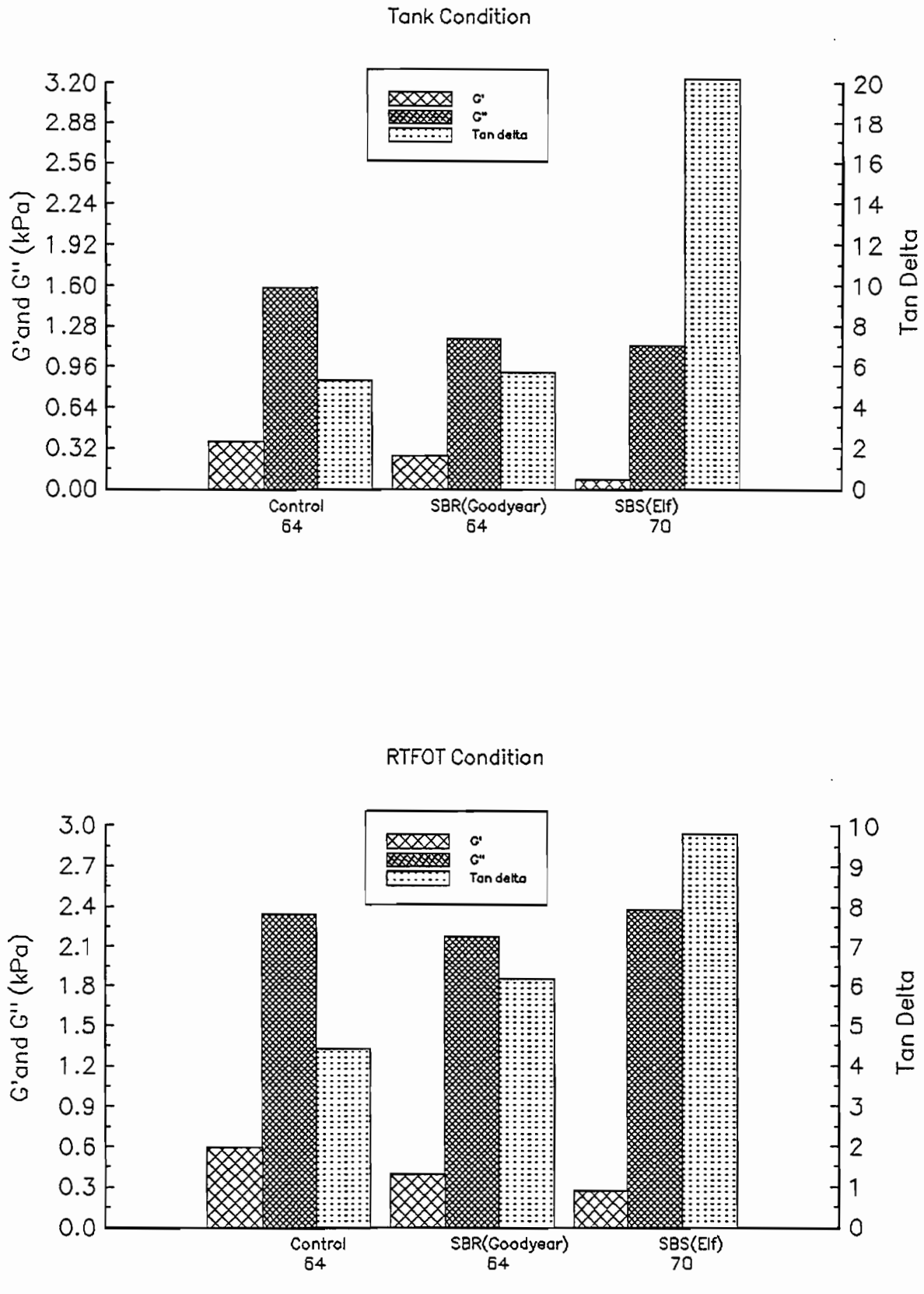

Figure B-10 Storage, loss modulus, and tan delta for District 11 binders (RTFOT condition)

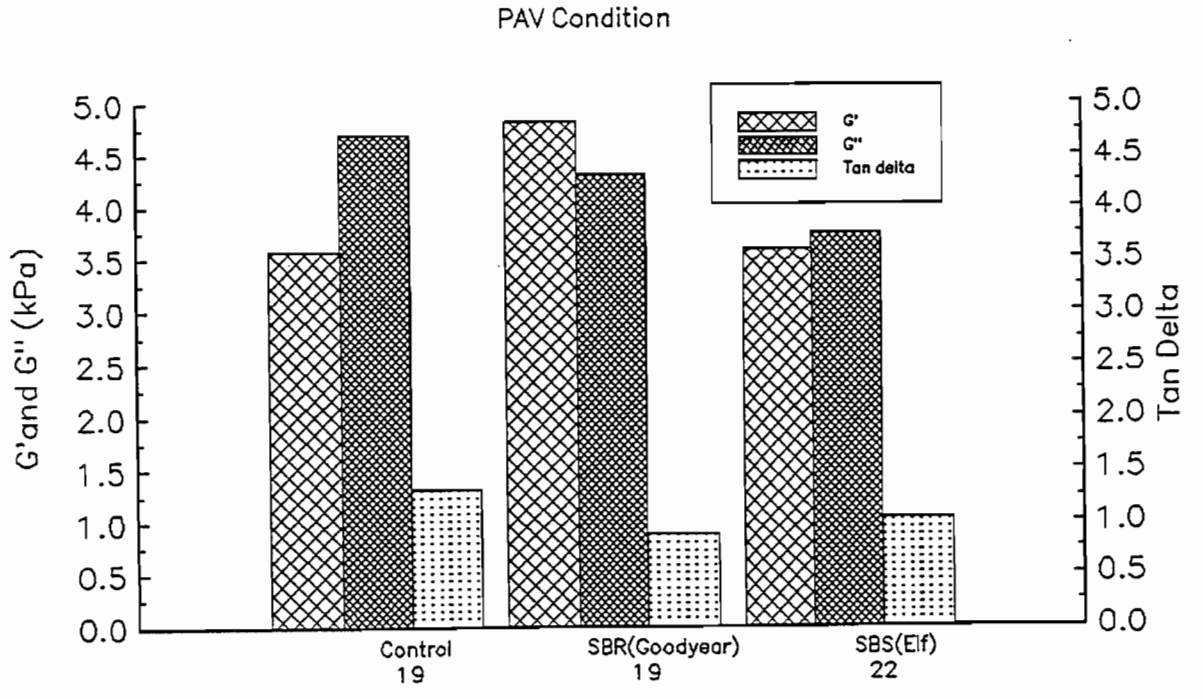

Figure B-11 Storage, loss modulus, and tan delta for District 11 binders (PAV condition)

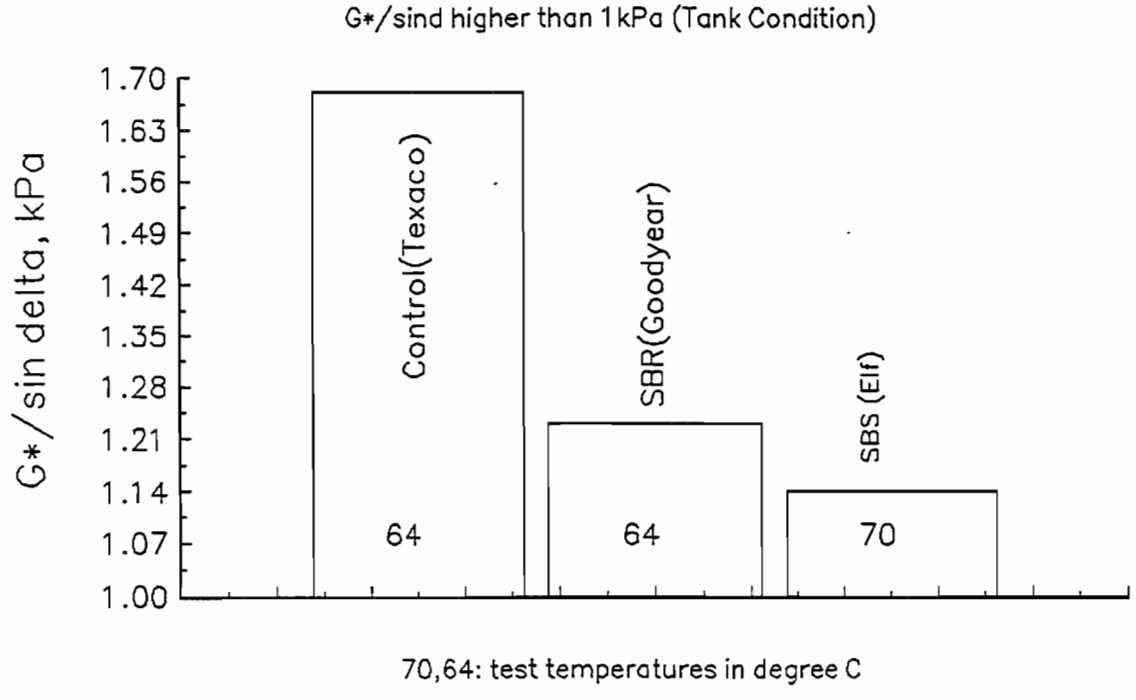

Figure B-12 Ranking of District 11 binders (tank condition)

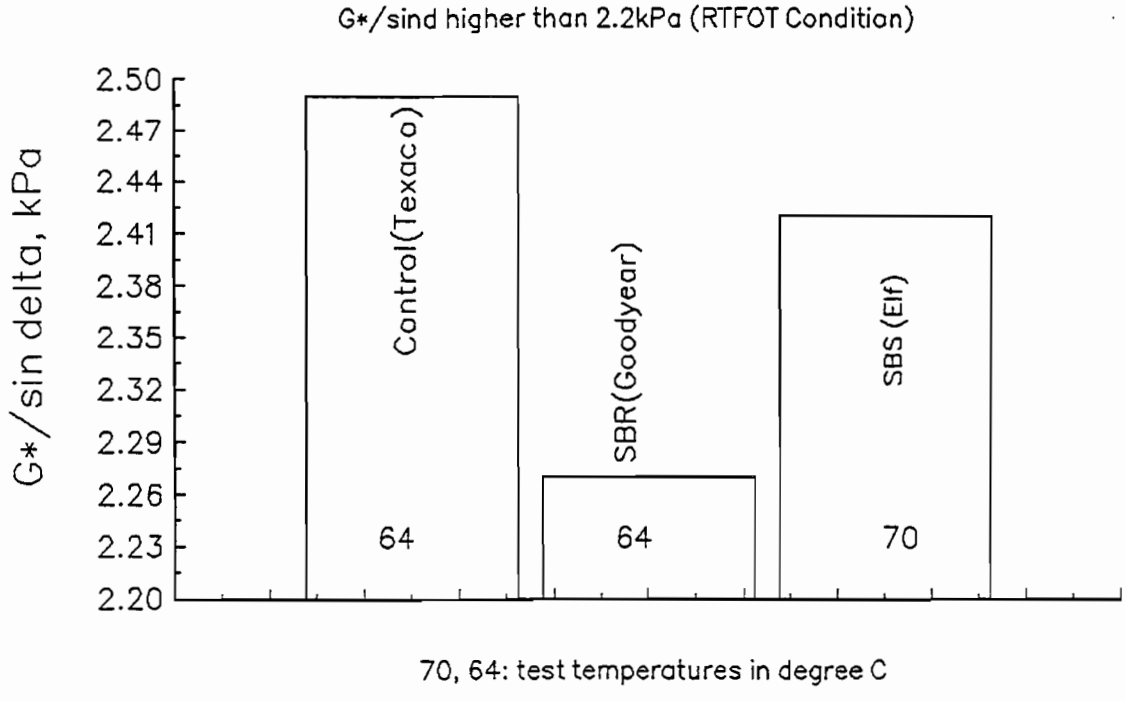

Figure B-13 Ranking of District 11 binders (RTFOT condition)

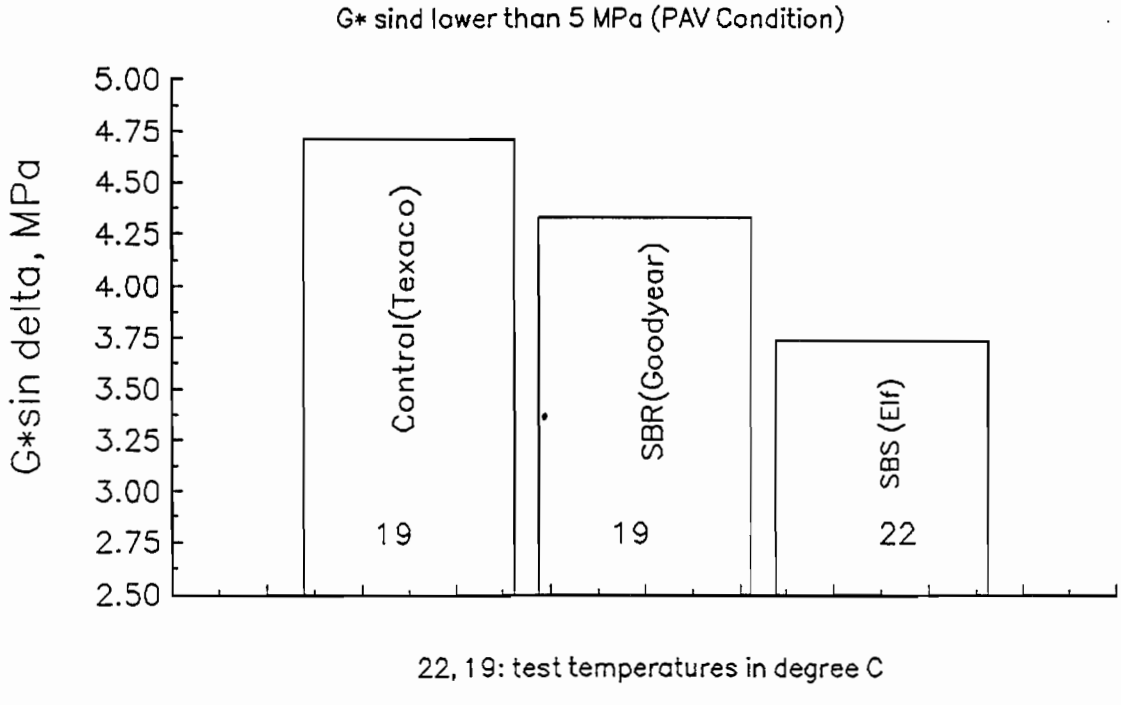

Figure B-14 Ranking of District 11 binders (PAV condition)

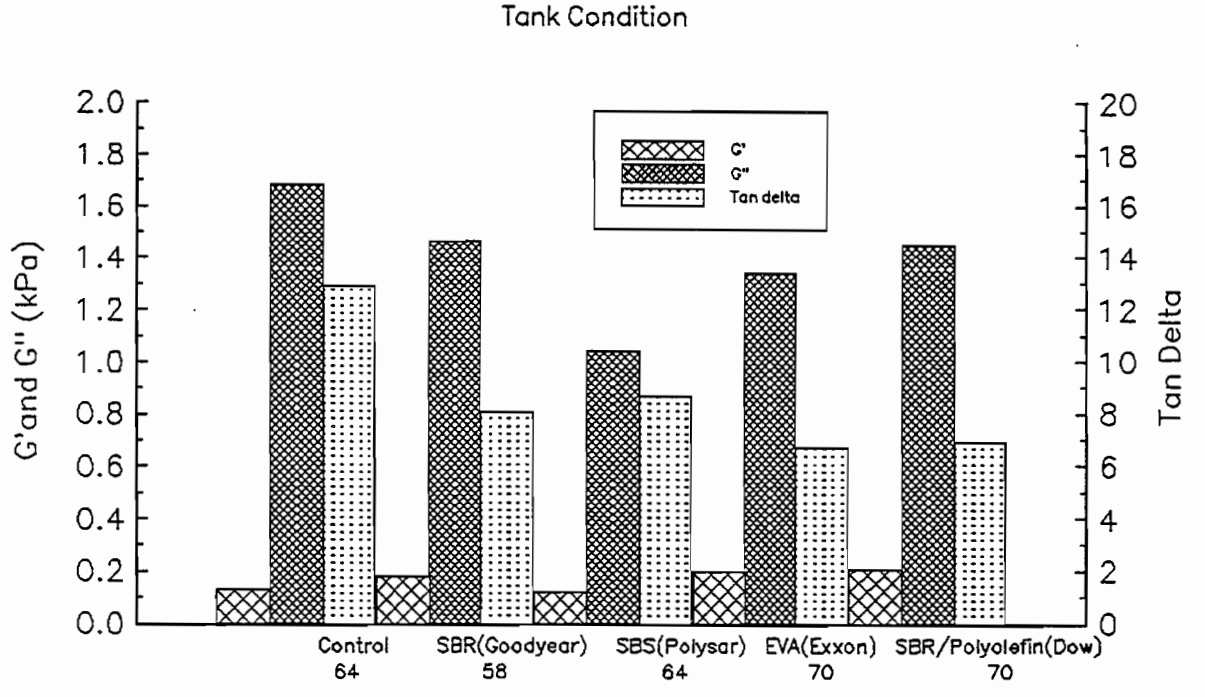

Figure B-15 Storage, loss modulus, and tan delta for District 15 binders (tank condition)

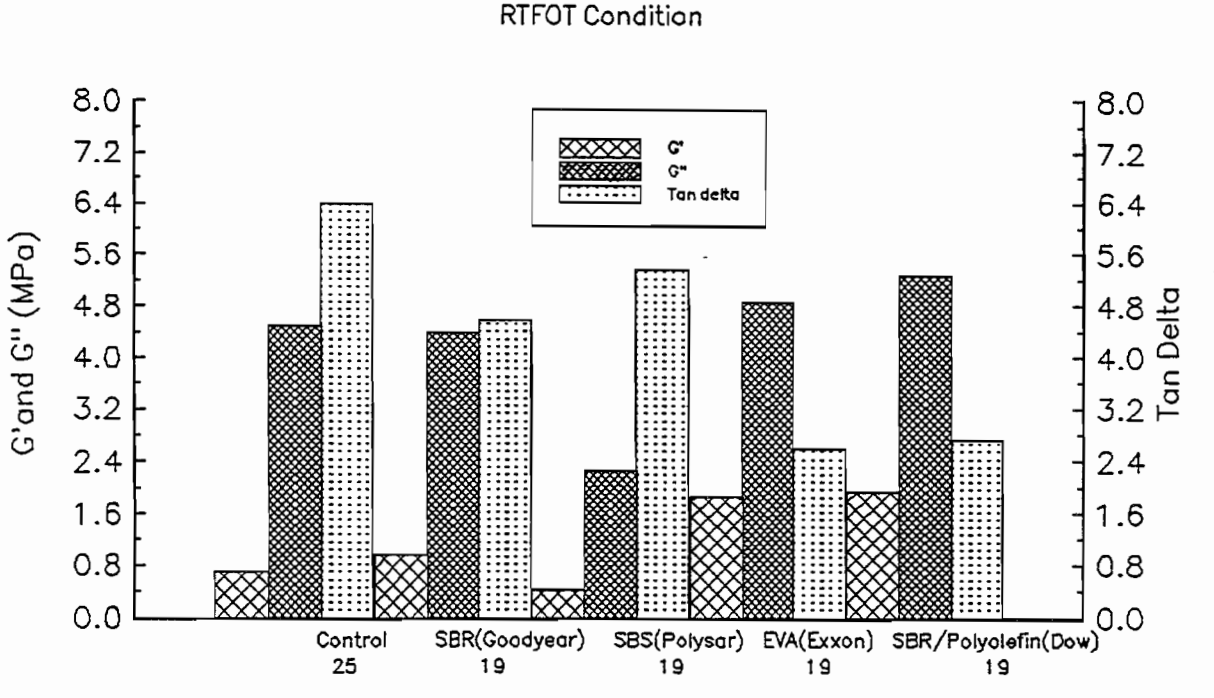

Figure B-16 Storage, loss modulus, and tan delta for District 15 binders (RTFOT condition)

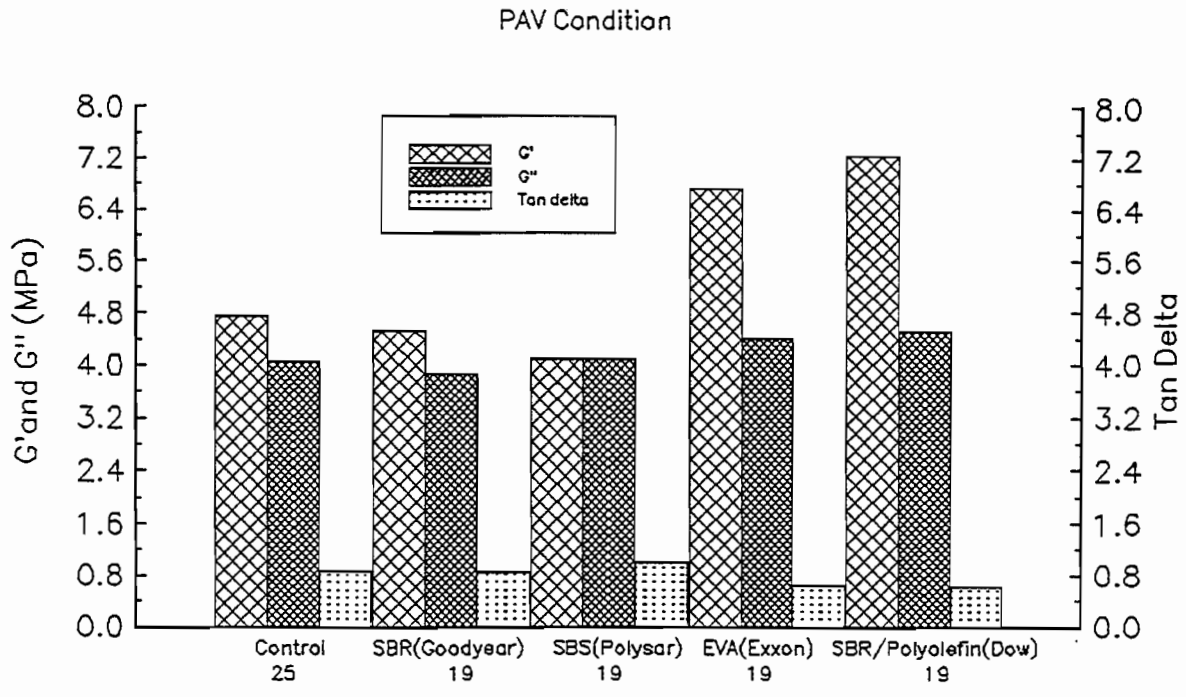

Figure B-17 Storage, loss modulus, and tan delta for District 15 binders (PAV condition)

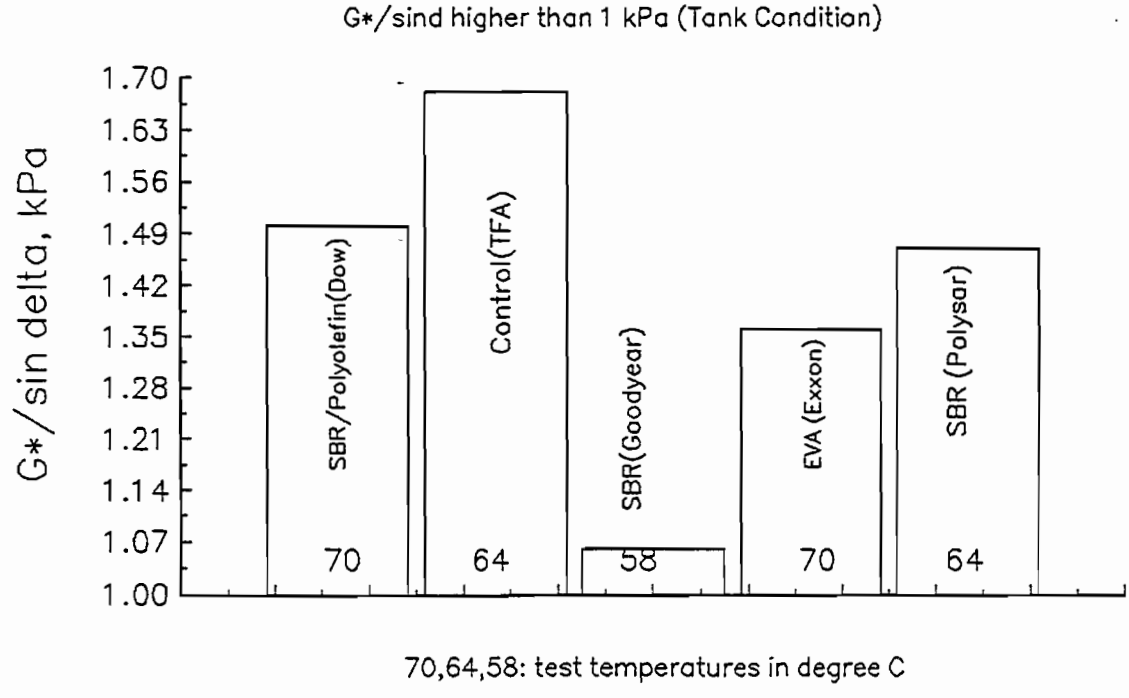

Figure B-18 Ranking of District 15 binders (tank condition)

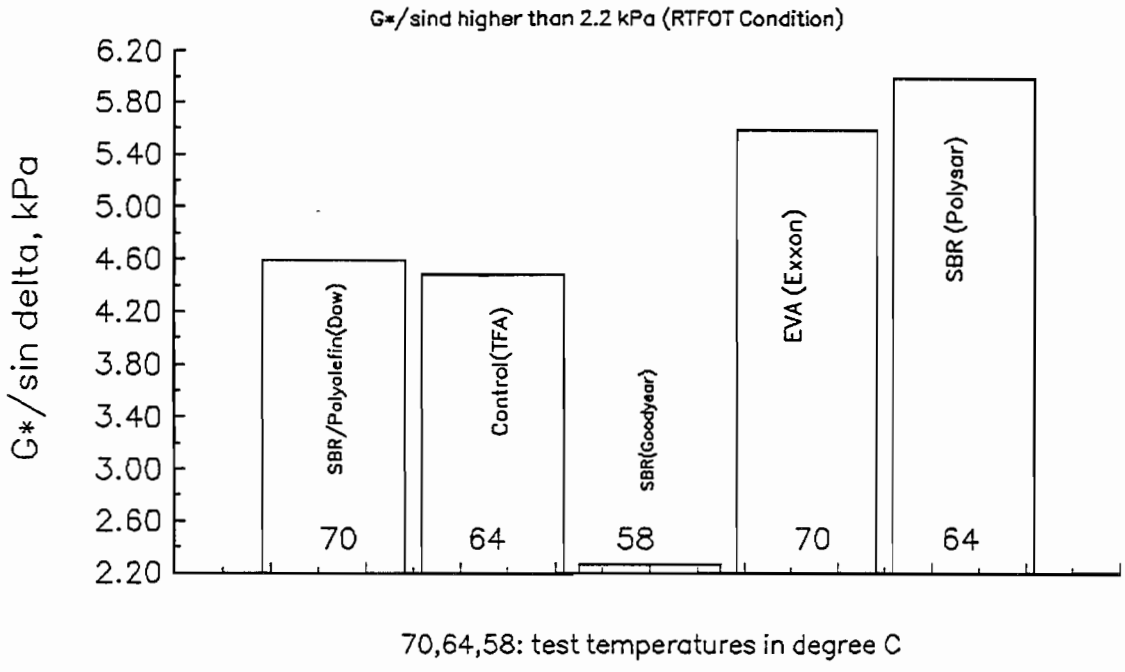

Figure B-19 Ranking of District 15 binders (RTFOT condition)

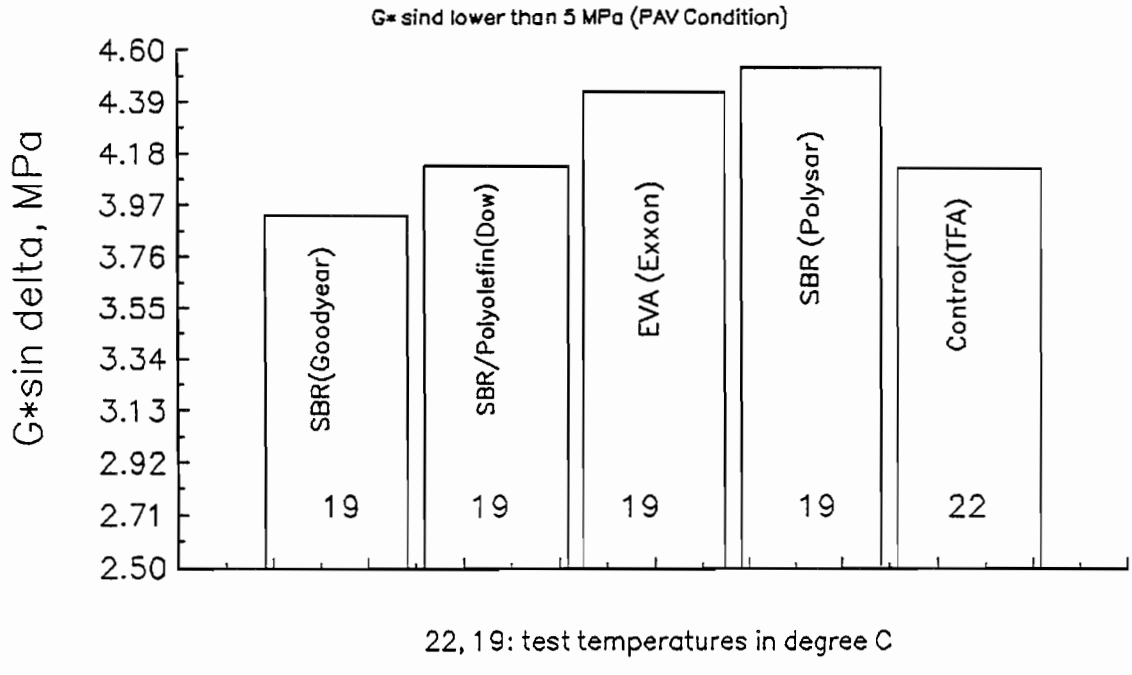

Figure B-20 Ranking of District 15 binders (PAV condition)

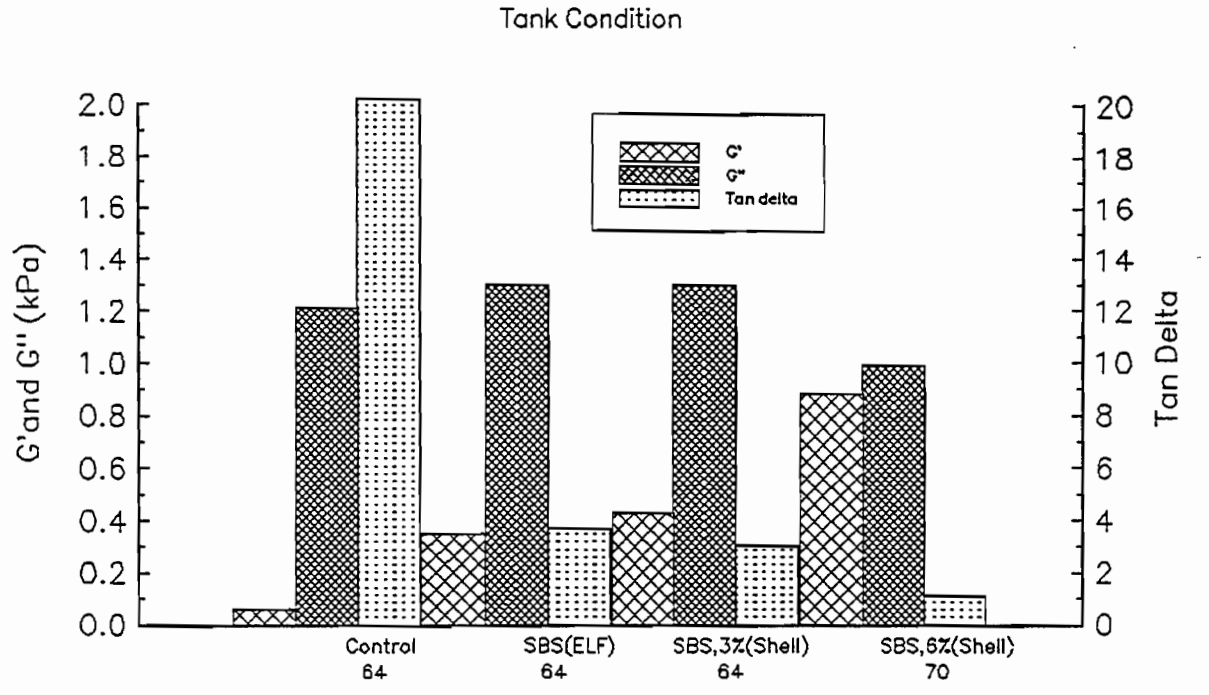

Figure B-21 Storage, loss modulus, and tan delta for District 25 binders (tank condition)

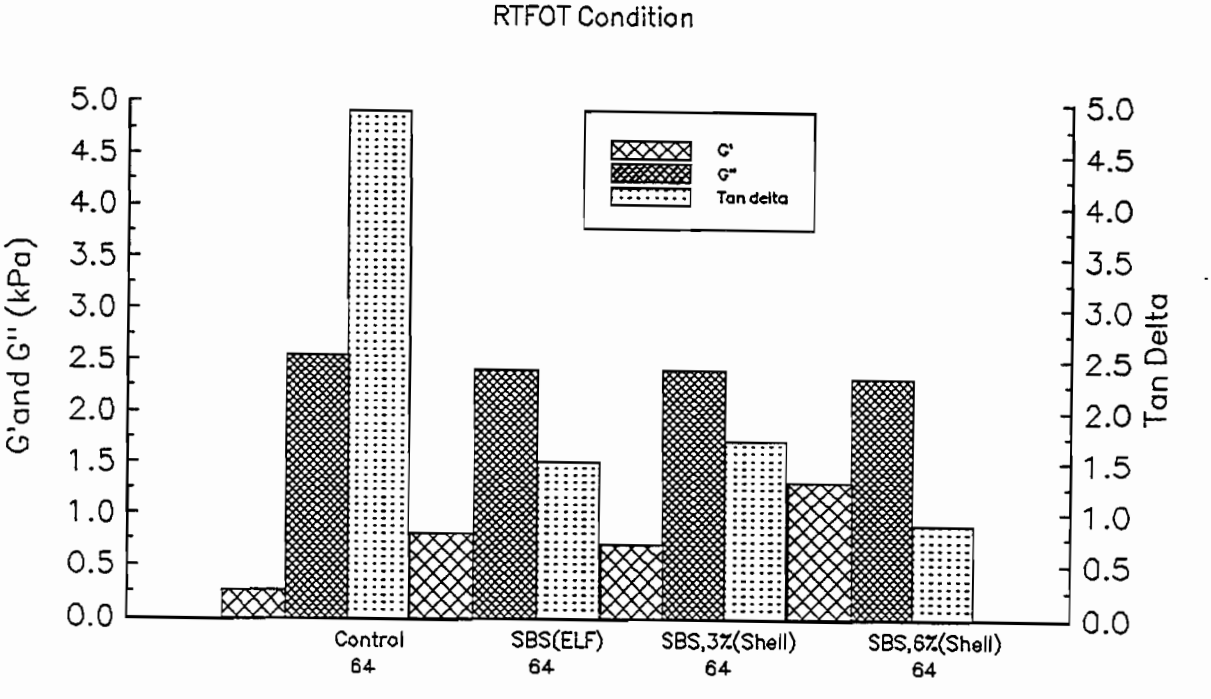

Figure B-22 Storage, loss modulus, and tan delta for District 25 binders (RTFOT condition)

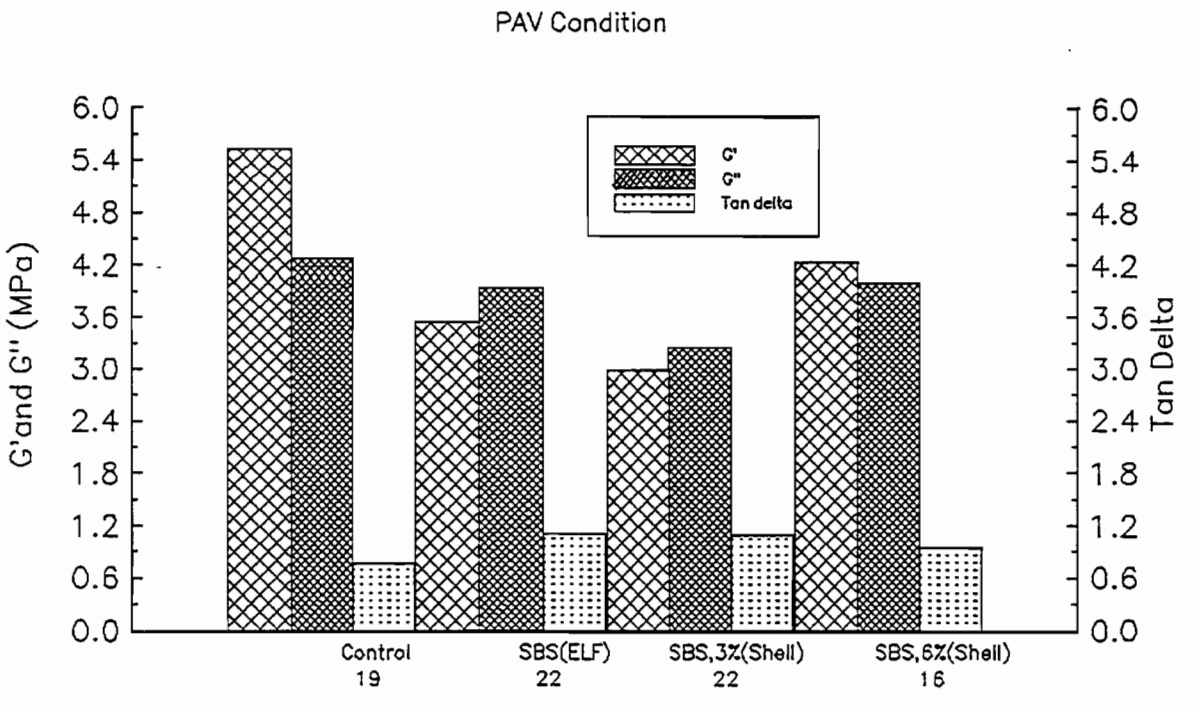

Figure B-23 Storage, loss modulus, and tan delta for District 25 binders (PAV condition)

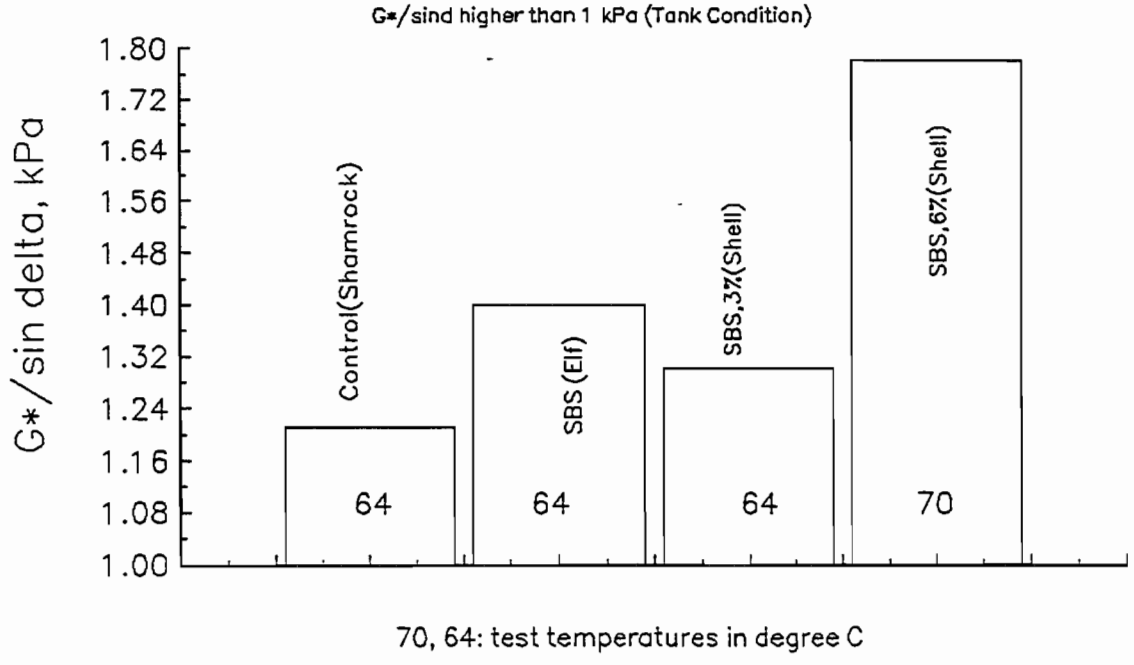

Figure B-24 Ranking of District 25 binders (tank condition)

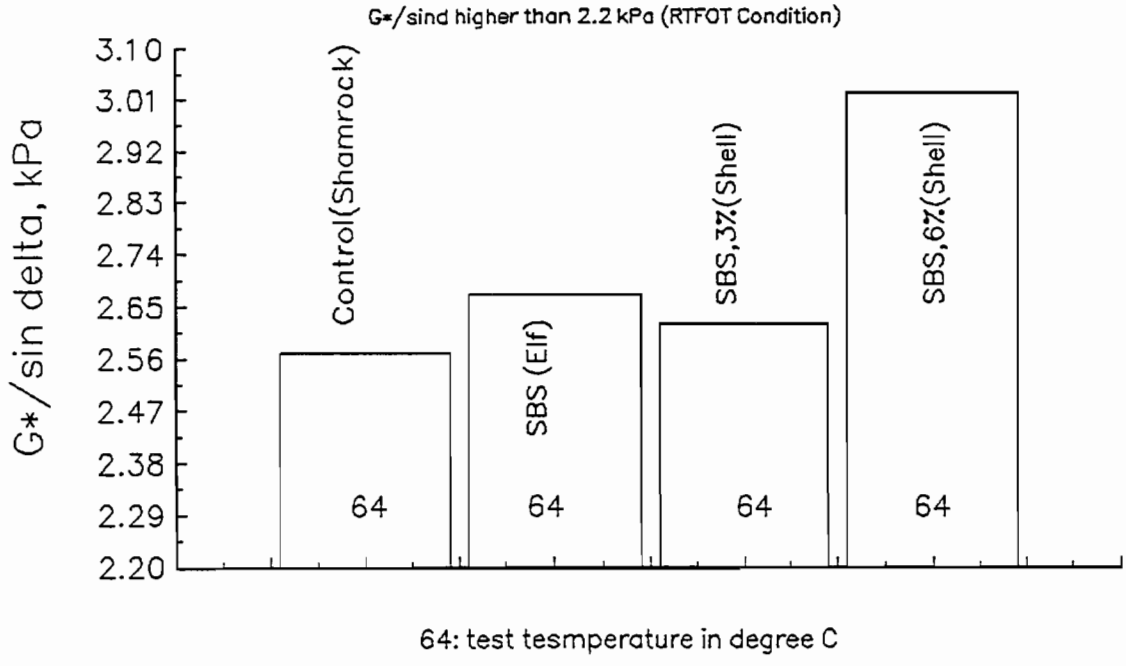

Figure B-25 Ranking of District 25 binders (RTFOT condition)

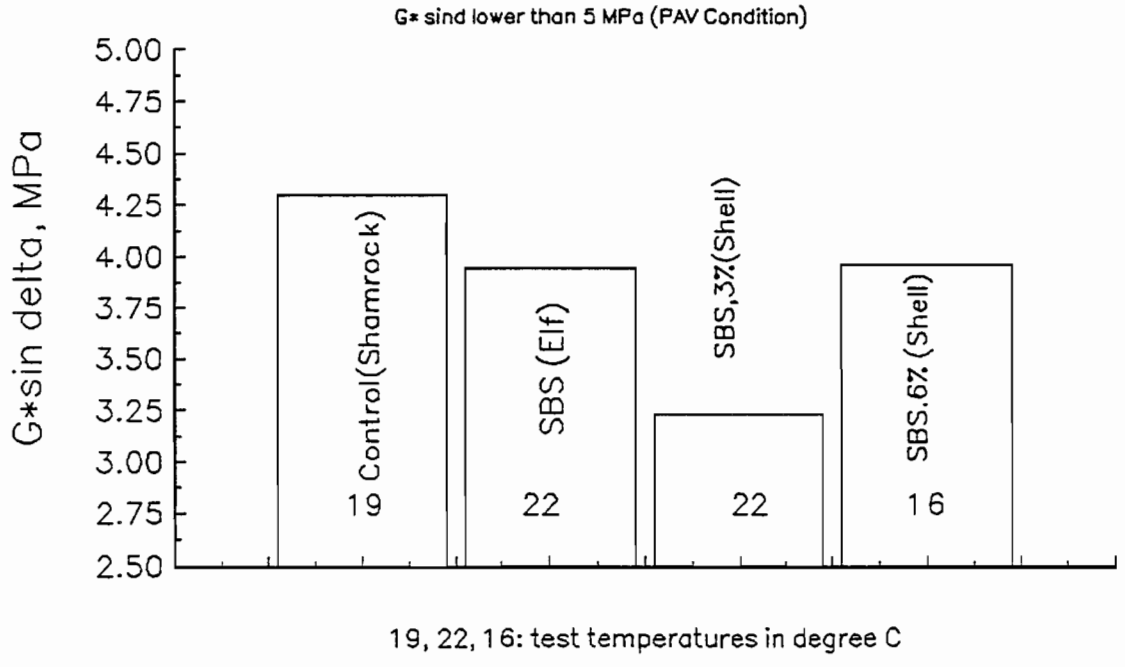

Figure B-26 Ranking of District 25 binders (PAV condition)

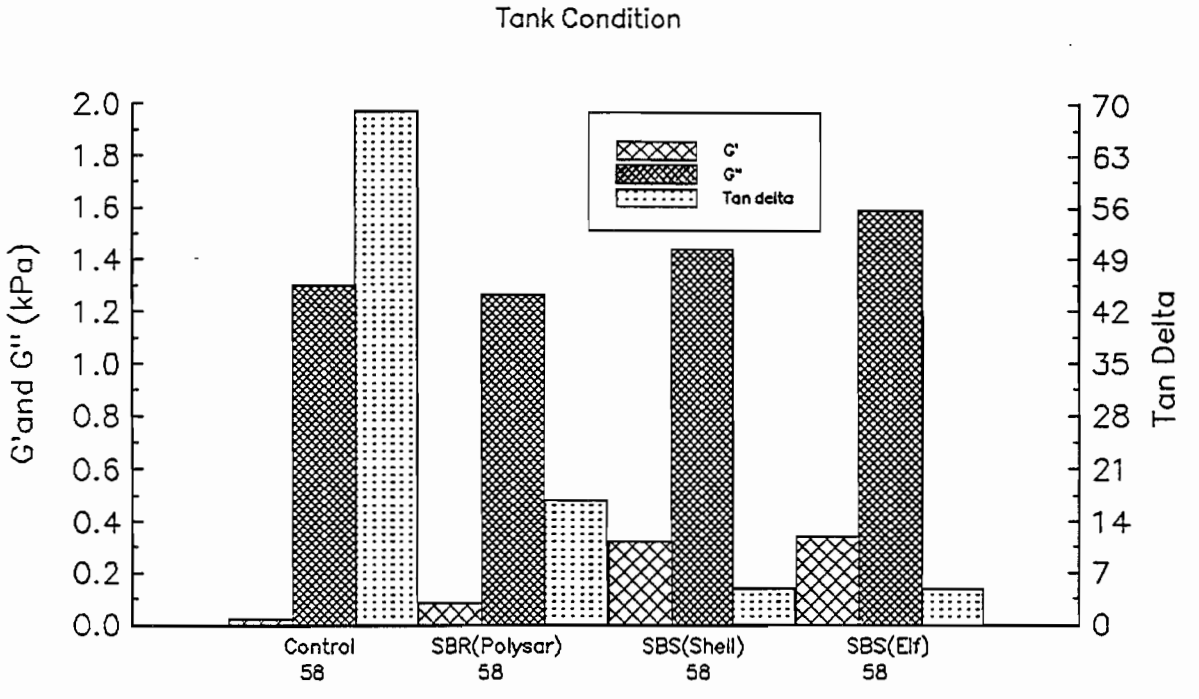

Figure B-27 Storage, loss modulus, and tan delta for District 17 binders (tank condition)

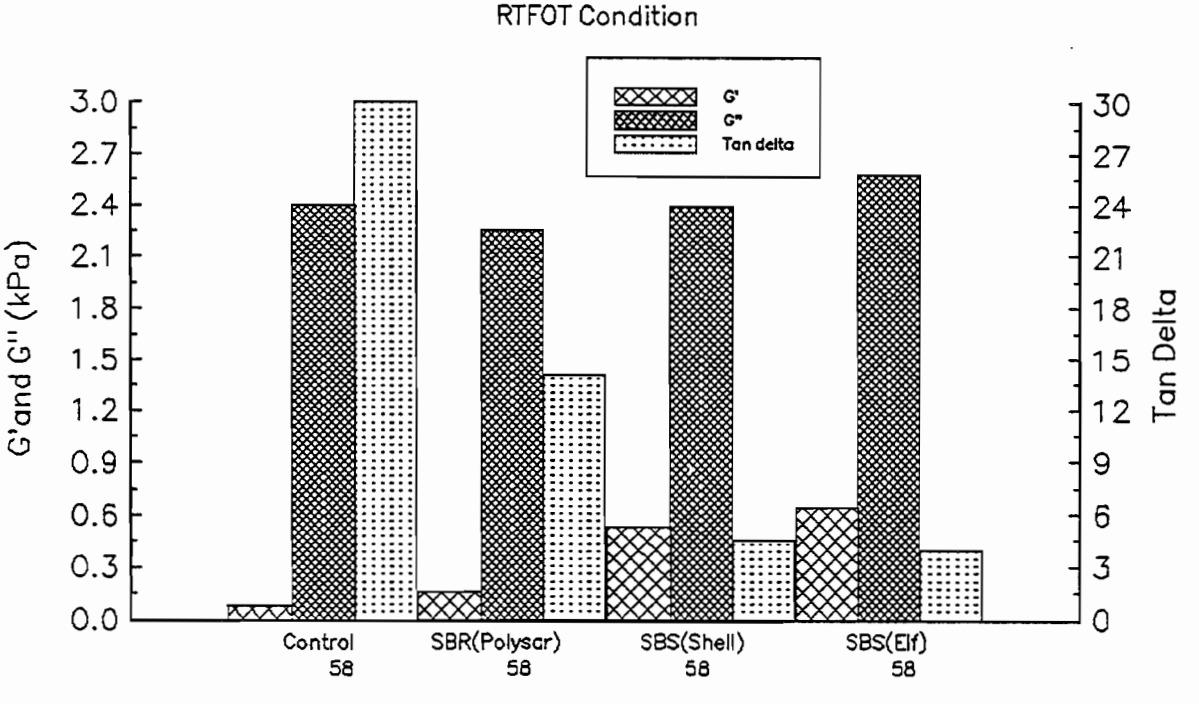

Figure B-28 Storage, loss modulus, and tan delta for District 17 binders (RTFOT condition)

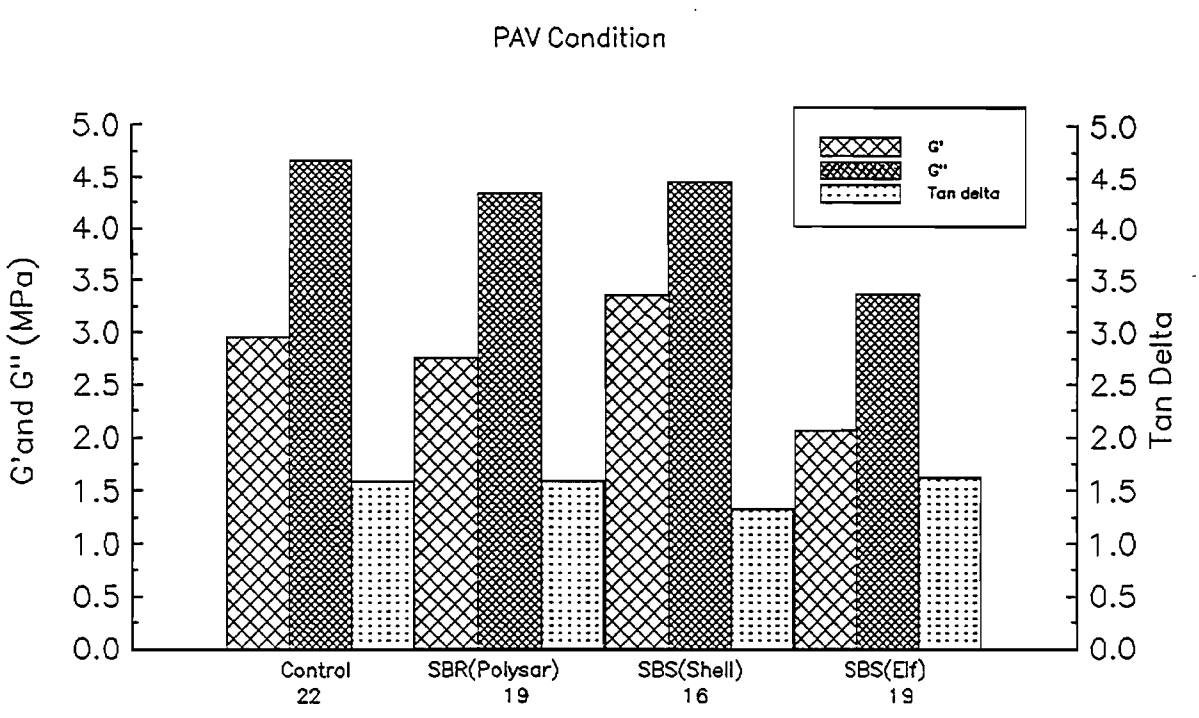

Figure B-29 Storage, loss modulus, and tan delta for District 17 binders (PAV condition)

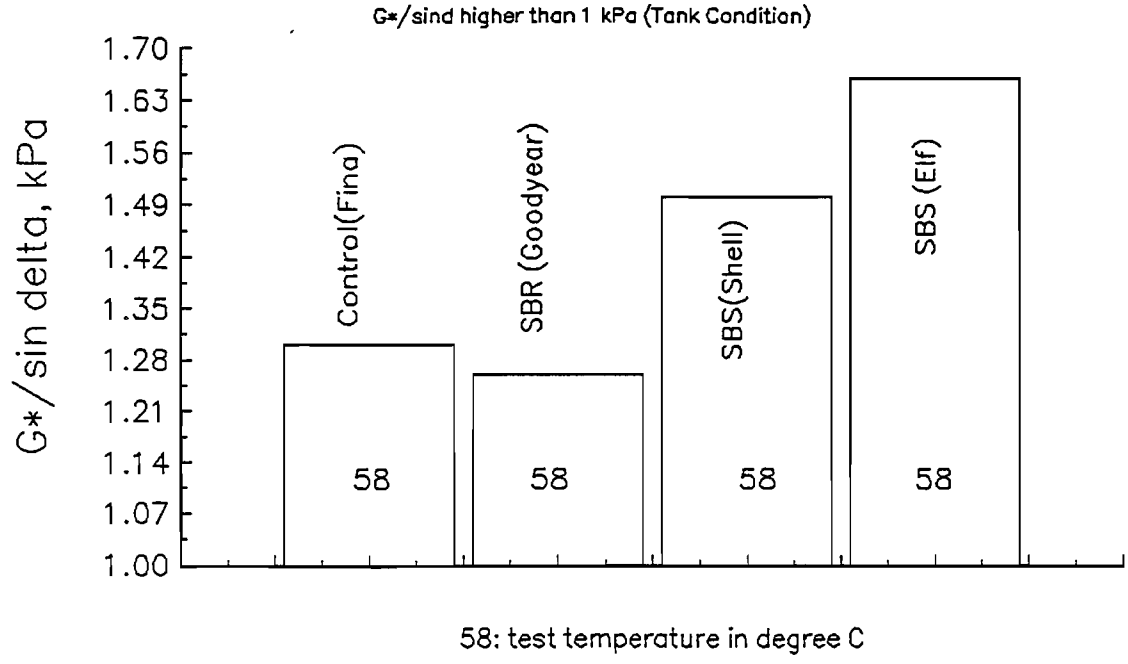

Figure B-30 Ranking of District 17 binders (tank condition)

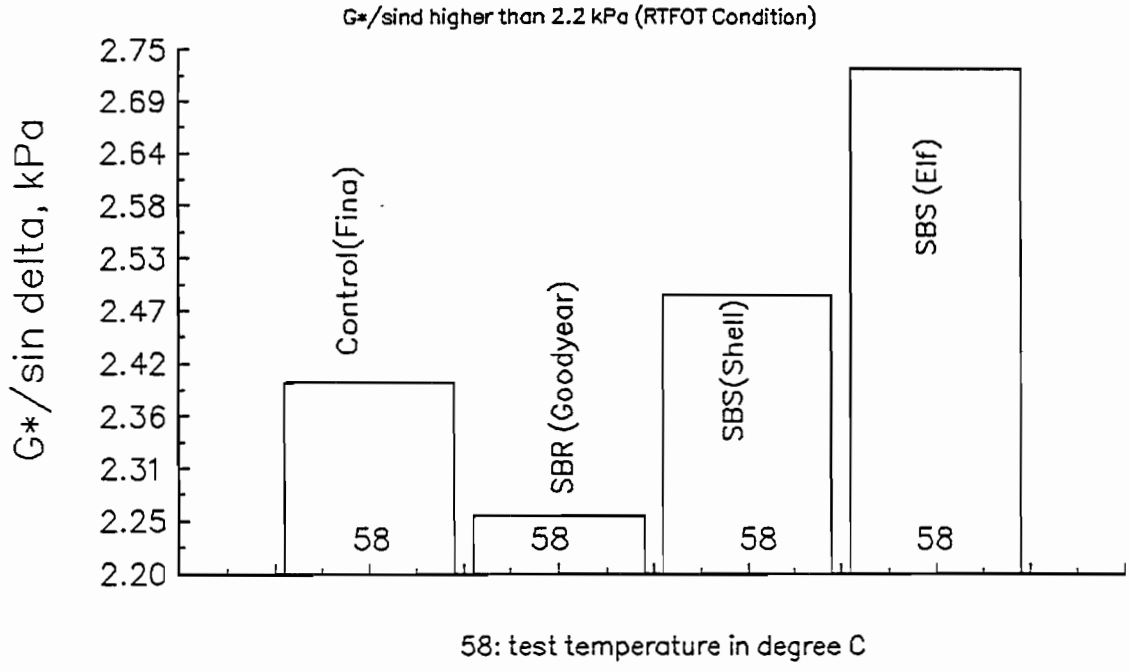

Figure B-31 Ranking of District 17 binders (RTFOT condition)

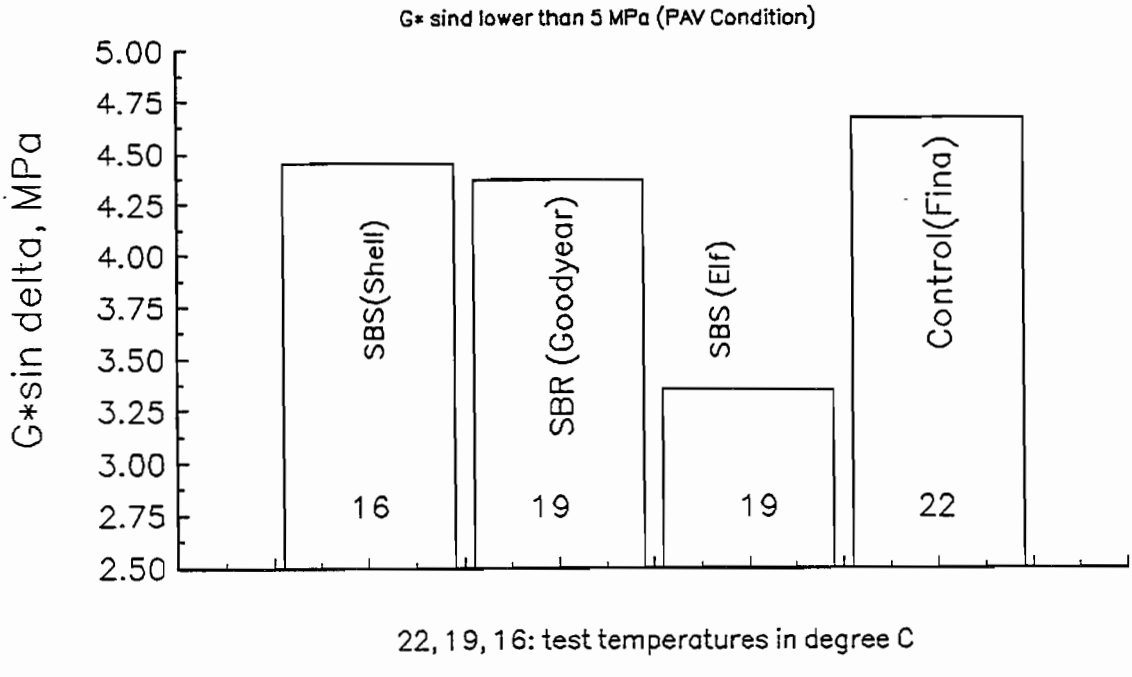

Figure B-32 Ranking of District 17 binders (PAV condition)

APPENDIX C

TABLES AND GRAPHS — BINDER CONVENTIONAL TESTING

TABLE C-1 ASPHALT BINDER DURABILITY PROPERTIES AS MEASURED BY PENETRATION TESTS (ASTM D 5) ON ORIGINAL, LABORATORY-AGED, AND FIELD-AGED BINDERS (DISTRICT 10)

District 10

Binder	Control (Total)	SBR (Goodyear)	SBS (Elf)	EVA (Exxon)	SBS (Shell)
Penetration 25°C(77°F) Original (dmm)	74	93	89	112	104
Penetration 25°C(77°F) RTFOT (dmm)	44	56	61	77	69
Lab Retained Penetration %	60	60	69	69	66
Penetration 25°C(77°F) Field-Aged (dmm)	44	37	34	90	61
Field Retained Penetration %	60	40	38	80	59
In-service* time,months	34	34	34	34	34

* as of May 1993

TABLE C-2 ASPHALT BINDER DURABILITY PROPERTIES AS MEASURED BY CAPILLARY VISCOSITY TESTS (ASTM D 2171) ON ORIGINAL, LABORATORY-AGED, AND FIELD-AGED BINDERS (DISTRICT 10)

District 10

Binder	Control (Total)	SBR (Goodyear)	SBS (Elf)	EVA (Exxon)	SBS (Shell)
Viscosity 60°C(140°F) Original Poises	2037	2373	2904	928	2644
Viscosity 60°C(140°F) RTFOT Poises	4798	5140	7416	2329	4251
Lab Aging Index	2.36	2.17	2.55	2.51	1.61
Viscosity 60°C(140°F) Field Aged Poises	5509	6210	11492	2621	3848
Aging Index	2.71	2.62	3.96	2.82	1.46
In-service* time,months	34	34	34	34	34

* as of May 1993

TABLE C-3 ASPHALT BINDER DURABILITY PROPERTIES AS MEASURED BY CAPILLARY VISCOSITY TESTS (ASTM D 2170) ON ORIGINAL, LABORATORY-AGED, AND FIELD-AGED BINDERS (DISTRICT 10)

District 10

Binder	Control (Total)	SBR (Goodyear)	SBS (Elf)	EVA (Exxon)	SBS (Shell)
Viscosity 135°C(275°F) Original cSt	510	650	763	380	480
Viscosity 135°C(275°F) RTFOT cSt	918	943	1098	1243	1055
Lab Aging Index	1.80	1.45	1.44	1.94	1.35
Viscosity 135°C(275°F) Field Aged cSt	670	1658	1242	507	572
Field Aging Index	1.31	2.55	1.63	1.33	1.19
In-service* time,months	34	34	34	34	34

* as of May 1993

TABLE C-4 ASPHALT BINDER DURABILITY PROPERTIES AS MEASURED BY PENETRATION TESTS (ASTM D 5) ON ORIGINAL, LABORATORY-AGED, AND FIELD-AGED BINDERS (DISTRICT 11)

District 11

Asphalt Binder	Control (Texaco)	SBR (Goodyear)	SBS (Elf)
Penetration 25°C(77°F) Original (dmm)	71	87	93
Penetration 25°C(77°F) RTFOT (dmm)	46	50	67
Lab Retained Penetration %	65	58	72
Penetration 25°C(77°F) Field-Aged (dmm)	21	27	23
Field Retained Penetration %	30	31	25
In-service* time,months	49	49	49

* as of May 1993

TABLE C-5 ASPHALT BINDER DURABILITY PROPERTIES AS MEASURED BY CAPILLARY VISCOSITY TESTS (ASTM D 2171) ON ORIGINAL, LABORATORY-AGED, AND FIELD-AGED BINDERS (DISTRICT 11)

District 11

Asphalt Binder	Control (Texaco)	SBR (Goodyear)	SBS (Elf)
Viscosity 60°C(140°F) Original Poises	2375	2330	3060
Viscosity 60°C(140°F) RTFOT Poises	7002	4327	58825
Lab Aging Index	2.95	1.86	1.92
Viscosity 60°C(140°F) Field-Aged Poises	21283	29556	33921
Field Aging Index	8.96	12.69	11.1
In-service* time,months	49	49	49

* as of May 1993

TABLE C-6 ASPHALT BINDER DURABILITY PROPERTIES AS MEASURED BY CAPILLARY VISCOSITY TESTS (ASTM D 2170) ON ORIGINAL, LABORATORY-AGED, AND FIELD-AGED BINDERS (DISTRICT 11)

District 11

Asphalt Binder	Control (Texaco)	SBR (Goodyear)	SBS (Elf)
Viscosity 135°C(275°F) Original cSt	496	822	715
Viscosity 135°C(275°F) RTFOT cSt	751	1049	897
Lab Aging Index	1.51	1.28	1.26
Viscosity 135°C(275°F) Field-Aged cSt	856	2695	1954
Field Aging Index	1.73	3.28	2.73
In-service* time,months	49	49	49

* as of May 1993

TABLE C-7 ASPHALT BINDER DURABILITY PROPERTIES AS MEASURED BY PENETRATION TESTS (ASTM D 5) ON ORIGINAL, LABORATORY-AGED, AND FIELD-AGED BINDERS (DISTRICT 15)

District 15

Asphalt Binder	Control (TFA)	SBR (Goodyear)	SBR (Polysar)	EVA (Exxon)	SBR/P (Dow)	SBS (Elf)
Penetration 25°C(77°F) Original (dmm)	70	100	93	70	66	101
Penetration 25°C(77°F) RTFOT (dmm)	46	67	70	49	43	73
Lab Retained Penetration %	65	67	75	70	64	72
Penetration 25°C(77°F) Field-Aged (dmm)	16	23	25	16	43	18
Field Retained Penetration %	23	23	27	23	65	18
In-service* time,months	73	73	73	73	73	73

* as of May 1993

TABLE C-8 ASPHALT BINDER DURABILITY PROPERTIES AS MEASURED BY CAPILLARY VISCOSITY TESTS (ASTM D 2171) ON ORIGINAL, LABORATORY-AGED, AND FIELD-AGED BINDERS (DISTRICT 15)

District 15

Binder	Control (TFA)	SBR (Goodyear)	SBR (Polysar)	EVA (Exxon)	SBR/P (Dow)	SBS (Elf)
Viscosity 60°C(140°F) Original Poises	2087	1311	1318	3296	5198	3332
Viscosity 60°C(140°F) RTFOT Poises	7401	3932	3780	26266	31592	6331
Lab Aging Index	3.55	3.00	2.87	7.97	6.08	1.90
Viscosity 60°C(140°F) Field-Aged Poises*	---	---	---	---	---	---
Field Aging Index	---	---	---	---	---	---
In-service** time,months	73	73	73	73	73	73

* unable to run due to the very stiff nature of the material recovered

** as of May 1993

TABLE C-9 ASPHALT BINDER DURABILITY PROPERTIES AS MEASURED BY CAPILLARY VISCOSITY TESTS (ASTM D 2170) ON ORIGINAL, LABORATORY-AGED, AND FIELD-AGED BINDERS (DISTRICT 15)

District 15

Binder	Control (TFA)	SBR (Goodyear)	SBR (Polysar)	EVA (Exxon)	SBR/P (Dow)	SBS (Elf)
Viscosity 135°C(275°F) Original cSt	416	503	495	919	1202	754
Viscosity 135°C(275°F) RTFOT cSt	697	729	682	1830	2329	967
Lab Aging Index	1.68	1.45	1.38	1.99	1.94	1.28
Viscosity 135°C(275°F) Field-Aged cSt	4300	1587	1340	10357	1425	1428
Field Aging Index	10.34	3.16	2.71	11.27	1.19	1.89
In-service* time,months	73	73	73	73	73	73

* as of May 1993

TABLE C-10 ASPHALT BINDER DURABILITY PROPERTIES AS MEASURED BY PENETRATION TESTS (ASTM D 5) ON ORIGINAL, LABORATORY-AGED, AND FIELD-AGED BINDERS (DISTRICT 25)

District 25

Asphalt Binder	Control (Shamrock)	SBS (Elf)	SBS,3% (Shell)	SBS,6% (Shell)
Penetration 25°C(77°F) Original (dmm)	67	90	82	98
Penetration 25°C(77°F) RTFOT (dmm)	45	56	47	67
Lab Retained Penetration %	68	63	57	69
Penetration 25°C(77°F) Field Aging (dmm)	14	16	25	36
Field Retained Penetration %	21	18	31	37
In-service* time,months	56	56	56	56

* as of May 1993

TABLE C-11 ASPHALT BINDER DURABILITY PROPERTIES AS MEASURED BY CAPILLARY VISCOSITY TESTS (ASTM D 2171) ON ORIGINAL, LABORATORY-AGED, AND FIELD-AGED BINDERS (DISTRICT 25)

District 25

Asphalt Binder	Control (Shamrock)	SBS (Elf)	SBS,3% (Shell)	SBS,6% (Shell)
Viscosity 60°C(140°F) Original Poises	1998	2770	8127	*
Viscosity 60°C(140°F) RTFOT Poises	5202	7481	13,749	*
Lab Aging Index	2.60	2.70	1.69	*
Viscosity 60°C(140°F) Field-Aged Poises	64800	33700	22100	20900
Field Aging Index	32.43	12.17	2.72	---
In-service** time,months	56	56	56	56

* the original values were not available

** as of May 1993

TABLE C-12 ASPHALT BINDER DURABILITY PROPERTIES AS MEASURED BY CAPILLARY VISCOSITY TESTS (ASTM D 2170) ON ORIGINAL, LABORATORY-AGED, AND FIELD-AGED BINDERS (DISTRICT 25)

District 25

Asphalt Binder	Control (Shamrock)	SBS (Elf)	SBS,3% (Shell)	SBS,6% (Shell)
Viscosity 135°C(275°F), Original cSt	624	781	584	1013
Viscosity 135°C(275°F), RTFOT cSt	894	1009	736	1050
Lab Aging Index	1.43	1.29	1.26	1.04
Viscosity 135°C(275°F) Field-Aged cSt	1637	1991	1241	1114
Field-Aging Index	2.62	2.55	2.13	1.10
In-service* time, months	56	56	56	56

* as of May 1993

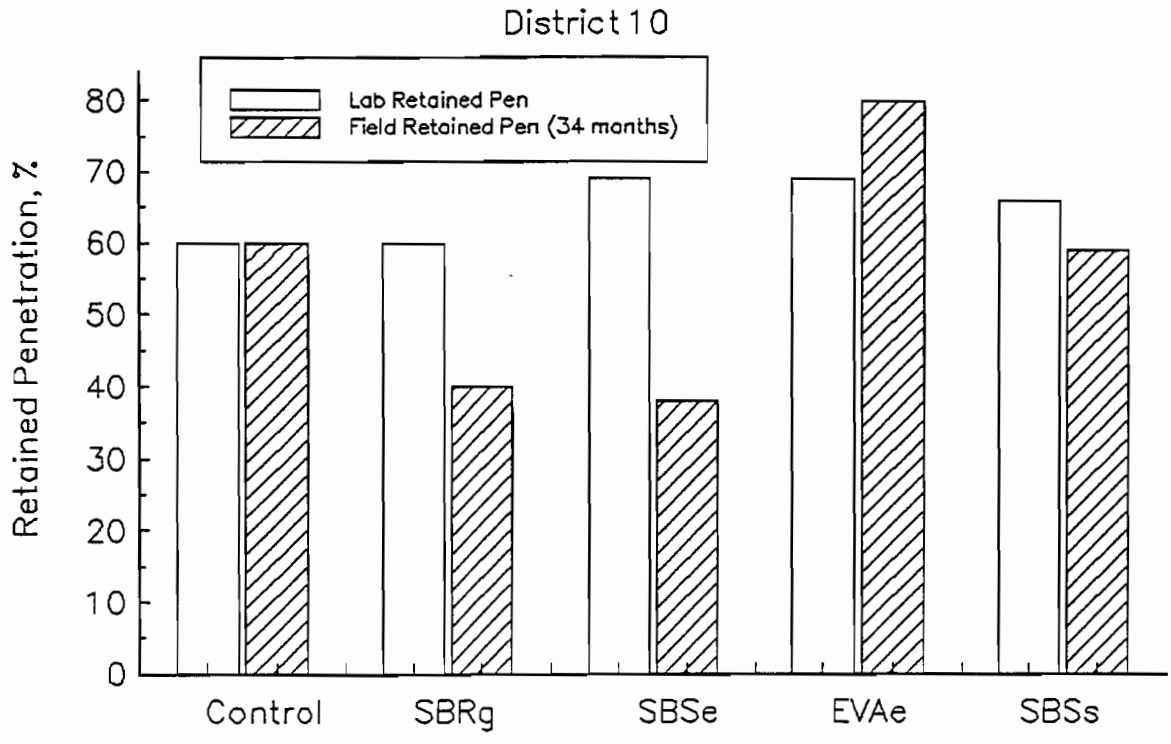

Figure C-1 Laboratory retained penetration versus field retained penetration (District 10)

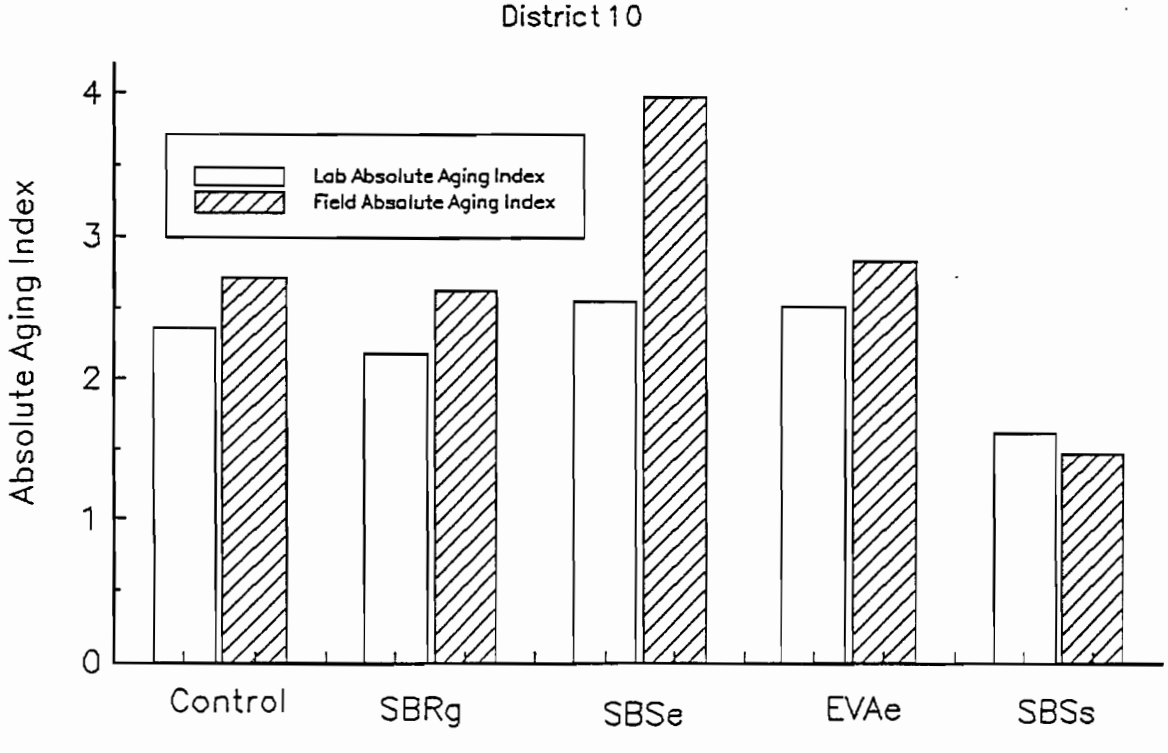

Figure C-2 Laboratory absolute aging index versus field absolute aging index (District 10)

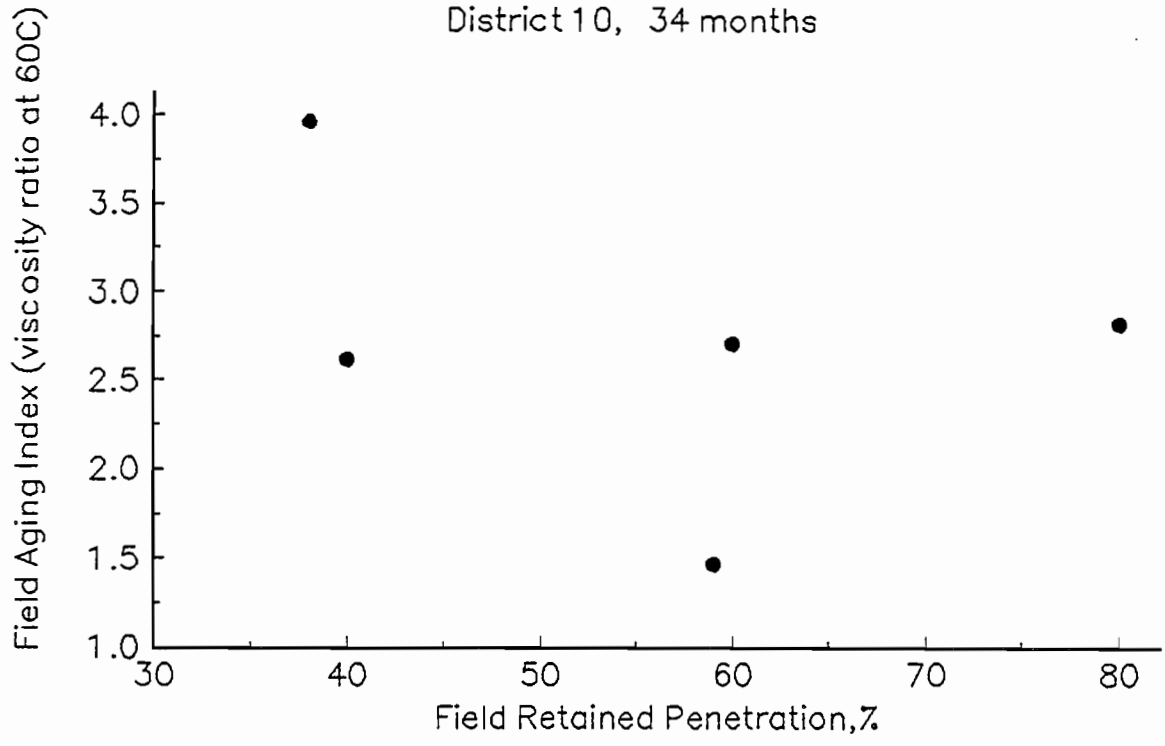

Figure C-3 Field retained penetration versus field aging index at 60°C (District 10)

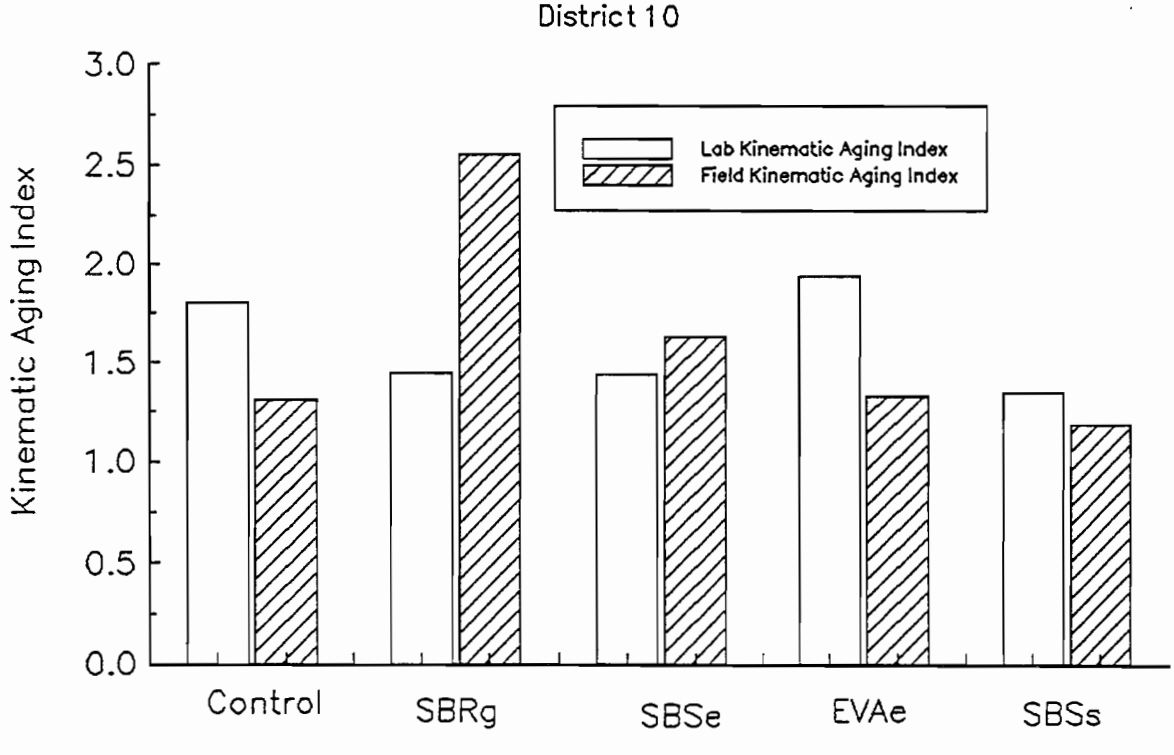

Figure C-4 Laboratory kinematic aging index versus field kinematic aging index (District 10)

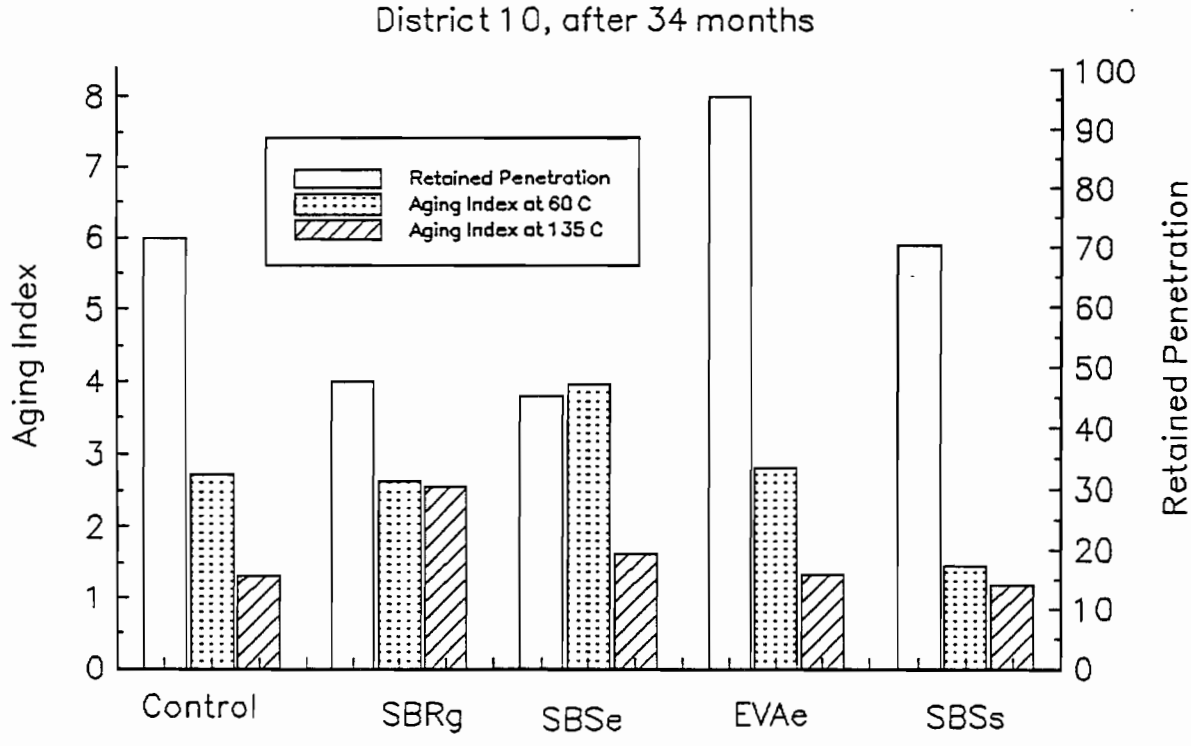

Figure C-5 Aging indexes and retained penetration (District 10)

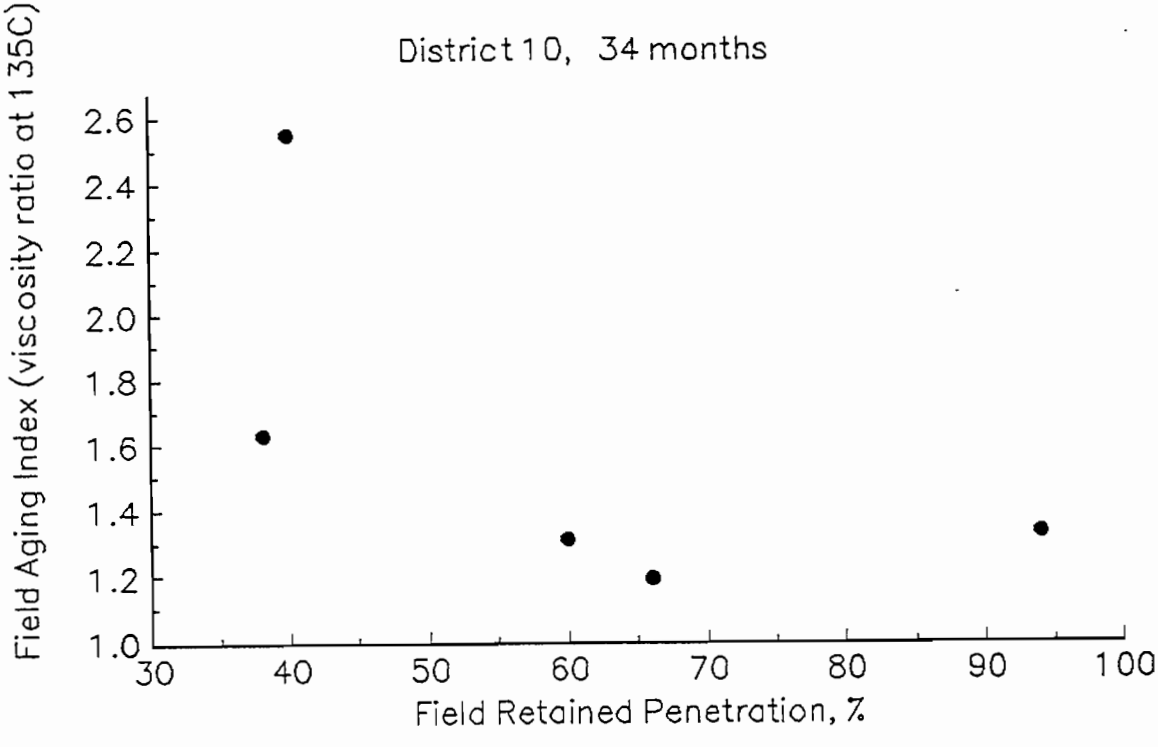

Figure C-6 Field retained penetration versus field aging index at 135°C (District 10)

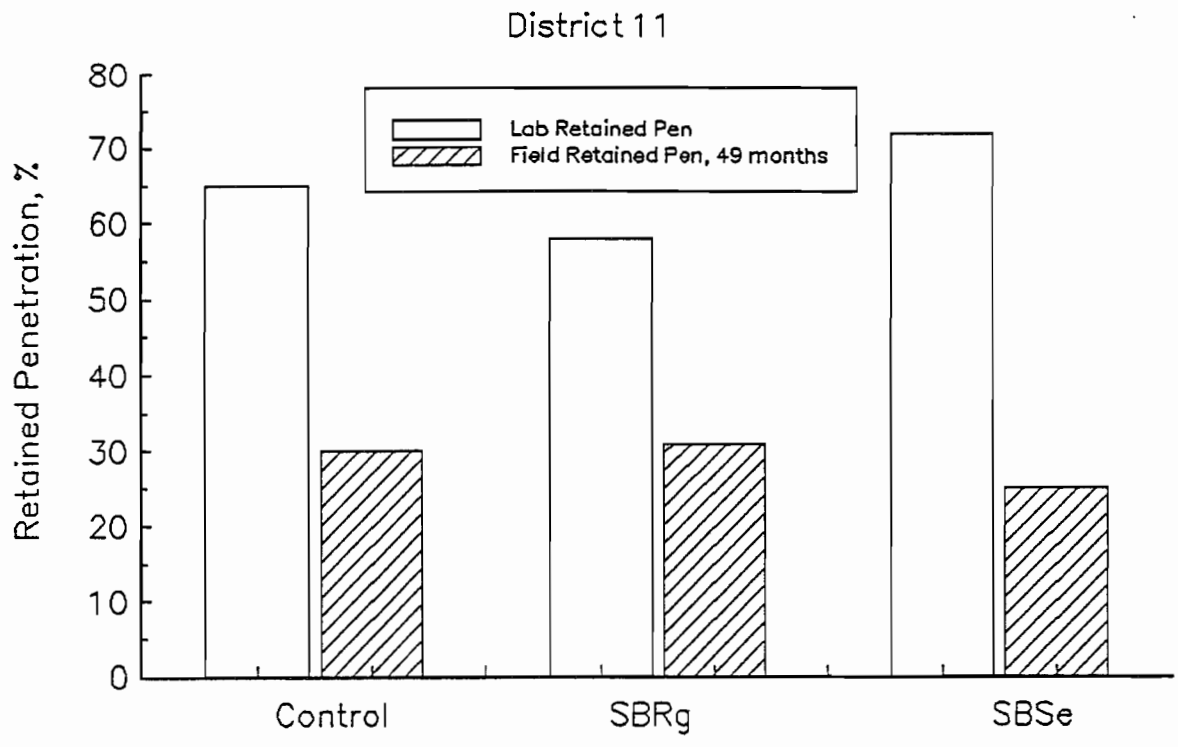

Figure C-7 Laboratory retained penetration versus field retained penetration (District 11)

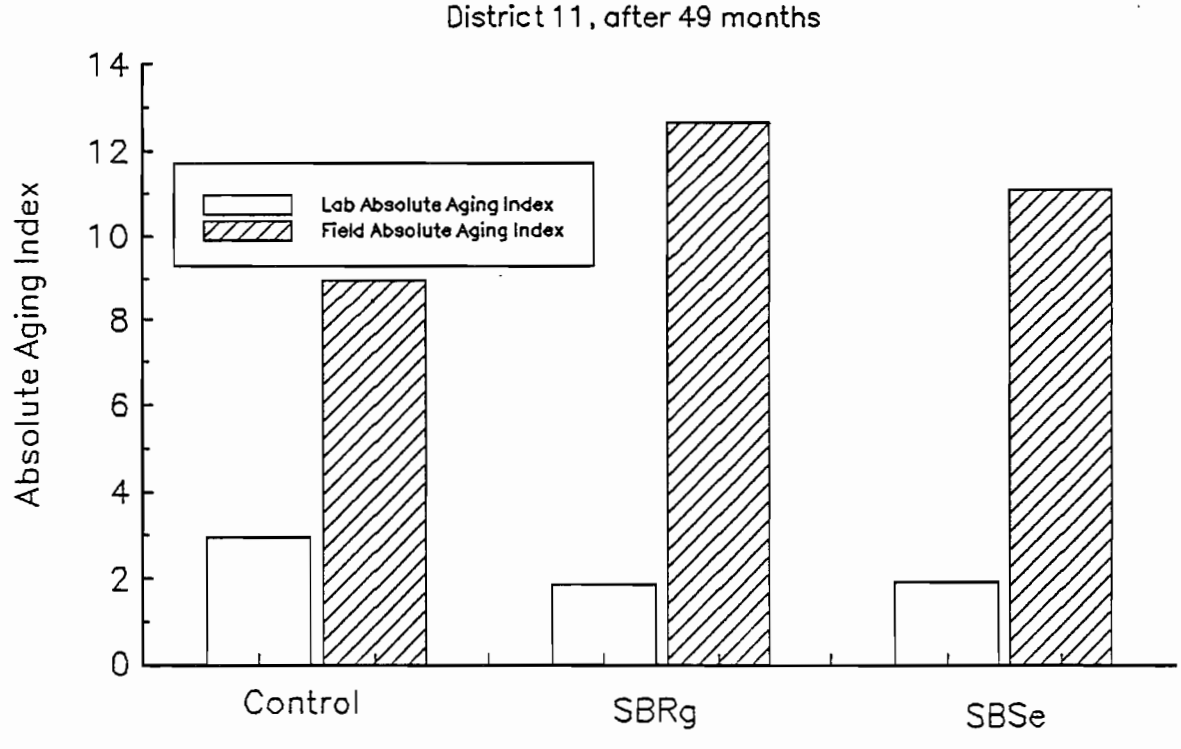

Figure C-8 Laboratory absolute aging index versus field absolute aging index (District 11)

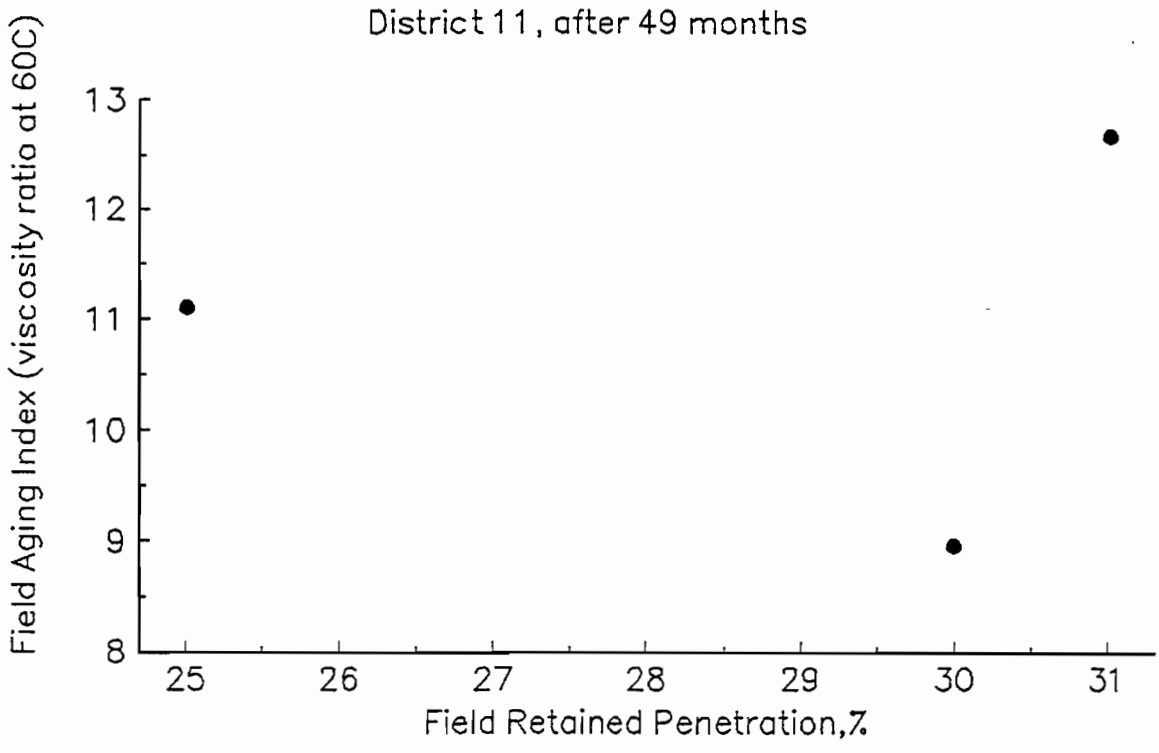

Figure C-9 Field retained penetration versus field aging index at 60°C (District 11)

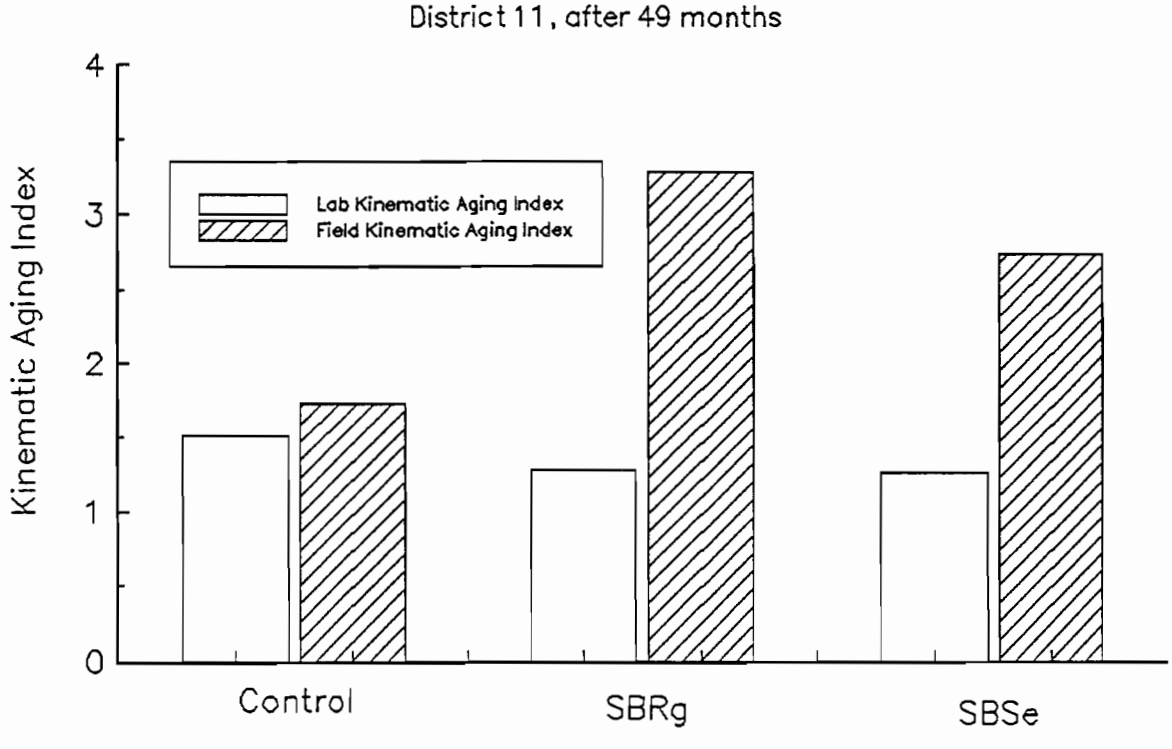

Figure C-10 Laboratory kinematic aging index versus field kinematic aging index (District 11)

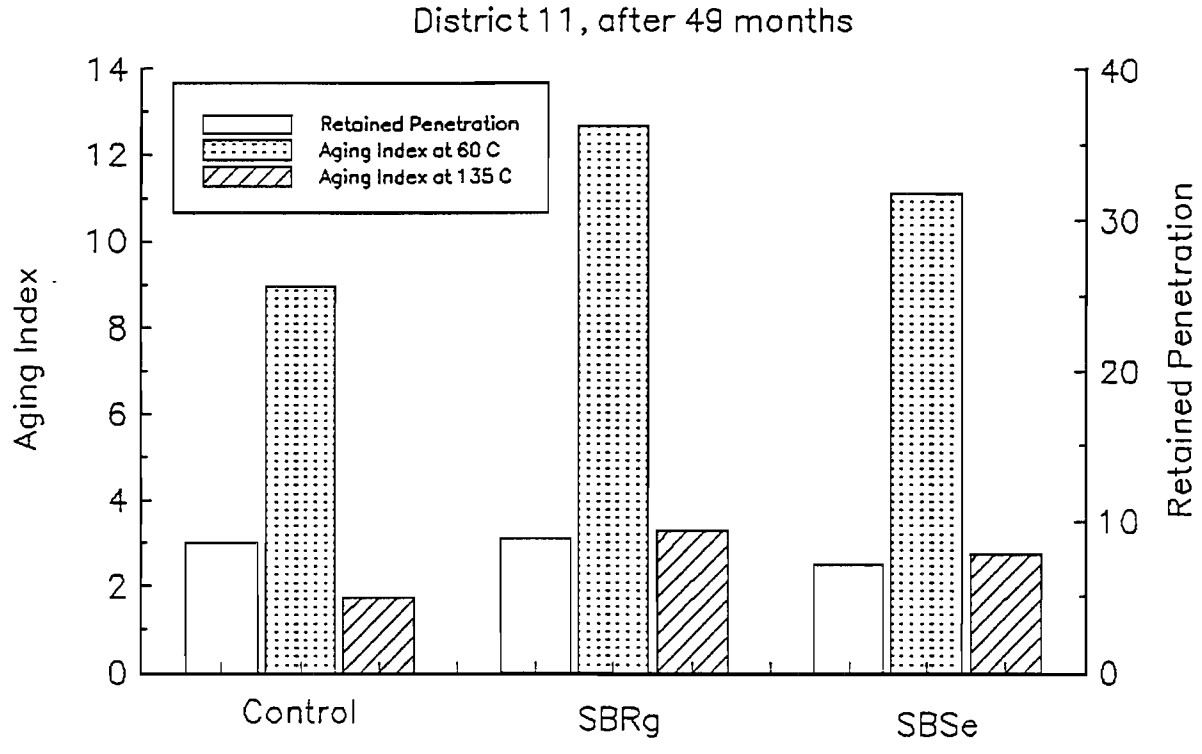

Figure C-11 Aging indexes and retained penetration (District 11)

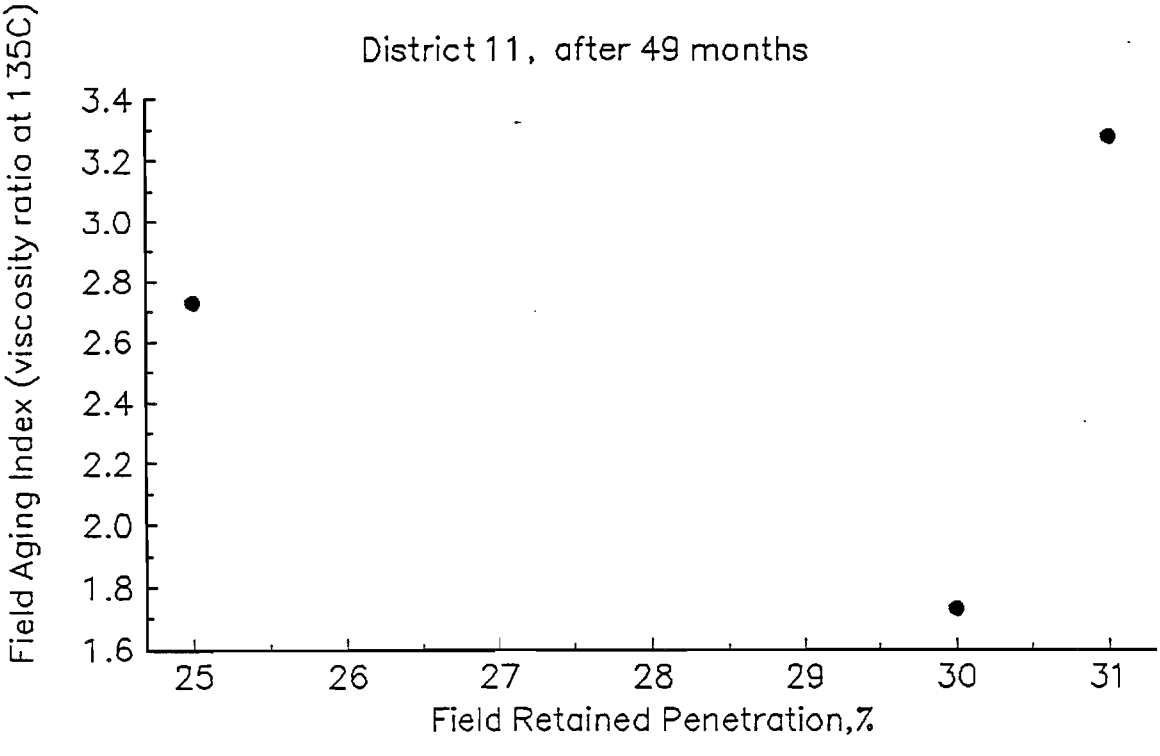

Figure C-12 Field retained penetration versus field aging index at 135°C (District 11)

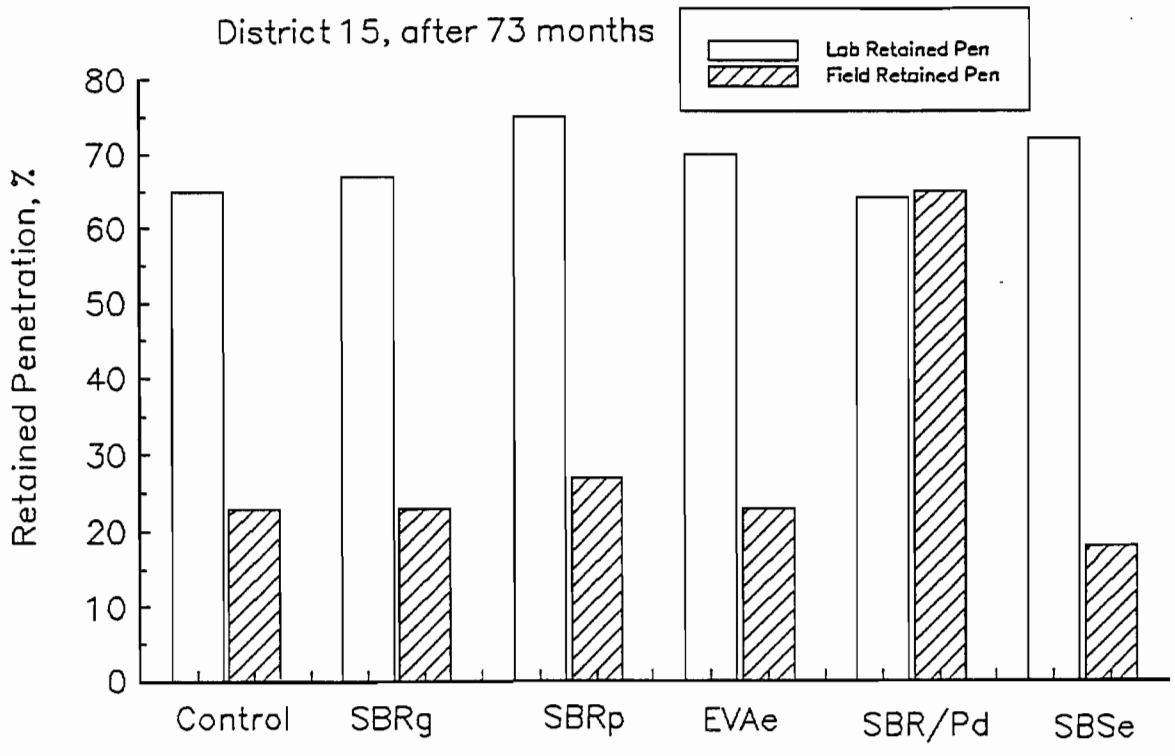

Figure C-13 Laboratory retained penetration versus field retained penetration (District 15)

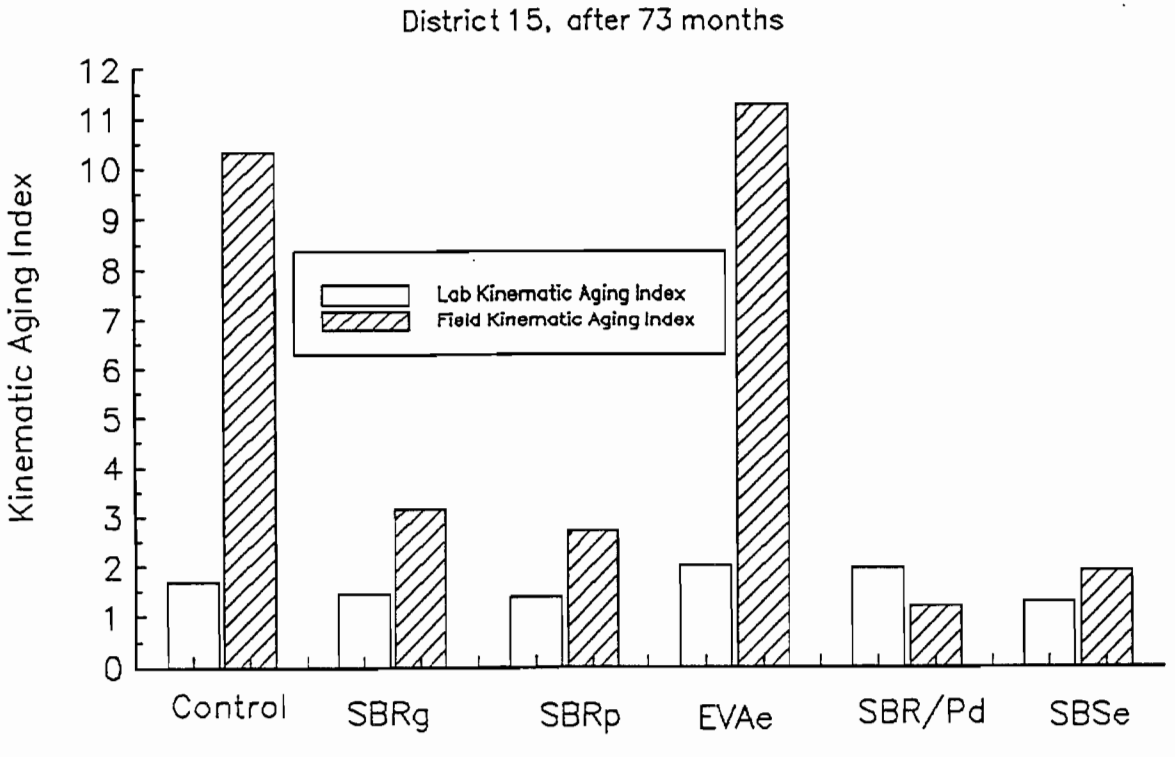

Figure C-14 Laboratory kinematic aging index versus field kinematic aging index (District 15)

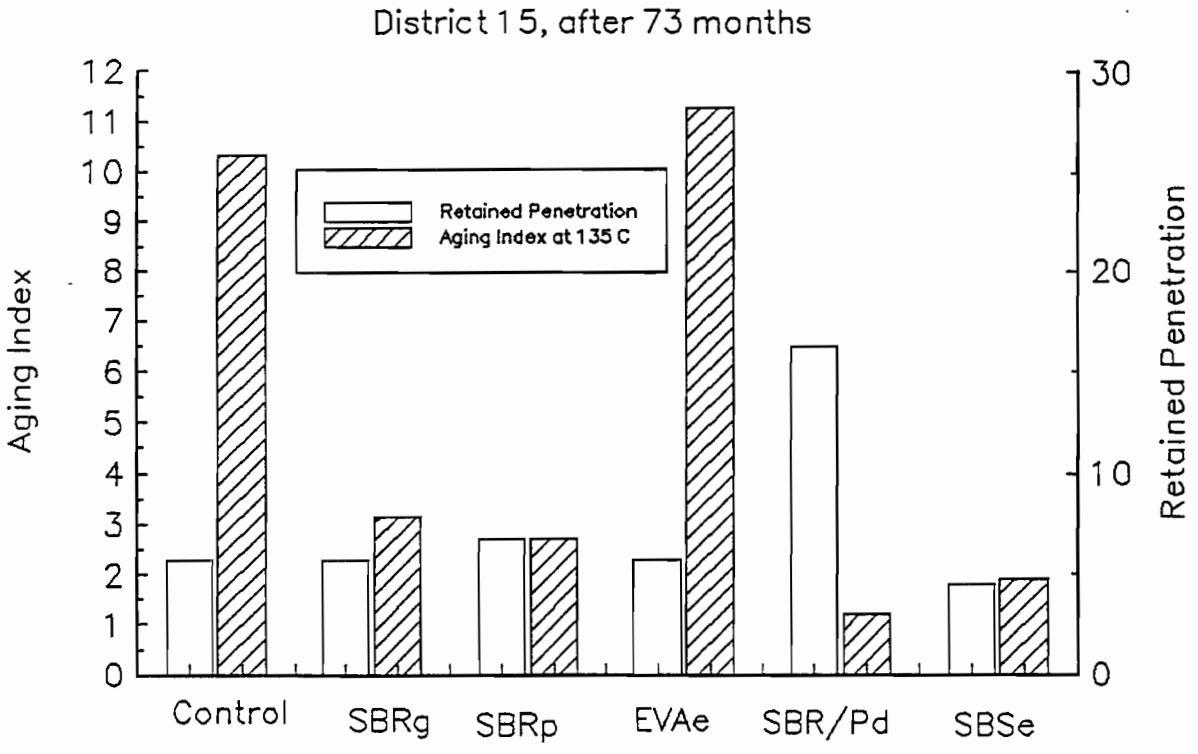

Figure C-15 Aging indexes and retained penetration (District 15)

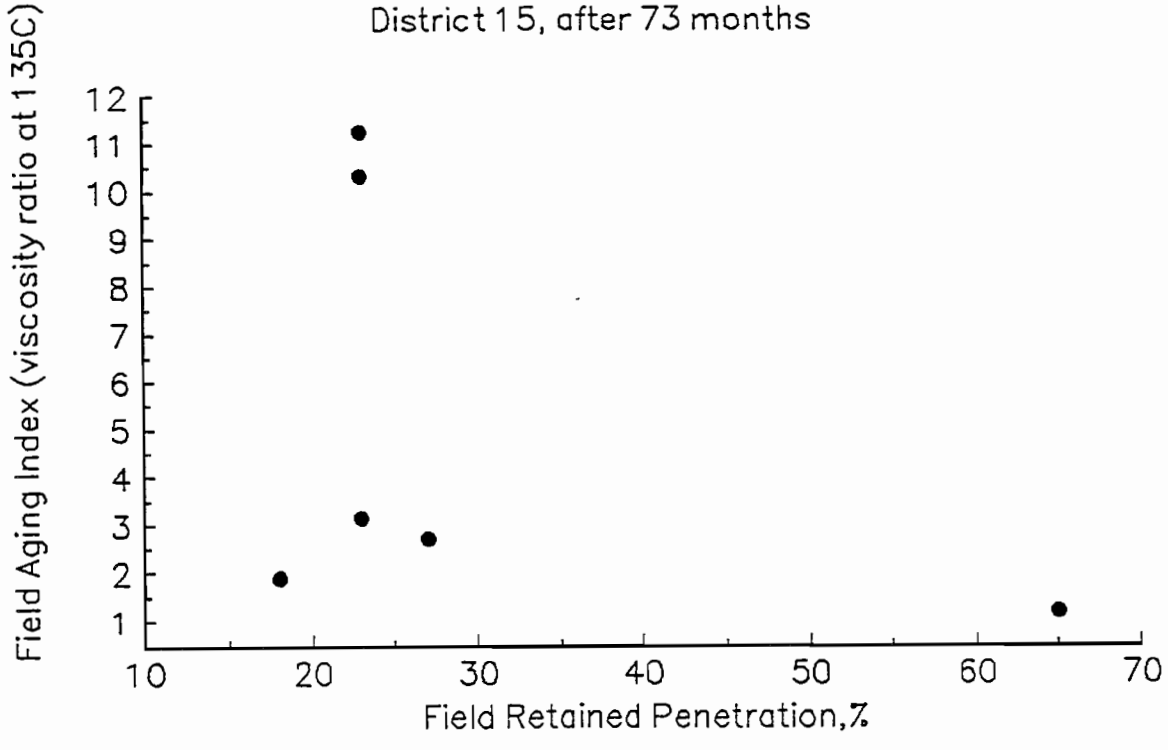

Figure C-16 Field retained penetration versus field aging index at 135°C (District 15)

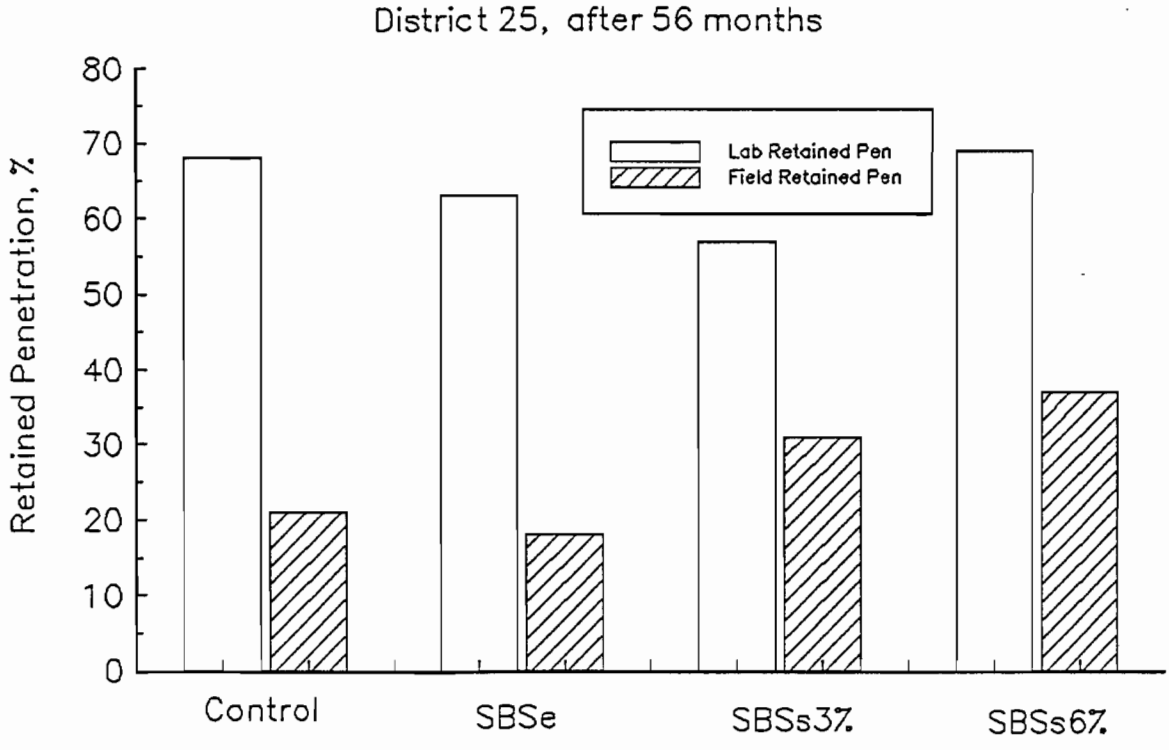

Figure C-17 Laboratory retained penetration versus field retained penetration (District 25)

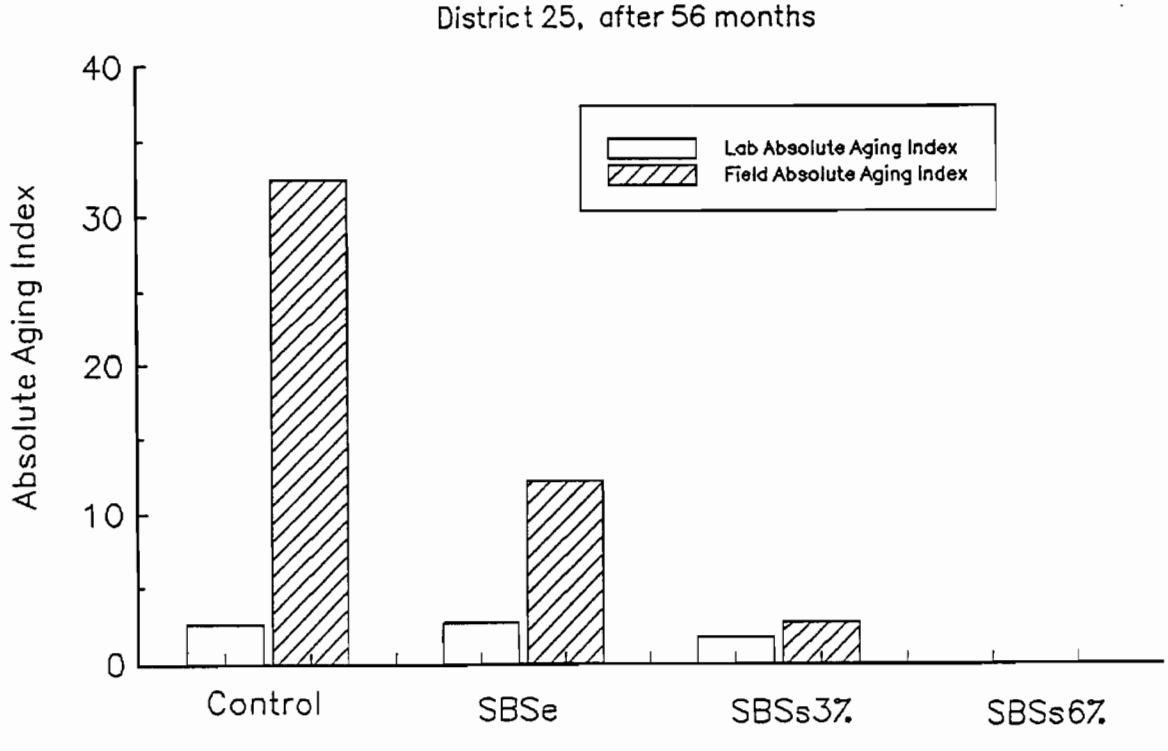

Figure C-18 Laboratory absolute aging index versus field absolute aging index (District 25)

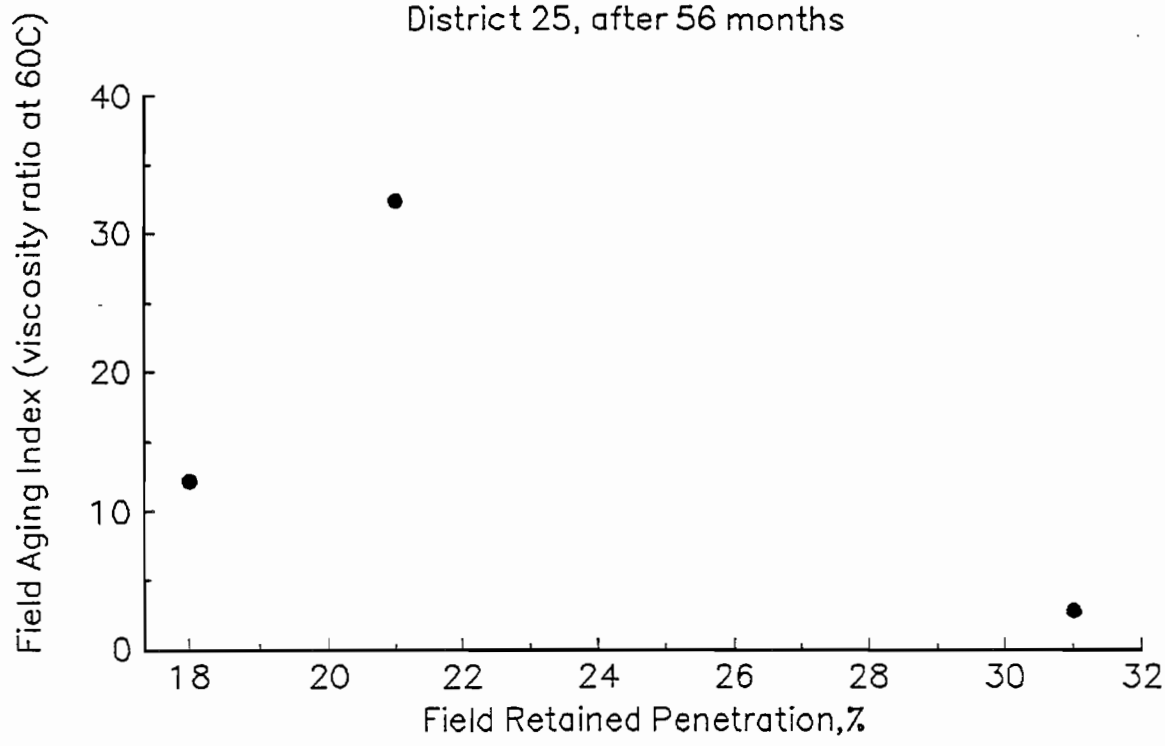

Figure C-19 Field retained penetration versus field aging index at 60°C (District 25)

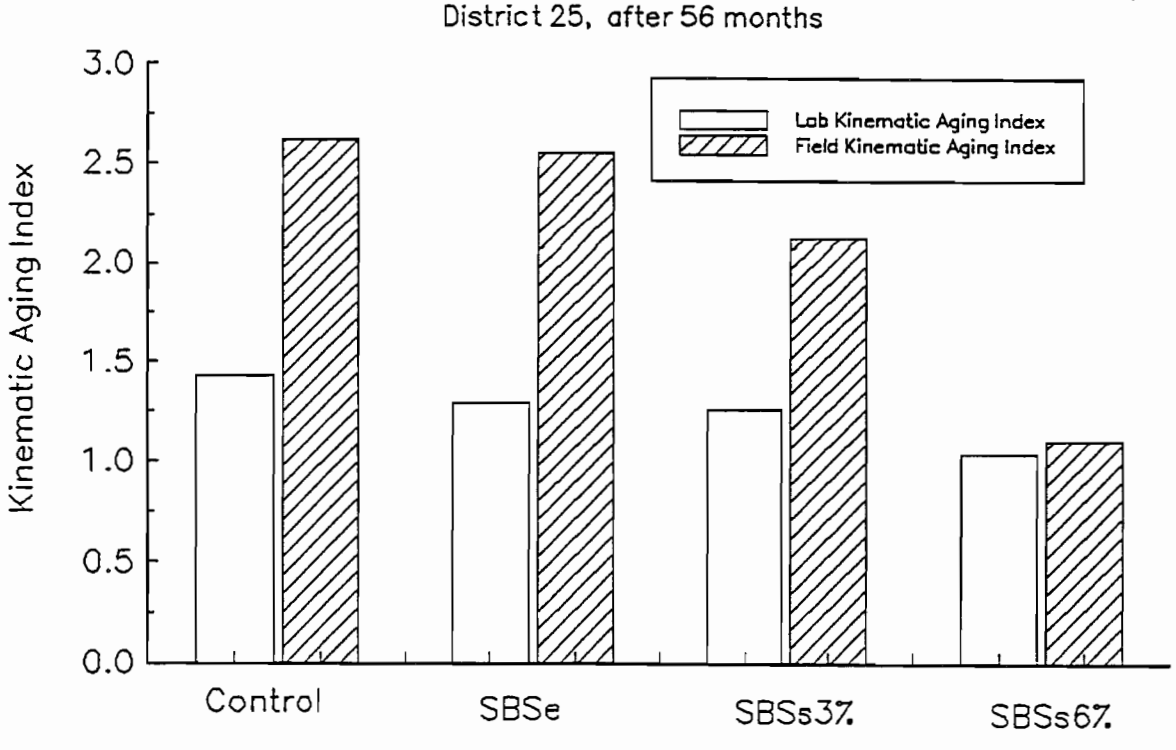

Figure C-20 Laboratory kinematic aging index versus field kinematic aging index (District 25)

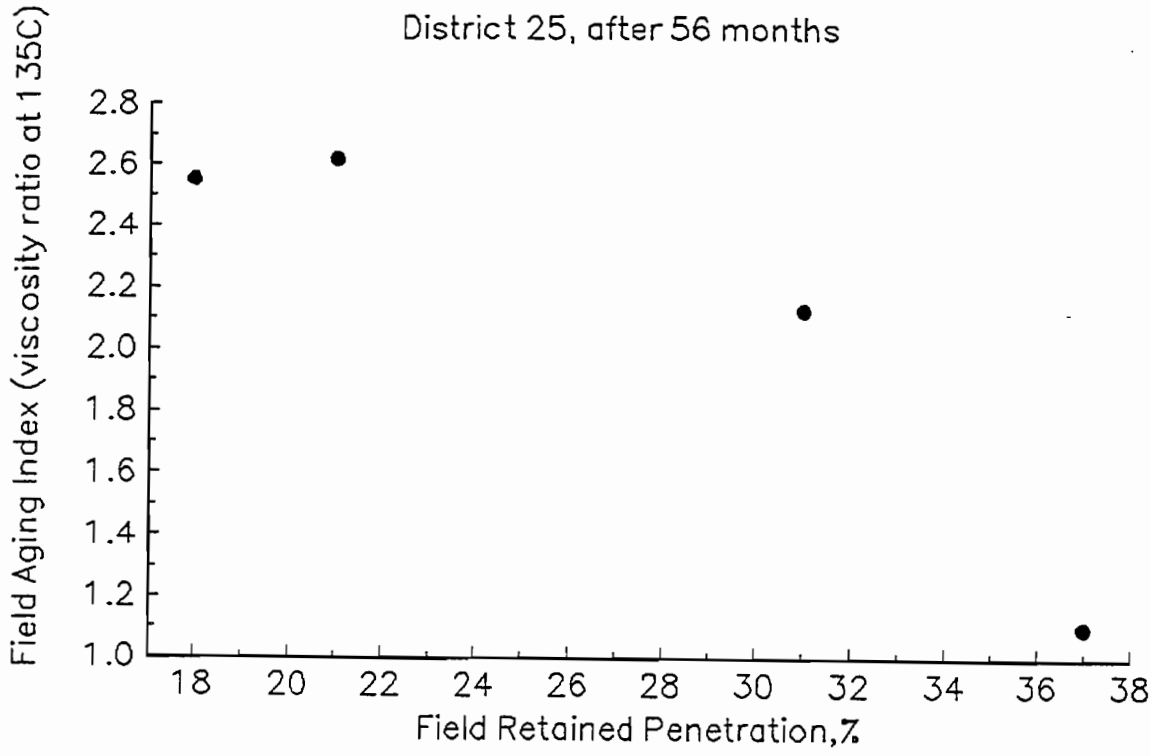

Figure C-21 Field retained penetration versus field aging index at 135°C (District 25)

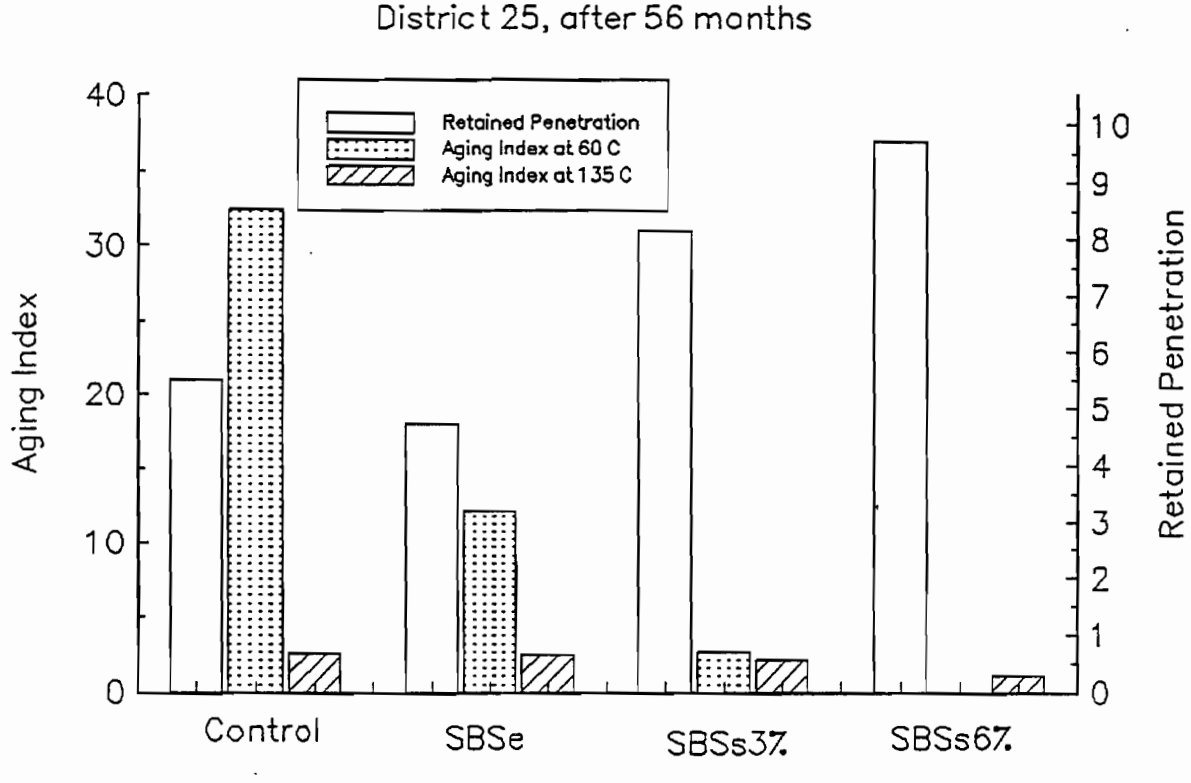

Figure C-22 Aging indexes and retained penetration (District 25)

APPENDIX D

TABLES AND GRAPHS — FIELD AND LABORATORY MIXTURE TESTING

TABLE D-1 DISTRIBUTION OF AIR VOIDS FOR DIFFERENT PROJECTS

District 10				District 11		District 15				District 25			
The following are the percent air voids													
Control	6.7	EVA	5.7	Control	2.2	Control	7.0	Rubber	4.6	Control	7.6	SBSs 6%	7.1
	6.6		6.1		2.3		5.4		7.4		7.6		10.3
	5.4		6.1		2.2		5.7		7.8		7.4		9.1
	5.7		6.4		2.5		7.5		7.2		7.8		10.6
	6.0		5.7		3.2		6.6		4.5		6.8		9.4
	7.0		6.1		2.2		7.3		8.2		8.2		8.5
	10.3		6.0		3.0		5.2		7.9		8.6		8.8
	6.5		6.4		3.5		6.1		8.2		7.1		7.9
	5.7		6.6		2.9		5.9		6.7		6.5		7.2
AVG	**6.7**		**6.1**		**2.7**		**6.3**		**6.9**		**7.5**		**8.8**
SBRg	3.7	SBSe	4.2	SBRg	2.7	SBRg	5.2	SBRp	3.2	SBRg	8.6	SBSe	7.8
	4.0		4.0		2.5		7.5		2.8		7.7		8.1
	3.6		4.4		1.6		5.7		3.9		7.7		7.8
	3.9		4.2		1.2		7.6		4.5		8.6		8.4
	4.9		3.8		1.8		5.9		3.9		10.4		8.5
	5.0		3.9		1.7		7.7		3.2		7.5		9.0
	5.0		4.4		1.8		5.9		4.1		7.9		9.1
	4.6		3.8		2.0		5.9		3.9		7.8		8.2
	7.2		3.5		1.8		5.9		5.1		8.1		7.8
AVG	**4.7**		**4.0**		**1.9**		**6.4**		**3.8**		**8.3**		**8.3**
SBSs 3%	4.7			SBSe	1.7	SBSe	6.0	Fiber	3.2	SBSs 3%	6.8		
	6.2				1.3		5.1		6.6		7.7		
	6.4				1.6		7.2		7.0		7.0		
	4.9				1.1		7.3		6.4		7.3		
	5.5				1.2		6.0		7.8		7.1		
	6.8				1.5		6.1		6.0		7.4		
	5.0				1.4		6.0		6.9		7.2		
	4.9				1.9		6.4		6.6		6.5		
	4.9				1.3		5.8		7.4		6.4		
AVG	**5.5**				**1.4**		**6.2**		**6.4**		**7.0**		
						EVA	6.2	SBR/ Pd	7.7				
							7.7		7.3				
							6.3		8.2				
							7.8		6.9				
							6.7		8.8				
							7.3		9.6				
							7.1		9.6				
							10.3		9.1				
							7.4		7.8				
AVG							**7.4**		**8.3**				

Dist →	**10**	**11**	**15**	**25**
Mean	5.4	2.0	6.5	8.0
Max	10.3	3.5	10.3	10.6
Min	3.5	1.1	2.8	6.4
StdDv	1.3	0.7	1.6	1.0

TABLE D-2 INDIRECT TENSILE STRENGTH, STRAIN AT FAILURE, AND SECANT MODULUS AT 39°F (4°C) FOR FIELD CORES OF DISTRICT 10

Age : 34 months Cored in May 1993

Section	Height inches	Rice Sp.Gr.	Air Voids %	ITS psi 39F	StF E-03 39F	MS psi,E03 39F
	2.00	2.509	6.6	333	1.18	455
Control	1.96	2.509	6.6	364	1.39	422
	1.92	2.509	5.4	378	1.18	517
Avg.			**6.2**	**358**	**1.25**	**465**
	2.00	2.482	3.7	487	1.18	667
SBRg	2.06	2.482	4.0	448	1.07	675
	2.04	2.482	3.6	540	1.61	542
Avg.			**3.7**	**492**	**1.29**	**628**
	2.08	2.458	4.2	436	0.80	875
SBSe	2.03	2.458	4.0	450	1.07	678
	2.06	2.458	4.4	385	0.64	966
Avg.			**4.2**	**423**	**0.84**	**839**
	1.88	2.492	4.7	355	2.25	255
SBSs	1.87	2.492	6.2	365	2.79	211
	1.88	2.492	6.4	320	2.68	193
Avg.			**5.8**	**347**	**2.57**	**220**
	2.06	2.494	5.7	412	1.66	401
EVAe	2.06	2.494	6.1	403	1.82	357
	2.02	2.494	6.1	360	2.14	271
Avg.			**6.0**	**392**	**1.88**	**343**

Sp.Gr. : specific gravity
ITS : indirect tensile strength
StF : strain at failure
MS : secant modulus
SBRg : UP 70, Goodyear
SBSe : Styrelf-13, Elf
SBSs : Kraton D 1101, Shell
EVAe : Polybilt 103, Exxon

1 inch = 25.4 mm
1 lb = 453 grams
1 psi = 6895 Pa
1 Δ°F = 0.556 Δ°C

TABLE D-3 INDIRECT TENSILE STRENGTH, STRAIN AT FAILURE, AND SECANT MODULUS AT 77°F (25°C) FOR FIELD CORES OF DISTRICT 10

Age: 34 months Cored in May 1993

Section	Height inches	Rice Sp.Gr.	Air Voids %	ITS psi 77F	StF E-03 77F	MS psi,E03 77F
	2.05	2.509	5.7	195	6.20	59
Control	2.02	2.509	6.0	229	7.30	59
	1.96	2.509	7.0	219	6.83	61
AVG.			**6.2**	**215**	**6.77**	**60**
	2.06	2.482	3.9	249	8.40	56
SBRg	2.01	2.482	4.9	225	7.88	54
	2.05	2.482	5.0	269	7.35	69
AVG.			**4.6**	**248**	**7.88**	**60**
	2.06	2.458	4.2	254	7.46	64
SBSe	1.94	2.458	3.8	243	9.98	46
	1.92	2.458	3.9	246	6.83	68
AVG.			**4.0**	**248**	**8.09**	**59**
	1.98	2.492	4.9	150	7.35	38
SBSs	1.86	2.492	5.5	159	7.35	41
	2.12	2.492	6.8	109	12.86	16
AVG.			**5.7**	**139**	**9.19**	**32**
	2.03	2.494	6.4	156	7.88	37
EVAe	2.08	2.494	5.7	169	6.30	51
	1.95	2.494	6.1	127	7.14	33
AVG.			**6.1**	**151**	**7.11**	**41**

Sp.Gr. : specific gravity
ITS : indirect tensile strength
StF : strain at failure
MS : secant modulus
SBRg : UP 70, Goodyear
SBSe : Styrelf-13, Elf
SBSs : Kraton D 1101, Shell
EVAe : Polybilt 103, Exxon

1 inch = 25.4 mm
1 lb = 453 grams
1 psi = 6895 Pa
1 Δ°F = 0.556 Δ°C

TABLE D-4 INDIRECT TENSILE STRENGTH, STRAIN AT FAILURE, AND SECANT MODULUS AT 104°F (40°C) FOR FIELD CORES OF DISTRICT 10

Age: 34 months Cored in May 1993

Section	Height inches	Rice Sp.Gr.	Air Voids %	ITS psi 104F	StF E-03 104F	MS psi,E03 104F
	1.70	2.509	10.3	66	7.98	18
Control	1.84	2.509	6.5	66	6.22	23
	2.13	2.509	5.7	69	9.07	17
Avg.			**7.5**	**67**	**7.75**	**19**
	1.61	2.482	5.0	46	9.53	11
SBRg	1.73	2.482	4.6	56	11.40	11
	1.82	2.482	7.2	50	11.09	10
Avg.			**5.6**	**51**	**10.67**	**10**
	1.93	2.458	4.4	35	8.08	9
SBSe	2.15	2.458	3.8	43	----	5
	1.88	2.458	3.5	71	8.81	18
Avg.			**3.9**	**49**	**8.44**	**11**
	2.18	2.492	5.0	47	5.70	18
SBSs	2.15	2.492	4.9	45	8.81	11
	2.03	2.492	4.9	33	8.08	9
Avg.			**4.9**	**42**	**7.53**	**13**
	1.91	2.494	6.0	30	7.46	9
EVAe	1.78	2.494	6.4	38	7.51	11
	2.01	2.494	6.6	34	5.08	15
Avg.			**6.3**	**34**	**6.68**	**12**

Sp.Gr. : specific gravity
ITS : indirect tensile strength
StF : strain at failure
MS : secant modulus
SBRg : UP 70, Goodyear
SBSe : Styrelf-13, Elf
SBSs : Kraton D 1101, Shell
EVAe : Polybilt 103, Exxon

1 inch = 25.4 mm
1 lb = 453 grams
1 psi = 6895 Pa
1 Δ°F = 0.556 Δ°C Δ°C

TABLE D-5 INDIRECT TENSILE STRENGTH, STRAIN AT FAILURE, AND SECANT MODULUS AT 39°F (4°C) FOR FIELD CORES OF DISTRICT 11

Age: 49 months Cored in May 1993

Section	Height inches	Rice Sp.Gr.	Air Voids %	ITS psi 39F	StF E-03 39F	MS psi,E03 39F
	1.39	1.985	2.2	511	1.88	440
Control	1.54	1.985	2.3	479	1.88	412
	1.47	1.985	2.2	461	2.36	316
Avg.			**2.2**	**484**	**2.04**	**389**
	1.54	1.996	2.7	443	1.82	393
SBRg	1.65	1.996	1.4	550	1.88	474
	1.76	1.996	1.5	527	1.93	441
Avg.			**1.8**	**507**	**1.88**	**436**
	1.30	2.008	1.4	527	2.14	397
SBSe	1.18	2.008	1.9	505	2.68	304
	1.36	2.008	1.3	544	2.95	298
Avg.			**1.5**	**525**	**2.59**	**333**

Sp.Gr.: specific gravity
ITS: indirect tensile srength
StF: strain at failure
MS: secant modulus
SBRg : UP 70 ,Goodyear
SBSe : Styrelf-13, Elf

1 inch = 25.4 mm

1 lb = 453 grams
1 psi = 6895 Pa
1 Δ°F = 0.556 Δ°C

TABLE D-6 INDIRECT TENSILE STRENGTH, STRAIN AT FAILURE, AND SECANT MODULUS AT 77°F (25°C) FOR FIELD CORES OF DISTRICT 11

Age: 49 months Cored in May 1993

Section	Height inches	Rice Sp.Gr.	Air Voids %	ITS psi 77F	StF E-03 77F	MS psi,E03 77F
	1.47	1.985	2.5	195	9.45	40
Control	1.55	1.985	3.2	216	9.12	45
	1.49	1.985	2.2	235	8.93	50
Avg.			**2.6**	**215**	**9.19**	**45**
	1.76	1.996	1.2	247	10.08	47
SBR g	1.79	1.996	1.8	239	9.19	50
	1.71	1.996	1.7	265	8.09	63
Avg.			**1.6**	**250**	**9.12**	**53**
	1.30	2.008	1.1	227	9.71	45
SBSe	1.28	2.008	1.2	200	11.55	33
	1.32	2.008	1.5	233	9.45	47
Avg.			**1.3**	**220**	**10.24**	**42**

Sp.Gr.: specific gravity
ITS: indirect tensile srength
StF: strain at failure
MS: secant modulus
SBRg : UP 70 ,Goodyear
SBSe : Styrelf-13, Elf

1 inch = 25.4 mm

1 lb 453 grams
1 psi 6895 Pa
1 Δ°F = 0.556 Δ°C

TABLE D-7 INDIRECT TENSILE STRENGTH, STRAIN AT FAILURE, AND SECANT MODULUS AT 104°F (40°C) FOR FIELD CORES OF DISTRICT 11

Age: 49 months Cored in May 1993

Section	Hight inches	Rice Sp.Gr.	Air Voids %	ITS psi 104F	StF e-03 104F	MS psi,e03 104F
	1.52	1.985	3.0	81	7.77	23
Control	1.53	1.985	3.5	73	10.88	15
	1.45	1.985	1.3	76	8.81	19
Avg.			**2.6**	**77**	**9.15**	**19**
	1.56	1.996	1.8	78	11.09	16
SBR g	1.83	1.996	2.0	78	11.03	16
	1.67	1.996	1.8	85	9.07	21
Avg.			**1.9**	**80**	**10.39**	**17**
	1.39	2.082	2.0	77	10.88	16
SBSe	1.32	2.082	3.4	57	11.34	11
	1.23	2.082	3.3	75	9.84	17
Avg.			**2.9**	**70**	**10.69**	**15**

Sp.Gr. :specific gravity
ITS: indirect tensile strength
StF: strain at failure
MS: secant modulus
SBRg : UP 70 ,Goodyear
SBSe : Styrelf-13, Elf

1 inch = 25.4 mm
1 lb = 453 grams
1 psi = 6895 Pa
1 Δ°F = 0.556 Δ°C

TABLE D-8 INDIRECT TENSILE STRENGTH, STRAIN AT FAILURE, AND SECANT MODULUS AT 39°F (4°C) FOR FIELD CORES OF DISTRICT 15

Age: 73 months — Cored in May 1993

Section	Height inches	Rice Sp.Gr.	Air Voids %	ITS psi 39F	StF E-03 39F	MS psi,E03 39F
	1.438	2.416	5.2	390	1.72	367
SBRg	1.410	2.416	7.5	377	1.07	567
	1.416	2.416	5.7	490	0.54	1476
Avg.			**6.1**	**419**	**1.11**	**804**
	1.300	2.420	6.0	432	1.39	501
SBSe	1.304	2.420	5.1	557	0.54	1679
	1.333	2.420	7.2	449	1.50	483
Avg.			**6.1**	**479**	**1.14**	**888**
	1.613	2.418	7.0	329	0.64	827
Control	1.624	2.418	5.4	363	1.23	476
	1.644	2.418	5.7	422	1.34	509
Avg.			**6.1**	**372**	**1.07**	**604**
	1.631	2.417	6.2	364	1.93	305
EVAe	1.596	2.417	7.7	358	1.45	399
	1.444	2.417	6.3	376	1.07	566
Avg.			**6.7**	**366**	**1.48**	**423**
	1.555	2.365	4.6	326	1.18	447
Rubber	1.561	2.365	7.4	256	1.29	322
	1.500	2.365	7.8	229	1.50	246
Avg.			**6.6**	**270**	**1.32**	**338**
	1.774	2.393	3.2	460	1.39	533
SBRp	1.650	2.393	2.8	479	1.39	555
	1.701	2.393	3.9	485	1.61	487
Avg.			**3.3**	**475**	**1.47**	**525**
	1.518	2.421	1.6	277	3.22	139
Fiber	1.515	2.421	6.6	360	0.80	723
	1.510	2.421	7.0	372	0.96	623
Avg.			**5.1**	**336**	**1.66**	**495**
	2.014	2.421	7.7	341	1.34	410
SBR/Pd	1.951	2.421	7.7	338	1.72	318
	2.123	2.421	7.3	377	1.18	516
Avg.			**7.5**	**352**	**1.41**	**415**

Sp.Gr. : specific gravity
ITS : indirect tensile strength
StF : strain at failure
MS : secant modulus
SBRg : UP 70 ,Goodyear
SBSe : Styrelf-13, Elf
EVAe : Polybilt 103, Exxon
Rubber : Genstar C107,Crafco

1 inch = 25.4 mm
1 lb = 453 grams
1 psi = 6895 Pascal
1 Δ°F = 0.556 Δ°C

TABLE D-9 INDIRECT TENSILE STRENGTH, STRAIN AT FAILURE, AND SECANT MODULUS AT 77°F (25°C) FOR FIELD CORES OF DISTRICT 15

Age: 73 months Cored in May 1993

Section	Height inches	Rice Sp.Gr.	Air Voids %	ITS psi 77F	StF E-03 77F	MS psi,E03 77F
	1.46	2.416	7.6	155	3.10	96
SBRg	1.39	2.416	5.9	199	3.89	98
	1.28	2.416	7.7	186	3.68	97
Avg.			**7.1**	**180**	**3.55**	**97**
	1.50	2.420	7.3	199	2.89	132
SBSe	1.65	2.420	6.0	219	4.46	94
	1.38	2.420	6.1	169	5.88	55
Avg.			**6.5**	**196**	**4.41**	**94**
	1.83	2.418	7.5	193	3.68	101
Control	1.55	2.418	6.6	190	3.41	107
	1.43	2.418	7.3	174	3.68	91
Avg.			**7.1**	**186**	**3.59**	**100**
	1.63	2.417	7.8	152	2.52	116
EVAe	1.61	2.417	6.7	167	2.36	136
	1.24	2.417	7.3	163	2.21	142
Avg.			**7.3**	**161**	**2.36**	**131**
	1.72	2.365	7.2	132	3.05	83
Rubber	1.95	2.365	4.5	123	4.46	53
	1.42	2.365	8.2	104	2.63	76
Avg.			**6.6**	**120**	**3.38**	**71**
	1.72	2.393	4.5	204	4.10	96
SBRp	1.76	2.393	3.9	210	4.73	85
	1.71	2.393	3.2	207	6.46	61
Avg.			**3.9**	**207**	**5.09**	**81**
	1.45	2.421	6.4	196	3.57	105
Fiber	1.28	2.421	7.8	170	3.57	91
	1.72	2.421	6.0	177	3.78	90
Avg.			**6.7**	**181**	**3.64**	**96**
	1.61	2.421	8.2	149	2.57	111
SBR/Pd	1.85	2.421	6.9	154	4.41	67
	1.85	2.421	8.8	127	3.41	71
Avg.			**8.0**	**143**	**3.47**	**83**

Sp.Gr. : specific gravity
ITS : indirect tensile strength
StF : strain at failure
MS : secant modulus
SBRg : UP 70 ,Goodyear
SBSe : Styrelf-13, Elf
EVAe : Polybilt 103, Exxon
Rubber : Genstar C107,Crafco

1 inch = 25.4 mm
1 lb = 453 grams
1 psi = 6895 Pascal
1 Δ°F = 0.556 Δ°C

TABLE D-10 INDIRECT TENSILE STRENGTH, STRAIN AT FAILURE, AND SECANT MODULUS AT 104°F (40°C) FOR FIELD CORES OF DISTRICT 15

Age: 73 months — Cored in May 1993

Section	Height inches	Rice Sp.Gr.	Air Voids %	ITS psi 104F	StF E-03 104F	MS psi,E03 104F
	1.16	2.416	5.9	70	6.22	25
SBRg	1.57	2.416	5.9	75	5.70	29
	1.26	2.416	5.9	72	5.28	30
Avg.			**5.9**	**72**	**5.73**	**28**
	1.96	2.420	6.0	68	6.11	25
SBSe	1.63	2.420	6.4	76	6.22	27
	1.53	2.420	5.8	106	6.01	39
Avg.			**6.1**	**83**	**6.11**	**30**
	1.55	2.418	5.2	83	4.25	44
Control	1.59	2.418	6.1	68	4.92	31
	1.51	2.418	5.9	81	3.99	45
Avg.			**5.7**	**77**	**4.39**	**40**
	1.70	2.417	7.1	69	3.63	42
EVAe	1.56	2.417	10.3	72	3.11	52
	1.43	2.417	7.4	72	3.37	47
Avg.			**8.2**	**71**	**3.37**	**47**
	1.67	2.365	7.9	64	4.14	34
Rubber	1.67	2.365	8.2	56	10.36	12
	1.87	2.365	6.7	69	3.63	42
Avg.			**7.6**	**63**	**6.04**	**29**
	1.82	2.393	4.1	79	7.77	23
SBRp	1.75	2.393	3.9	95	5.96	35
	1.97	2.393	5.1	83	5.96	31
Avg.			**4.4**	**85**	**6.56**	**30**
	1.60	2.421	6.9	69	5.70	27
Fiber	1.40	2.421	6.6	91	3.63	56
	1.76	2.421	7.4	60	7.51	18
Avg.			**6.9**	**73**	**5.61**	**34**
	1.49	2.421	9.6	62	5.91	23
SBR/Pd	1.52	2.421	9.1	68	3.83	39
	1.69	2.421	7.8	73	3.63	45
Avg.			**8.8**	**68**	**4.45**	**36**

Sp.Gr. : specific gravity
ITS : indirect tensile strength
StF : strain at failure
MS : secant modulus
SBRg : UP 70 ,Goodyear
SBSe : Styrelf-13, Elf
EVAe : Polybilt 103, Exxon
Rubber : Genstar C107,Crafco
SBRp : NS 175, Polysar
SBR/Pd : SBR/Polyolefin, Dow

1 inch = 25.4 mm
1 lb = 453 grams
1 psi = 6895 Pascals
1 Δ°F = 0.556 Δ°C

TABLE D-11 INDIRECT TENSILE STRENGTH, STRAIN AT FAILURE, AND SECANT MODULUS AT 39°F (4°C) FOR FIELD CORES OF DISTRICT 25

Age: 56 months

Section	Height inches	Rice Sp.Gr.	Air Voids %	ITS psi 39F	StF E-03 39F	MS psi,E03 39F
	1.62	2.439	7.6	402	1.39	466
Control	1.53	2.439	7.6	362	1.07	545
	1.58	2.439	7.4	369	1.07	556
Avg.			**7.5**	**378**	**1.18**	**522**
	1.62	2.439	8.6	281	1.07	423
SBRg	1.67	2.439	7.7	411	1.18	563
	1.68	2.439	7.7	411	1.07	619
Avg.			**8.0**	**367**	**1.11**	**535**
	1.74	2.425	7.8	295	1.18	405
SBSe	1.88	2.425	8.1	389	1.61	390
	1.58	2.425	7.8	408	1.50	439
Avg.			**7.9**	**364**	**1.43**	**411**
	1.96	2.436	6.8	441	1.82	391
SBSs3%	1.93	2.436	7.7	339	1.18	465
	1.94	2.436	7.0	423	1.72	398
Avg.			**7.2**	**401**	**1.57**	**418**
	1.67	2.422	7.1	328	2.47	215
SBSs,6%	1.60	2.422	10.3	247	2.68	149
	1.54	2.422	9.1	312	2.68	188
Avg.			**8.8**	**295**	**2.61**	**184**

Sp.Gr. : specific gravity
ITS : indirect tensile strength
StF : strain at failure
MS : secant modulus
SBRg : UP 70, Goodyear
SBSe : Styrelf-13, Elf
SBSs,3% : Kraton D-1101,3% content, Shell
SBSs,6% : Kraton D-1101,6% content, Shell

1 inch = 25.4 mm
1 lb = 453 grams
1 psi = 6895 Pascals
1 Δ°F = 0.556 Δ°C

TABLE D-12 INDIRECT TENSILE STRENGTH, STRAIN AT FAILURE, AND SECANT MODULUS AT 77°F (25°C) FOR FIELD CORES OF DISTRICT 25

Age: 56 months Cored in May 1993

Section	Height inches	Rice Sp.Gr.	Air Voids %	ITS psi 77F	StF E-03 77F	MS psi,E03 77F
	1.54	2.439	7.8	160	6.51	47
Control	1.53	2.439	6.8	167	4.52	71
	1.45	2.439	8.2	152	3.41	86
Avg.			**7.6**	**160**	**4.81**	**68**
	1.73	2.439	8.6	158	4.73	64
SBRg	1.54	2.439	10.4	150	3.68	78
	1.74	2.439	7.5	191	5.78	64
Avg.			**8.8**	**166**	**4.73**	**69**
	1.59	2.425	8.4	162	3.94	79
SBSe	1.77	2.425	8.5	184	5.41	65
	1.61	2.425	9.0	159	4.31	71
Avg.			**8.6**	**168**	**4.55**	**72**
	1.95	2.436	7.3	204	6.20	63
SBSs3%	1.94	2.436	7.1	194	6.41	58
	1.87	2.436	7.4	174	6.83	49
Avg.			**7.3**	**191**	**6.48**	**57**
	1.67	2.422	10.6	110	7.61	28
SBSs,6%	1.52	2.422	9.4	121	7.35	32
	1.94	2.422	8.5	125	6.30	38
Avg.			**9.5**	**119**	**7.09**	**33**

Sp.Gr. : specific gravity
ITS : indirect tensile strength
StF : strain at failure
MS : secant modulus
SBRg : UP 70, Goodyear
SBSe : Styrelf-13, Elf
SBSs,3% : Kraton D-1101,3% content, Shell
SBSs,6% : Kraton D-1101,6% content, Shell

1 inch = 25.4 mm
1 lb = 453 grams
1 psi = 6895 Pascal
1 Δ°F = 0.556 Δ°C

TABLE D-13 INDIRECT TENSILE STRENGTH, STRAIN AT FAILURE, AND SECANT MODULUS AT 104°F (40°C) FOR FIELD CORES OF DISTRICT 25

Age: 56 months Cored in May 1993

Section	Height inches	Rice Sp.Gr.	Air Voids %	ITS psi 104F	StF E-03 104F	MS psi,E03 104F
	1.63	2.439	8.6	51	7.77	15
Control	1.55	2.439	7.1	51	7.77	15
	1.80	2.439	6.5	53	9.01	13
Avg.			**7.4**	**52**	**8.18**	**14**
	2.01	2.439	7.9	47	8.55	12
SBRg	1.93	2.439	7.8	55	8.29	15
	1.71	2.439	8.1	52	7.51	15
Avg.			**7.9**	**52**	**8.12**	**14**
	1.80	2.425	9.1	59	8.39	16
SBSe	1.78	2.425	8.2	59	7.04	19
	1.66	2.425	7.8	55	8.81	14
Avg.			**8.4**	**58**	**8.08**	**16**
	2.19	2.436	7.2	56	8.81	14
SBSs3%	2.19	2.436	6.5	60	8.91	15
	2.23	2.436	6.4	56	9.84	13
Avg.			**6.7**	**58**	**9.19**	**14**
	1.72	2.422	8.8	50	8.91	13
SBSs,6%	1.60	2.422	7.9	52	10.10	11
	1.44	2.422	7.3	56	10.62	12
Avg.			**8.0**	**53**	**9.88**	**12**

Sp.Gr. : specific gravity
ITS : indirect tensile strength
StF : strain at failure
MS : secant modulus
SBRg : UP 70, Goodyear
SBSe : Styrelf-13, Elf
SBSs,3% : Kraton D-1101,3% content, Shell
SBSs,6% : Kraton D-1101,6% content, Shell

1 inch = 25.4 mm
1 lb = 453 grams
1 psi = 6895 Pascal
1 Δ°F = 0.556 Δ°C

TABLE D-14 TENSILE STRAIN AT FAILURE OF AGED FIELD CORES COMPARED WITH TENSILE STRAIN AT FAILURE OF LABORATORY-COMPACTED LABORATORY MIXES (1)

District	Polymer	field core TSF,% 39F	lab mix TSF,% 39F	field core TSF,% 77F	lab mix TSF,% 77F	field core TSF,% 104F	lab mix TSF,% 104F
10	control	0.13	0.24	0.68	1.23	0.78	1.58
	SBRg	0.13	0.23	0.79	1.33	1.07	1.52
	SBSe	0.08	0.26	0.81	2.25	0.84	2.86
	SBSs,3%	0.26	0.64	0.19	1.79	0.75	2.08
	EVAe	0.19	0.77	0.71	1.33	0.67	1.31
11	control	0.20	0.37	0.92	1.28	0.92	1.30
	SBRg	0.19	0.36	0.91	1.51	1.04	1.57
	SBSe	0.26	0.75	1.02	2.15	1.07	2.41
15	Control	0.11	0.18	0.36	0.55	0.44	0.78
	SBRg	0.11	0.31	0.36	0.94	0.57	1.33
	SBSe	0.11	0.51	0.44	1.38	0.61	1.91
	EVAe	0.15	0.20	0.24	0.55	0.32	0.77
	Rubber	0.13	0.58	0.34	1.80	0.60	2.71
	SBRp	0.15	0.33	0.51	0.90	0.66	1.04
	Fiber	0.17		0.36		0.56	
	SBR/pd	0.14	0.22	0.35	3.60	0.45	0.43
25	Control	0.12	0.29	0.48	0.58	0.78	1.26
	SBRg	0.11		0.47		0.81	
	SBSe	0.14	0.41	0.46	1.76	0.81	2.26
	SBSs,3%	0.16	0.42	0.65	1.84	0.92	2.47
	SBSs,6%	0.21	1.06	0.71	3.38	0.99	3.82

(1) NOTE:
The results are reported as the average of testing three specimens.
The field cores were tested during this research study (RS1306)
The laboratory compacted mixtures were tested during research study 492.

(2) Data were not available for blank cells

TSF: Tensile Strain at Failure $1\ \Delta°F = 0.556\ \Delta°C$

SBRg : UP 70 ,Goodyear
SBSe : Styrelf-13, Elf
EVAe : Polybilt 103, Exxon
Rubber : Genstar C107,Crafco
SBRp : NS 175, Polysar
SBR/Pd : SBR/Polyolefin, Dow
SBSs,3% : Kraton D-1101,3% content, Shell
SBSs,6% : Kraton D-1101,6% content, Shell

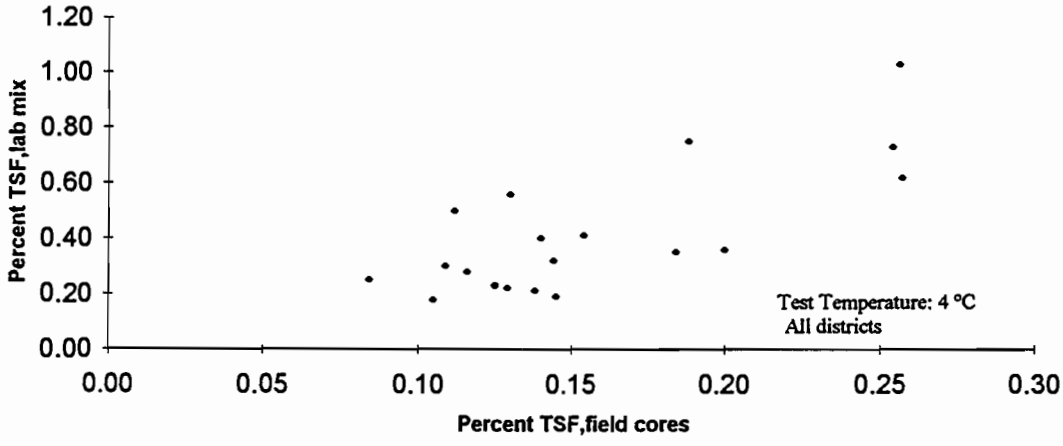

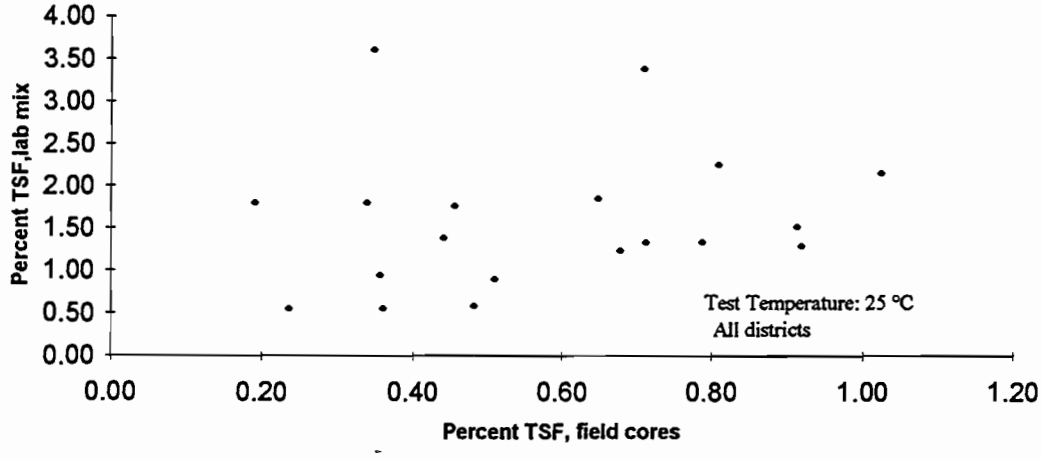

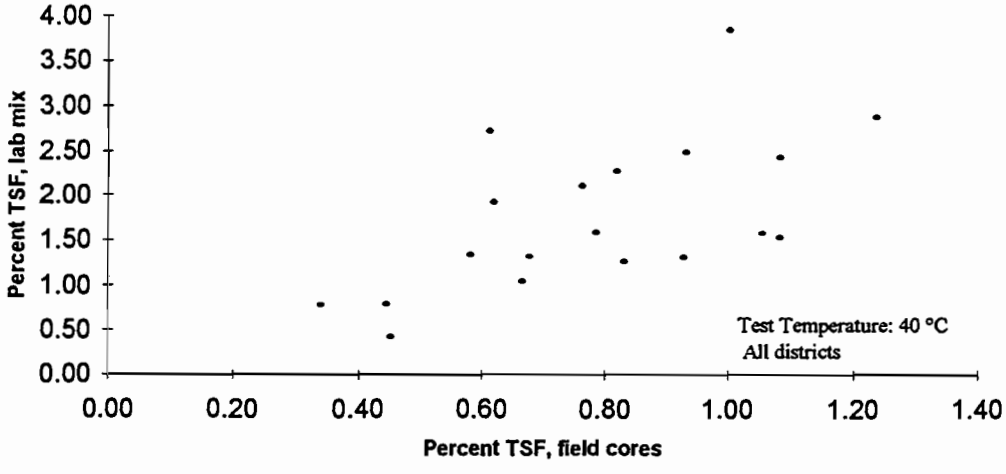

Figure D-1 Tensile strain at failure (TSF) of field cores versus tensile strain at failure of laboratory-compacted mixtures

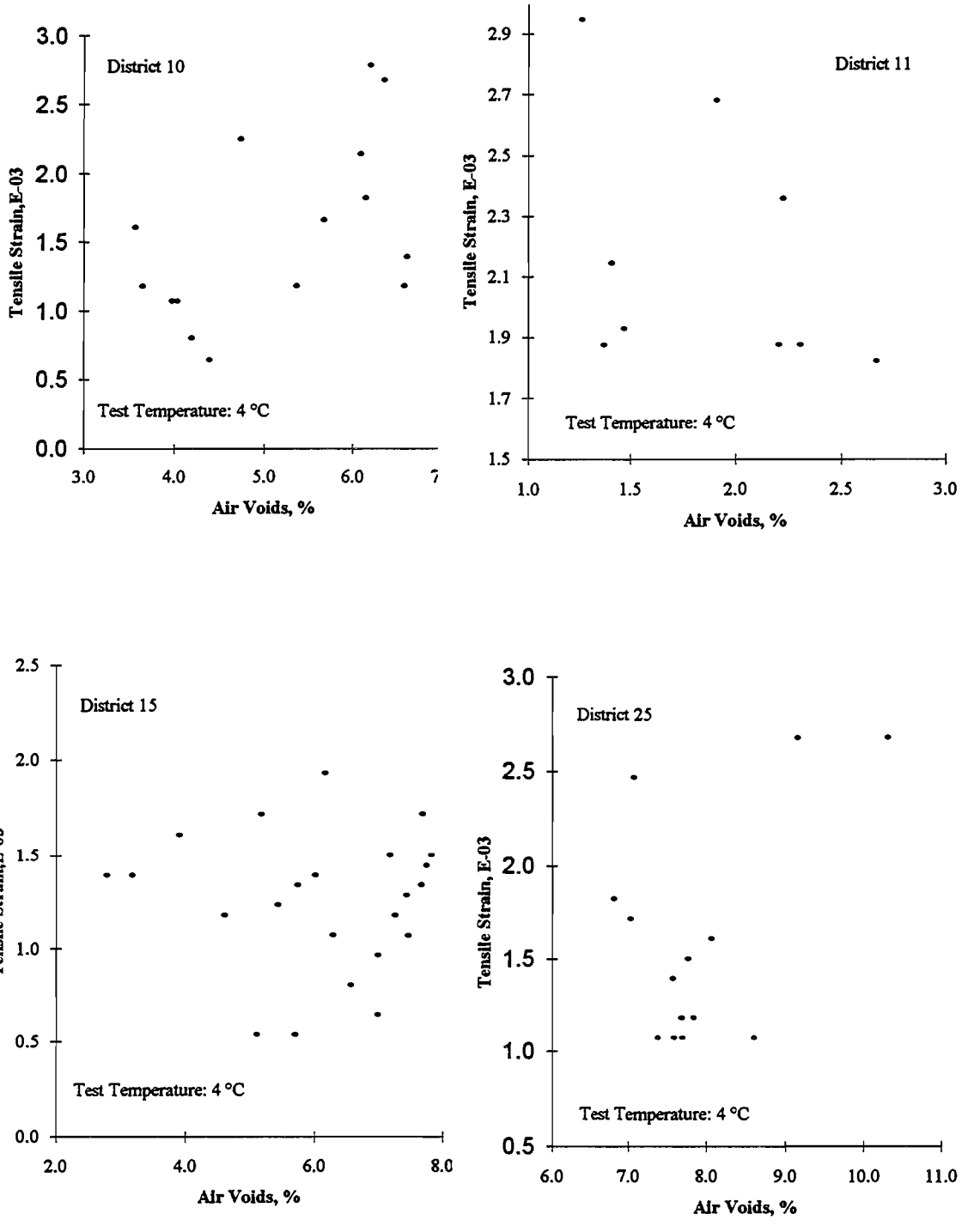

Figure D-2 Maximum tensile strain at failure as a function of air voids from indirect tensile test at 4°C

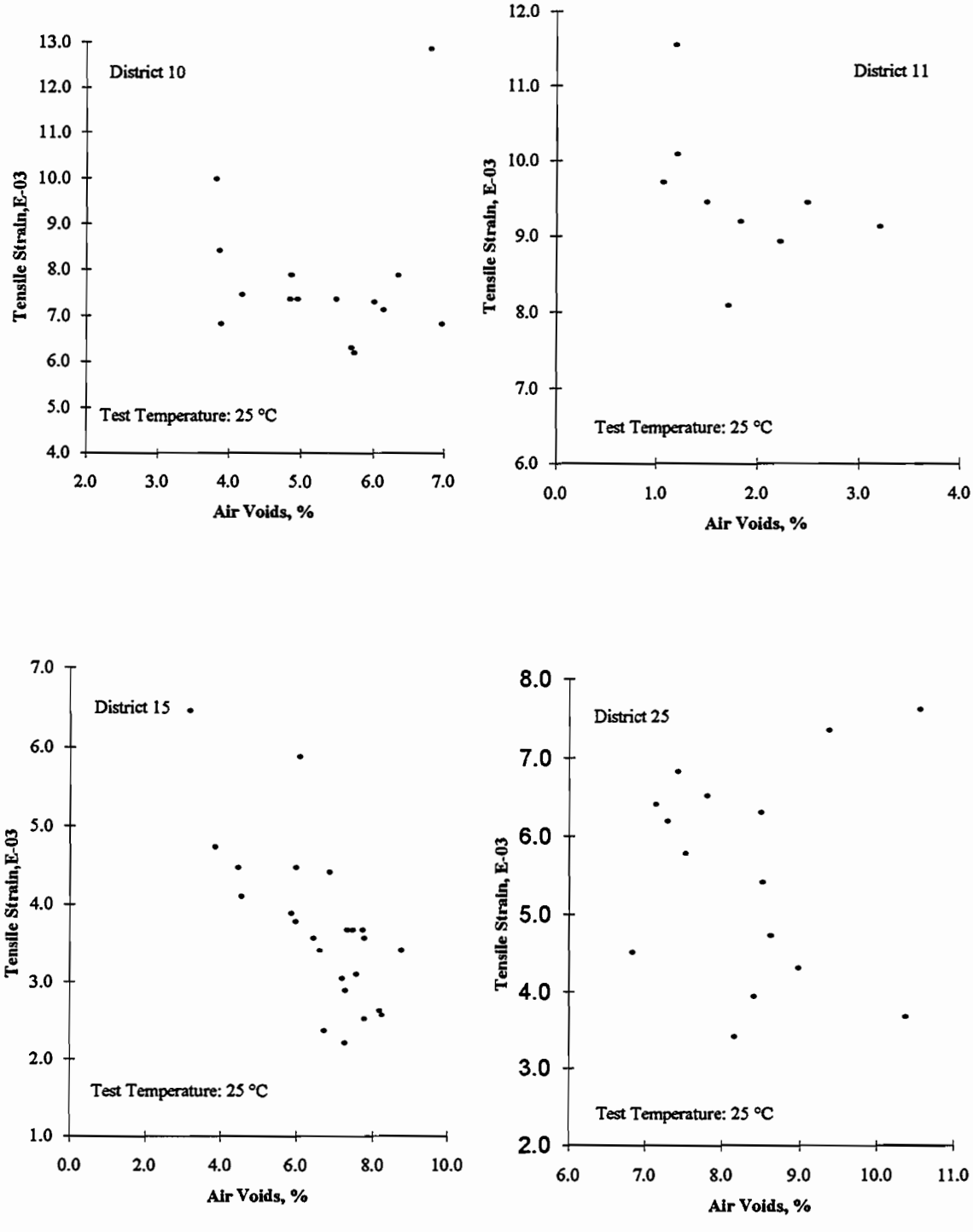

Figure D-3 Maximum tensile strain at failure as a function of air voids from indirect tensile test at 25°C

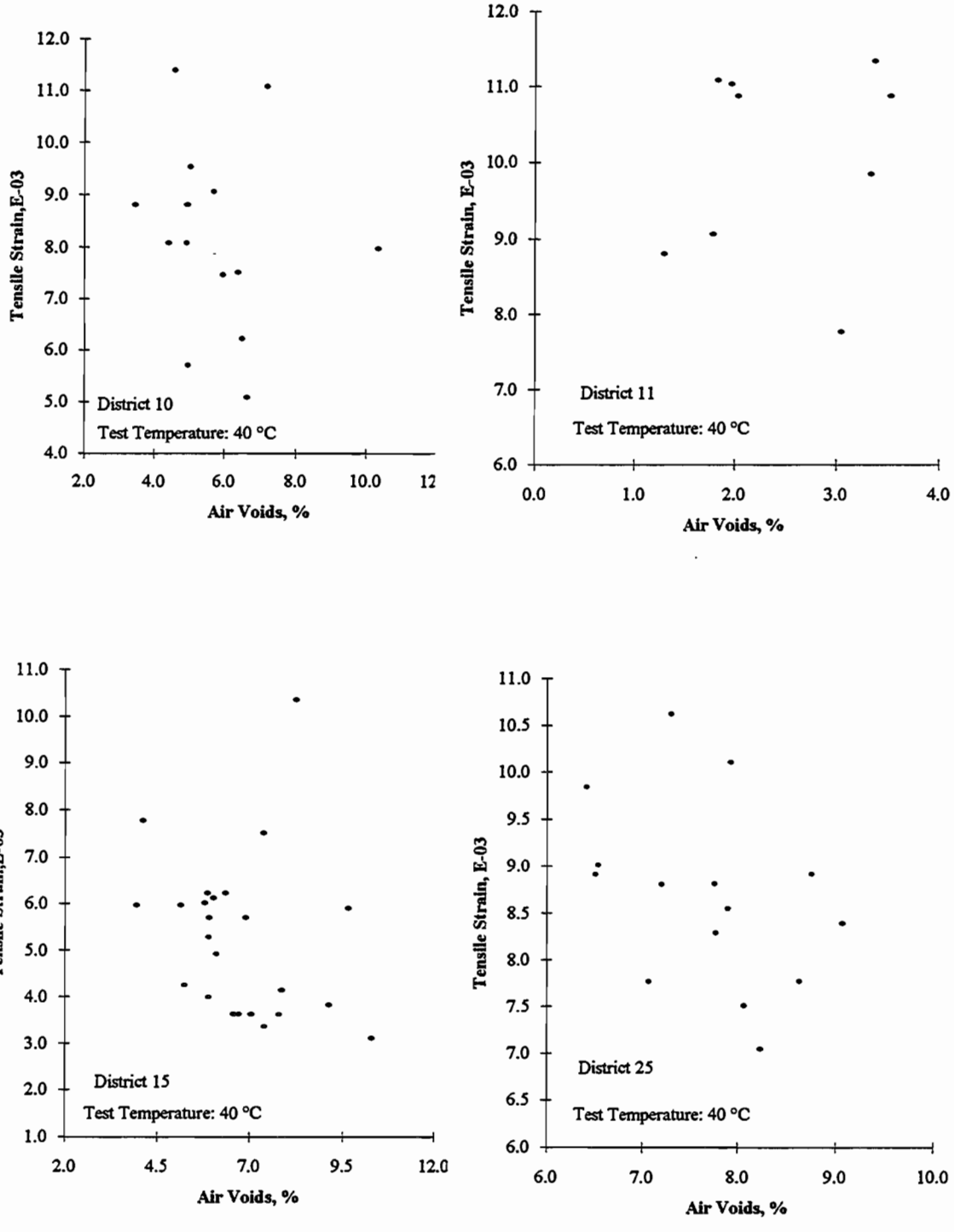

Figure D-4 Maximum tensile strain at failure as a function of air voids from indirect tensile test at 40°C

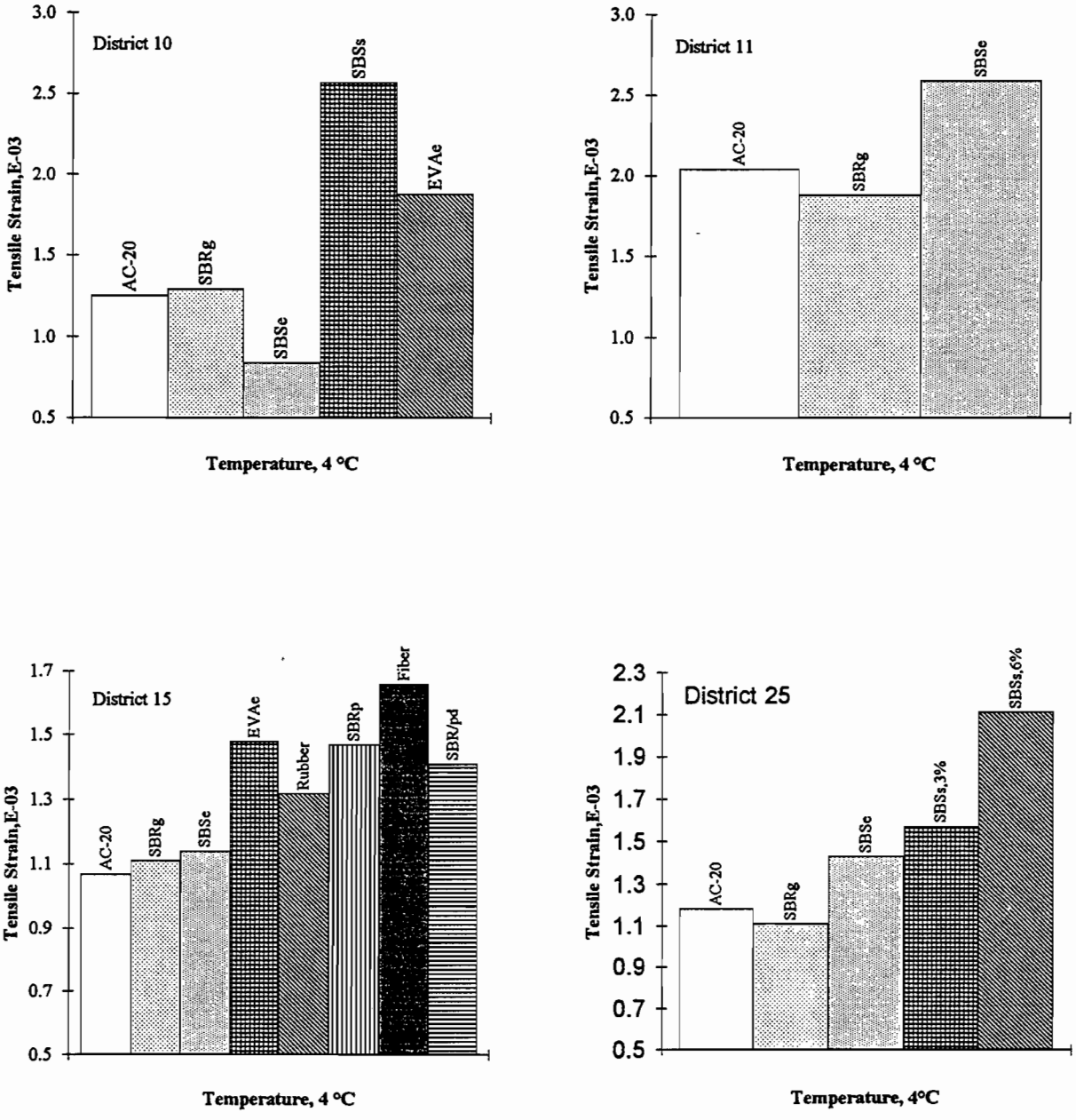

Figure D-5 Maximum tensile strain at failure for different polymer-modified asphalts at 4°C

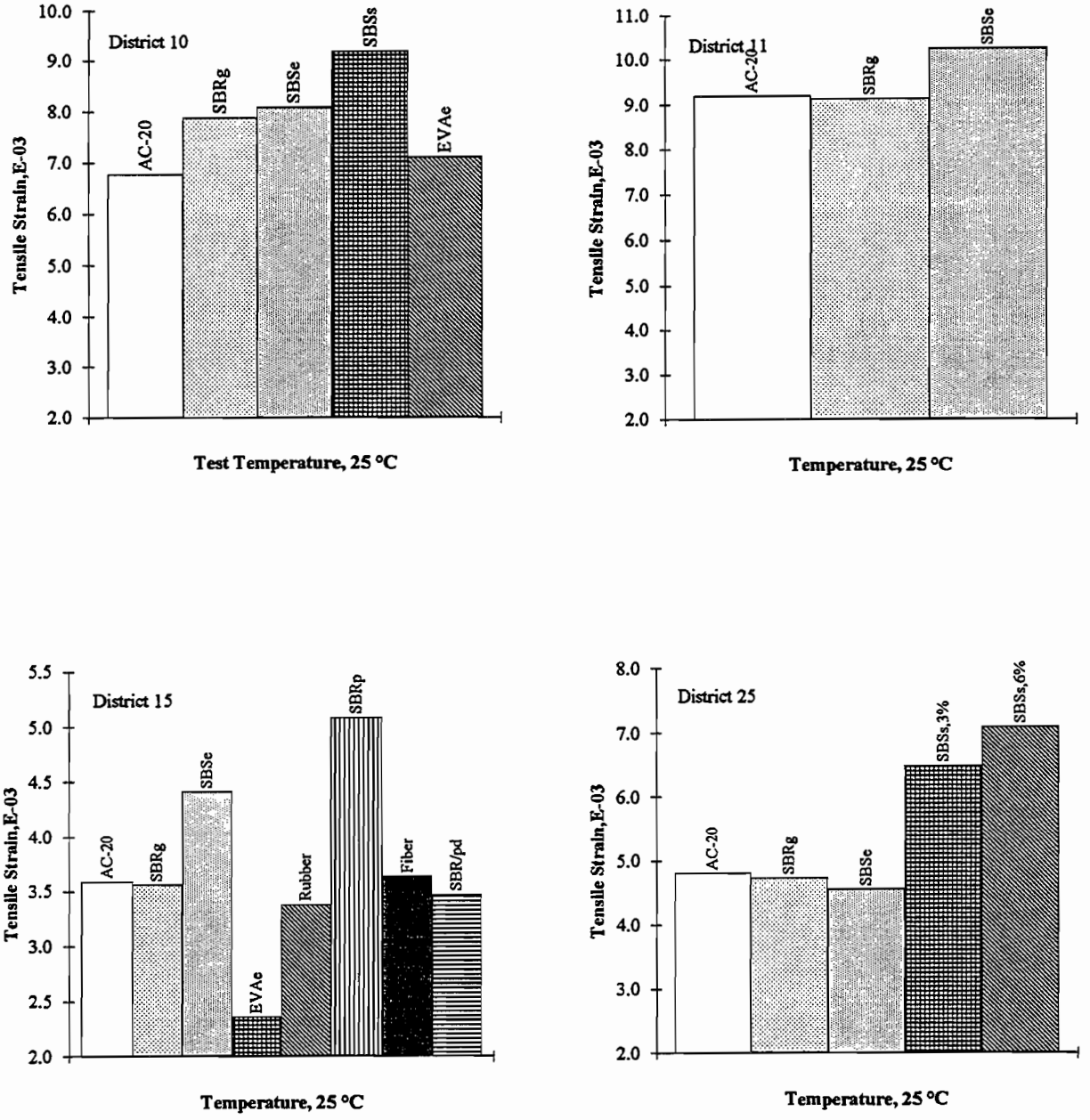

Figure D-6 Maximum tensile strain at failure for different polymer-modified asphalts at 25°C

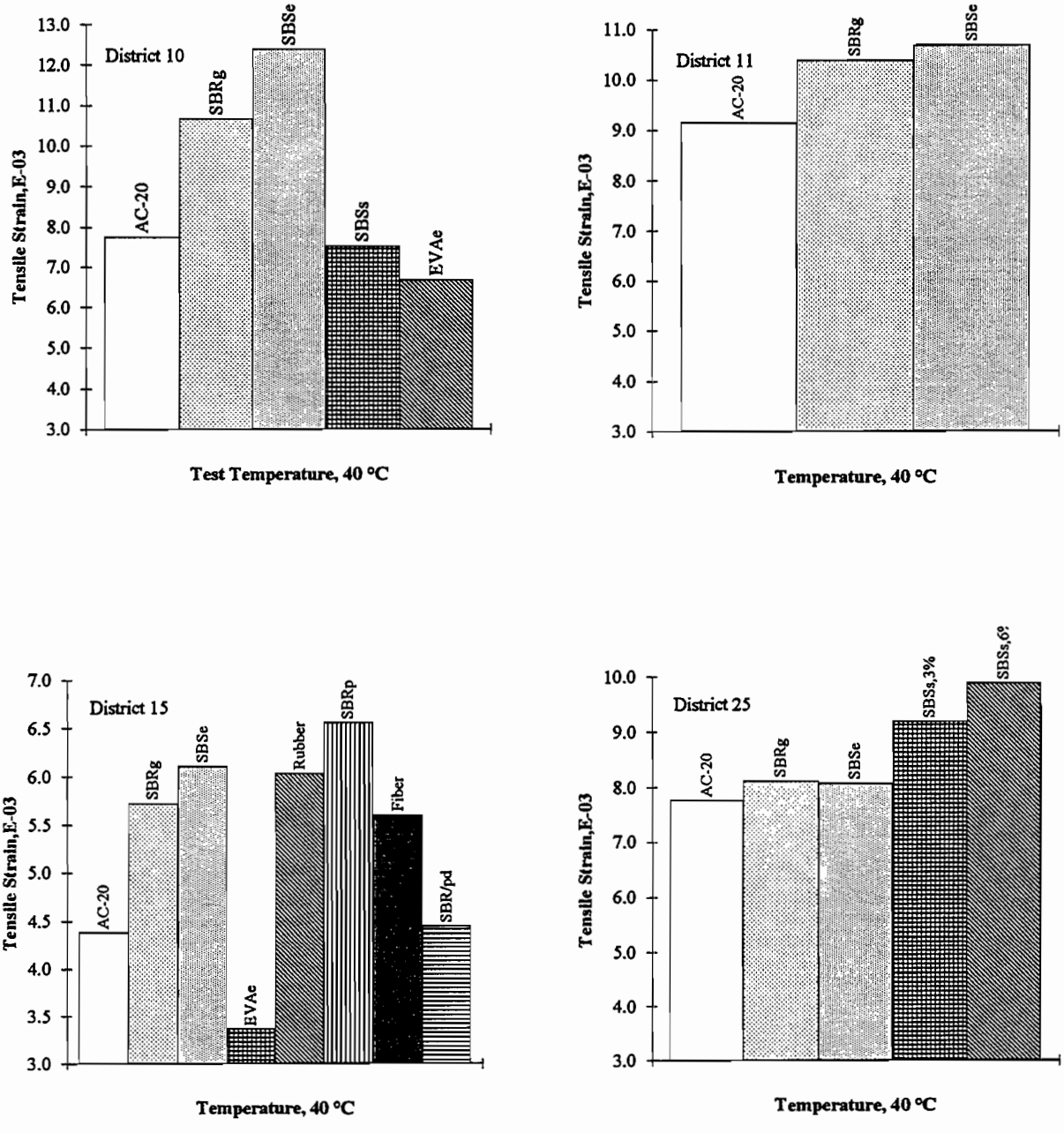

Figure D-7 Maximum tensile strain at failure for different polymer-modified asphalts at 40°C

TABLE D-15 INDIRECT TENSILE STRENGTH OF AGED FIELD CORES COMPARED WITH INDIRECT TENSILE STRENGTH OF LABORATORY-COMPACTED LABORATORY MIXES (1)

District	Polymer	field core ITS,psi 39F	lab mix ITS,psi 39F	field core ITS,psi 77F	lab mix ITS,psi 77F	field core ITS,psi 104F	lab mix ITS,psi 104F
10	control	358	332	215	86	67	21
	SBRg	492	435	248	79	51	18
	SBSe	423	397	248	100	49	20
	SBSs	347	374	139	60	42	11
	EVAe	392	273	151	37	34	8
11	control	484	303	215	70	77	20
	SBRg	507	363	250	84	80	20
	SBSe	525	304	220	64	70	15
15	Control	372	320	186	79	77	32
	SBRg	419	285	180	67	72	24
	SBSe	479	319	196	76	83	25
	EVAe	366	284	161	80	71	31
	Rubber	270	112	120	36	63	15
	SBRp	475	286	207	70	85	28
	Fiber	336		181		73	
	SBR/pd	352	305	143	74	68	36
25	Control	378	399	160	88	52	27
	SBRg	367		166		52	
	SBSe	364	467	168	123	58	42
	SBSs,3%	401	414	191	98	58	31
	SBSs,6%	295	286	119	80	53	28

NOTE:
The results are reported as the average of testing three specimens.
The field cores were tested during this research study (RS1306)
The laboratory compacted specimens were tested during research study 492.

ITS: Indirect Tensile Strength
SBRg : UP 70 ,Goodyear
SBSe : Styrelf-13, Elf
EVAe : Polybilt 103, Exxon
Rubber : Genstar C107,Crafco
SBRp : NS 175, Polysar
SBR/Pd : SBR/Polyolefin, Dow
SBSs,3% : Kraton D-1101,3% content, Shell
SBSs,6% : Kraton D-1101,6% content, Shell

1 psi = 6895 Pascals

$1\ \Delta°F = 0.556\ \Delta°C$

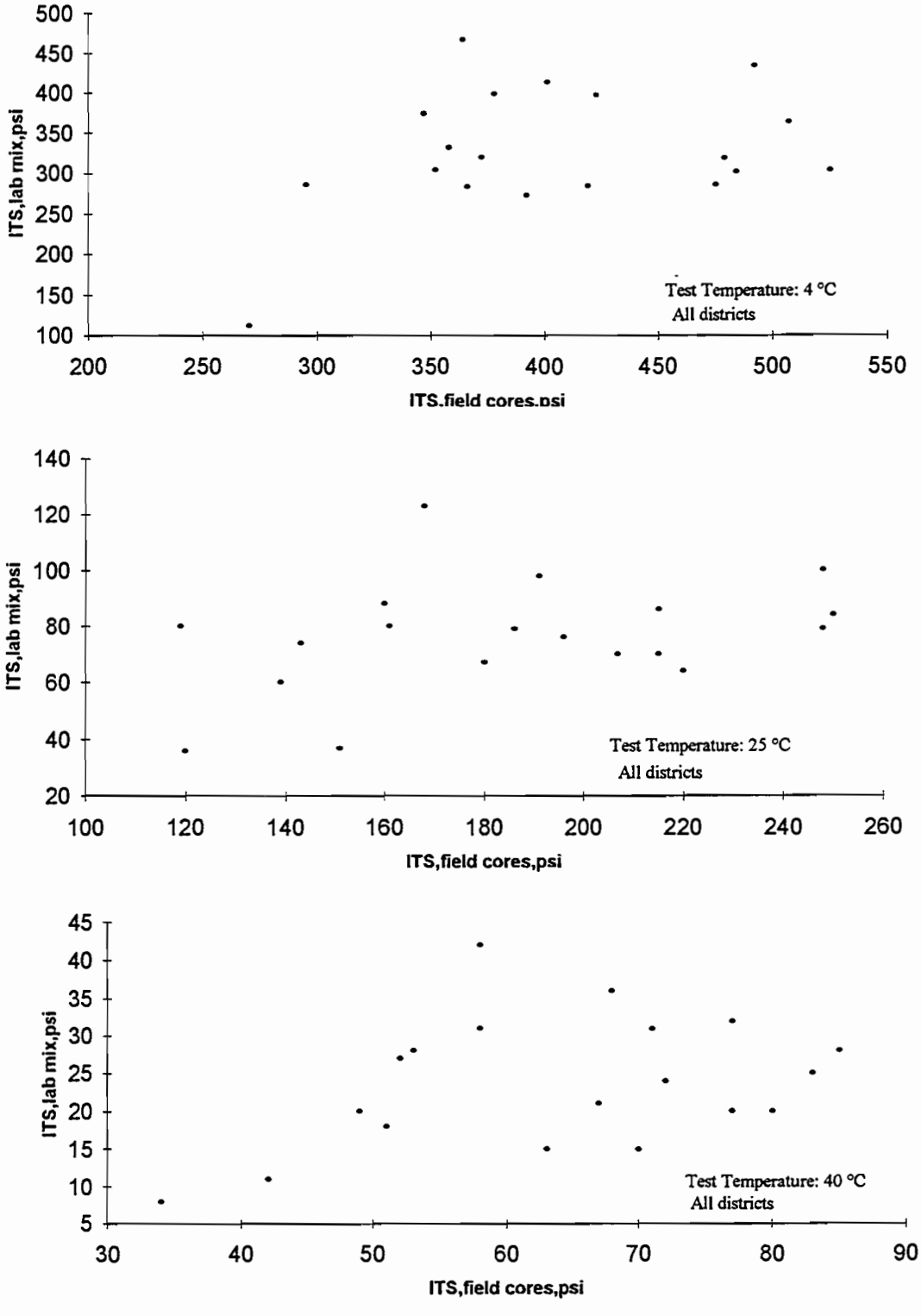

Figure D-8 Indirect tensile strength (ITS) of field cores versus indirect tensile strength of laboratory-compacted mixtures at different temperatures

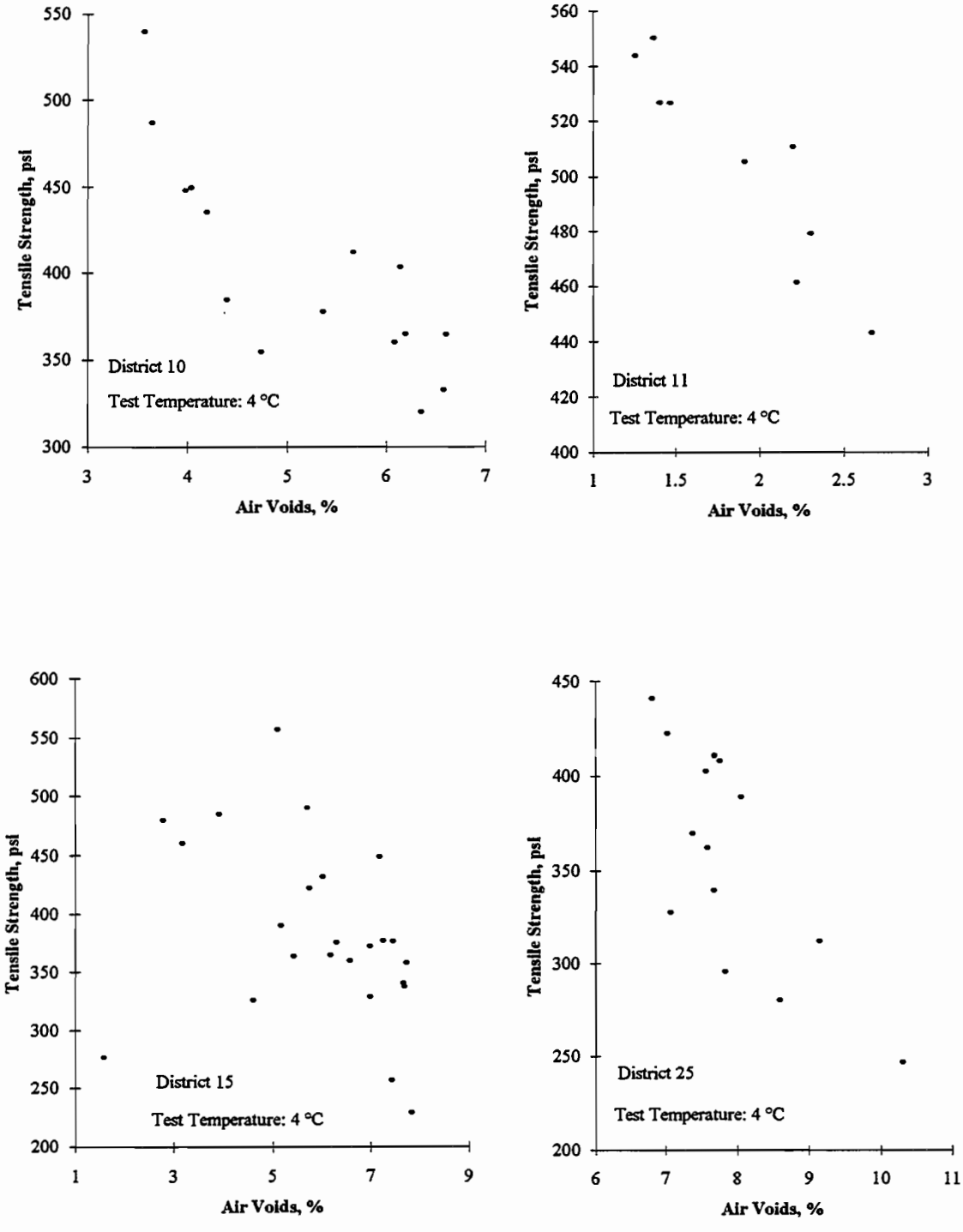

Figure D-9 Indirect tensile strength as a function of air voids at 4°C

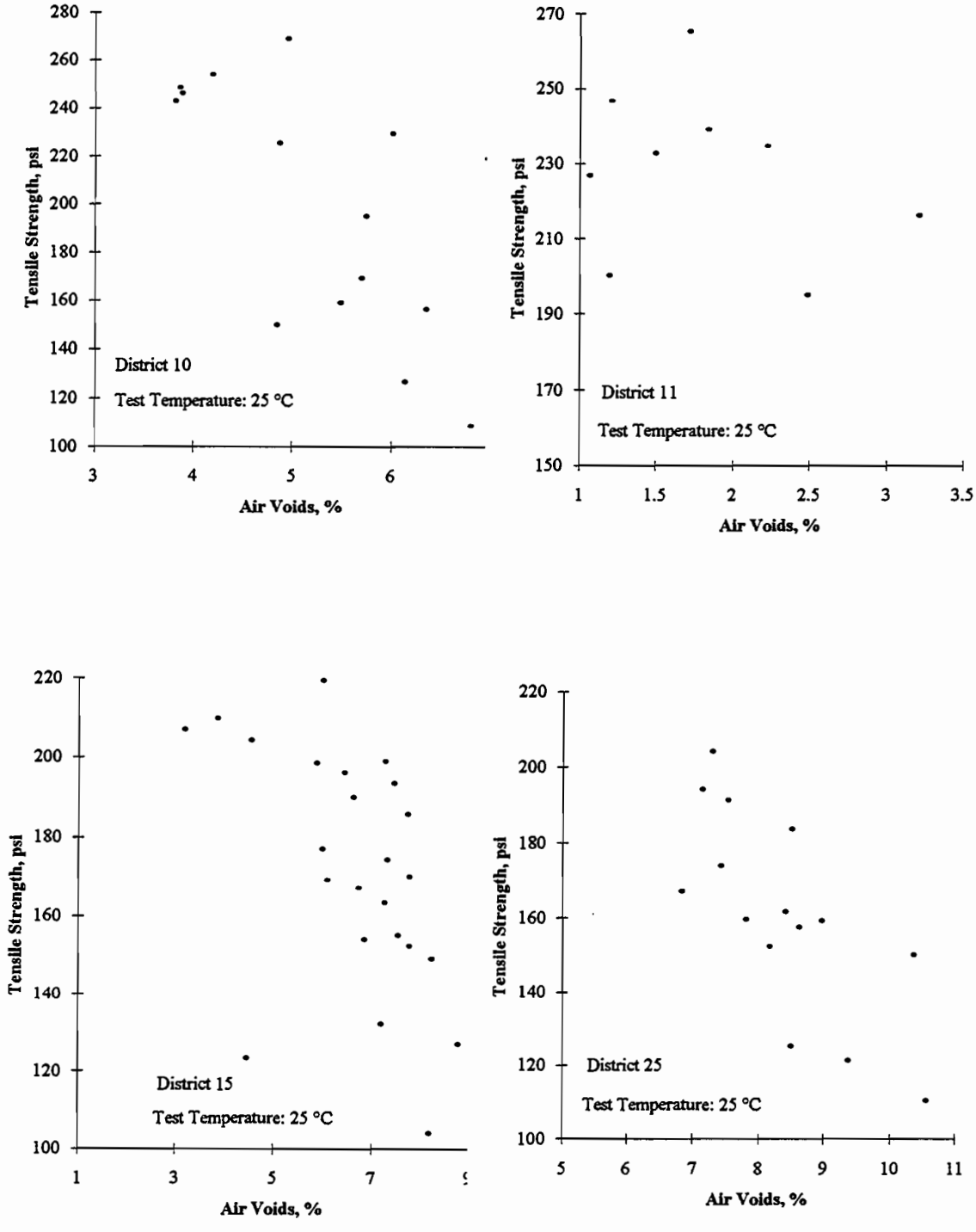

Figure D-10 Indirect tensile strength as a function of air voids at 25°C

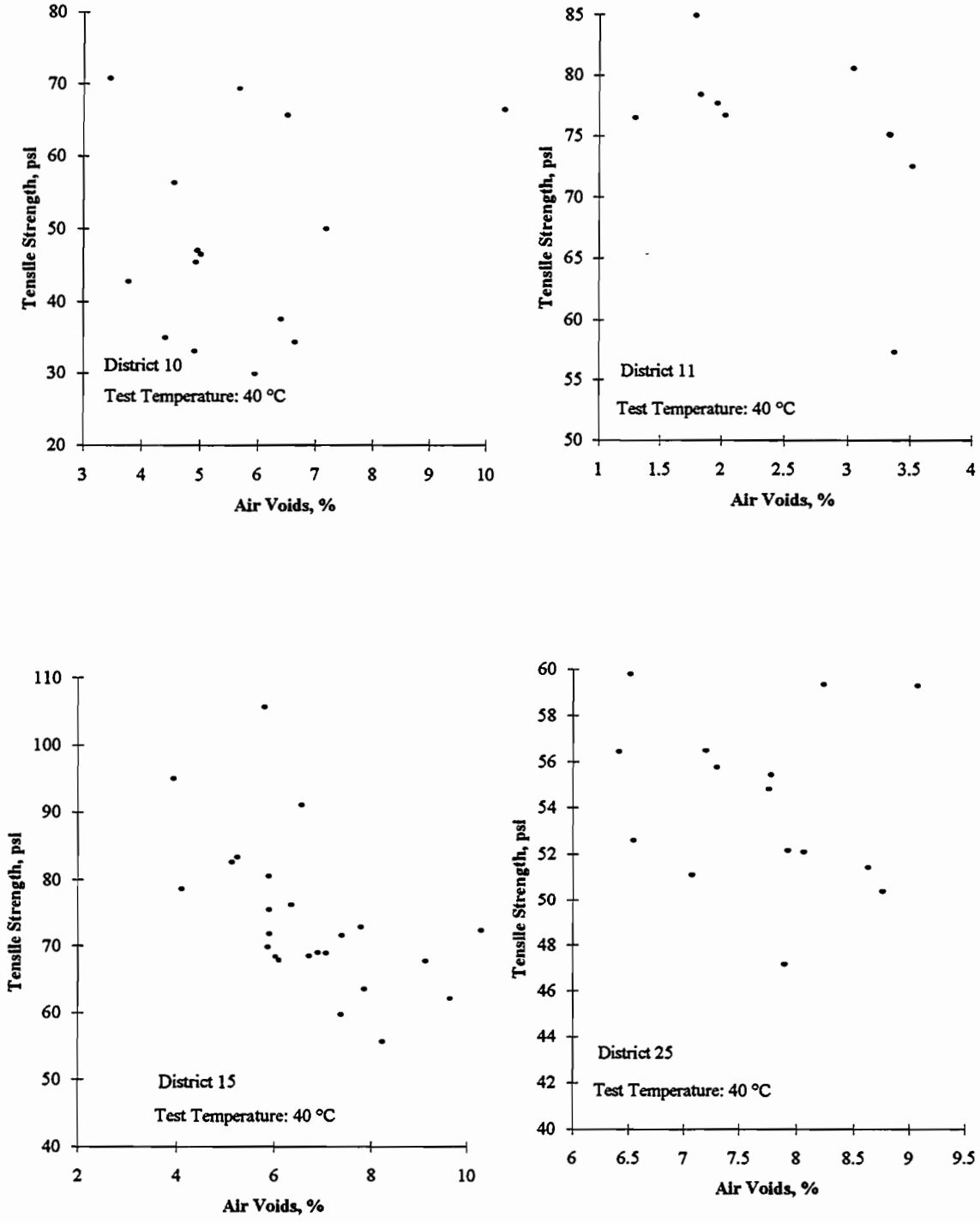

Figure D-11 Indirect tensile strength as a function of air voids at 40°C

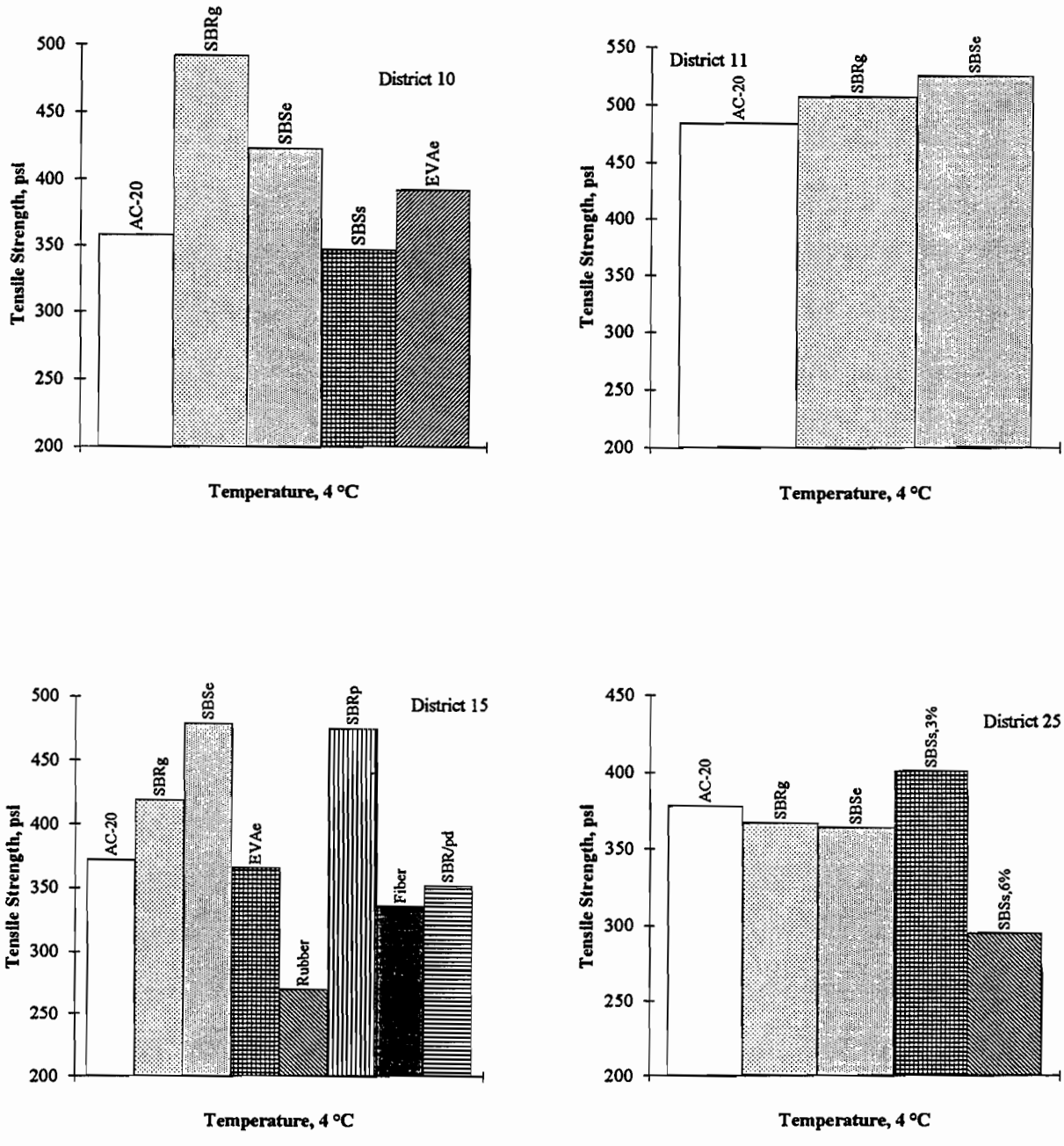

Figure D-12 Indirect tensile strength for different polymer-modified mixtures at 4°C

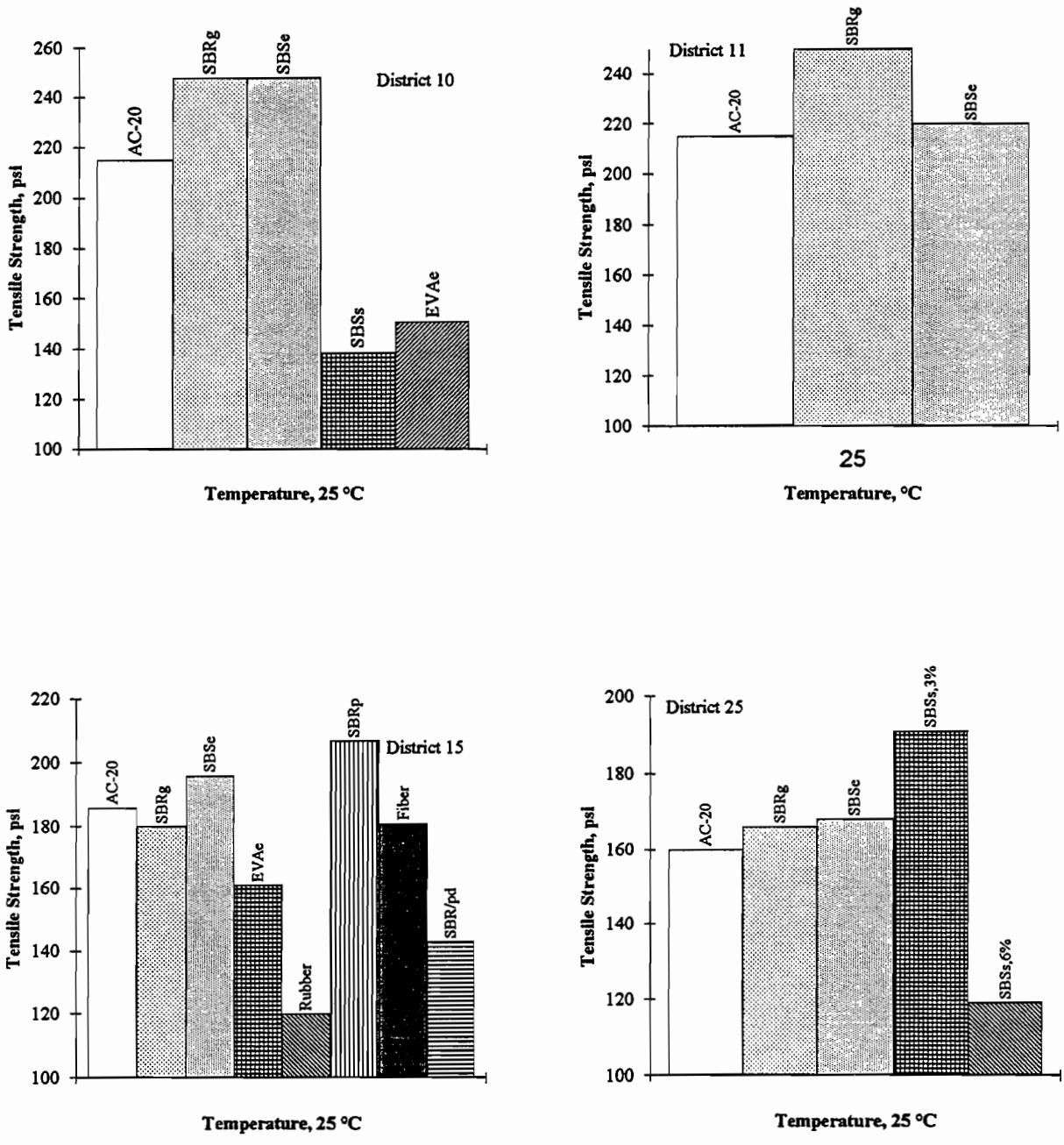

Figure D-13 Indirect tensile strength for different polymer-modified mixtures at 25°C

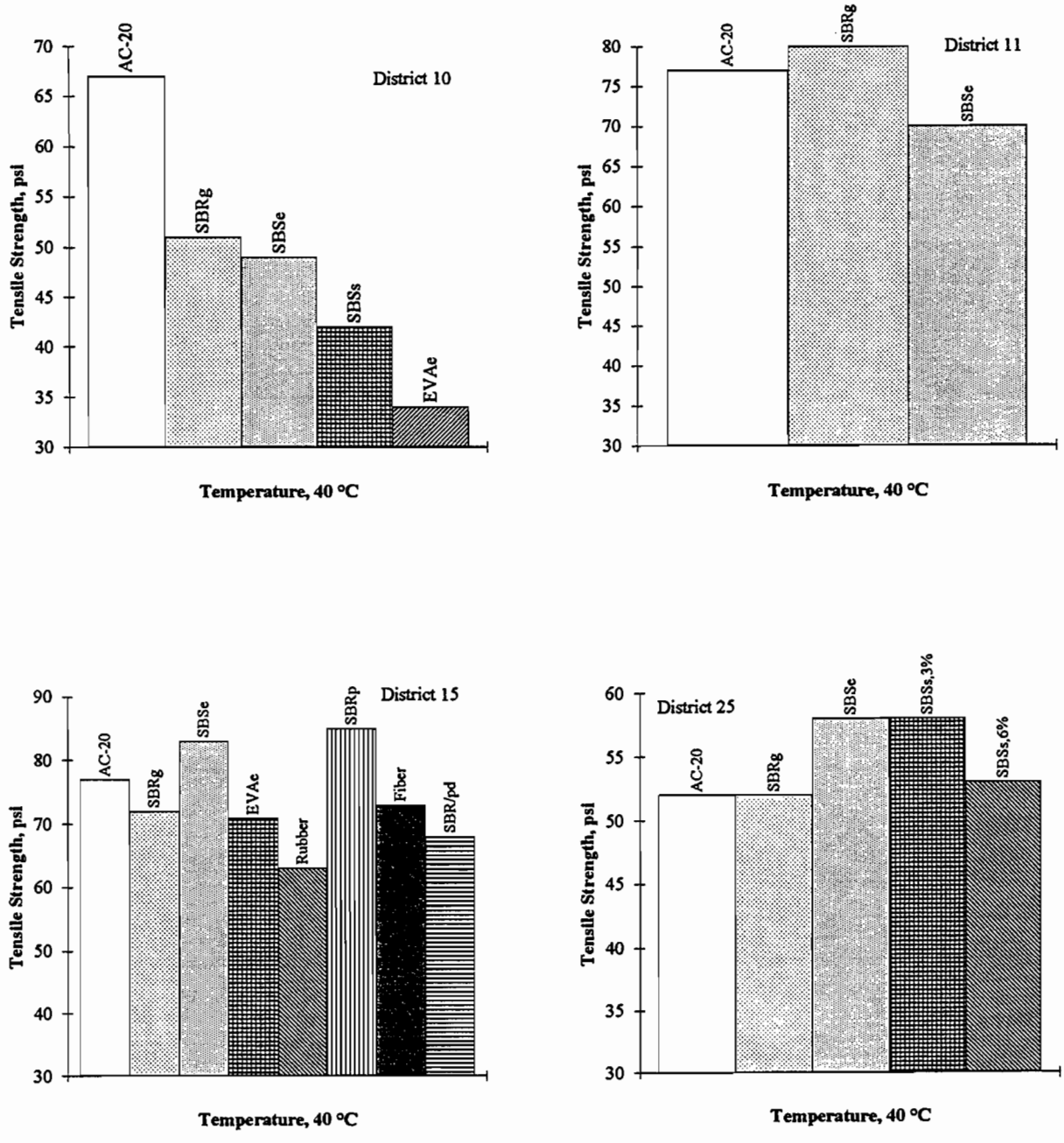

Figure D-14 Indirect tensile strength for different polymer-modified mixtures at 40°C

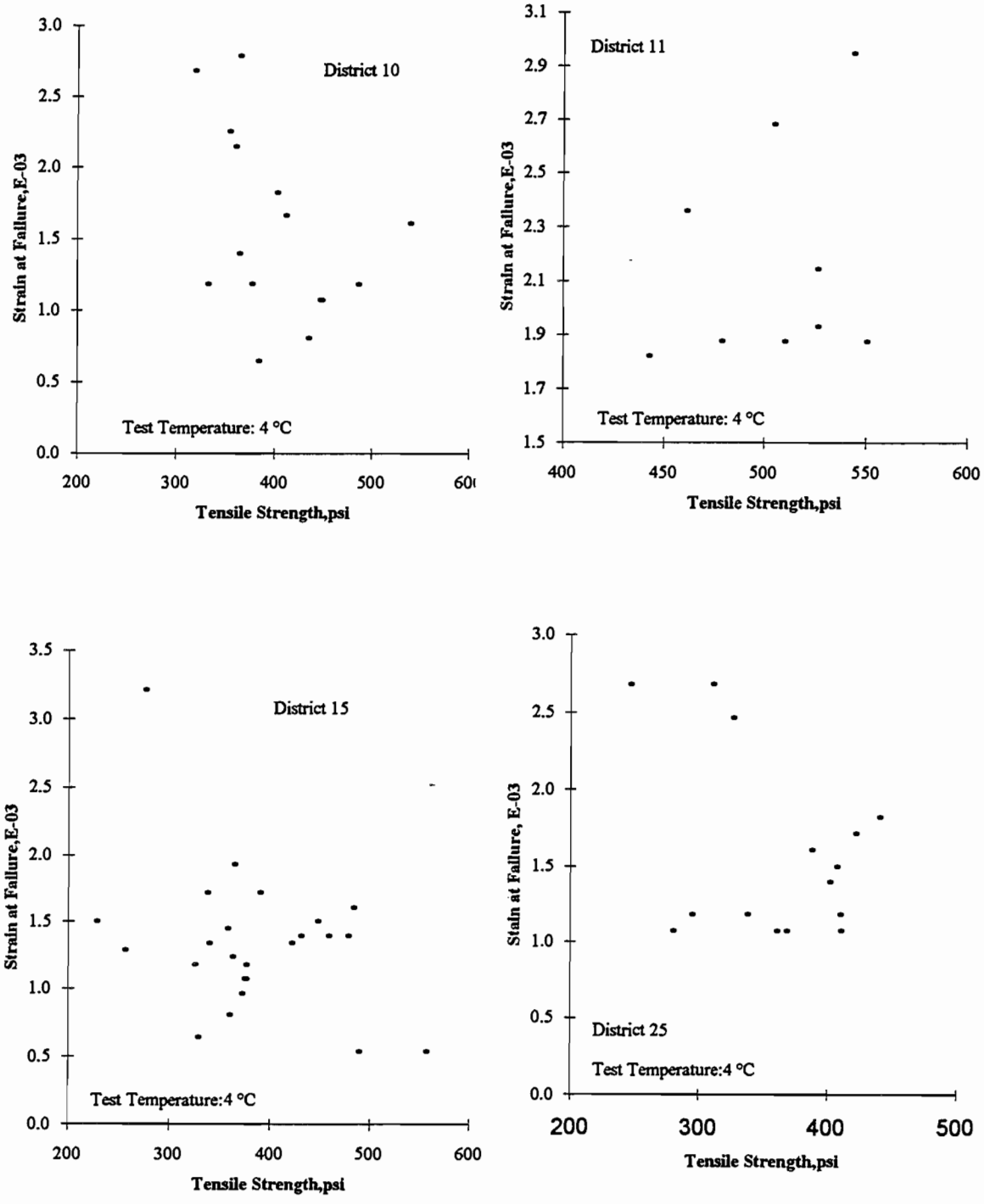

Figure D-15 Maximum tensile strain at failure versus indirect tensile strength at 4°C

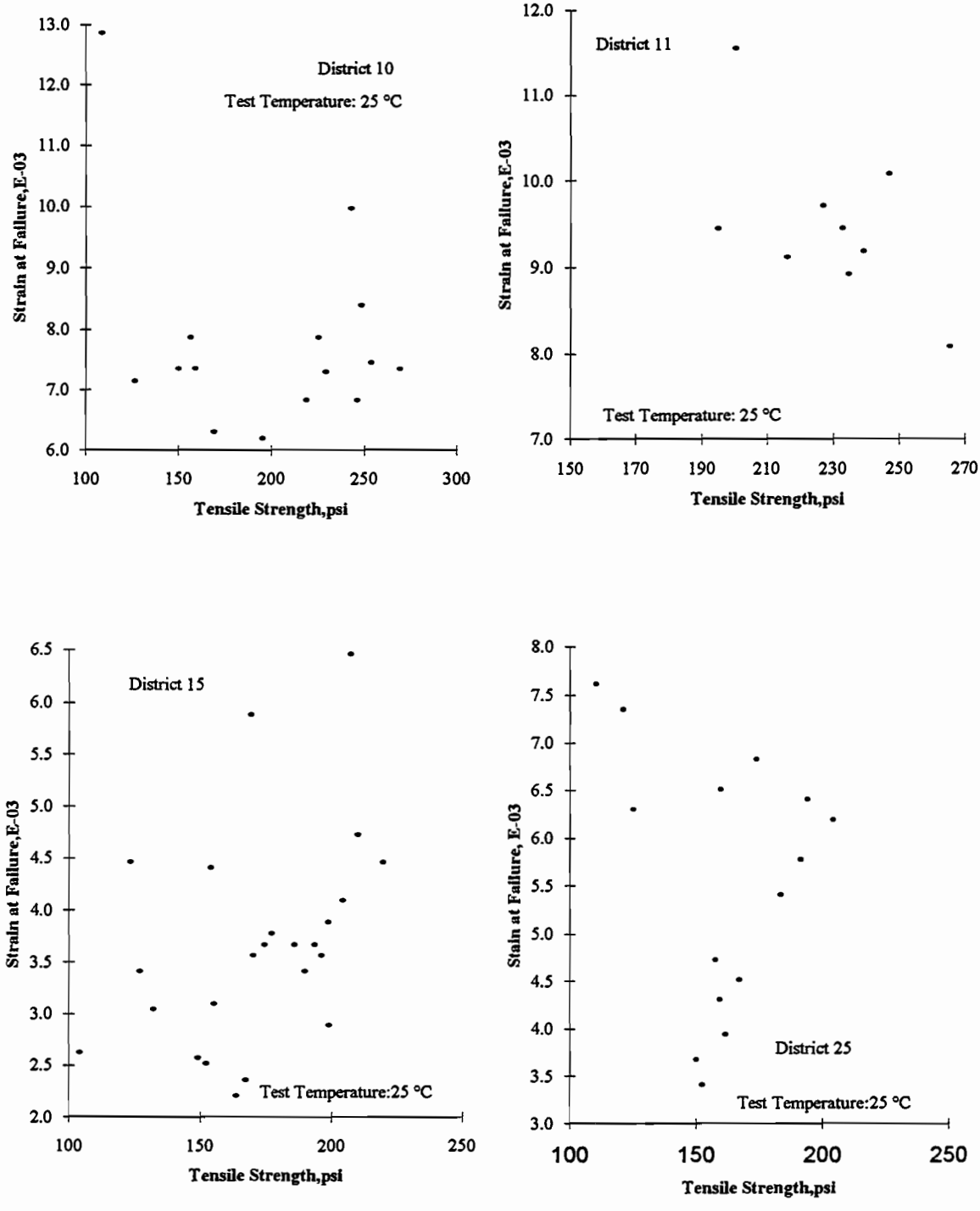

Figure D-16 Maximum tensile strain at failure versus indirect tensile strength at 25°C

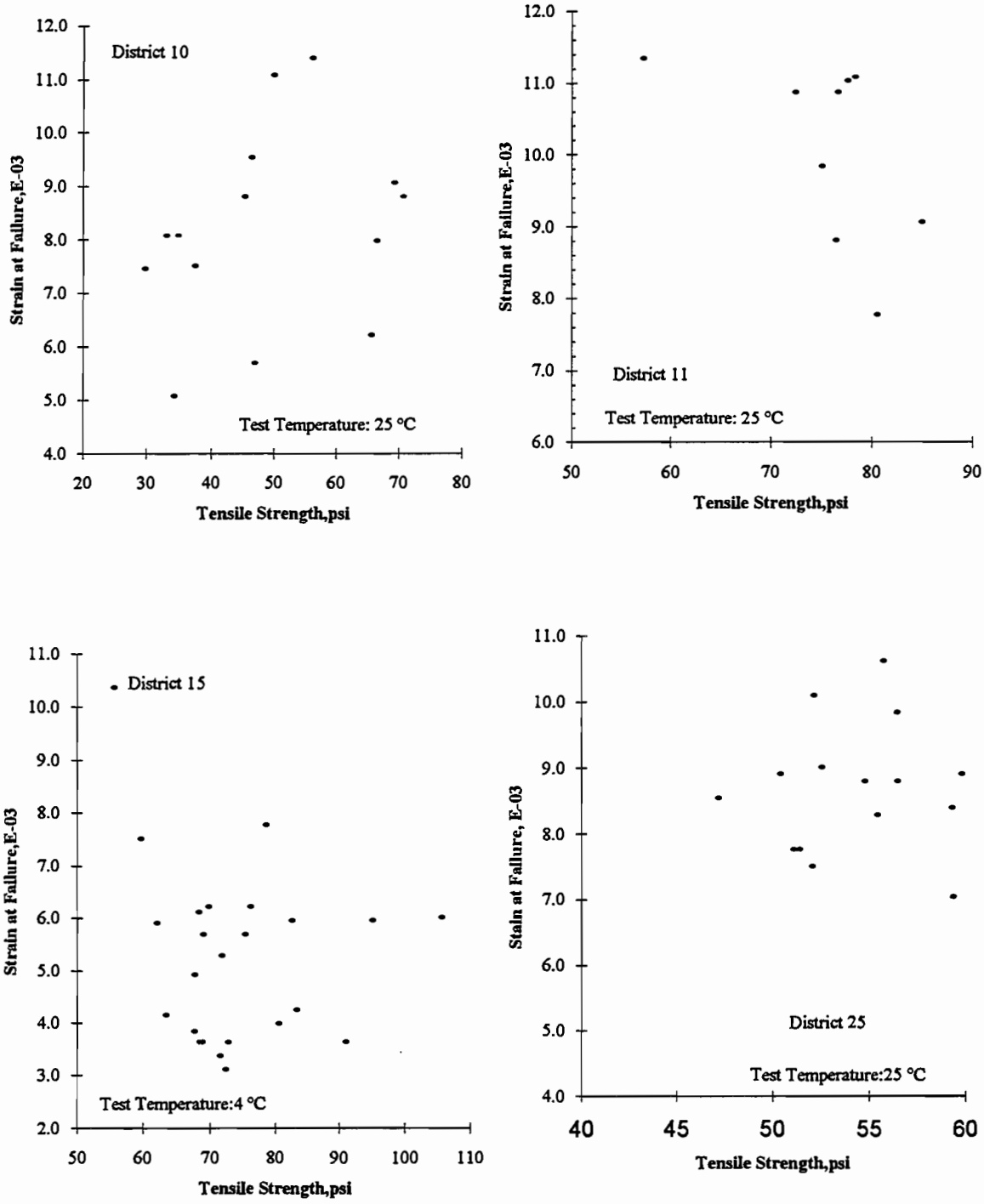

Figure D-17 Maximum tensile strain at failure versus indirect tensile strength at 40°C

TABLE D-16 SECANT MODULI OF AGED FIELD CORES COMPARED WITH SECANT MODULI OF LABORATORY-COMPACTED LABORATORY MIXES (1)

District	Polymer	field core MS,ksi 39 F	lab mix MS,ksi 39 F	field core MS,ksi 77 F	lab mix MS,ksi 77 F	field core MS,ksi 104 F	lab mix MS,ksi 104 F
10	control	465	234	60	14	19	2.9
	SBRg	628	309	60	12	10	2.7
	SBSe	839	248	59	9	14	1.6
	SBSs,3%	220	95	32	7	13	1.1
	EVAe	343	56	41	6	12	1.5
11	control	389	135	45	11	19	3.4
	SBRg	436	161	53	11	17	2.9
	SBSe	333	65	42	6	15	1.3
15	Control	604	274	100	29	40	9.0
	SBRg	804	150	97	14	28	4.0
	SBSe	888	99	94	11	30	2.9
	EVAe	423	237	131	30	47	8.9
	Rubber	338	31	71	4	29	1.2
	SBRp	525	143	81	16	30	5.9
	Fiber	495		96		34	
	SBR/pd	415	233	83	41	36	18.8
25	Control	522	230	68	20	14	4.7
	SBRg	535		69		14	
	SBSe	411	181	72	14	16	4.1
	SBSs,3%	418	160	57	11	14	2.8
	SBSs,6%	184	43	33	5	12	1.7

NOTE:
The results are reported as the average of testing three specimens.
The field cores were tested during this research study (RS1306)
The laboratory mixed were tested during research 492.

(2) Data was not available for blank cells

MS: Secant Modulus at Peak Load

1 ksi = 6895 kPascals

1 Δ°F = 0.556 Δ°C

SBRg : UP 70 ,Goodyear
SBSe : Styrelf-13, Elf
EVAe : Polybilt 103, Exxon
Rubber : Genstar C107,Crafco
SBRp : NS 175, Polysar
SBR/Pd : SBR/Polyolefin, Dow
SBSs,3% : Kraton D-1101,3% content, Shell
SBSs,6% : Kraton D-1101,6% content, Shell

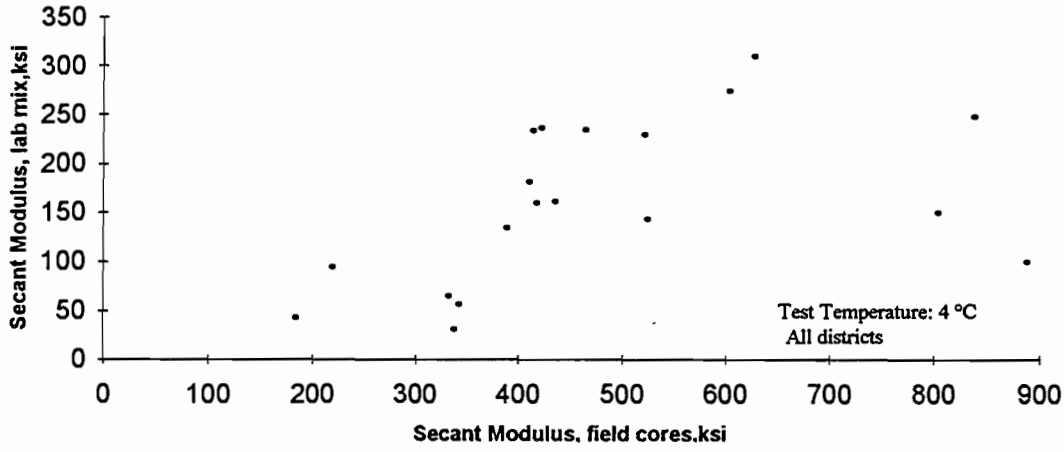

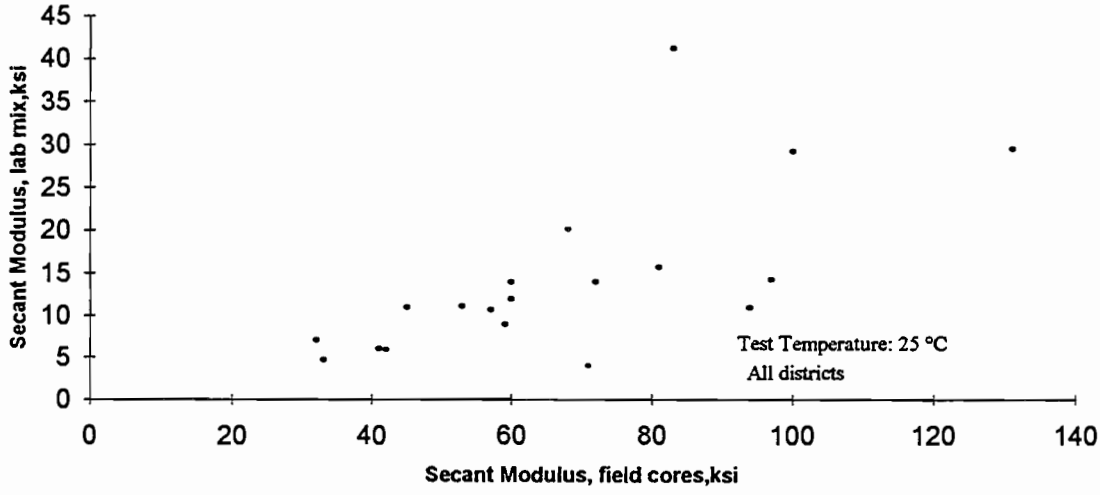

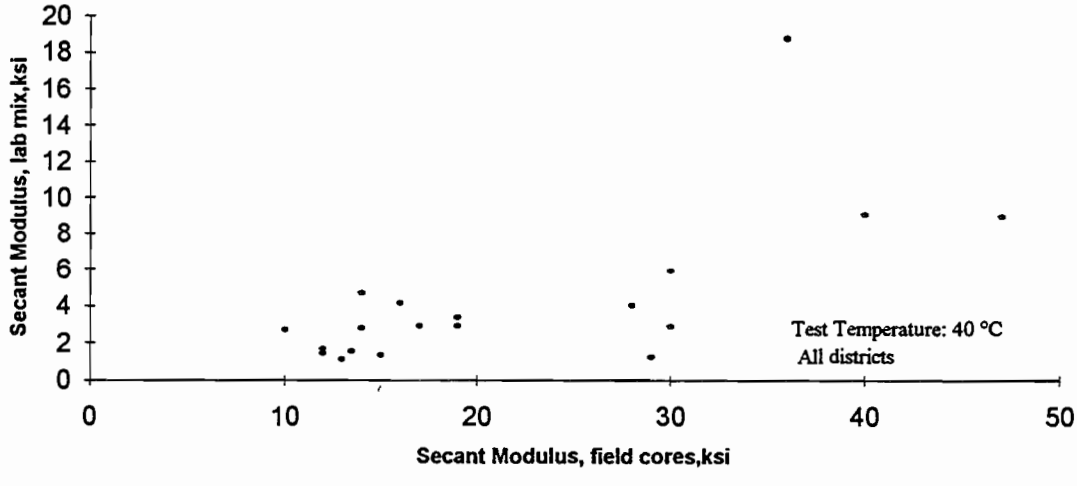

Figure D-18 Secant modulus of field cores versus secant modulus of laboratory-compacted specimens at different temperatures

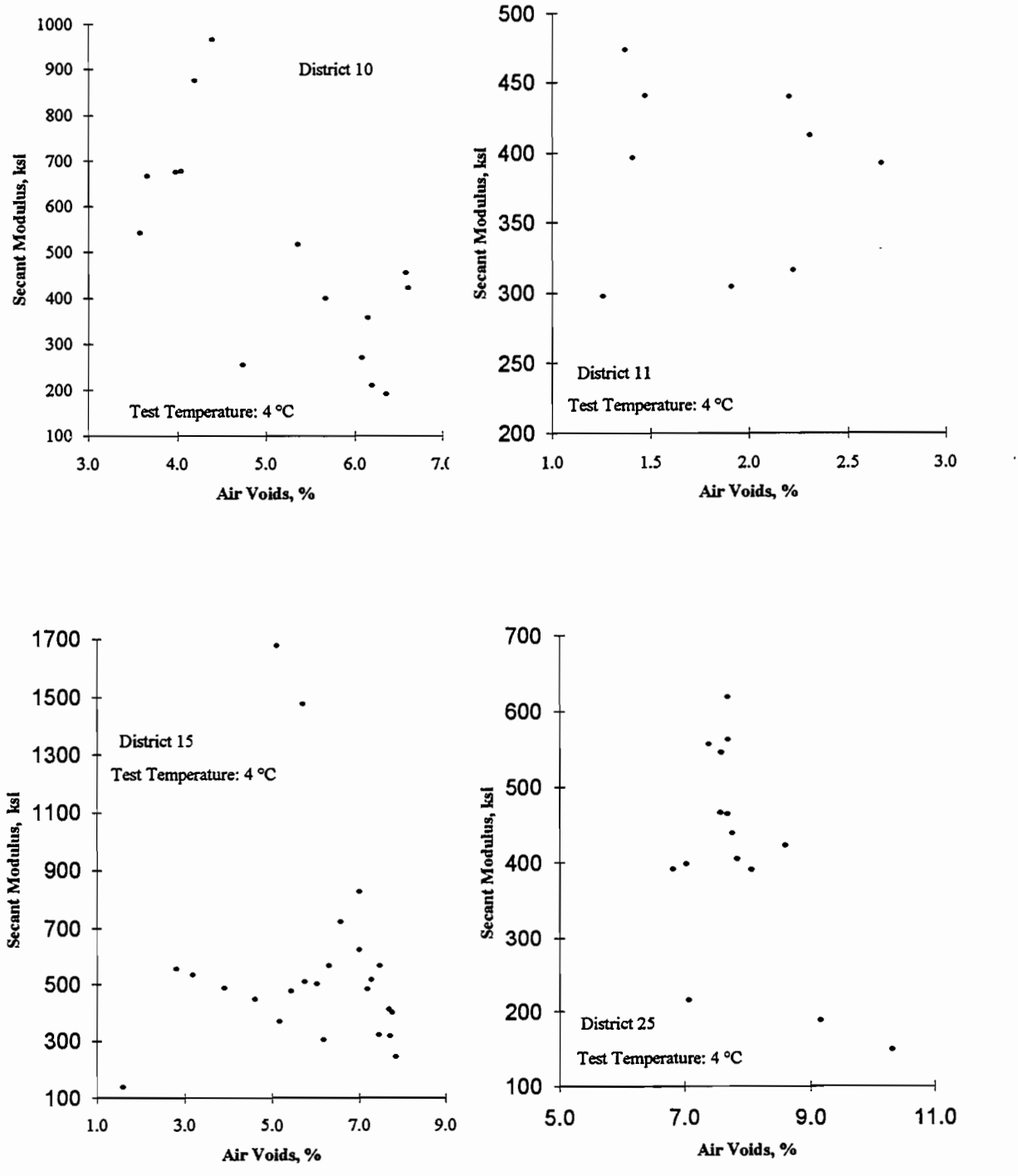

Figure D-19 Secant modulus at peak load from indirect tensile test as a function of air voids at 4°C

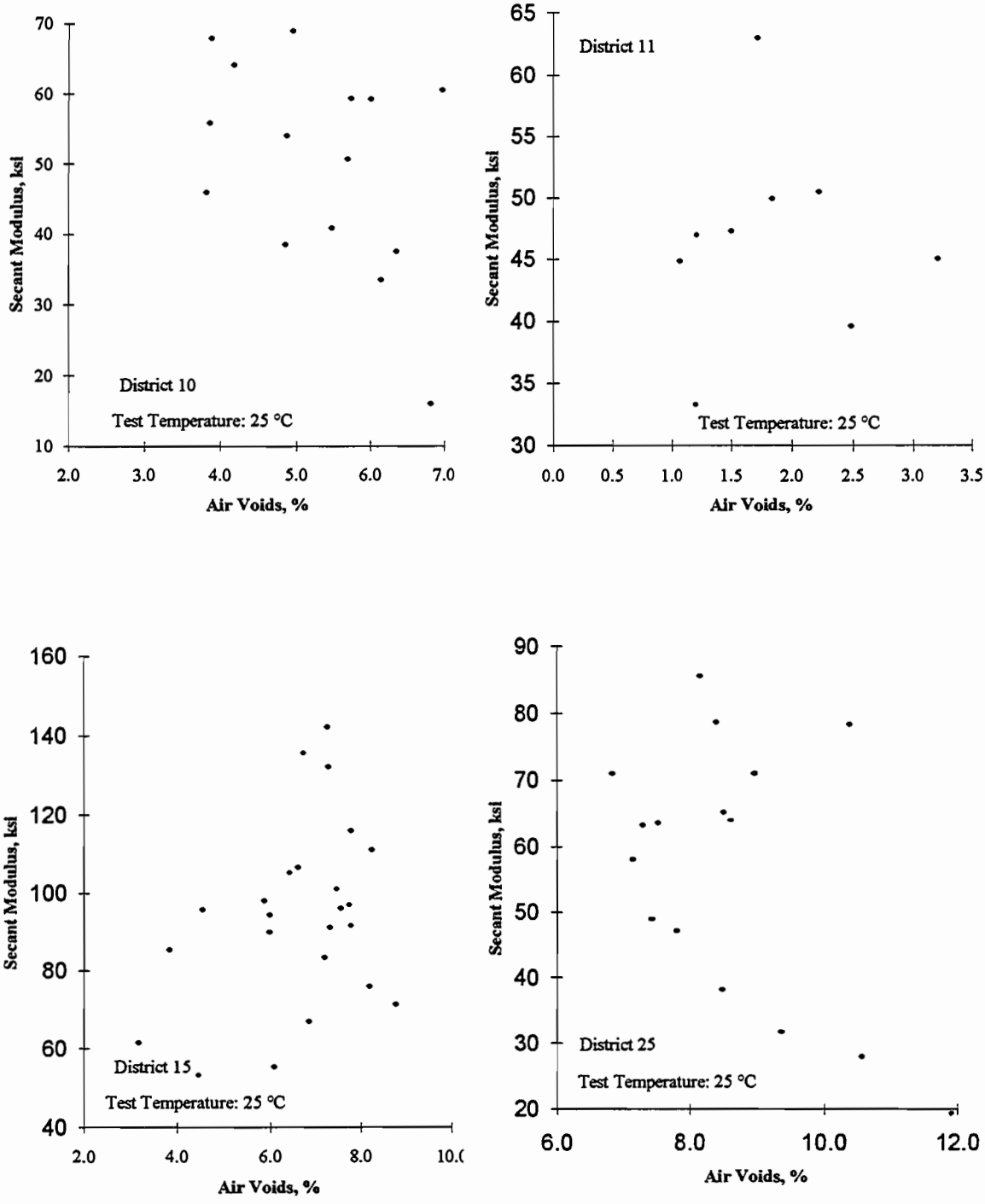

Figure D-20 Secant modulus at peak load from indirect tensile test as a function of air voids at 25°C

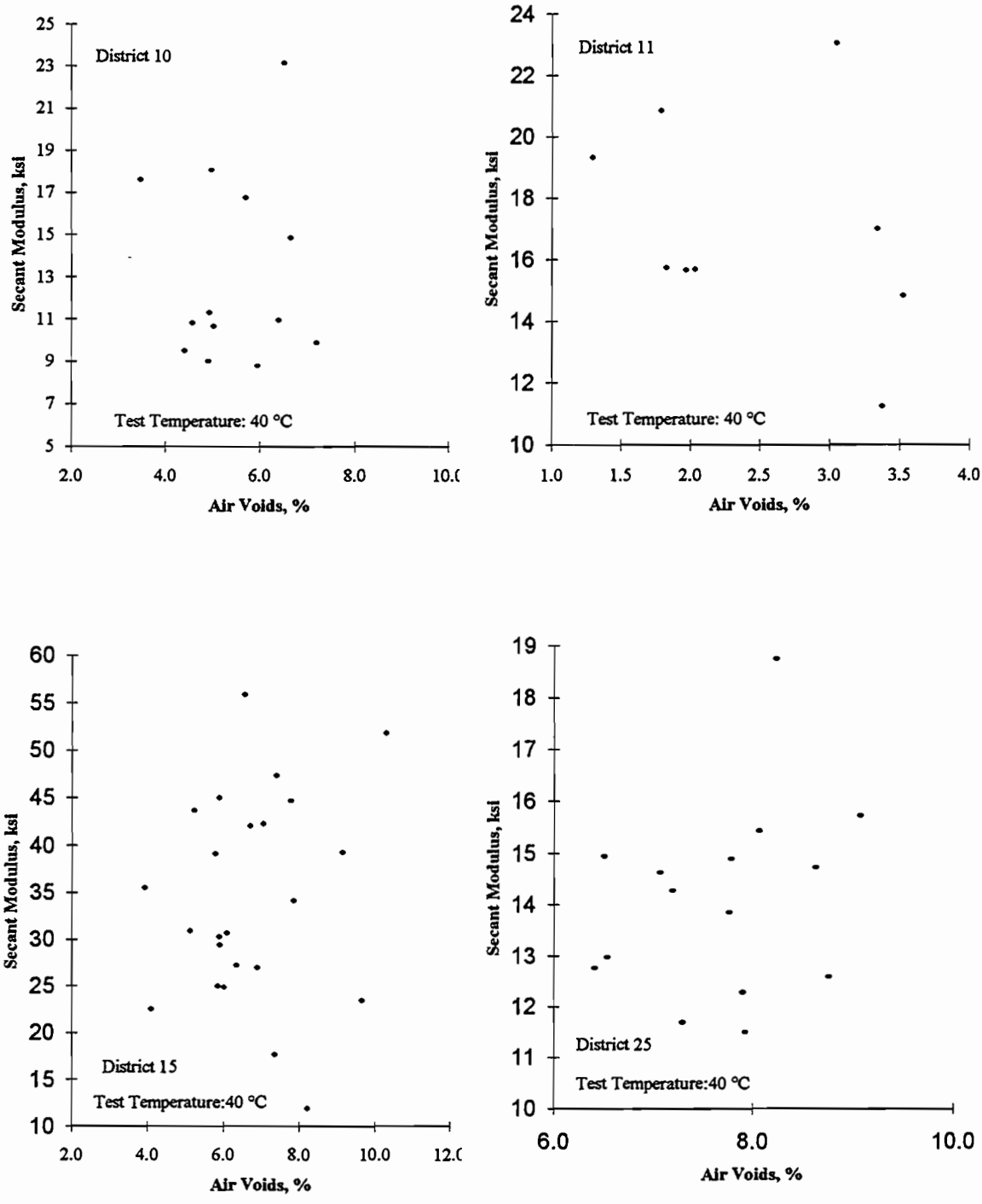

Figure D-21 Secant modulus at peak load from indirect tensile test as a function of air voids at 40°C

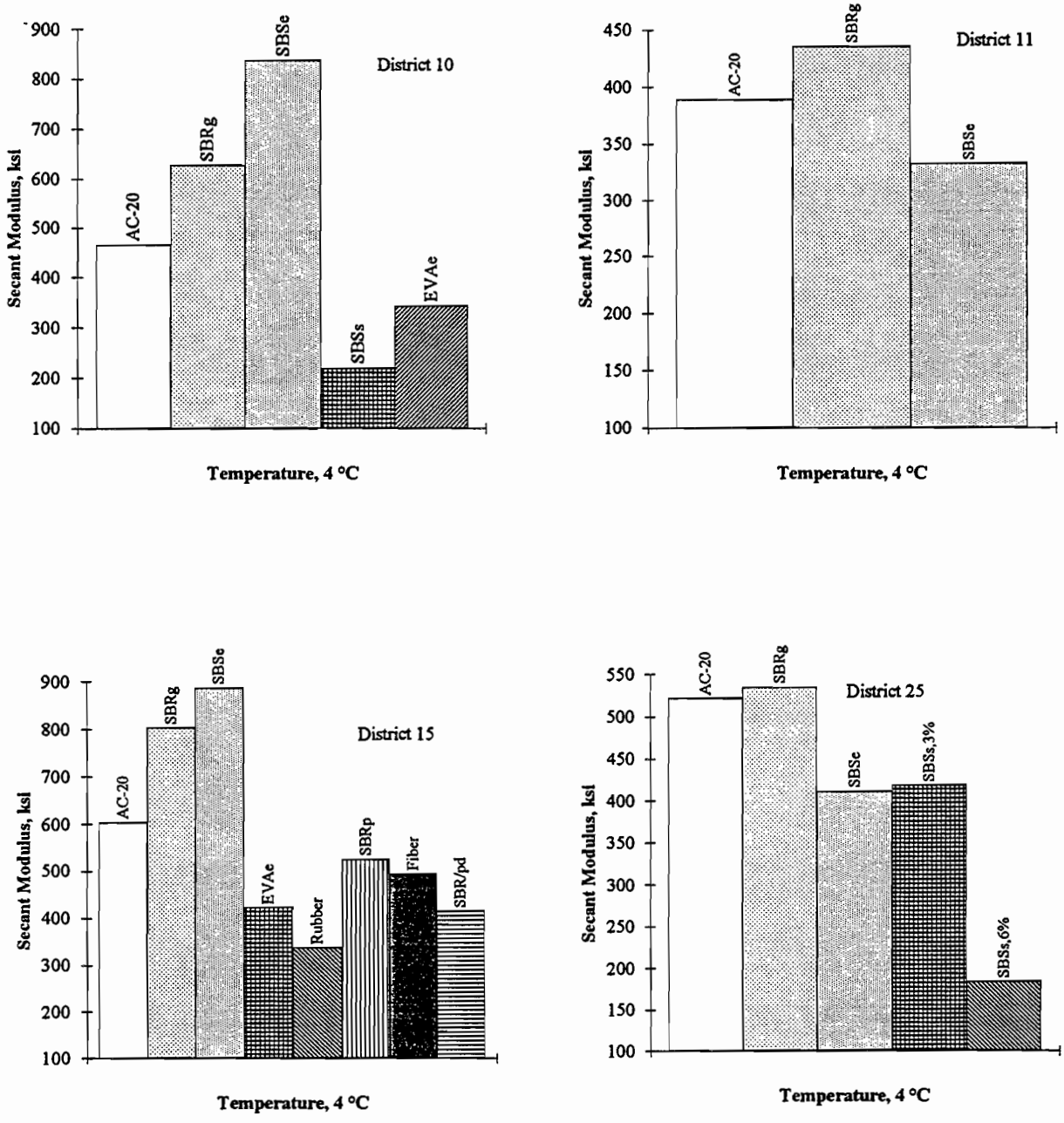

Figure D-22 Secant modulus at peak load for different polymer-modified mixtures at 4°C

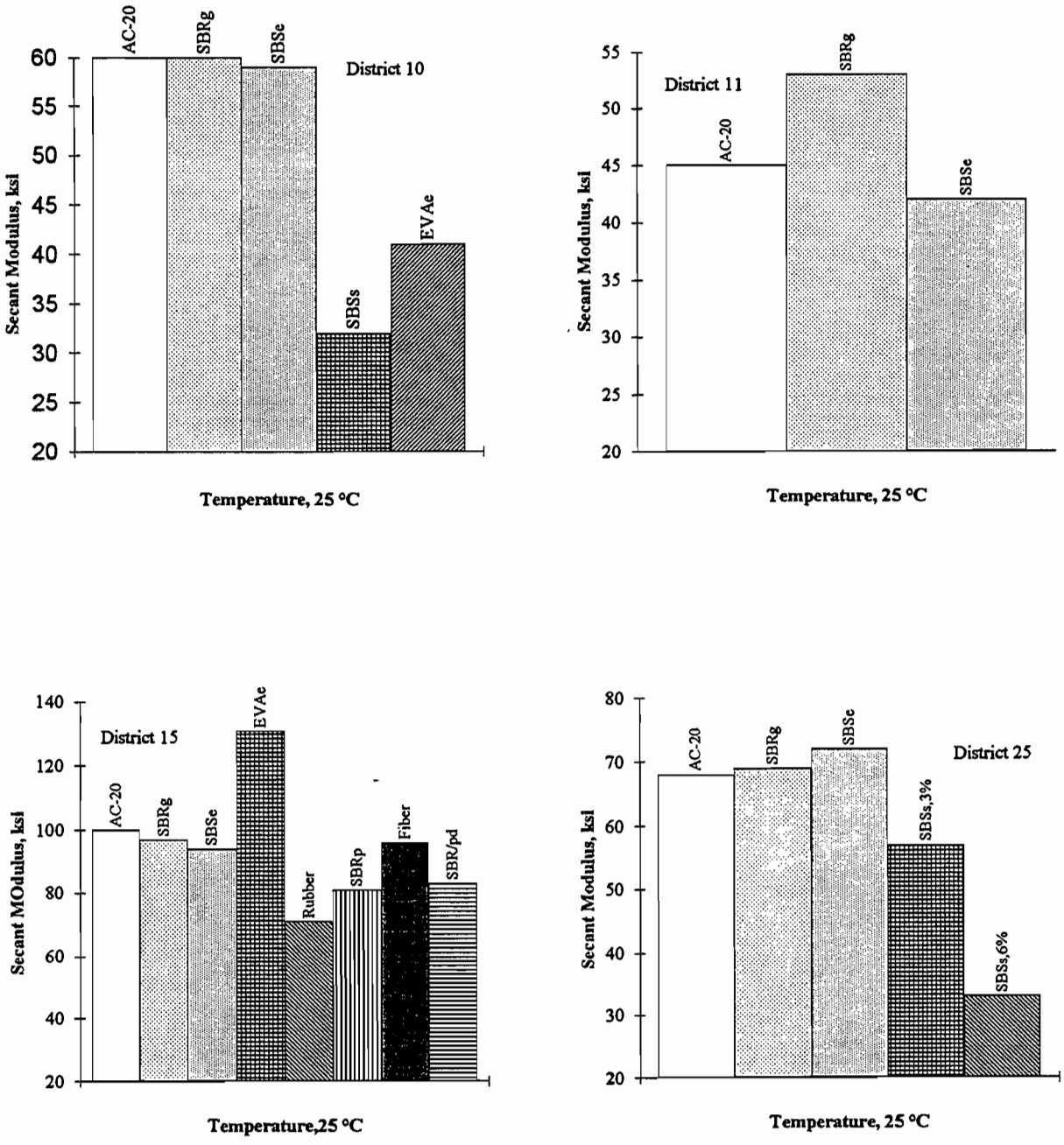

Figure D-23 Secant modulus at peak load for different polymer-modified mixtures at 25°C

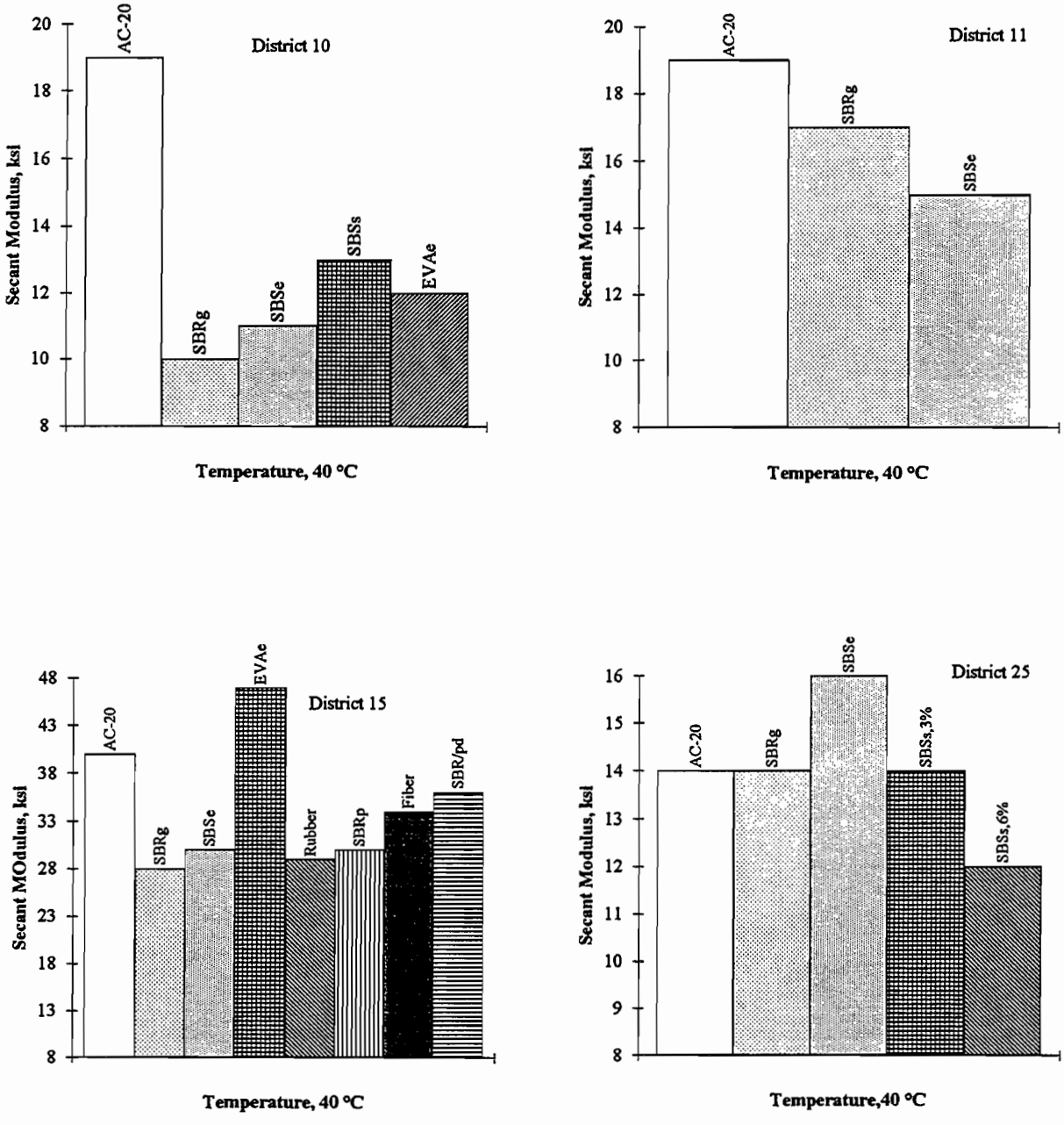

Figure D-24 Secant modulus at peak load for different polymer-modified mixtures at 40°C

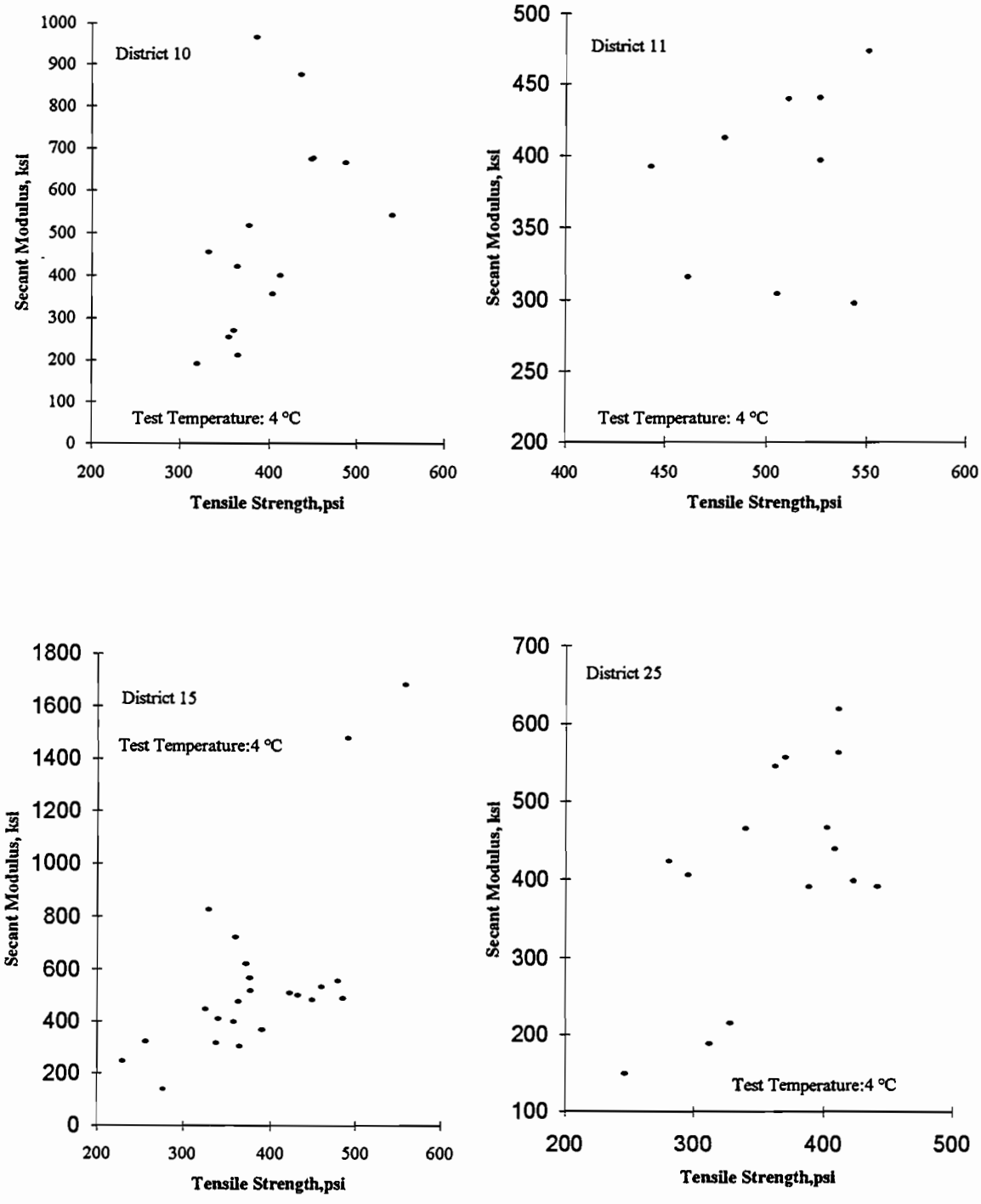

Figure D-25 Secant modulus as a function of indirect tensile strength at 4°C

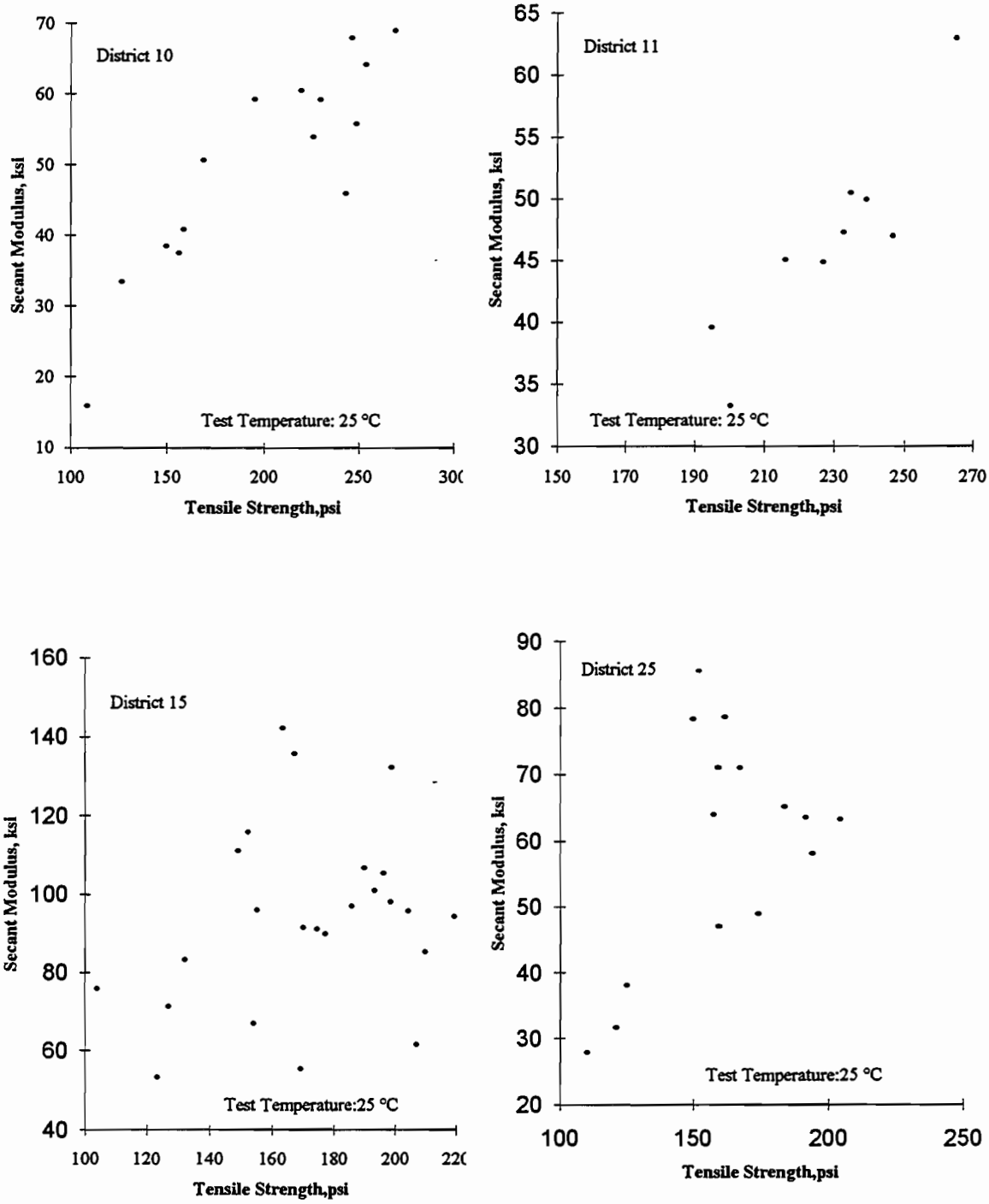

Figure D-26 Secant modulus as a function of indirect tensile strength at 25°C

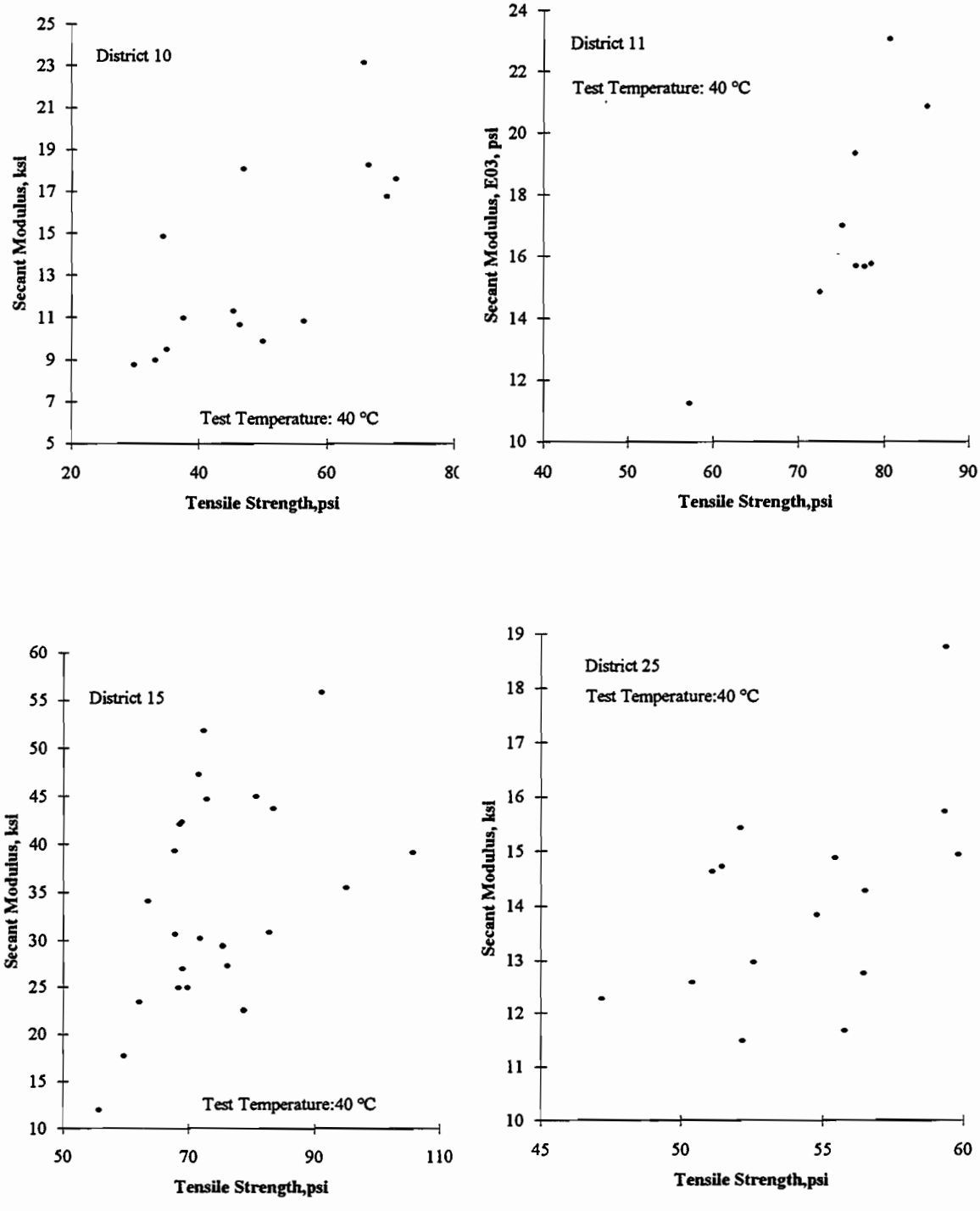

Figure D-27 Secant modulus as a function of indirect tensile strength at 40°C

TABLE D-17 TOTAL AND INSTANTANEOUS RESILIENT MODULUS AT TWO TEMPERATURES FOR FIELD CORES OF DISTRICT 10

Age : 34 months Cored in May 1993

Section	Height inches	Rice Sp.Gr.	Air Voids %	MRi psi,e06 77F	MRi psi,e06 39F	MRt psi,e06 77F	MRt psi,e06 39F
	2.00	2.509	6.6	2.711	4.525	2.259	3.908
Control	1.96	2.509	6.6	2.660	6.419	1.862	5.658
	1.92	2.509	5.4	2.191	4.999	1.693	4.777
Avg.			**6.2**	**2.521**	**5.314**	**1.938**	**4.781**
	2.00	2.482	3.7	2.864	7.995	1.998	7.510
SBRg	2.06	2.482	4.0	2.453	7.625	1.789	6.521
	2.04	2.482	3.6	2.564	8.268	1.909	7.087
Avg.			**3.7**	**2.627**	**7.963**	**1.899**	**7.039**
	2.08	2.458	4.2	2.987	6.014	2.458	5.400
SBSe	2.03	2.458	4.0	2.457	5.224	1.911	4.682
	2.06	2.458	4.4	3.814	7.740	2.601	7.506
Avg.			**4.2**	**3.086**	**6.326**	**2.323**	**5.862**
	1.88	2.492	4.7	1.615	7.172	1.211	5.827
SBSs	1.87	2.492	6.2	1.651	7.985	1.209	6.075
	1.88	2.492	6.4	1.172	8.467	0.835	6.985
Avg.			**5.8**	**1.479**	**7.874**	**1.085**	**6.296**
	2.06	2.494	5.7	1.592	5.662	1.222	5.058
EVAe	2.06	2.494	6.1	1.614	2.886	1.312	2.706
	2.02	2.494	6.1	1.520	6.060	1.192	4.591
Avg.			**6.0**	**1.576**	**4.869**	**1.242**	**4.118**

Sp.Gr. : specific gravity
MRi : instantaneous resilient modulus
MRt : total resilient modulus
SBRg : UP 70, Goodyear
SBSe : Styrelf-13, Elf
SBSs : Kraton D 1101, Shell
EVAe : Polybilt 103, Exxon

1 inch = 25.4 mm
1 lb = 453 grams
1 psi = 6895 Pa
1 Δ°F = 0.556 Δ°C

TABLE D-18 TOTAL AND INSTANTANEOUS RESILIENT MODULUS AT TWO TEMPERATURES FOR FIELD CORES OF DISTRICT 11

Age: 49 months Cored in May 1993

Section	Height inches	Rice Sp.Gr.	Air Voids %	MRi psi,e06 77F	MRi psi,e06 39F	MRt psi,e06 77F	MRt psi,e06 39F
	1.41	1.985	2.2	1.840	7.734	1.417	7.090
Control	1.54	1.985	2.3	2.162	5.081	1.622	4.799
	1.47	1.985	2.2	1.741	6.903	1.273	6.547
Avg.			**2.2**	**1.914**	**6.573**	**1.437**	**6.145**
	1.54	1.996	2.7	1.743	4.790	1.259	4.335
SBR g	1.65	1.996	2.3	1.509	5.742	1.056	5.467
	1.76	1.996	1.4	1.800	5.918	1.238	5.240
Avg.			**2.1**	**1.684**	**5.483**	**1.184**	**5.014**
	1.30	2.008	1.7	1.176	5.201	0.904	4.334
SBSe	1.18	2.008	1.3	1.034	3.154	1.034	2.509
	1.36	2.008	1.6	1.499	4.207	1.183	3.681
Avg.			**1.5**	**1.236**	**4.187**	**1.041**	**3.508**

Sp.Gr.: specific gravity
MRi: instantaneous resilient modulus
MRt: total resilient modulus
SBRg: UP 70, Goodyear
SBSe: Styrelf-13, Elf

1 inch = 25.4 mm
1 lb 453 gram
1 psi 6895 Pa
1 Δ°F = 0.556 Δ°C

TABLE D-19 TOTAL AND INSTANTANEOUS RESILIENT MODULUS AT TWO TEMPERATURES FOR FIELD CORES OF DISTRICT 15

Age: 73 months Cored in May 1993

Section	Height inches	Rice Sp.Gr.	Air Voids %	MRi psi,e06 77F	MRi psi,e-06 39F	MRt psi,E06 77F	MRt psi,E06 39F
	1.44	2.416	5.2	2.089	5.834	1.694	5.480
SBRg	1.41	2.416	7.5	1.793	6.714	1.459	6.474
	1.42	2.416	5.7	3.124	10.314	2.232	10.028
Avg.			**6.1**	**2.335**	**7.621**	**1.795**	**7.327**
	1.30	2.420	6.0	3.889	6.710	2.723	6.554
SBSe	1.30	2.420	5.1	1.951	8.279	1.707	7.881
	1.33	2.420	7.2	2.720	8.431	2.061	7.858
Avg.			**6.1**	**2.854**	**7.807**	**2.163**	**7.431**
	1.61	2.418	7.0	7.343	10.190	3.231	9.324
Control	1.62	2.418	5.4	2.867	11.091	1.290	9.807
	1.64	2.418	5.7	4.690	7.471	2.157	6.918
Avg.			**6.1**	**4.967**	**9.584**	**2.226**	**8.683**
	1.55	2.417	6.2	2.356	7.527	2.243	6.473
EVAe	1.60	2.417	7.7	2.698	5.404	2.494	4.988
	1.44	2.417	6.3	2.902	7.035	2.546	6.472
Avg.			**6.7**	**2.652**	**6.655**	**2.428**	**5.978**
	1.56	2.365	4.6	2.793	3.900	2.095	3.454
Rubber	1.56	2.365	7.4	3.693	8.603	3.024	8.029
	1.50	2.365	7.8	2.001	6.329	1.850	6.329
Avg.			**6.6**	**2.829**	**6.277**	**2.323**	**5.938**
	1.77	2.393	3.2	3.785	9.229	2.820	8.306
SBRp	1.65	2.393	2.8	2.620	11.401	2.217	10.404
	1.70	2.393	3.9	2.186	7.569	1.803	6.405
Avg.			**3.3**	**2.864**	**9.400**	**2.280**	**8.372**
	1.52	2.421	3.2	1.227	4.541	0.932	3.824
Fiber	1.52	2.421	6.6	2.190	6.618	2.102	6.067
	1.51	2.421	7.0	2.517	7.269	2.392	6.608
Avg.			**5.6**	**1.978**	**6.143**	**1.809**	**5.500**
	2.01	2.421	7.7	1.425	4.431	1.247	4.236
SBR/Pd	1.92	2.421	7.7	2.900	4.580	2.475	4.336
	2.12	2.421	7.3	1.173	6.606	1.108	6.051
Avg.			**7.5**	**1.833**	**5.206**	**1.610**	**4.874**

Sp.Gr. : specific gravity
MRi : instantaneous resilient modul
MRt : total resilient modulus
SBRg : UP 70 ,Goodyear
SBSe : Styrelf-13, Elf
EVAe : Polybilt 103, Exxon
Rubber : Genstar C107,Crafco
SBRp : NS 175, Polysar
SBR/Pd : SBR/Polyolefin, Dow

1 inch = 25.4 mm
1 lb = 453 grams
1 psi = 6895 Pascals
1 Δ°F = 0.556 °C

TABLE D-20 TOTAL AND INSTANTANEOUS RESILIENT MODULUS AT TWO TEMPERATURES FOR FIELD CORES OF DISTRICT 25

Age: 56 months Cored in May 1993

Section	Height inches	Rice Sp.Gr.	Air Voids %	MRi psi,e06 77F	MRi psi,e06 39F	MRt psi,e06 77F	MRt psi,e06 39F
	1.621	2.439	7.6	2.471	3.209	2.138	2.971
Control	1.530	2.439	7.6	1.826	6.705	1.688	5.364
	1.584	2.439	7.4	2.363	6.283	1.983	5.169
Avg.			**7.5**	**2.220**	**5.399**	**1.936**	**4.501**
	1.621	2.439	8.6	1.745	7.388	1.340	5.732
SBRg	1.673	2.439	7.7	1.155	8.637	0.996	6.945
	1.675	2.439	7.7	2.003	5.550	1.648	4.757
Avg.			**8.0**	**1.635**	**7.191**	**1.328**	**5.811**
	1.738	2.425	7.8	1.797	6.748	1.425	6.025
SBSe	1.881	2.425	8.1	2.449	5.903	1.666	5.608
	1.576	2.425	7.8	1.464	6.954	1.301	6.035
Avg.			**7.9**	**1.904**	**6.535**	**1.464**	**5.889**
	1.964	2.436	6.8	2.936	8.478	1.887	7.630
SBSs3%	1.926	2.436	7.7	1.389	4.007	1.064	3.660
	1.940	2.436	7.0	1.942	6.930	1.436	6.572
Avg.			**7.2**	**2.089**	**6.472**	**1.462**	**5.954**
	1.670	2.422	7.1	1.699	3.098	1.086	2.909
SBSs,6%	1.597	2.422	10.3	0.873	4.885	0.691	4.603
	1.538	2.422	9.1	1.354	5.966	1.087	4.972
Avg.			**8.8**	**1.309**	**4.650**	**0.955**	**4.161**

Sp.Gr. : specific gravity
MRi : instantaneous resilient modulus
MRt : total resilient modulus
SBRg : UP 70, Goodyear
SBSe : Styrelf-13, Elf
SBSs,3% : Kraton D-1101,3% content, Shell
SBSs,6% : Kraton D-1101,6% content, Shell

1 inch = 25.4 mm
1 lb = 453 grams
1 psi = 6895 Pasc
1 Δ°F = 0.556 °C

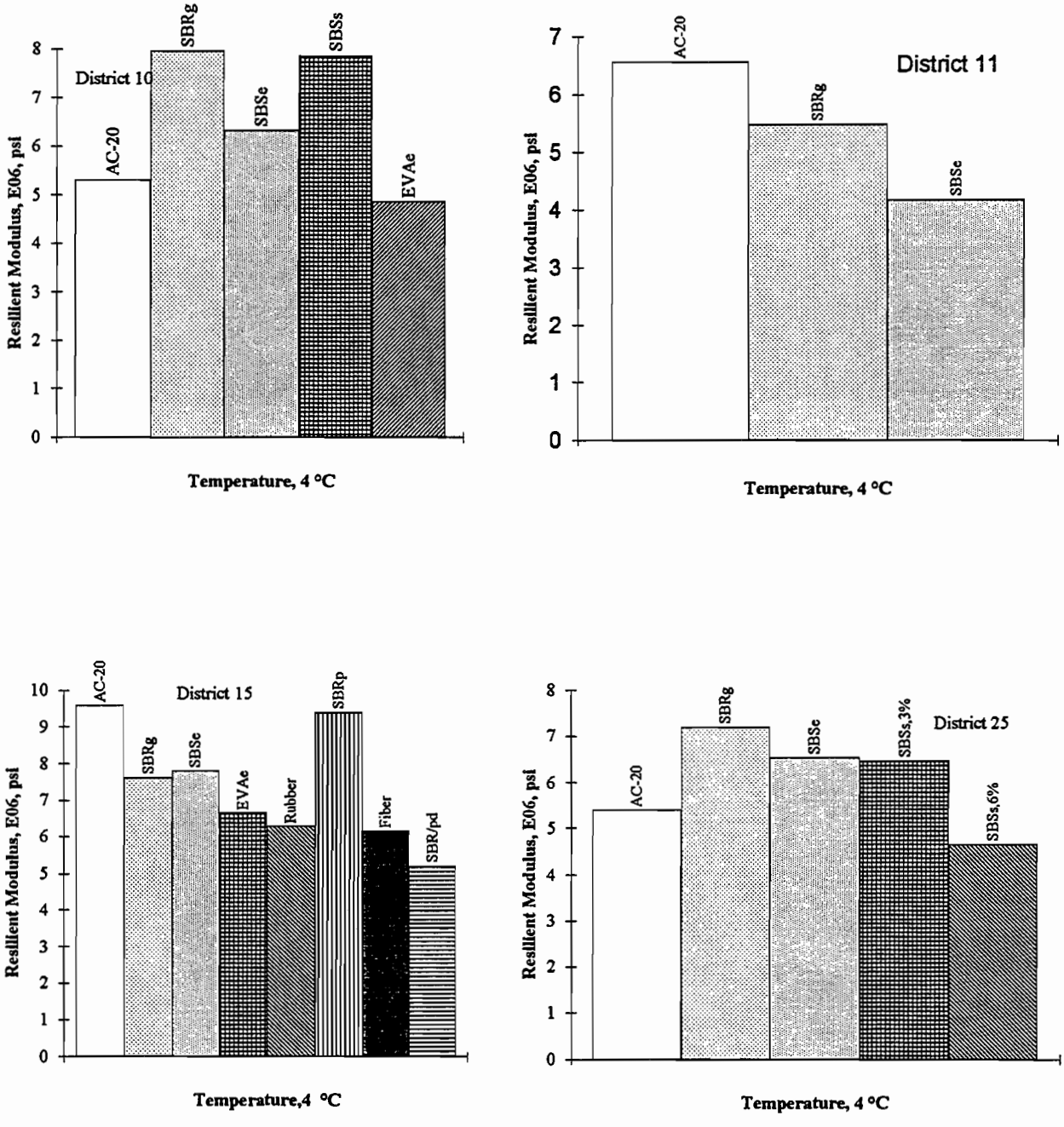

Figure D-28 Resilient modulus for different polymer-modified mixtures at 4°C

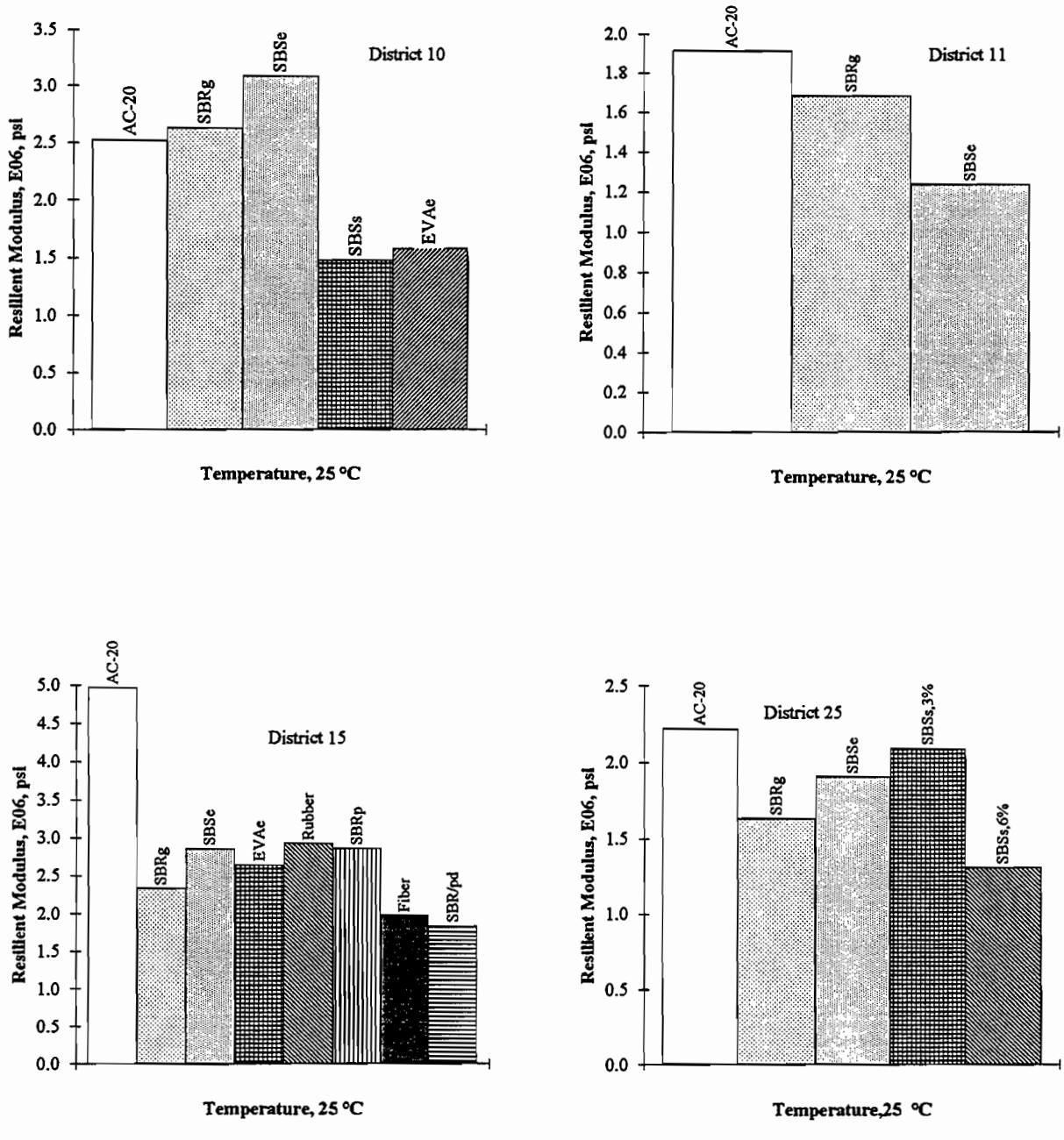

Figure D-29 Resilient modulus for different polymer-modified mixtures at 25°C

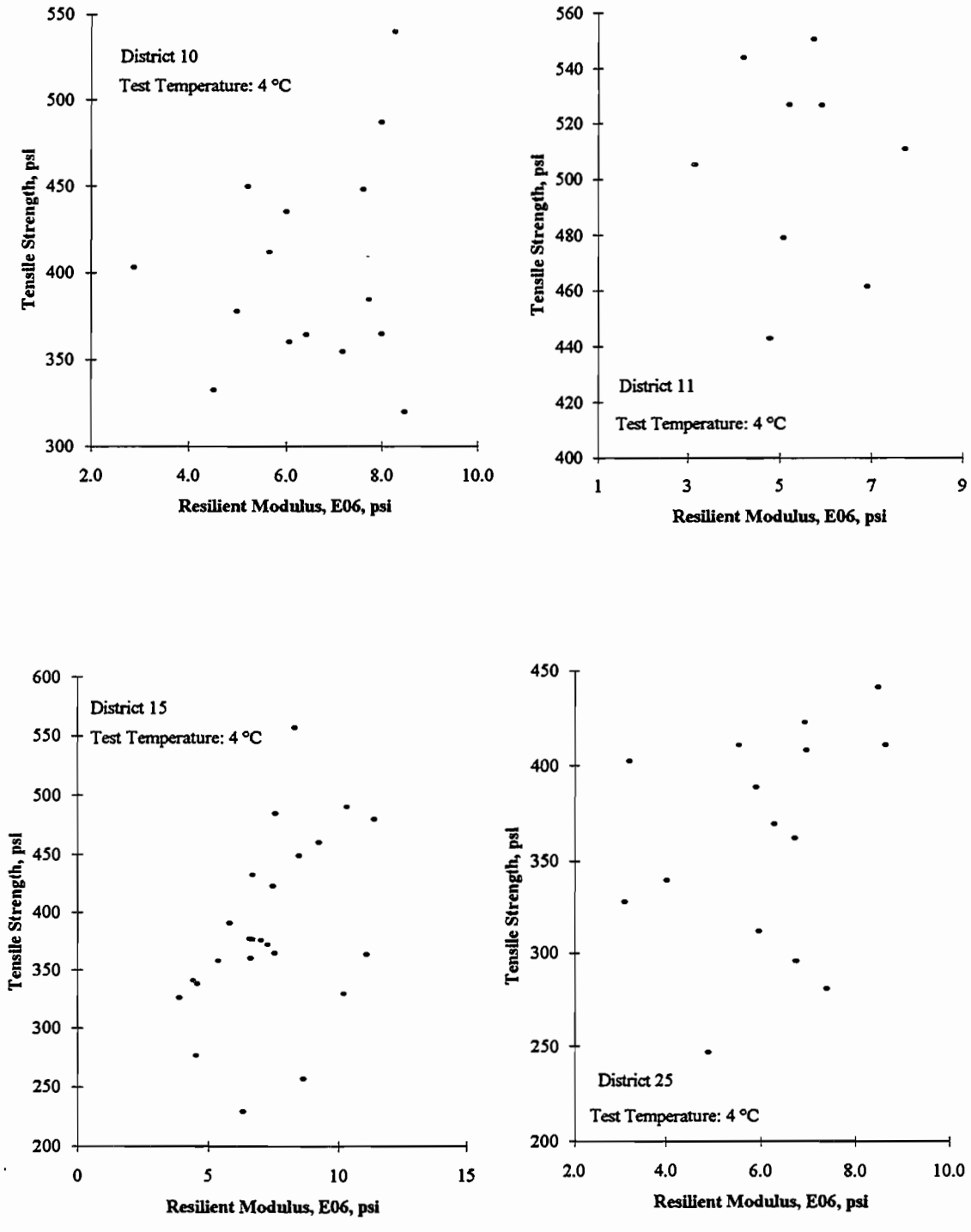

Figure D-30 Indirect tensile strength as a function of resilient modulus at 4°C

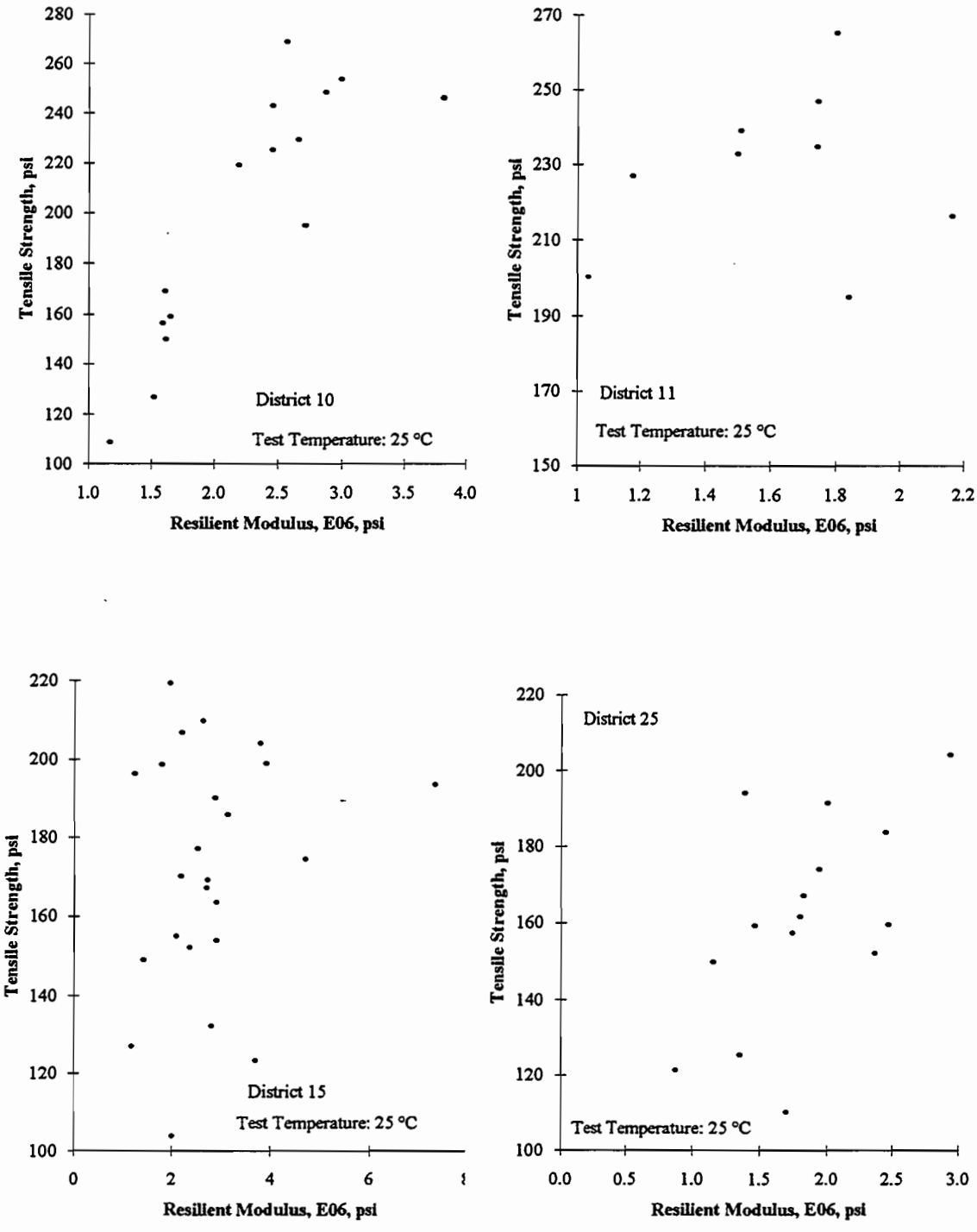

Figure D-31 Indirect tensile strength as a function of resilient modulus at 25°C

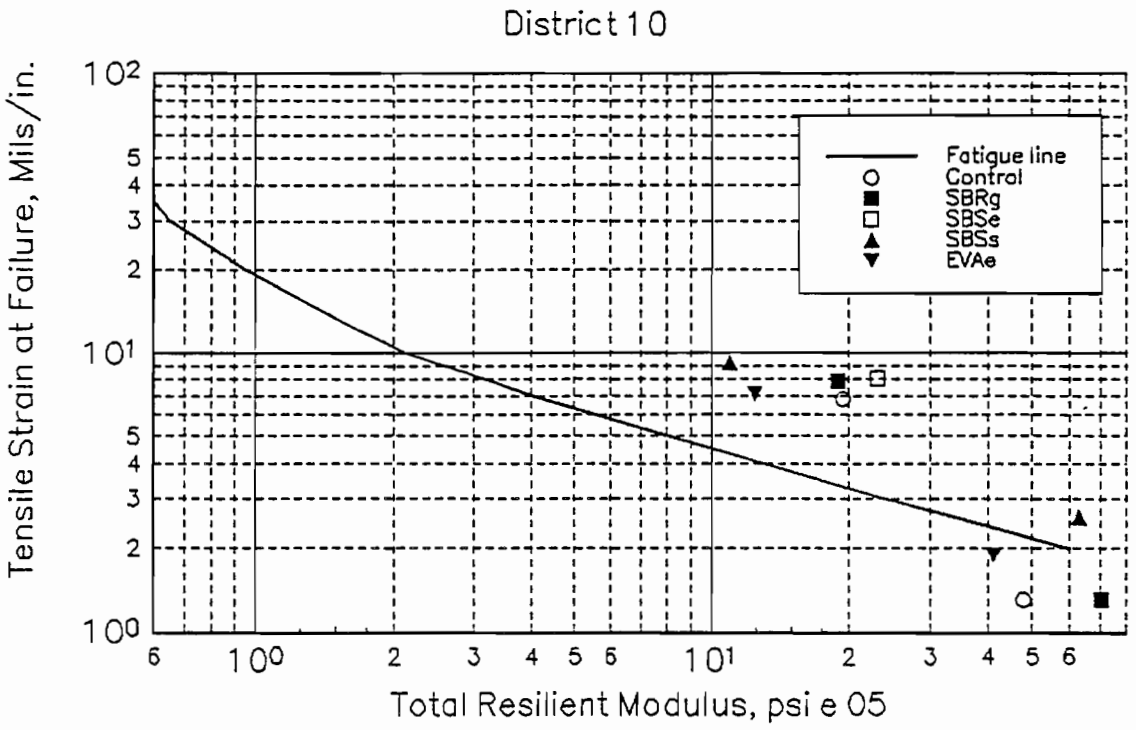

Figure D-32 Failure tensile strain as a function of total resilient modulus plotted on AAMAS fatigue chart for District 10

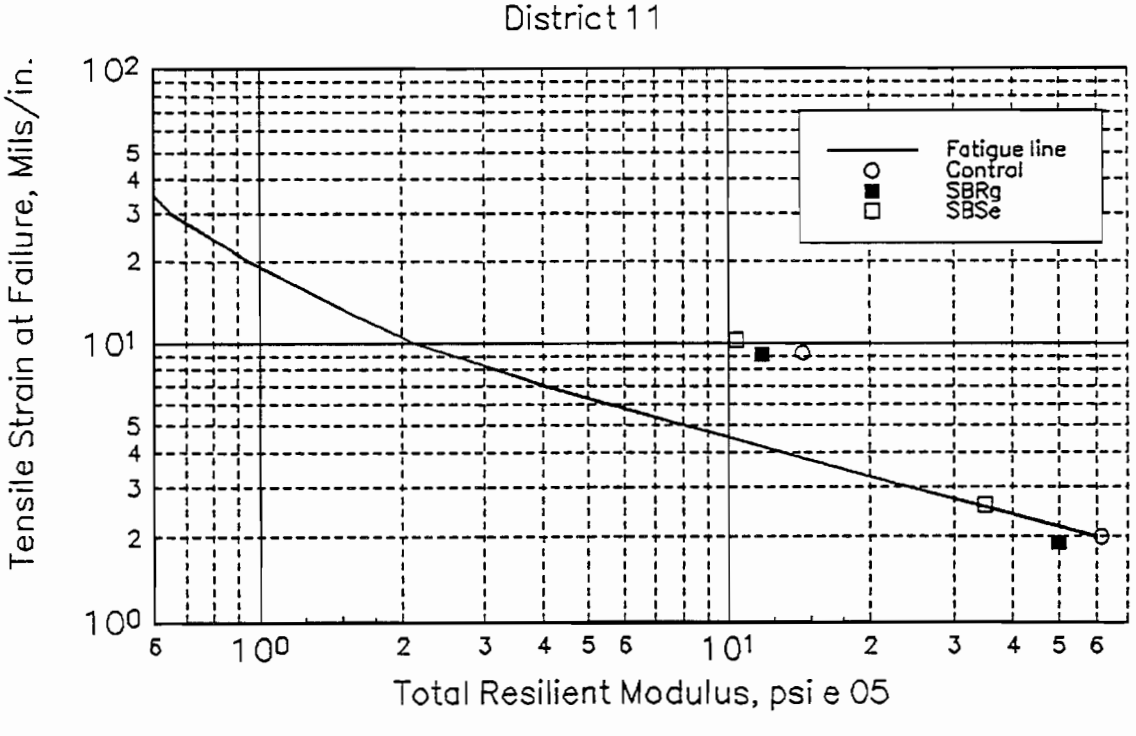

Figure D-33 Failure tensile strain as a function of total resilient modulus plotted on AAMAS fatigue chart for District 11

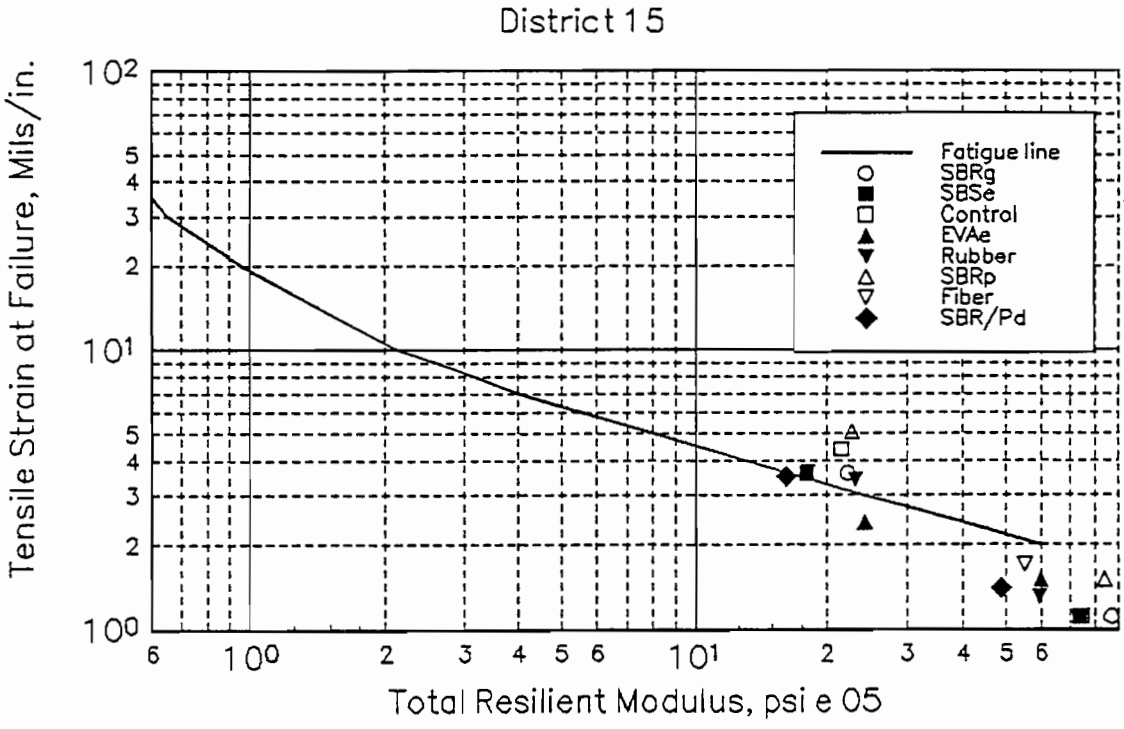

Figure D-34 Failure tensile strain as a function of total resilient modulus plotted on AAMAS fatigue chart for District 15

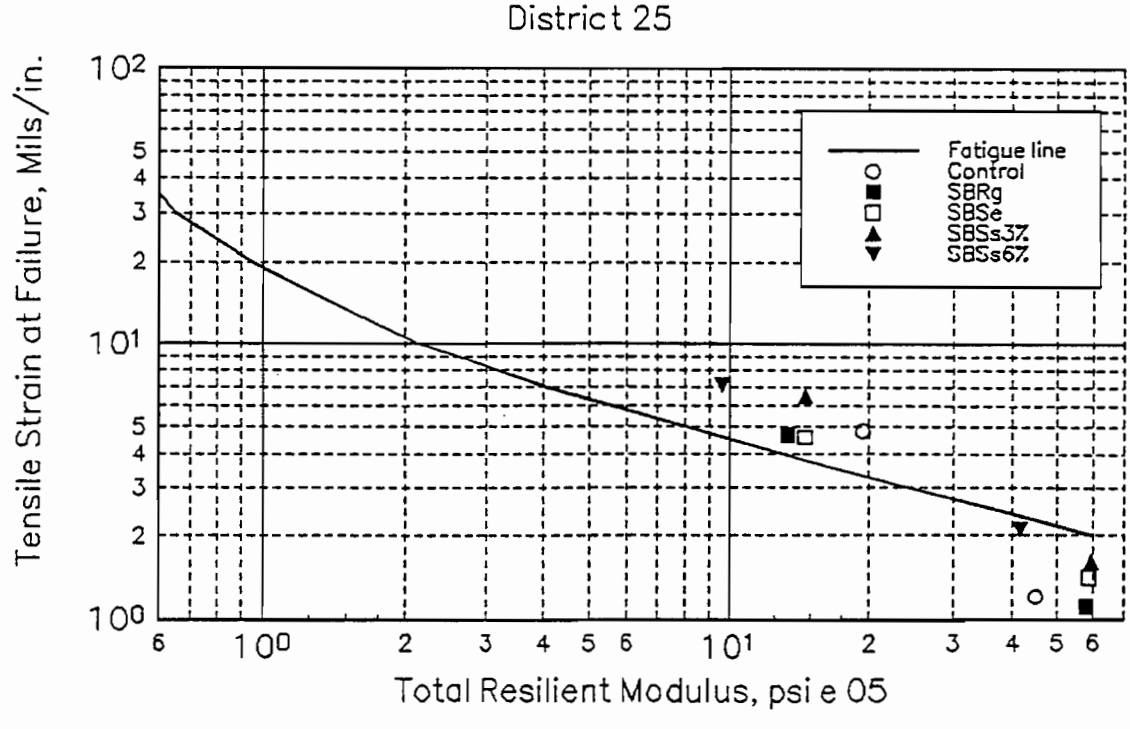

Figure D-35 Failure tensile strain as a function of total resilient modulus plotted on AAMAS fatigue chart for District 25